

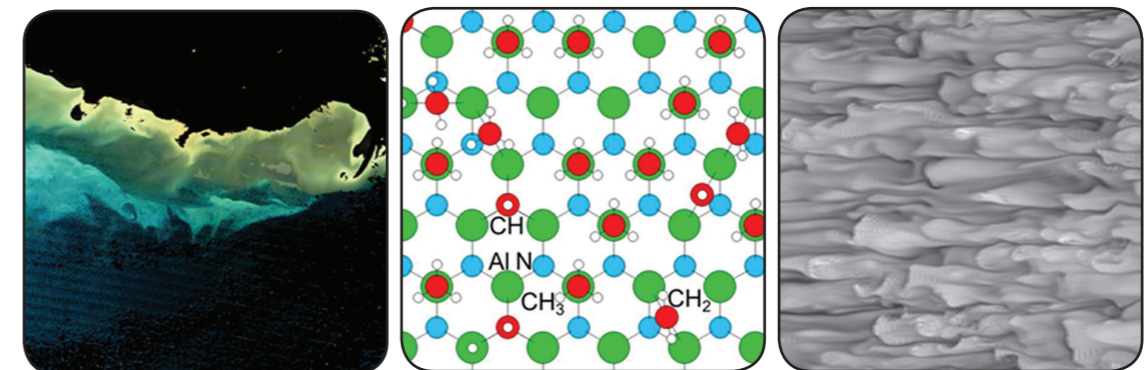


FY18 NRL DoD High Performance Computing Modernization Program Annual Reports

PREPARED BY
PORTIA A. SHINGLER
AND
BETH A. HOWELL

*Center for Computational Science
Information Technology Division*

November 7, 2019



Introduction

This book is a compilation of reports on all the work accomplished by NRL scientists and engineers and their collaborators using the DoD High Performance Computing Modernization Program's (HPCMP) resources for fiscal year 2018. The reports encompass work performed by researchers at all three NRL sites: Washington, DC; Stennis Space Center, Mississippi; and Monterey, California.

These reports are categorized according to the primary Computational Technology Area (CTA) as specified by the HPCMP, and include resources at the DoD Supercomputing Resource Centers (DSRC) as well as the Affiliated Resource Centers (ARC). This volume includes three indices for ease of reference. These are an author index, a site index, and an NRL hierarchical index of reports from the Branches and Divisions in the Laboratory.

THIS PAGE INTENTIONALLY LEFT BLANK

Table of Contents

Computational Structural Mechanics (CSM)

Computational Analysis of Warfighter Brain Injury and Protective Equipment.....2

X.G. Tan and R.N. Saunders

Naval Research Laboratory, Washington, DC

Stochastic Methods for Uncertainty Quantification in Computational Mechanics4

K. Teferra,¹ R. Saunders,¹ and V. Ha²

¹*Naval Research Laboratory, Washington, DC*

²*NRC Postdoctoral Fellow, Naval Research Laboratory, Washington, DC*

Geometric, Constitutive, and Loading Complexities in Structural Materials6

S.A. Wimmer,¹ R.N. Saunders,¹ A. Achuthan,² A. Arcari,³ J.R. Franke,¹ A.B.

Geltmacher,¹ D.J. Hasler,⁴ D.J. Horton,¹ L.P. Kuna,¹ J.A. Mancias,¹ T.J. Martin,¹ and J.G. Michopoulos,¹

¹*Naval Research Laboratory, Washington, DC*

²*Clarkson University, Potsdam, NY*

³*Excet, Inc., Springfield, VA*

⁴*Naval Operational Support Center, Green Bay, WI*

Computational Fluid Dynamics (CFD)

The Impact of Foam and Aerosol Dynamics on Fire, Explosion Safety, and Suppression (Mechanisms of Water Mist Suppression of a Burning Solid Surface)10

X. Zhuang¹ and R. Ananth²

¹*ASEE Postdoctoral Fellow, Naval Research Laboratory, Washington, DC*

²*Naval Research Laboratory, Washington DC*

Direct Numerical Simulation of Fluid-Sediment Wave Bottom Boundary Layer.....12

A. Levenson, S.P. Bateman, J.A. Simeonov, and J. Calantoni

Naval Research Laboratory, Stennis Space Center, MS

Numerical Simulations of Turbulence Impact on Optical Signal Transmission and Near-Surface Turbulence.....14

S. Matt and W. Hou

Naval Research Laboratory, Stennis Space Center, MS

Numerical Investigation of Advanced Military Aircraft Noise Reduction Concepts.....16

J. Liu, A. Corrigan, R.F. Johnson and R. Ramamurti

Naval Research Laboratory, Washington, DC

Deflagration-to-Detonation Transition in Terrestrial Systems and Type Ia Supernovae	18
V.N. Gamezo, ¹ and A.Y. Poludnenko ²	
¹ <i>Naval Research Laboratory, Washington, DC</i>	
² <i>Texas A&M University, College Station, TX</i>	
Predicting Fluid-Structure Interaction for Military Applications.....	20
D.R. Mott and A.D. Kercher	
<i>Naval Research Laboratory, Washington, DC</i>	
Multidimensional Chemically Reacting Fluid Dynamics with Application to Flameless Combustors	22
R.F. Johnson, A.D. Kercher, and D.A. Schwer	
<i>Naval Research Laboratory, Washington, DC</i>	
Optimization of the Spectral Dopant Concentration and Distribution in High Energy Density Deuterium Z-Pinch Plasmas as a Pulsed Neutron Source	24
Y.K. Chong	
<i>Naval Research Laboratory, Washington, DC</i>	
Hypersonic Reactive Flow Modeling.....	26
G. Goodwin	
<i>Naval Research Laboratory, Washington, DC</i>	
Advanced Two Phase CFD Model.....	28
T.D. Holman	
<i>Naval Research Laboratory, Washington, DC</i>	
High-Temperature and Rarefied Gas Dynamics in Hypersonic Flows	30
R.E. Rogers and J.R. Maxwell	
<i>Naval Research Laboratory, Washington, DC</i>	
Detonations with Multi-Phase Flows for Propulsion.....	32
D.A. Schwer	
<i>Naval Research Laboratory, Washington, DC</i>	
Simulations of the Ionosphere/Plasmasphere/Thermosphere System	34
J. Krall ¹ and J.D. Huba ²	
¹ <i>Naval Research Laboratory, Washington, DC</i>	
² <i>Berkeley Research Associates, Springfield, VA</i>	
Numerical Simulations of Noise Generated by Non-Circular Advanced Military Aircraft Nozzles.....	36
K. Viswanath and R. Ramamurti	
<i>Naval Research Laboratory, Washington, DC</i>	

Applications of FEFLO Incompressible Flow Solver	38
R. Ramamurti	
<i>Naval Research Laboratory, Washington, DC</i>	
Particle-in-Cell Simulations of Large-Area Electron-Beam Diodes	40
S.B. Swanekamp, A.S. Richardson, I. Rittersdorf, J.W. Schumer, P.F. Ottinger and S.P. Obenschain	
<i>Naval Research Laboratory, Washington, DC</i>	
Fine Scale Structure of the Air-Sea Interface	42
G.B. Smith, ¹ R. Leighton, ² I. Savelyev, ¹ and T. Evans ¹	
¹ <i>Naval Research Laboratory, Washington, DC</i>	
² <i>SRI-International, Ann Arbor, MI</i>	
 <u>Computational Biology, Chemistry, and Materials Science (CCM)</u>	
Quantum-Chemical Simulation of Surface-Science Experiments.....	46
V.M. Bermudez and P.E. Pehrsson	
<i>Naval Research Laboratory, Washington, DC</i>	
Marine Biofilm Metaproteomics	48
W.J. Hervey, IV, C. Ames, M.A. Rimmer, S.M. Colston, D.H. Leary, and G.J. Vora	
<i>Naval Research Laboratory, Washington, DC</i>	
Synthetic Biology for Military Environments	50
W.J. Hervey, IV, D.H. Leary, M.A. Rimmer, S.N. Dean, S. Kim, and G.J. Vora	
<i>Naval Research Laboratory, Washington, DC</i>	
First-Principles Simulations of Condensed-Phase Decomposition of Energetic Materials	52
I.V. Schweigert	
<i>Naval Research Laboratory, Washington, DC</i>	
Growth and Control of Metal Films on Semiconductor Substrates.....	54
S.C. Erwin	
<i>Naval Research Laboratory, Washington, DC</i>	
Sequence Clustering.....	56
D. Zabetakis, J.L. Liu, G.P. Anderson, and E.R. Goldman	
<i>Naval Research Laboratory, Washington, DC</i>	
Calculation of Materials Properties Via Density Functional Theory and Its Extensions	58
J.L. Lyons	
<i>Naval Research Laboratory, Washington, DC</i>	

Materials for Energy Storage and Generation.....	60
M. Johannes <i>Naval Research Laboratory, Washington, DC</i>	
Surfaces and Interfaces in Oxides and Semiconductors	62
C.S. Hellberg <i>Naval Research Laboratory, Washington, DC</i>	
Multiple Length and Time Scale Simulations of Material Properties	64
N. Bernstein <i>Naval Research Laboratory, Washington, DC</i>	
IR Absorption Spectra for Chlorinated Hydrocarbons in Water Using Density Functional Theory.....	66
S. Lambrakos, ¹ L. Huang, ² and L. Massa ³ ¹ <i>Naval Research Laboratory, Washington, DC</i> ² <i>Volunteer Emeritus, Naval Research Laboratory, Washington, DC</i> ³ <i>City University of New York, NY</i>	
High-Throughput Search for New Magnetic Materials and Noncollinear Magnetism	68
I. Mazin ¹ and J. Glasbrenner ² ¹ <i>Naval Research Laboratory, Washington, DC</i> ² <i>George Mason University, Fairfax, VA</i>	
Numerical Studies of Semiconductor Nanostructures.....	70
T.L. Reinecke ¹ and S. Mukhopadhyay ² ¹ <i>Naval Research Laboratory, Washington, DC</i> ² <i>National Research Council Postdoctoral Program, Washington, DC</i>	
<u>Computational Electromagnetics and Acoustics (CEA)</u>	
Acoustic Parameter Variability over an Ocean Reanalysis (AVORA).....	74
J.P. Fabre <i>Naval Research Laboratory, Stennis Space Center, MS</i>	
Forward Simulations of Diffusive Wave Algorithms	76
D. Photiadis <i>Naval Research Laboratory, Washington, DC</i>	
Flowfield and Transport Models for Navy Applications	78
W.G. Szymczak and A.J. Romano <i>Naval Research Laboratory, Washington, DC</i>	

Intense Laser Physics and Advanced Radiation Sources.....	80
D.F. Gordon, ¹ J. Penano, ¹ L. Johnson, ¹ D. Kaganovich, ¹ Y. Chen, ¹ M. Helle, ¹ B. Hafizi, ¹ and Y. Khine ²	
¹ Naval Research Laboratory, Washington, DC	
² Engility Corporation, Chantilly, VA	
Optomechanical Systems.....	82
M. Zalalutdinov, S. Carter, S. Dey	
Naval Research Laboratory, Washington, DC	
Small Slope Approximation Rough-Surface Back-Scattering Analysis	84
J. Alatishe	
Naval Research Laboratory, Washington, DC	
Multidimensional Particle-in-Cell Modeling of Ultrashort Pulse Laser with Solid Targets.....	86
G.M. Petrov	
Naval Research Laboratory, Washington, DC	
Low Grazing Angle Radar Backscatter	88
J.V. Toporkov, M.A. Sletten, and J.D. Ouellette	
Naval Research Laboratory, Washington, DC	
Computer-Aided Design of Vacuum Electronic Devices.....	90
G. Stantchev, ¹ S. Cooke, ¹ J. Petillo, ² A. Jensen, ² and S. Ovtchinnikov ²	
¹ Naval Research Laboratory, Washington, DC	
² Leidos, Billerica, MA	
 <u>Climate Weather Ocean Modeling (CWO)</u>	
Data Assimilation Studies Project	94
W.F. Campbell and B. Ruston	
Naval Research Laboratory, Monterey, CA	
Bio-Optical Modeling and Forecasting	96
J.K. Jolliff, S.Ladner, T. Smith, and J. Dykes	
Naval Research Laboratory, Stennis Space Center, MS	
Modeling Cloud-Aerosol Interactions in Long-Lived Polluted Clouds	98
P. Caffrey and S. Rabenhorst	
Naval Research Laboratory, Washington, DC	
Atmospheric Process Studies	100
N.P. Barton, ¹ T. Whitcomb, ¹ J. Ridout, ¹ K. Viner, ¹ J. McLay, ¹ W. Crawford, ² M. Liu, ¹ and C. Reynolds ¹	
¹ Naval Research Laboratory, Monterey, CA	
² American Society for Engineering Education, Washington, DC	

Multi-scale Characterization and Prediction of the Global Atmosphere from the Ground to the Edge of Space using Next-Generation Navy Modeling Systems.....102

J.P. McCormack,¹ S.D. Eckermann,¹ C.A. Barton,^{1,3} F. Sassi,¹ M.A. Herrera,^{1,3} K.W. Hoppel,¹ D.D. Kuhl,¹ D.R. Allen,¹ J. Ma,² and J. Tate²

¹Naval Research Laboratory, Washington, DC

²Computational Physics, Inc., Springfield, VA

³National Research Council Postdoctoral Research Fellow, Washington, DC

Variational Data Assimilation104

S. Smith,¹ C. Amerault,² C. Barron,¹ T. Campbell,¹ M. Carrier,¹ J. D'Addezio,³ J. Dastugue,¹ S. DeRada,¹ E. Douglas,¹ P. Martin,¹ J. May,¹ W. Mulberry,⁴ H. Ngodock,¹ J. Osborne,⁵ C. Rowley,¹ R. Schaefer,⁵ J. Shriver,¹ O. Smedstad,⁶ T. Smith,¹ I. Souopgui,⁷ and P. Spence,⁶

¹Naval Research Laboratory, Stennis Space Center, MS

²Naval Research Laboratory, Monterey, CA

³University of Southern Mississippi, Stennis Space Center, MS

⁴University of North Carolina, Greensboro, NC

⁵American Society for Engineering Education, Stennis Space Center, MS

⁶QinetiQ North America, Stennis Space Center, MS

⁷University of New Orleans, Stennis Space Center, MS

Rogue Wave Probability Estimator for WAVEWATCH III.....106

M. Orzech,¹ J. Simeonov,¹ and M. Manolidis²

¹Naval Research Laboratory, Stennis Space Center, MS

²National Research Council Postdoctoral Research Associate, Naval Research Laboratory, Stennis Space Center, MS

Dynamics of Coupled Models108

I. Shulman, B. Pent, S. Cayula, and C. Rowley

Naval Research Laboratory, Stennis Space Center, MS

Probabilistic Prediction to Support Ocean Modeling Projects.....110

C.D. Rowley,¹ L.F. Smedstad,¹ C.N. Barron,¹ R.S. Linzell,² M. Yaremchuk,¹ J.C. May,¹ J.M. Dastugue,¹ P.L. Spence,² T.L. Townsend,¹ T.A. Smith,¹ J.J. Osborne V,³ G.G. Panteleev¹, N. VandeVoorde,² B.P. Bartels,² and B.R. Maloy¹

¹Naval Research Laboratory, Stennis Space Center, MS

²Perspecta, Stennis Space Center, MS

³Naval Research Laboratory Postdoctoral Program, Stennis Space Center, MS

Guidance for Heterogeneous Observation System (GHOST)112

L.F. Smedstad,¹ C.N. Barron,¹ G.A. Jacobs,¹ P.L. Spence,² C.J. DeHaan,² T.A. Smith,¹ R.S. Linzell,² and B.P. Bartels²

¹Naval Research Laboratory, Stennis Space Center, MS

²Perspecta, Stennis Space Center, MS

Coupled Ocean-Wave-Air-Ice Prediction System.....114

R. Allard,¹ T. Campbell,¹ J. Crout,² D. Hebert,¹ T. Jensen,¹ T. Smith,¹ and E. Rogers¹

¹Naval Research Laboratory, Stennis Space Center, MS

²Perspecta, Stennis Space Center, MS

The Effect of Langmuir Turbulence in Upper Ocean Mixing.....116

Y. Fan, E. Rogers, and T. Jensen

Naval Research Laboratory, Stennis Space Center, MS

Eddy-resolving Global/Basin-SOM.....118

E.J. Metzger,¹ J.F. Shriver,¹ M. Buijsman,² and C.H. Jeon²

¹Naval Research Laboratory, Stennis Space Center, MS

²University of Southern Mississippi, Stennis Space Center, MS

Coastal Meoscale Modeling – COAMPS-TC Intensity Prediction.....120

J.D. Doyle

Naval Research Laboratory, Monterey, CA

Coastal Mesoscale Modeling122

P.A. Reinecke

Naval Research Laboratory, Monterey, CA

Signal Image Processing (SIP)

Reducing the Burden of Massive Training Data for Deep Learning126

L.N. Smith, S.N. Blisard, and K.M. Sullivan

Naval Research Laboratory, Washington, DC

Common Ground Learning and Explanation (COGLE)128

L.N. Smith,¹ M. Youngblood,² M. Stefik,² and B. Krivacic²

¹Naval Research Laboratory, Washington, DC

²Palo Alto Research Center, (PARC, a Xerox Company), Palo Alto, CA

Space and Astrophysical Science (SAS)

Radiative Signatures and Dynamical Interactions of AGN Jets132

M.T. Wolff¹ and J.H. Beall²

¹Naval Research Laboratory, Washington, DC

²St. John's College, Annapolis, MD

Development of a Weather Model of the Ionosphere	134
S.E. McDonald, ¹ F. Sassi, ¹ C.A. Metzler, ¹ D.P. Drob, ¹ J.L. Tate, ³ M.S. Dhadly, ² and B.D. Curtis ⁴	
¹ <i>Naval Research Laboratory, Washington, DC</i>	
² <i>National Research Council Postdoctoral Fellow, Naval Research Laboratory, Washington, DC</i>	
³ <i>Computational Physics, Inc., Springfield, VA</i>	
⁴ <i>Praxis, Inc., Arlington, VA</i>	
Navy Ionosphere Model for Operations	136
S.E. McDonald, ¹ C.A. Metzler, ¹ J.L. Tate, ² B.D. Curtis, ³ R.K. Schaefer, ⁴ P.B. Dandenault, ⁴ A.T. Chartier, ⁴ G. Romeo, ⁴ G.S. Bust, ⁴ and R. Calfas ⁵	
¹ <i>Naval Research Laboratory, Washington, DC</i>	
² <i>Computational Physics, Inc., Springfield, VA</i>	
³ <i>Praxis, Inc., Arlington, VA</i>	
⁴ <i>The Johns Hopkins Applied Physics Laboratory, Laurel, MD</i>	
⁵ <i>The University of Texas at Austin, Applied Research Laboratories, Austin, TX</i>	
Meteorology and Climatology of the Thermosphere	138
D.P. Drob, ¹ M. Jones, ¹ and M. Dhadly ²	
¹ <i>Naval Research Laboratory, Washington, DC</i>	
² <i>National Research Council Postdoctoral Program, Washington</i>	
Electromagnetic Pulses from Hypervelocity Impacts on Spacecraft	140
A. Fletcher	
<i>Naval Research Laboratory, Washington, DC</i>	
Dynamic Phenomena in the Solar Atmosphere.....	142
M.G. Linton	
<i>Naval Research Laboratory, Washington, DC</i>	
Radio and Gamma-ray Searches for Millisecond Pulsars and Radio Transients ...	144
P.S. Ray and J. Deneva	
<i>Naval Research Laboratory, Washington, DC</i>	
<u>Other (OTH)</u>	
Simulation of High Energy-Radiation Environments	148
J. Finke and A. Hutcheson	
<i>Naval Research Laboratory, Washington, DC</i>	
Author Index	151
Division/Branch Index	154
Site Index	156



Computational Structural Mechanics

CSM covers the high resolution multidimensional modeling of materials and structures subjected to a broad range of loading conditions including quasistatic, dynamic, electromagnetic, shock, penetration, and blast. It also includes the highly interdisciplinary research area of materials design, where multiscale modeling from atomistic scale to macro scale is essential. CSM encompasses a wide range of engineering problems in solid mechanics, such as material or structural response to time- and history-dependent loading, large deformations, fracture propagation, shock wave propagation, isotropic and anisotropic plasticity, frequency response, and nonlinear and heterogeneous material behaviors. High performance computing for CSM addresses the accurate numerical solution of conservation equations, equation of motion, equations of state, and constitutive relationships to model simple or complex geometries and material properties, subject to external boundary conditions and loads. CSM is used for basic studies in continuum mechanics, stress analysis for engineering design studies, predicting structural and material response to impulsive loads, and modeling response of heterogeneous embedded sensors/devices. DoD application areas include conventional underwater explosion and ship response, structural acoustics, coupled field problems, space debris, propulsion systems, structural analysis, total weapon simulation, weapon systems' lethality/survivability (e.g., aircraft, ships, submarines, and tanks), theater missile defense lethality analyses, optimization techniques, and real-time, large-scale soldier- and hardware-in- the-loop ground vehicle dynamic simulation.

Title: Computational Analysis of Warfighter Brain Injury and Protective Equipment

Author(s): X.G. Tan and R.N. Saunders

Affiliation(s): Naval Research Laboratory, Washington, DC

CTA: CSM

Computer Resources: SGI ICE X [AFRL, OH]; Cray XC40 [ARL, MD]; Cray XC40/50 [ERDC, MS]; SGI ICE X [ERDC, MS]; SGI Altix ICE [NRL, DC]

Research Objectives: The research objective of this project is developing methods to prevent and mitigate injury to warfighters. This involves computational analysis of ballistic/blunt impacts on personal protective equipment (PPE) and blast induced traumatic brain injury (TBI). Computational methods, such as finite element analysis, are used to conduct the analysis. The use of HPC resources is vitally important to this project due to the high fidelity of the models of interest. A typical model to analyze TBI requires approximately 24 hours on 216 computer cores. One of the primary outcomes of this research will be the accumulation of a significant number of simulations, which will be used to construct correspondence relationships between humans, pigs, and their surrogates.

Methodology: The project uses finite element methods extensively, but the work is not restricted to finite element methodologies. Nonlinear material mechanical constitutive response features are highlighted in much of the work performed. Implicit and explicit solution methods are used as appropriate. The primary finite element codes used are Abaqus and CoBi. User subroutines are used for specialized material constitutive response when applicable. Multi-physics modeling capability is used to couple the fluid and structure analysis. Typically Abaqus/Viewer, ParaView, IDL, Matlab, and Tecplot are used for visualization of results, including the animation. For model development, the project typically uses CUBIT, ABAQUS/CAE, SimpleWare, IDL, and in-house software. Large run times and large model size are often required for the multi-physics/multi-step nonlinear finite element analysis jobs.

Results: This project involves work in several topical areas. Work has been performed on creating image-based head and helmet models, modeling biological tissues, biomechanics of trauma, and modeling ballistic shell and suspension pad materials. Representative results for the analysis of the protective role of combat helmets against blast induced brain injury are presented. A full-size shock tube is modeled to replicate the actual explosion. Figure 1 shows the slice view of the shock wave interaction with the head with helmet in the shock tube. The analysis results shown in Fig. 2 reveal blast induced brain injury pathways, including the shock wave focusing in the ocular cavity and ear, wave infiltration under the helmet, and pressure loading transmission into the brain. The comparative study between the head with the combat helmet and head without helmet suggests that current combat helmets provide the protection against blast-induced TBI when both the positive pressure in the brain and head acceleration are used as the injury metrics (Fig. 3).

DoD Impact/Significance: Insights gained from this project are necessary for the advancement from concept to application. Navy/DoD expected results are an improved understanding of TBI for Naval/DoD applications. New insights will be gained through quantifying the effects of anatomical and material property differences on the mechanical response of quantities correlated with TBI, which will impact warfighter health in terms of improved protective gear and improved understanding of the correlation between mechanical response thresholds and TBI. The development of techniques to model population-wide anatomical variability will provide insight into the importance of the fit of protective gear.

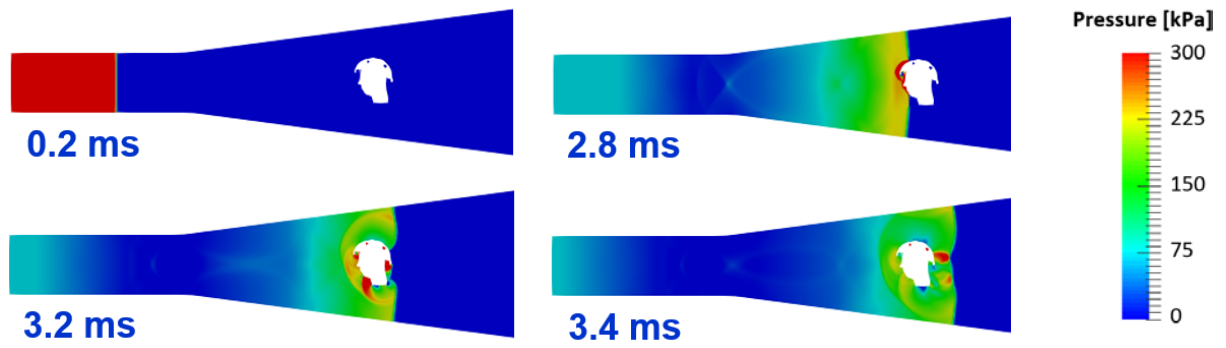


Figure 1. Contour plots of overpressure (kPa) of shock wave interaction with the head with combat helmet in a helium-air shock tube.

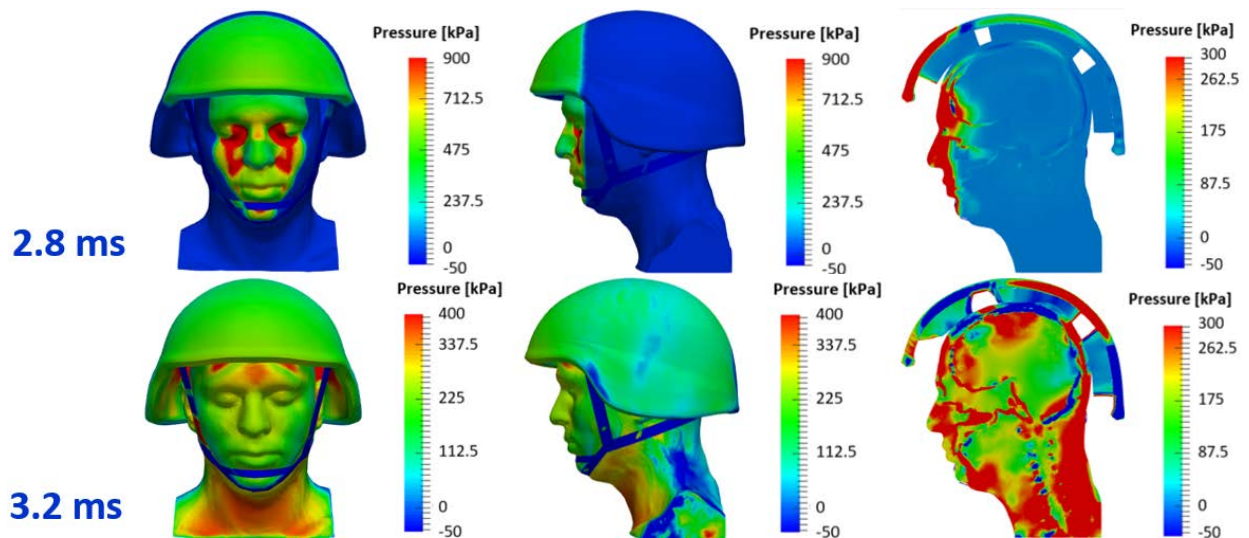


Figure 2. Contour plots of pressure (kPa) on the helmet and head and at the middle sagittal plane due to the shock wave loading.

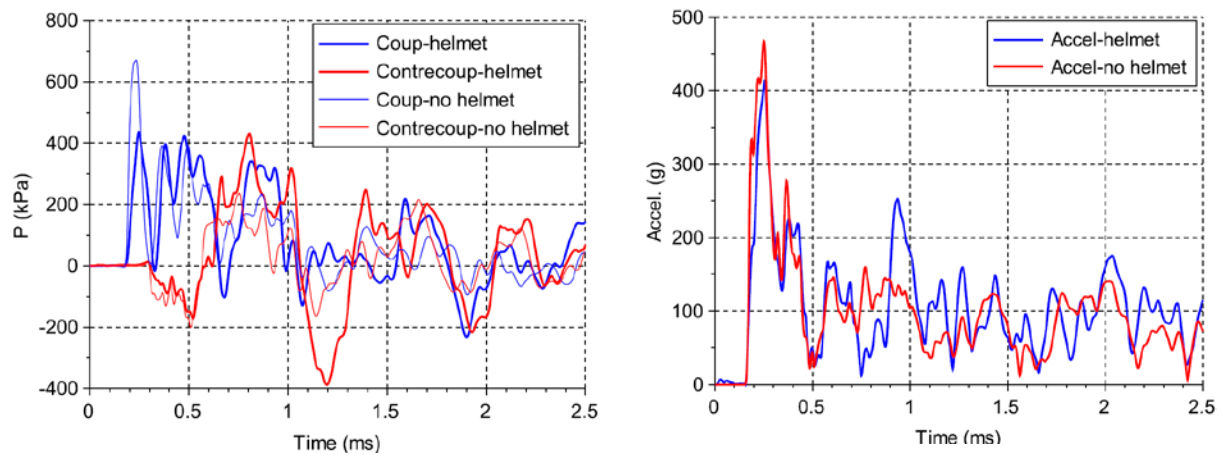


Figure 3. Pressure in the brain (left) and head acceleration (right) for the head with helmet and head without helmet due to the shock wave loading. Time offset is 2.6 msec.

Title: Stochastic Methods for Uncertainty Quantification in Computational Mechanics

Author(s): K. Teferra,¹ R. Saunders,¹ and V. Ha²

Affiliation(s): ¹Naval Research Laboratory, Washington, DC; ²NRC Postdoctoral Fellow, Naval Research Laboratory, Washington, DC

CTA: CSM

Computer Resources: SGI ICE X [AFRL, OH]; SGI ICE X [ERDC, MS]

Research Objectives: The research objective is to develop and integrate uncertainty quantification methods into computational mechanics simulations in order to understand the effects of input uncertainty on response quantities of interest. Inherent to problems in structural mechanics is the existence of many uncertainties, such as material properties, boundary conditions, material interfaces, component morphologies, and modeling errors as simulation techniques diverge from first-principles calculations as a result of their computational intractability for meso- and macro- length scales. In order to understand the effects of these uncertainties on mechanical response quantities of interest, the uncertainties must be characterized, parameterized, and then simulated. A simulated sample is a single instantiation of one of many possible system states, while it is desired to understand the mechanical response for the ensemble of possible system states. Therefore, extensive simulations must be conducted along with the development of optimal sampling techniques and accurate stochastic simulation algorithms.

Methodology: The project uses finite element methods extensively along with in-house developed scripts and compiled codes. Nonlinear material constitutive response, complex component geometry, and large mechanical deformations are common features of the scenarios simulated. Implicit and explicit solution methods are used as appropriate. The range of finite element codes used are Abaqus, CoBi, Sierra, and Moose. Model development is done with CUBIT, ABAQUS/CAE, SimpleWare, or in-house software. Large run times and large model size are often required for the multi-step nonlinear finite element analysis jobs.

Results: While this project involves work in several research areas, the topic of modeling the biomechanical response of the human brain due to blast loading and the effects of intersubject head morphological variability is highlighted. In this particular study, population-wide analysis is conducted to model how the mechanical response in the brain differs based on head shape. A database of approximately 200 magnetic resonance imaging (MRI) scans of human heads is obtained, and the brain and head components of each subject are segmented from the gray scale values using image processing techniques. A previously developed, detailed model of a median male subject is morphed into each subject's geometry. A morphing is a displacement field applied to one model to match the geometry of another, and determined through optimization. The morphed median model is auto-meshed and finite element analysis is conducted. Schematic of the morphing strategy, time histories of the peak pressure in the brain, and trend with respect head shape parameters are show in Figs. 1, 2, and 3, respectively, with detailed explanations provided in the figure captions.

DoD Impact/Significance: Traumatic brain injury caused by an insult to the brain leading to neuro-degeneration has been a pressing issue for the Navy and Marine Corps because it is an impediment to warfighter performance and health. The warfighter health and survivability support area aims to improve protection against insults associated with traumatic brain injury as well as to improve our understanding of this disease for better treatment. Understanding and quantifying the uncertainty associated with population-wide variability regarding anthropometry, anatomy, and biomechanical behavior can improve the design of personal protective equipment.

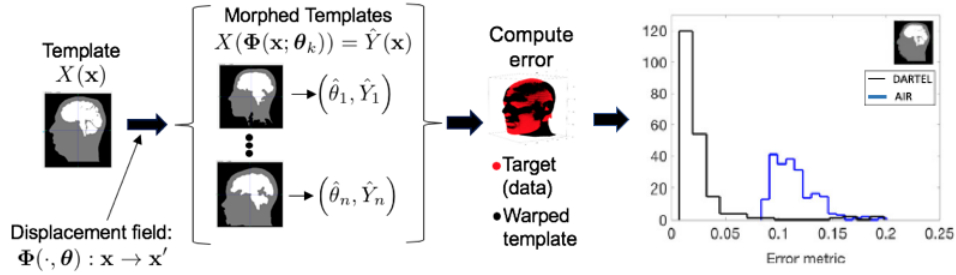


Figure 1. Schematic of the morphing strategy: a displacement field is applied to the template model to match different subjects. A loss function based on mismatch volume is minimized. This error is evaluated for two different modeling techniques (DARTEL and AIR).

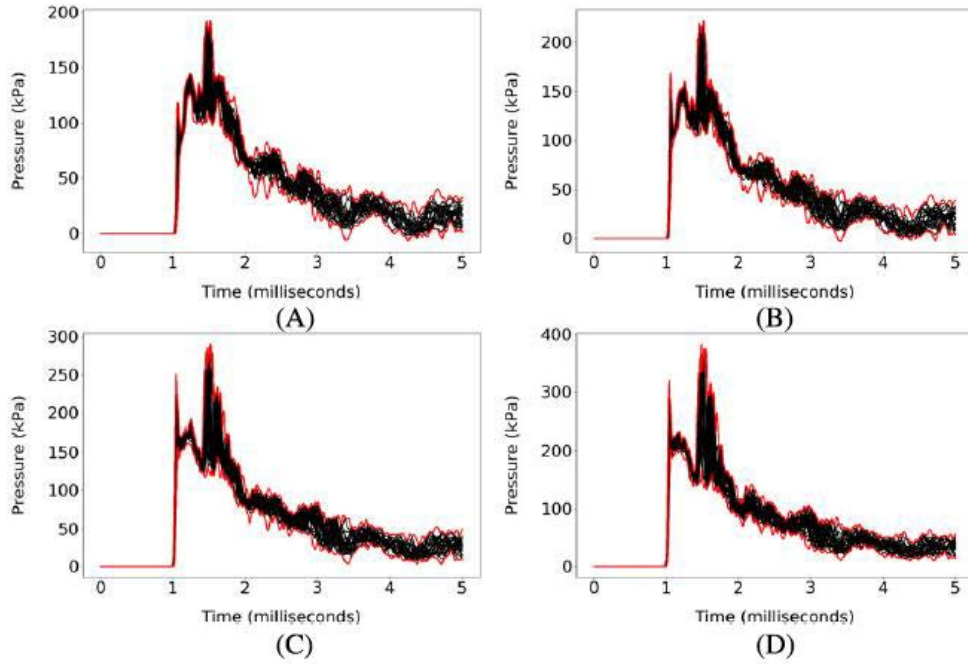


Figure 2. Time history plots of (a) 90th (b) 95th (c) 99th (d) 99.9th percentile pressure values for 25 subjects simulated. Red lines indicate bounds.

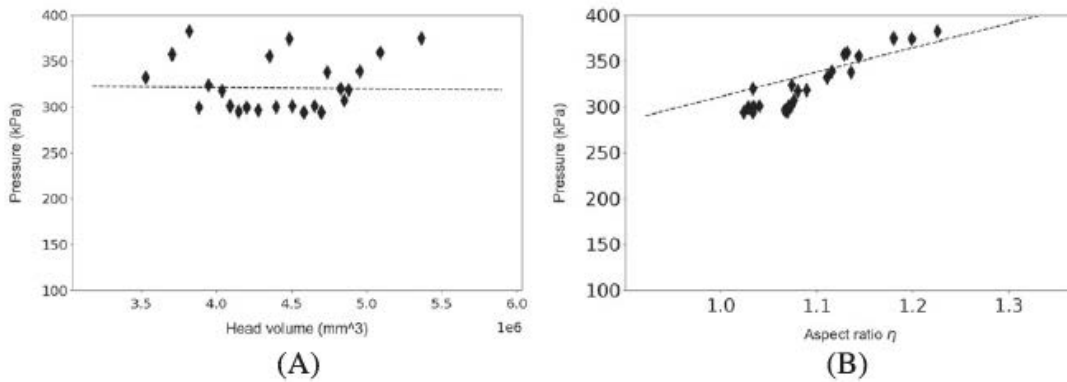


Figure 3. Peak pressure versus (a) head volume and (b) a measure of head width to depth. Black diamonds are simulation results and the dashed line is a least square fit of the data.

Title: Geometric, Constitutive, and Loading Complexities in Structural Materials

Author(s): S.A. Wimmer,¹ R.N. Saunders,¹ A. Achuthan,² A. Arcari,³ J.R. Franke,¹ A.B. Geltmacher,¹ D.J. Hasler,⁴ D.J. Horton,¹ L.P. Kuna,¹ J.A. Mancias,¹ T.J. Martin,¹ and J.G. Michopoulos,¹

Affiliation(s): ¹Naval Research Laboratory, Washington, DC; ²Clarkson University, Potsdam, NY; ³Excet, Inc., Springfield, VA; ⁴Naval Operational Support Center, Green Bay, WI

CTA: CSM

Computer Resources: SGI ICE X [AFRL, OH]; SGI ICE X [ERDC, MS]

Research Objectives: The research objective is developing a rational basis and mathematical description of complex material responses for structural and novel evolving materials. Structural integrity and life cycle evaluations require an understanding of material responses. Analytical models and techniques cannot describe complex materials and often do not account for interactions, complex geometries, or multi-physics loading. Finite element methods are used to develop models involving multi-functional materials, novel evolving materials, and multi-physics. In order to accurately model the nonlinear response of conventional structural materials, rate dependence, large deformation, and damage accumulation mechanisms must be understood and accurately represented. The performance of the overall structure or system is also examined via parameters such as kinematics, geometric complexities, loading path dependencies, and interaction between loading types.

Methodology: The project uses finite element methods extensively. Nonlinear material constitutive response features are highlighted in much of the work. Implicit and explicit solution methods are used as appropriate. The primary finite element code used is ABAQUS. Coupled material responses, such as electric-thermal or electrical-mechanical-thermal are exercised for evaluation of these effects. Model development is done with CUBIT, ABAQUS/CAE, SimpleWare, or in-house software. Large run times and large model size are often required for the multi-step nonlinear finite element analysis jobs.

Results: This project involves work in several topical areas. Work has been performed on creating image-based microstructural models, modeling multi-layer ceramic structures, modeling stress corrosion cracking, and modeling biofoulants. Representative results for the Thermal Barrier Coatings topic are discussed here. Existing models of thermal barrier coatings are typically two-dimensional (2D). The porosity of the ceramic material affects the thermal conductivity and mechanical strength (modulus) of the coating. The ideal coating would have high through thickness thermal conductivity while maintaining high longitudinal and shear strength. A series of three-dimensional (3D) models were constructed of randomly placed pores, voids, and cracks for a range of porosities. Figure 1 shows contour plots of von Mises stresses and Fig. 2 shows contour plots of heat flux. These plots show different defect interactions, such as chaining, even though the porosity is similar. Effective moduli and effective thermal conductivity versus porosity is shown in Fig. 3 to highlight the fact that effective properties from 2D models are always lower than 3D models, yet the peak von Mises stress and peak heat flux around defects is higher with more defect interactions. ABAQUS/Standard was used for the stress analysis and can require 36 cores for one to two days for the 3D models.

DoD Impact/Significance: Thermal barrier coatings are vital for metallic parts, such as turbine blades. Improving the thermal conductivity of a coating increases operational temperatures of the turbine, saving fuel and increasing the component lifetime. Improvement to thermal conductivity must not diminish mechanical properties of the ceramic. Large 3D models are being developed for characterization and computational analysis of these ceramic microstructures for accurate prediction and optimization of material properties.

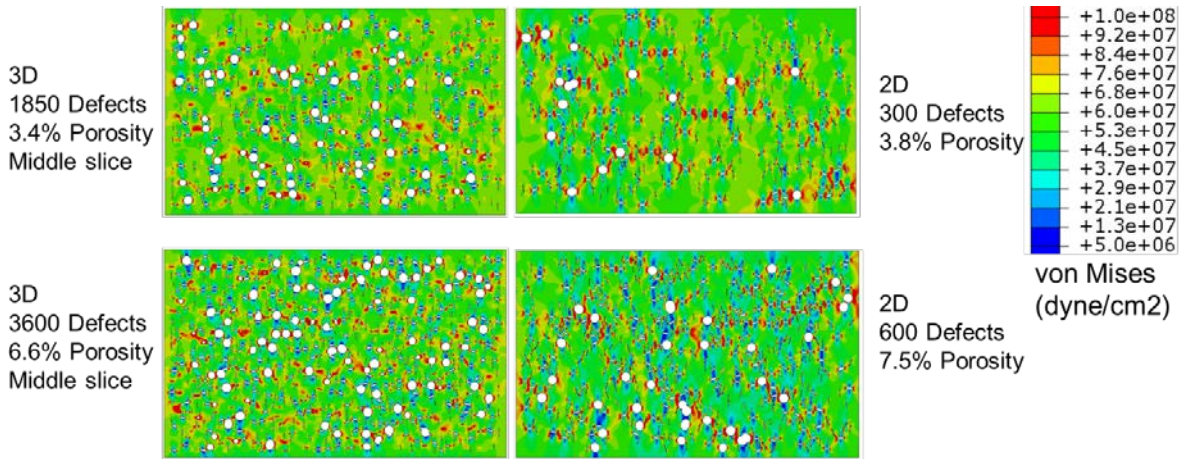


Figure 1. Contour plots of von Mises stress (dyne/cm²) for through thickness displacement for 2D and 3D models with various amounts of porosity due to randomly distributed defects.

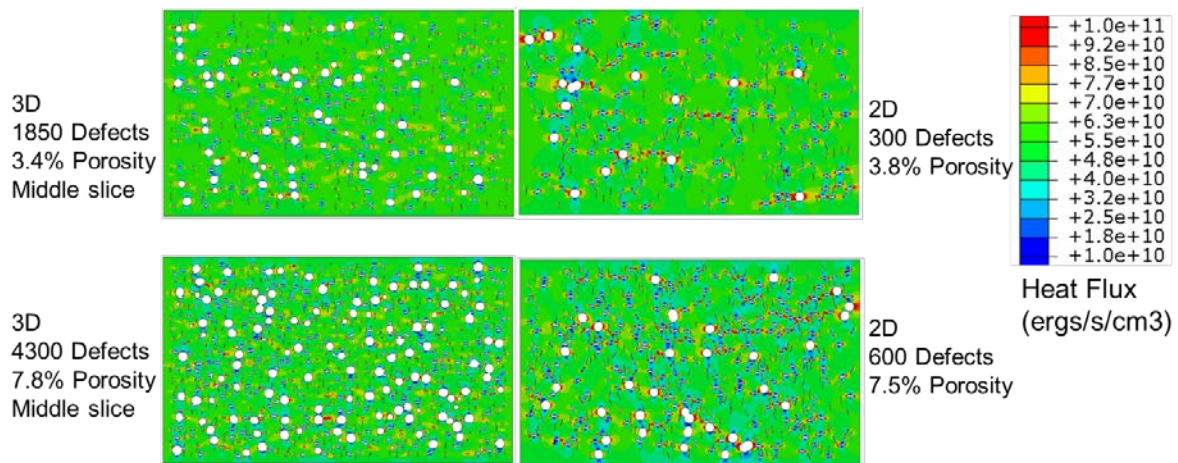


Figure 2. Contour plots of heat flux (ergs/s/cm³) for through thickness thermal loading for 2D and 3D models with various amounts of porosity due to randomly distributed defects.

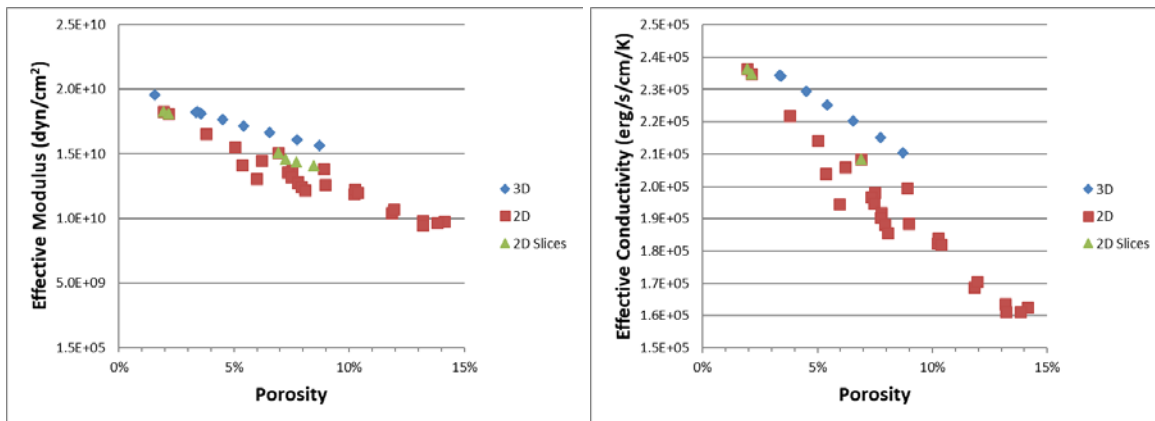


Figure 3. Effective Modulus and Effective Conductivity versus porosity for through thickness loading for a variety of 2D and 3D geometries with randomly distributed defects.

THIS PAGE INTENTIONALLY LEFT BLANK

CFD

Computational Fluid Dynamics

CFD covers high performance computations whose goal is the accurate numerical solution of the equations describing fluid motion and the related use of digital computers in fluid dynamics research. CFD is used for basic studies of fluid dynamics for engineering design of complex flow configurations and for predicting the interactions of chemistry with fluid flow for combustion and propulsion. It is also used to interpret and analyze experimental data and to extrapolate into regimes that are inaccessible or too costly to study. Work in the CFD CTA encompasses all Reynolds number flow regimes and scales of interest to the DoD. Incompressible flows are generally slow (e.g., governing the dynamics of submarines, slow airplanes, pipe flows, and air circulation) while compressible flows are important at higher speeds (e.g., controlling the behavior of transonic and supersonic planes, missiles, and projectiles). Fluid dynamics itself involves some very complex physics, such as boundary layer flows, transition to turbulence, and turbulence dynamics that require continued scientific research. CFD also must incorporate complex additional physics to deal with many real world problems. These effects include additional force fields, coupling to surface atomic physics and microphysics, changes of phase, changes of chemical composition, and interactions among multiple phases in heterogeneous flows. Examples of these physical complexities include Direct Simulation Monte Carlo and plasma simulation for atmospheric re-entry, microelectromechanical systems (MEMS), materials processing, and magnetohydrodynamics (MHD) for advanced power systems and weapons effects. CFD has no restrictions on the geometry and includes motion and deformation of solid boundaries defining the flow.

Title: The Impact of Foam and Aerosol Dynamics on Fire, Explosion Safety, and Suppression (Mechanisms of Water Mist Suppression of a Burning Solid Surface)

Author(s): X. Zhuang¹ and R. Ananth²

Affiliation(s): ¹ASEE Postdoctoral Fellow, Naval Research Laboratory, Washington, DC; ²Naval Research Laboratory, Washington DC

CTA: CFD

Computer Resources: SGI ICE X, Cray XC30 [AFRL, OH]

Research Objectives: The objective of this work is to develop a computational models to study the interfacial properties of the surfactant monolayers at fuel/water and air/water interfaces and their interactions with heptane and gasoline fuels.

Methodology: Develop molecular dynamics (MD) models using CHARMM36 with TIP3P force fields for surfactants studied in the literature. Simulate fuel/surfactant-monolayer/water interface with constant molecule number, pressure, and temperature (NPT) ensemble and the air/surfactant-monolayer/water interface with constant molecule number, volume, and temperature (NVT) ensemble. Use NAMD for the MD simulations, and VMD, CHARMM, and Python for the trajectory analyses and properties calculations. Validate the models/force fields with experimental data available in the literature. Using the validated models, investigate the effects of changes to surfactant's tail and head structures on the interfacial properties relating to lamella stability and fuel/surfactant packing at the interface.

Results: We simulated SDS, CTAB, PFOA, and Silwet L77 surfactants at air/water and heptane/water interfaces. The MD simulations using CHARMM36 force field show quantitative agreement with experimental data for the interface-area per surfactant molecule, surface tension, and Gibbs elasticity. We developed a method to predict the most probable interface-area per surfactant molecule based on maximum in Gibbs elasticity. We also show quantitative agreement between the predictions and experiments for surface tension as a function of surfactant concentration as shown in Fig. 1. We are using the validated models to simulate an alkyl-glucoside and polyethoxy-trisiloxane surfactants at air/water interface and predicting the effect of varying the tail length (alkyl or trisiloxane) and head group size (glucoside or polyethoxy-) on the interface area, surface tension, and Gibbs elasticity.

Significance: Computational models of the lamella interfaces in the aqueous foam will be used to develop understanding of the dependence of lamella properties on the surfactant's molecular structure. This will provide structural features of potential surfactants for synthesis and experimental investigations and facilitate the development of the new effective firefighting aqueous foams.

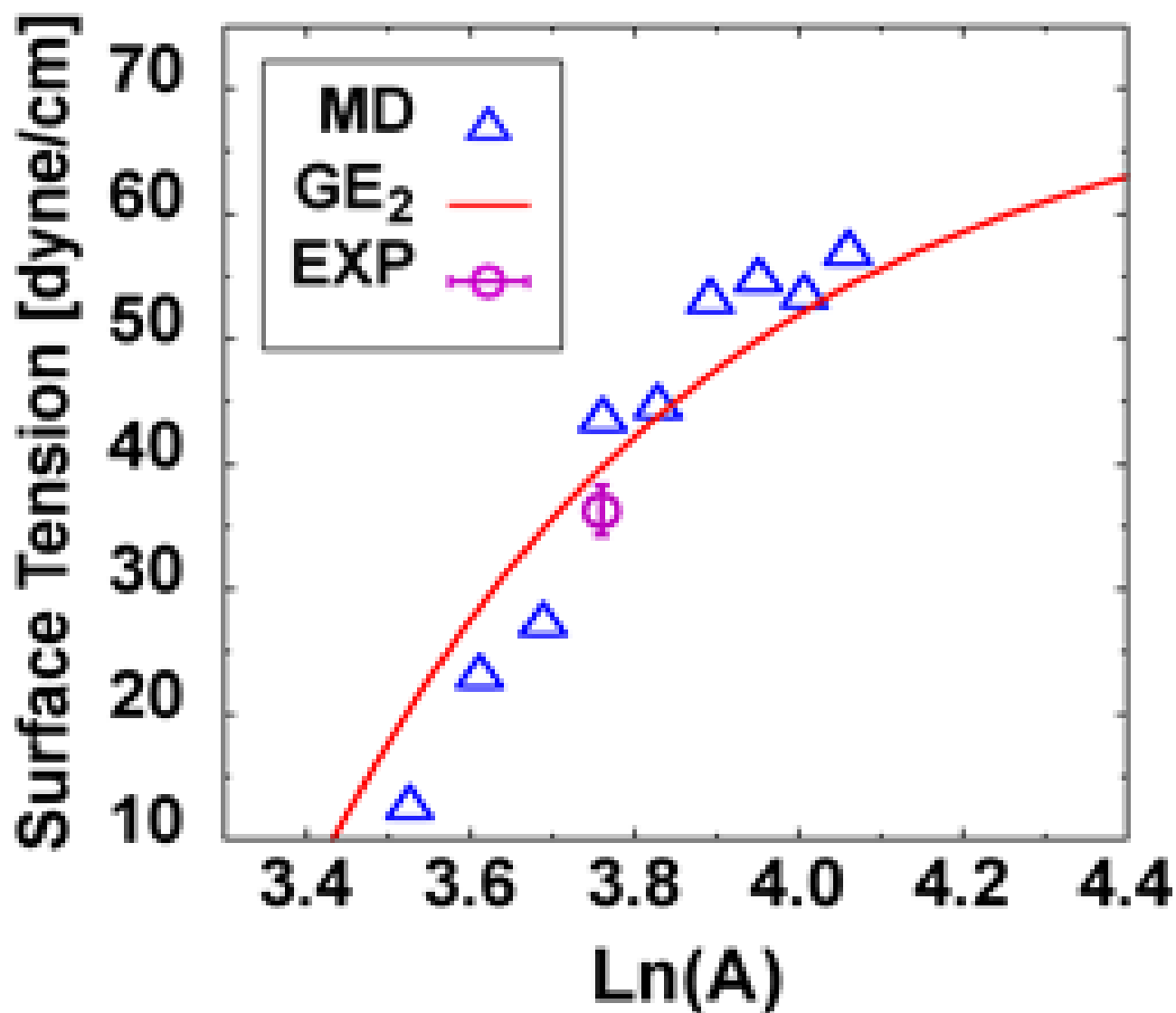


Figure 1. Comparison of the MD predicted surface tension for perfluorooctanoic acid (PFOA) with the experimental data as a function of interface area per molecule, A . The experimental data include direct measurements of the A and γ (EXP), and the values of A derived from experimental measurements of γ as a function of surfactant concentration in solution using Gibbs equation.

Title: Direct Numerical Simulation of Fluid-Sediment Wave Bottom Boundary Layer
Author(s): A.P. Levenson, S.P. Bateman, J.A. Simeonov, and J. Calantoni
Affiliation(s): Naval Research Laboratory, Stennis Space Center, MS
CTA: CFD

Computer Resources: Cray XE6m, XC40/50 [ERDC, MS]; Cray XC40 [ARL, MD]

Research Objectives: Predictive models for nearshore bathymetric evolution require a complete understanding of the physics of fluid-sediment interactions in the wave bottom boundary layer (WBBL). We performed coupled fluid sediment numerical simulations to increase our understanding of the sediment and hydrodynamics in the WBBL. Fundamental concepts used in describing the phenomena of sediment transport such as mixture viscosity and diffusivity, hindered settling, reference concentration, bed failure criterion, and the concept of acceleration-induced transport are addressed with our models. The models produce high-resolution results necessary to gain insight into the small-scale boundary layer (BL) processes and clarify new directions for measurement techniques needed to improve predictive capabilities.

Methodology: We develop and use a suite of discrete and continuum WBBL models for simulating sediment transport in the nearshore environment from the microscale (cm-m) to the mesoscale (km). At the microscale (<10 cm), the three-dimensional sediment phase is simulated with discrete element method that allows individual grains to be uniquely specified. The fluid phase model varies in complexity from a simple one-dimensional eddy viscosity to a fully three-dimensional direct numerical simulation. Coupling between the fluid and sediment phases varies from one-way coupling to a system fully coupled at every fluid time step. Between the micro- and mesoscale (1-50 m), a spectral sea floor model simulates sea floor roughness dependent on changing wave conditions. At the mesoscale (1-10 km): (1) a model simulates high-resolution three-dimensional flow over the inner continental shelf in domains $O(4 \times 10^4 \text{ m}^2)$, and (2) nearshore hydro- and morphodynamics are simulated with the coupled wave-circulation morphology model, Delft3D.

Results: Ensembles of 2D hydro- and morphodynamic nearshore simulations (Delft3D) were run in order to assess the uncertainty in wave, current, and bed elevation change predictions. Delft3D includes a system of coupled models (wave, circulation, and morphology) to simulate the hydrodynamic flow and resulting bathymetric change within a model domain. Thirty-two ensemble simulations were set up at Duck, NC (Fig. 1) with three parameters varying over given input ranges and the results were compared to field observations. The 50% and 90% uncertainties of the predicted current magnitude and bed elevation change were calculated (Fig. 2). The current observations fell within the model uncertainty bands for only a portion of the simulation, suggesting that more input parameters need to be investigated. The model uncertainty of bed elevation change increases with time and is within a range of 7 cm at its maximum.

DoD Impact/Significance: All process-based models for nearshore bathymetric evolution are limited by shortcomings in fundamental knowledge of multiphase BL physics. The microscale simulations provide an unprecedented level of detail for the study of fluid-sediment interactions that is impossible to obtain experimentally. These results improve parameterizations of small-scale processes in larger-scale models. At the mesoscale, our models are highly efficient and well suited for coupling to regional operational hydrodynamic models in order to include the effects of an evolving sea floor. This work directly supports NRL base programs: “Forecasting bathymetric evolution in shallow coastal regions: Linking operational prediction systems with remote sensing,” “Observation and modeling of bottom boundary layer turbulence in stratified shallow water,” “Modeling Wave Interactions with Arctic Ice Floes,” “Sensing, Observing, and Forecasting High Frequency Resuspension Events in Coastal Proximity (SOFREX),” and “Using remote sensing and numerical models to quantify the role of rip currents in circulation and the resulting sediment transport.”

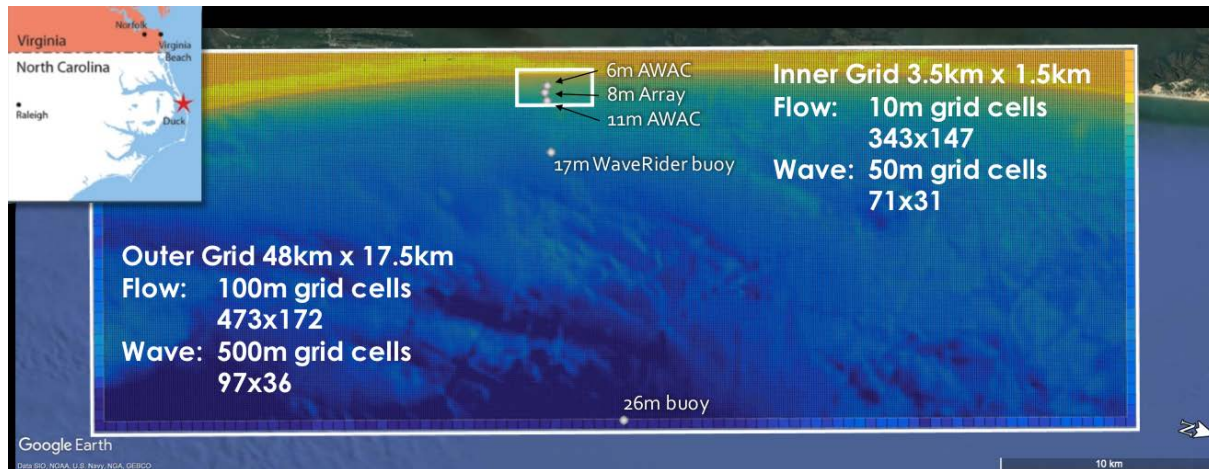


Figure 1. Plot of the model domains for the Delft3D simulations imposed on a Google Earth image of the region surrounding Duck, NC. The outer and inner grids are outlined in white. The color contour denotes the bathymetry.

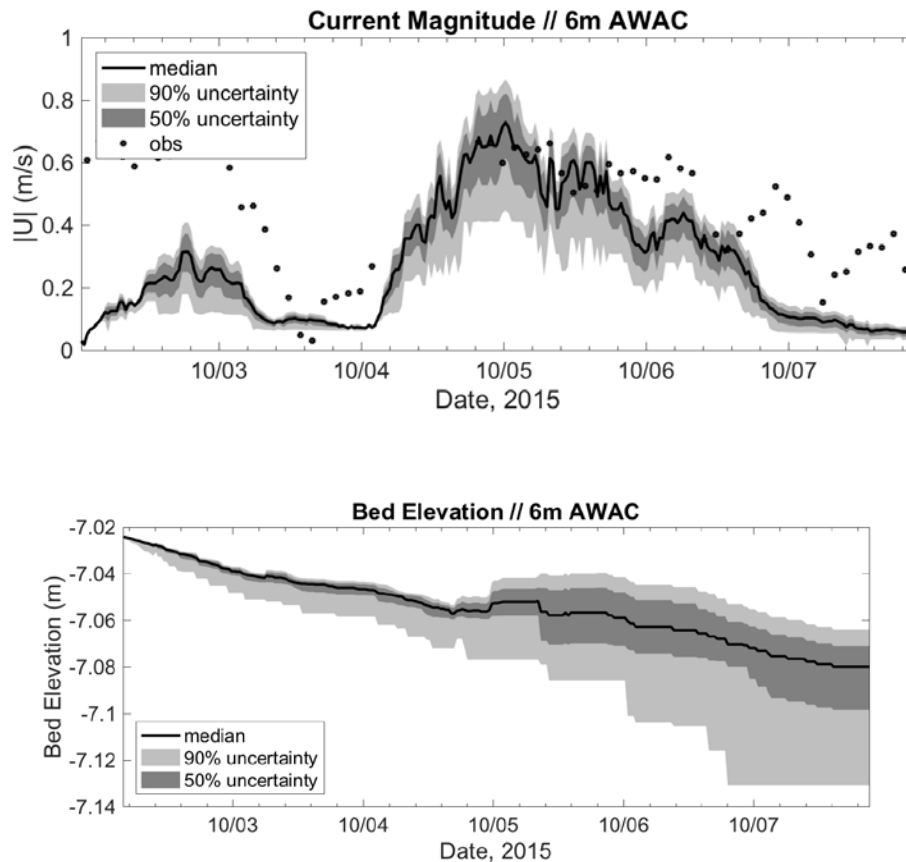


Figure 2. Plots include model predictions from 32 Delft3D simulations and observations in 6m water depth offshore of Duck, NC. Plotted are the modeled uncertainty (gray patches) and observed (dots) (a) current magnitude and (b) bed elevation change over a six-day period. The 90% and 50% uncertainties of the 32 simulations are denoted by light and dark gray bands, respectively. The median (black line) is also shown.

Title: Numerical Simulations of Turbulence Impact on Optical Signal Transmission and Near-Surface Turbulence

Author(s): S. Matt and W. Hou

Affiliation(s): Naval Research Laboratory, Stennis Space Center, MS

CTA: CFD

Computer Resources: Cray XC40 [ARL, MD]

Research Objectives: The objective of this project is to continue computational fluid dynamics (CFD) characterizations of numerical tanks emulating convective turbulence at the Simulated Turbulence and Turbidity Environment (SiTTE) and laminar to turbulent transition in the new flow tank flowSiTTE. The project also tests parameterizations of Langmuir turbulence by simulating laboratory-scale Langmuir circulation with and without the addition of the Craik-Leibovich vortex force, and emulates laboratory experiments at the University of Miami SUSTAIN facility, as well as coastal field experiments (CASPER-EAST). Combined with the accompanying laboratory and field results, the numerical simulations support work on a new underwater imager, novel methodologies and mechanisms for active boundary layer control, as well as insight into the dynamics and processes underlying near-surface turbulence, including Langmuir turbulence and boundary layer processes.

Methodology: To accurately reproduce the turbulence dynamics, the representation of these numerical tanks is accomplished by using a realistic domain size and resolving the flow down to the relevant scales: the Kolmogorov microscale for SiTTE, the scale of Tollmien-Schlichting (TS) waves for the flow tank, and the scale of Langmuir-type surface streaks for SUSTAIN. For the comparison to field experiments, the domain size and associated scales need to be increased considerably. The numerical experiments build on our previous work based on large-eddy simulation (LES) models using the open-source CFD code OpenFOAM, including custom developments to simulate Langmuir turbulence through the addition of the Craik-Leibovich vortex force.

Results: Following the success at SiTTE of using CFD together with laboratory experiments to characterize a controlled laboratory environment, this combined approach is employed to describe the new laminar to turbulent flow tank flowSiTTE (Fig. 1). A LES model is used to explore the parameter space and transition to turbulence in a numerical representation of the flow tank (Figs. 2, 3). For the study of Langmuir turbulence, a multi-phase LES model was implemented to test the performance of the Craik-Leibovich parameterization. In addition to the multi-phase modeling approach, a rigid-lid LES model with added Craik-Leibovich vortex force was developed for the study of coastal Langmuir circulation.

DoD Impact/Significance: Results from the model of near-surface turbulent coherent structures significantly advance our understanding of the dynamics of Langmuir turbulence and its parameterization in large-scale ocean models. CFD simulations of the numerical tanks continue to be critical for the implementation of the SiTTE laboratory, the convective turbulence tank to study and mitigate underwater optical turbulence impacts, as well as the new laminar to turbulent flow tank supporting the development of a novel methodology for active boundary layer control and associated drag reduction. This benefits research on optical communication, lidar sensing of turbulence, new fiber-optics sensor development (temperature, flow), near-surface turbulent flows, including air-sea interface, and boundary layer processes.

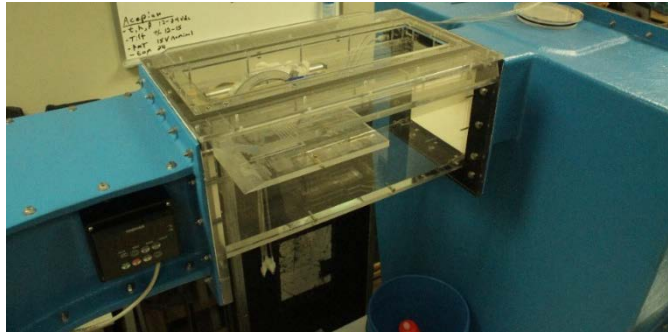


Figure 1. The laminar to turbulent flow tank “flowSiTTE” manufactured by Engineering Laboratory Design, Inc. (Eldinc). This tank is used to study laminar to turbulent transition and the development of TS waves in the transitional boundary layer, as well as active boundary layer control.

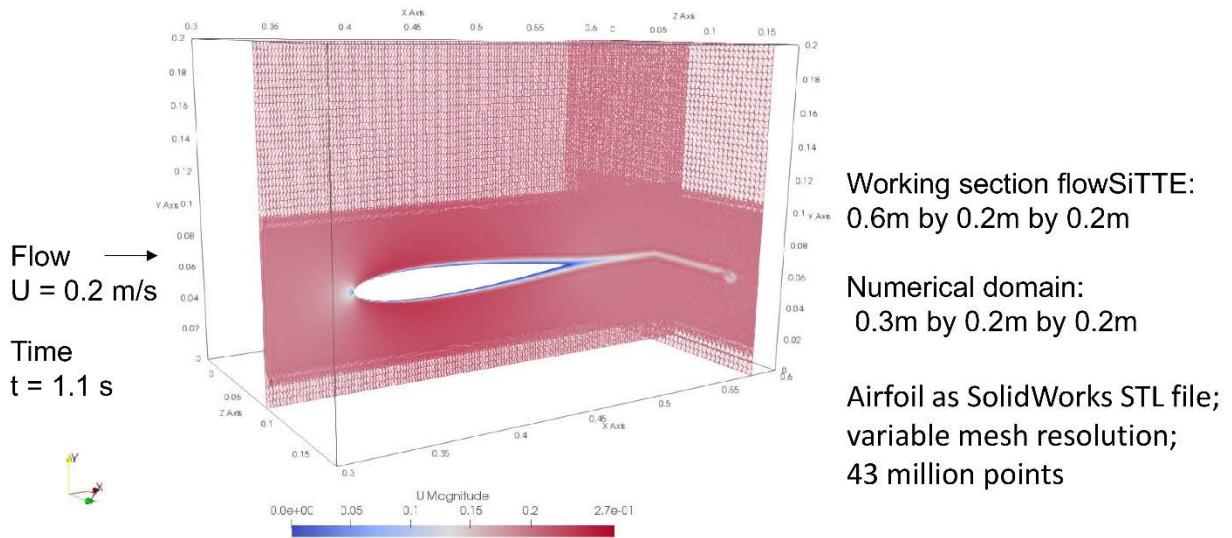


Figure 2. Model geometry and mesh (for centerline and a cross-section) for OpenFOAM model using pimpleFoam solver and snappyHexMesh to mesh around a Solidworks airfoil with a 6in cord. Color scale is in m/s and shows velocity magnitude.

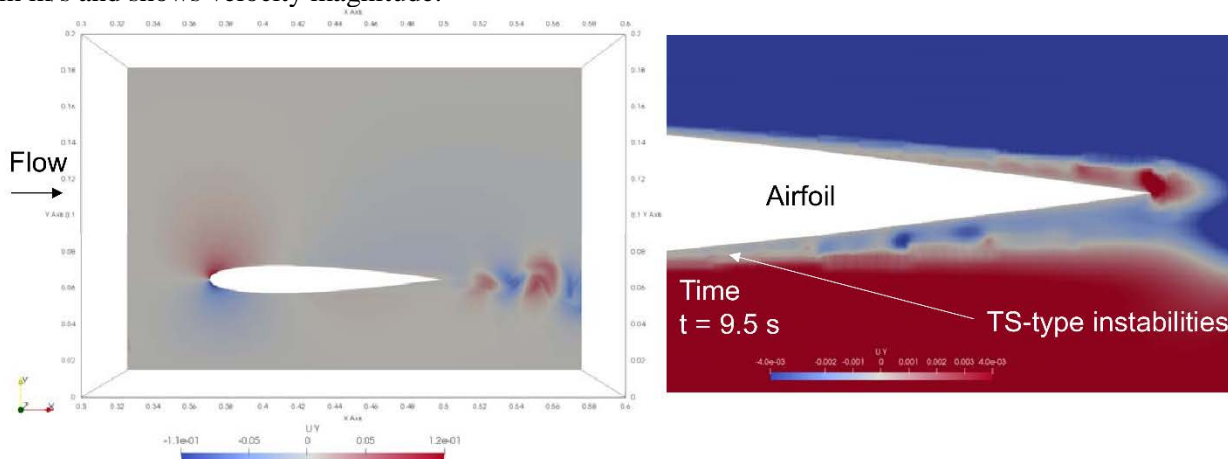


Figure 3. Along-channel velocity from CFD OpenFOAM model for flowSiTTE show boundary layer instabilities develop over the airfoil consistent with TS waves. Color scale is in m/s and shows along-tank velocity.

Title: Numerical Investigation of Advanced Military Aircraft Noise Reduction Concepts

Author(s): J. Liu, A. Corrigan, R.F. Johnson, and R. Ramamurti

Affiliation(s): Naval Research Laboratory, Washington, DC

CTA: CFD

Computer Resources: SGI ICE X [AFRL, OH]; SGI ICE X [ERDC, MS]; Cray XC40 [ARL, MD]; Cray XC40/50 [ERDC, MS]

Research Objectives: Use HPC computational resources to predict details of turbulent flow structures and noise generation in supersonic exhaust jets from representative military aircraft jet engine nozzles and to use this information to investigate and assess promising jet noise reduction concepts in support of the ongoing testing program.

Methodology: The flow solver is JENRE, a Navy-based and NRL-developed nodal finite-element code. JENRE can take structured meshes and unstructured meshes with arbitrary cell types and has multiple levels of parallelism: Multi-core CPUs or Multi-core GPUs, and MPI for inter-processor communication. JENRE has achieved an exceptional computational performance and scalability. Since using large-eddy simulations (LES) to fully resolve wall-bounded flows at high Reynolds numbers is computationally prohibitive due to the limitations of the available numerical methods and computational resources, the wall-layer model approach is used to simulate the boundary-layer effect of the wall-bounded flows. The far-field noise prediction tool, which uses the Ffowcs Williams & Hawkings (FW-H) surface integral method, has also been implemented in JENRE. To simulate the high-temperature effect observed in realistic jet engine exhausts, a temperature dependent function of the specific heat ratio is developed and implemented in JENRE.

Results: LES has become an important tool to enhance the understanding of the jet noise generation mechanism and assist the jet noise reduction effort. We have used LES to examine the flow field and jet noise generation of supersonic jets emanating from laboratory-scale simplified nozzle configurations. To move toward more realistic jet engine exhaust conditions, it is important to include nozzle geometries that mimic those used in the Navy relevant applications, for example, the F400 series nozzle used in the F404-GE-F400 engine which powers the F/A-18 aircraft. Figure 1(a) shows a model-scale nozzle developed by General Electric Aircraft Engines to mimic their F404 nozzle. This nozzle is a faceted biconic convergent and divergent nozzle made of twelve flaps. Figure 1(b) shows the inner surface contours of the nozzle without seals. NASA Glenn has obtained extensive flow-field and noise data at several nozzle design conditions over a broad range of nozzle pressure ratios using model-scale F404 series nozzle. This is very useful to the LES effort that extends to more realistic nozzle geometries and jet operating conditions. However, it is difficult to measure the nozzle internal turbulent flows, such as those associated with the nozzle turbulent boundary layer and extra internal flow features, for example, a bypass cooling flow is used in NASA's experiments. The effect of the nozzle internal flow conditions is often not clear and can add uncertainties to the numerical predictions. We have examined the effect of the nozzle boundary layer and a bypass cooling flow on the flow field and noise at overexpanded conditions, as shown in Fig. 2. Figures 3 and 4 show that the nozzle internal flow conditions affect both the downstream shock-cell structure and the far-field noise.

DoD Impact/Significance: There is a growing need to significantly reduce the noise generated by high performance, supersonic military aircraft. The noise generated during takeoff and landing on aircraft carriers has direct impact on shipboard health and safety issues. It is estimated that the US Veterans Administration pays \$4.2B or more for hearing disability claims each year. The results of our work will provide better understanding of the noise production for both industrial and military aircraft, and will aid the current effort of noise reduction, especially for supersonic aircraft.



Figure 1. Nozzle geometry: (a) F-400 series model puzzle geometry. (b) Nozzle inner surface contours.

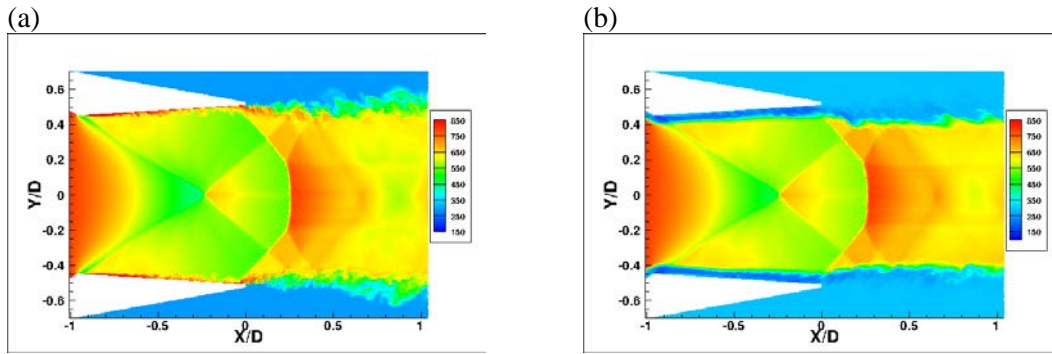


Figure 2. Instantaneous temperature distributions inside and around the nozzle. (a) Simulation that includes a small roughness on the divergent nozzle surface. (b) Simulation includes a bypass cooling flow.

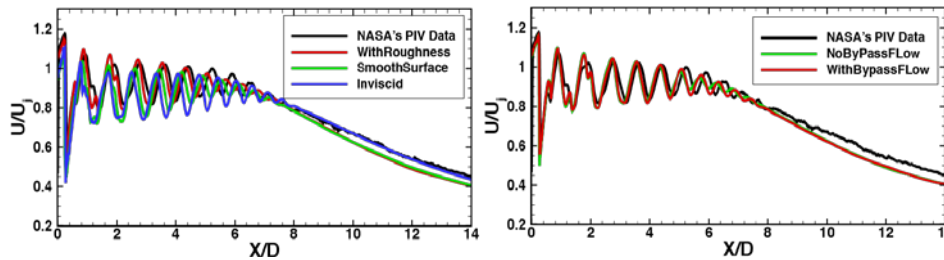


Figure 3. Impact of the nozzle internal flow conditions on the downstream shock-cell structure.

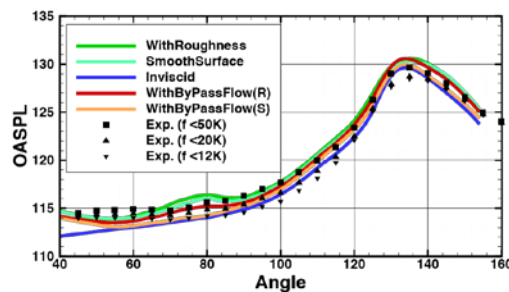


Figure 4. Impact of the nozzle internal flow conditions on the far-field overall sound pressure levels (OASPL). “f” stands for frequency, “(R)” stands for roughness added to the nozzle surface, and “(S)” stands for smooth nozzle surface.

Title: Deflagration-to-Detonation Transition in Terrestrial Systems and Type Ia Supernovae

Author(s): V.N. Gamezo¹ and A.Y. Poludnenko²

Affiliation(s): ¹ Naval Research Laboratory, Washington, DC; ² Texas A&M University, College Station, TX

CTA: CFD

Computer Resources: SGI ICE X [AFRL, OH]; SGI ICE X [ERDC, MS]; Cray XC30 [AFRL, OH]; Cray XE6m [ERDC, MS]

Research Objectives: Model, understand, and predict complex reactive-flow phenomena leading to the detonation initiation, including the deflagration-to-detonation transition (DDT).

Methodology: To study the ability of high-speed turbulent flames to generate shocks and detonations, we compute the interaction of a fully resolved premixed flame with a highly subsonic, statistically steady, homogeneous, isotropic turbulence. Turbulence-flame interactions are modeled using compressible reactive-flow equations solved on a uniform mesh using a fully unsplit corner transport upwind scheme with the Pulse-position Modulation (PPM) spatial reconstruction and the Harten-Lax vanLeer-Contact (HLLC) Riemann solver implemented in the code Athena-RFX. Turbulence is driven using a spectral method, which introduces in the flow divergence-free velocity fluctuations with a prescribed energy injection spectrum and rate. We consider chemical burning in H₂-air and CH₄-air mixtures, and thermonuclear burning of C¹² and O¹⁶ in relativistic, degenerate plasma typical of stellar interiors during Type Ia supernova explosions. The chemical burning is described by one-step Arrhenius or detailed reaction kinetics models. The thermonuclear burning is implemented using an α -chain network.

Results: The simulations show that the interaction of highly subsonic chemical or thermonuclear flames with a highly subsonic turbulence can produce strong shocks and detonations. Rapid runaway process resulting in pressure build-up occurs once the flame speed exceeds the critical Chapman-Jouguet (CJ) deflagration threshold in agreement with the developed theory. The strength of the resulting shock depends on the ratio of densities of fuel and burning products. For chemical flames considered here this ratio is ~ 8 , and this allows for a significant shock amplification leading to a detonation. For thermonuclear flames in degenerate plasmas, the ratio of densities is in the range 1.2-2.0, and the resulting shocks are not strong enough to ignite the detonations directly. These shocks, however, can further amplify by interacting with surrounding turbulent flames on larger scales, and eventually produce a detonation. This universal mechanism for the turbulence-induced DDT allows a detonation to form while the flame remains in the flamelet regime, in which the turbulent flame brush can be viewed as a folded laminar flame sheet with the internal structure minimally affected by turbulence. This is in contrast with prior theoretical models which suggested that turbulence-driven DDT requires formation of distributed flames, and thus necessitates significantly higher turbulence intensities.

DoD Impact / Significance: Understanding the mechanisms of flame acceleration and DDT provides insights for further development of turbulent combustion models for large-eddy simulations of high-speed regimes. These models are important for the theory of Type Ia supernova explosions, and critical for the design of the next generation of propulsion and energy conversion systems, such as scramjet engines, rotating-detonation engines, high-pressure turbines, etc. They can also be used to predict effects of accidental gas explosions in industrial environments and help to mitigate these effects.

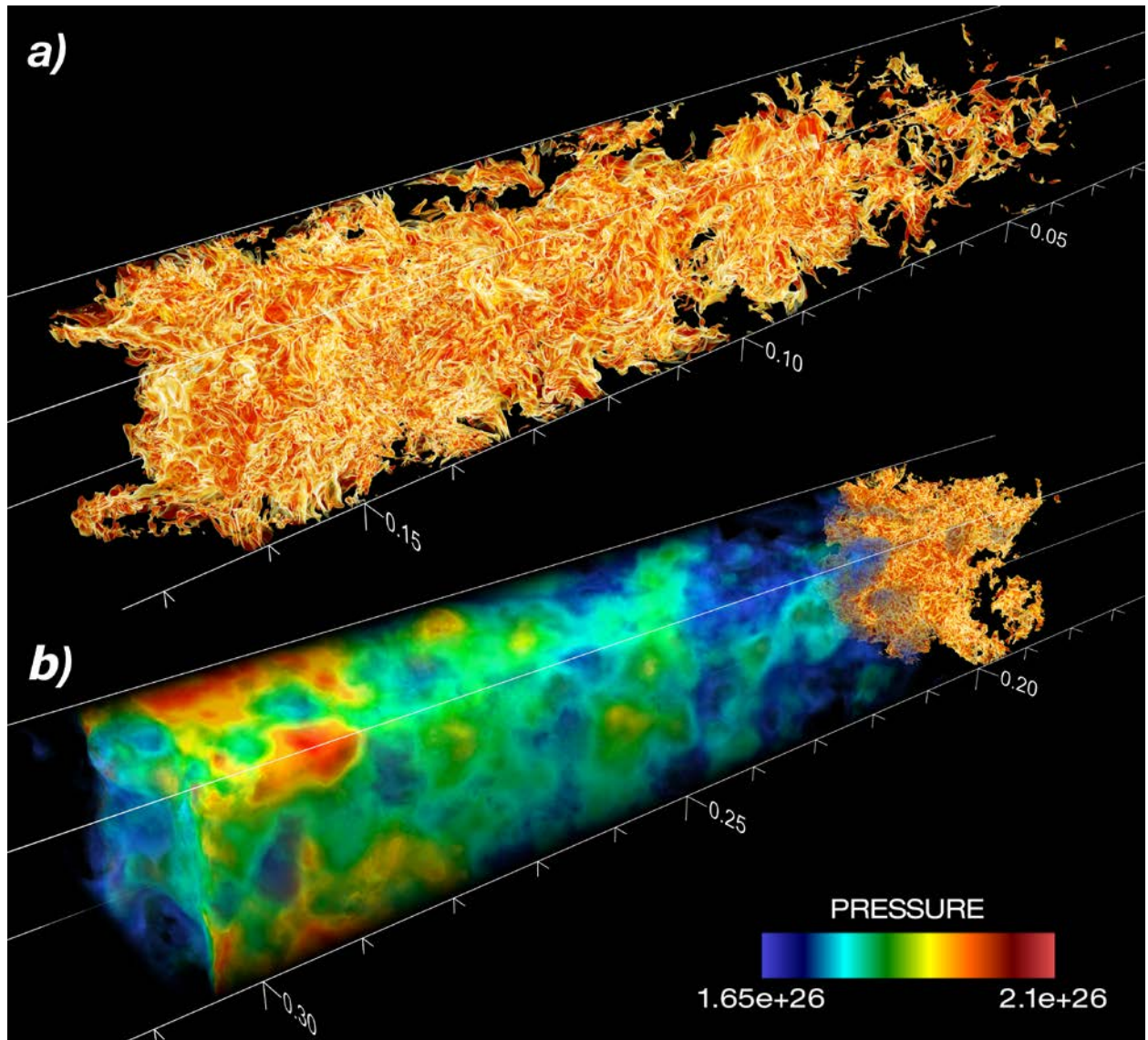


Figure 1. Turbulence-driven spontaneous shock formation in a turbulent thermonuclear flame. (a) Flame structure at the time when the turbulent burning velocity reaches its maximum. (b) Resulting flame-generated pressure field and the equilibrium structure of a turbulent flame at the end of the burn-out phase. The flame propagates to the left, and is shown as a semi-transparent light-emitting flame surface. Colors correspond to the light intensity, which increases from red to yellow to white. Pressure scale is in ergs/cm³. Length scales are in centimeters. The fuel is pure C¹² at the initial density 4×10^8 g/cm³.

Title: Predicting Fluid-Structure Interaction for Military Applications

Author(s): D.R. Mott and A.D. Kercher

Affiliation(s): Naval Research Laboratory, Washington, DC

CTA: CFD

Computer Resources: Cray XC30 [AFRL, OH]; SGI ICE X [ARL, MD]

Research Objectives: Create the computational capability to predict the interaction of fluids with flexible structures, including large, high-rate deformations due to blast loading, and convective and evaporative heat transfer and species transport at ambient atmospheric conditions. Use the new capability to design novel ventilated body armor and study other problems of defense relevance.

Methodology: The discontinuous Galerkin solver for incompressible flows, which is a part of the Hybrid Computational Cell (HYCC) infrastructure developed at NRL's Laboratories for Computational Physics and Fluid Dynamics, was used to simulate convection and diffusion of a target species within a flowing gas.

Results: Research this year included support of testing and development of vapor detection technologies. This testing required delivering a uniform concentration of target species to the inlet of a gas collector over an extended period of time, and the incompressible flow solver within the discontinuous Galerkin framework was used to develop a diffuser for this application. The diffuser feeds vapor into an expanding cone, and the collector being tested is placed downstream at the large end of the cone so that the gas bathes the collector's inlet with (ideally) a uniform target concentration. The diffuser resembles a capped 0.24-inch diameter cylinder with a collection of small holes staggered around the perimeter at different distances from the capped end. The gas mixture flows into the cylinder through the open bottom and is expelled through the collection of holes. The primary geometric parameters varied in the study are the number, cross-sectional area, and placement of these holes. The total area of the holes must be small enough for the jets' momentum to reach the walls of the enclosing cone and effectively sweep the entire volume, and the arrangement of holes must ensure that the entire area is engaged by the jets. A collection of simulations varying the geometric parameters was performed. The final two-dimensional (2D) diffuser consists of six holes through the sides of conical section and one hole through the cap. In three dimensions, the final design includes twelve holes through the conical section staggered at three distances from the cap. The total cross-sectional area of all the holes was equal to approximately 66% of the total cross-sectional area of the cylinder. Experiments confirmed that the design delivered a well-distributed mixture and quickly sweep the testing volume when concentrations and mixtures were changed between tests.

DoD Impact/Significance: Improved detection equipment for dangerous and illicit materials will make our warfighters safer and more effective. Designing complicated, multifunctional equipment for the warfighter is a difficult endeavor. Leveraging seemingly disparate applications (like body armor cooling and chemical detection) that share common underlying physics enables us to amplify the impact of our computational efforts. The overall computational capability that will arise from this effort will be applied to a range of Navy and Marine Corps applications as well as the larger DoD and defense communities.

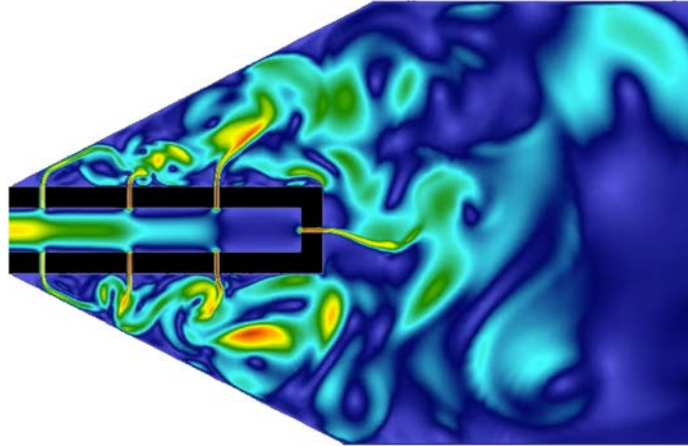


Figure 1. Instantaneous velocity magnitude in the xy-plane for a 2D diffuser design with a leading gap of 0.05. Flow from left to right.

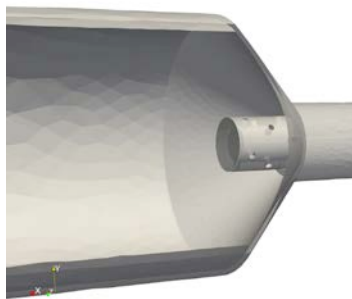


Figure 2. Three-dimensional (3D) diffuser geometry mounted inside the vapor cup. Flow from right to left.

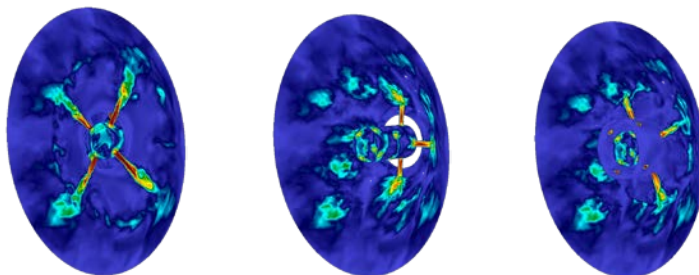


Figure 3. Velocity magnitude at planes aligned with the circumferential holes in the 3D diffuser geometry.

Title: Multidimensional Chemically Reacting Fluid Dynamics with Application to Flameless Combustors
Author(s): R.F. Johnson, A.D. Kercher, and D.A. Schwer
Affiliation: Naval Research Laboratory, Washington, DC
CTA: CFD

Computer Resources: Cray XC30 [AFRL, OH]; Cray XC40 [ARL, MD]; Cray XE6m [ERDC, MS]

Research Objectives: Use the HPC computational resources to simulate the computationally expensive chemically reacting fluid dynamics in various multidimensional configurations with the goal of better understanding various complex, multi-scale, combustion phenomena.

Methodology: The codes currently in use at The Laboratories for Computational Physics and Fluid Dynamics can accurately predict the flow field in many configurations. These codes employ high order methods, which are capable of simulating unsteady flows with strong shocks, chemical reactions, and other complex features. This work focuses on developments that are currently underway which will allow for the simulation of high speed and low speed reacting flows using state-of-the-art numerical methods. This year, we produced several important results as well as began to simulate experimental configurations for validation purposes.

Results: In the past two years, we dedicated research time to begin simulating a flameless combustor developed by the University of Cincinnati (UC). UC's combustion experiments were sensitive to invasive measurement techniques, so accurate computational fluid dynamics (CFD) results were seen as a way to assist in providing advanced diagnostics that UC's experiments would be incapable of measuring without perturbing the flow. The simulations could also guide modifications to experiments that would result in a more ideal flameless combustor.

The UC experimental configuration hosts complex three-dimensional physics and requires highly accurate simulations, which was made apparent with the shortcomings of the initial low-order CFD simulations. With the addition of advanced physics into the JENRE code, we have been able to produce initial simulations of the flameless combustor. Initial JENRE simulations modeled the entire experimental configuration with a simplified chemistry model for methane fuel at one of the UC's many experimental conditions. The simulations revealed areas that could help improve the effectiveness and efficiency of the combustor, such as exploiting unsteadiness with pulsating fuel injectors, changing fuel injectors to promote penetration, and configuration changes to dissuade pooling of fuels outside of recirculation zones. Figure 1 shows plane cuts of the flameless injectors at advancing points in time.

We also used advanced diagnostics techniques that require high performance computing. Figure 2 shows streamlines that were generated while simultaneously running the CFD to determine the trajectory of fuel in the recirculating combustor. These results will help reconfigure the flame injectors to better penetrate into the recirculation zone. One can see that not all the stream traces make it into the conical jet, which shows that better penetration can be achieved.

DoD Impact/Significance: Accurately predicting combustion has benefits to Navy engine technologies. The research in flameless combustion will yield a better grasp of a not well-understood phenomena that promises better combustion efficiency and lower heat signatures of Navy/DoD aircraft.

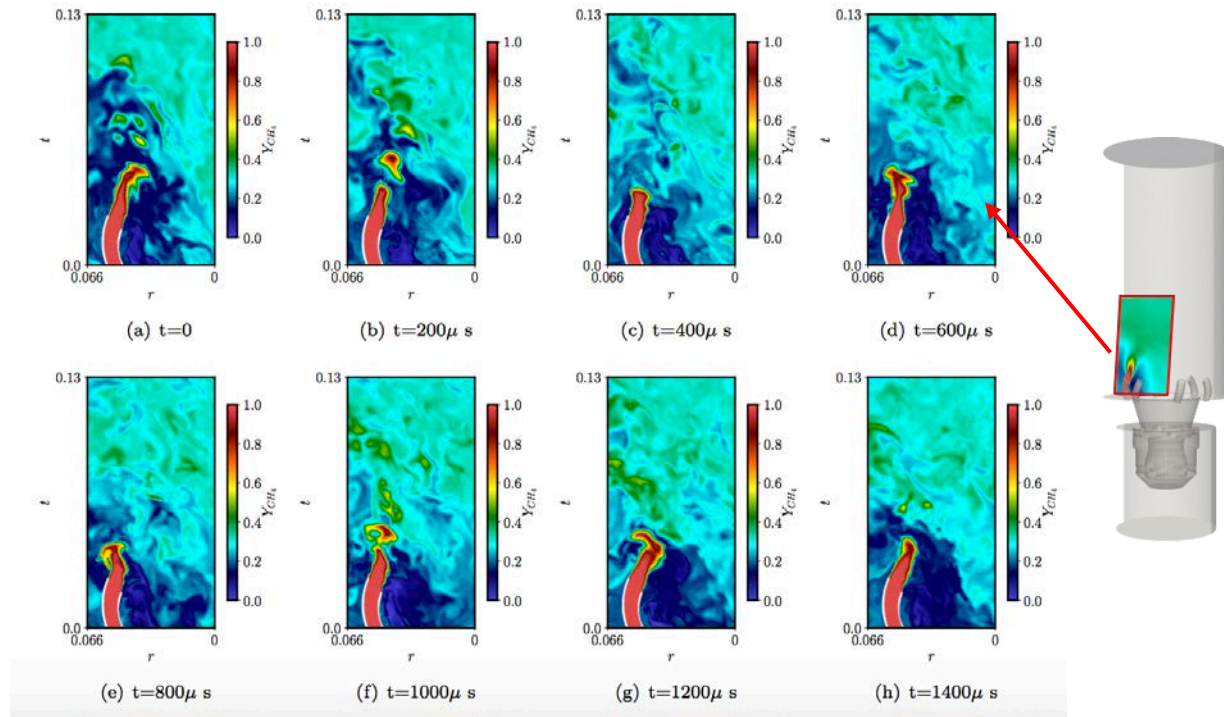


Figure 1. Time accurate results for one of the six methane injectors. Plane is sliced through the midpoint of the injector with directions radially, r , and at the angle of the injector, t .

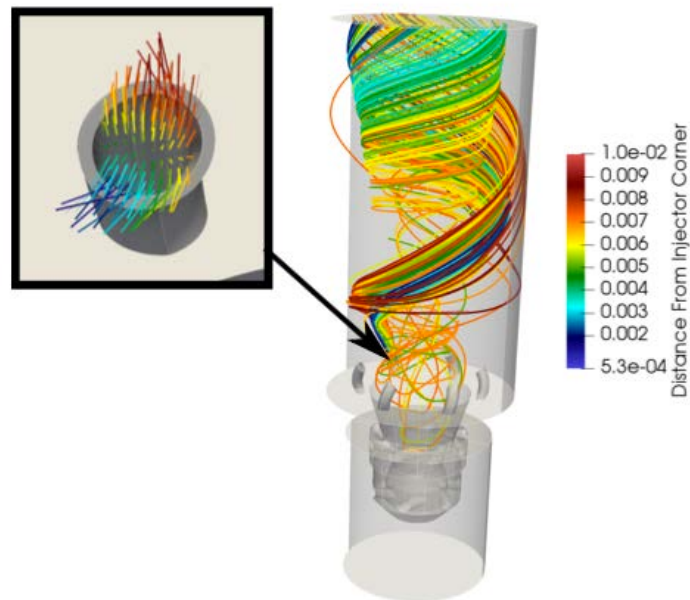


Figure 2. Stream traces of fuel injection.

Title: Optimization of the Spectral Dopant Concentration and Distribution in High Energy Density Deuterium Z-Pinch Plasmas as a Pulsed Neutron Source*

Author(s): Y.K. Chong

Affiliation(s): Naval Research Laboratory, Washington, DC

CTA: CFD

Computer Resources: Cray XC40 [ARL, MD]; Cray XC30 [NAVY, MS]; SGI ICE X [ERDC, MS]; Cray XC40/50 [ERDC, MS]

Research Objectives: The intense thermonuclear neutron sources such as deuterium Z-pinch plasmas produced from high power pulsed generators play an important role in the support of DoD missions such as the nuclear weapon effects study, hardness assessment analysis, and nuclear non-proliferation assays. The deuterium Z-pinch plasmas seeded with high Z spectral dopant materials offer an array of possibilities in inferring diagnostics and optimization of the pinch energetics and neutron emission characteristics toward meeting the machine operation criteria. Our objective is to investigate the effects of high Z spectral dopants on the physics and energetics of deuterium Z-pinch plasmas and to optimize their design and performance as a pulsed neutron source using a multiphase multidimensional radiation magnetohydrodynamics (RMHD) model.

Methodology: The multiphase multimaterial version of Machx+DDTCRE multidimensional RMHD code within the MPI framework will be employed in the study of the multimaterial Z-pinch plasma with spectral dopant load experiments on pulsed accelerators. The material interface tracking and interaction physics control needed for the multimaterial Z-pinch plasmas are possible through a PLIC volume of fraction model. An accurate treatment of the radiation transport and non-LTE ionization dynamics is handled using the multiphase version of the dynamical domain tabular collisional radiative equilibrium transport model. A dynamic transport domain radiation transport model that takes an advantage of the inherent compartmentalization nature of the physics will help toward an efficient parallelization of the codes using MPI. A detailed configuration non-LTE kinetics with a ray-based 3D integral radiation transport model will be applied to understand and analyze the spectral signature emanating from the dopant materials.

Results: The multiphase version of the Mach+DDTCRE model was employed to investigate the effects of spectral dopants on the implosion physics and dynamics of mixed material deuterium gas-puff Z-pinch loads on the ZR accelerator at the Sandia National Laboratories. Our simulation study indicates that the optimization of the thermal neutron yield of DD Z-pinch plasmas is predicated on the ability to understand and control their implosion physics and dynamics which are affected strongly by the multidimensional structure and nonuniform gradients formation and development due to the RT instabilities. In addition, there exists an appropriate choice of high Z dopant material and their distribution that can lead to the desired spectral diagnostics of the radiation emitted from them in an effective and non-intrusive method while at the same time yielding a control for directing the implosion toward an enhanced neutron emission.

DoD Impact/Significance: The optimization study of thermal neutron emissions from hot dense deuterium Z-pinch plasmas based on the understanding of the multidimensional structure and nonuniform gradients formation and RT instability development from on the RMHD simulations is an essential step toward their utilization as a choice tool for the DoD nuclear weapons effect and nonproliferation mission study. The spectral diagnostics of the dopant radiation is a valuable tool for understanding and controlling their implosion physics and dynamics toward their optimal design and performance as a pulsed neutron source.

*This work is supported by DOE/NNSA. Sandia is a multi-program laboratory operated by Sandia Corporation, a Lockheed Martin Company, for the US DOE's NNSA under contract DE-AC04-94AL85000.

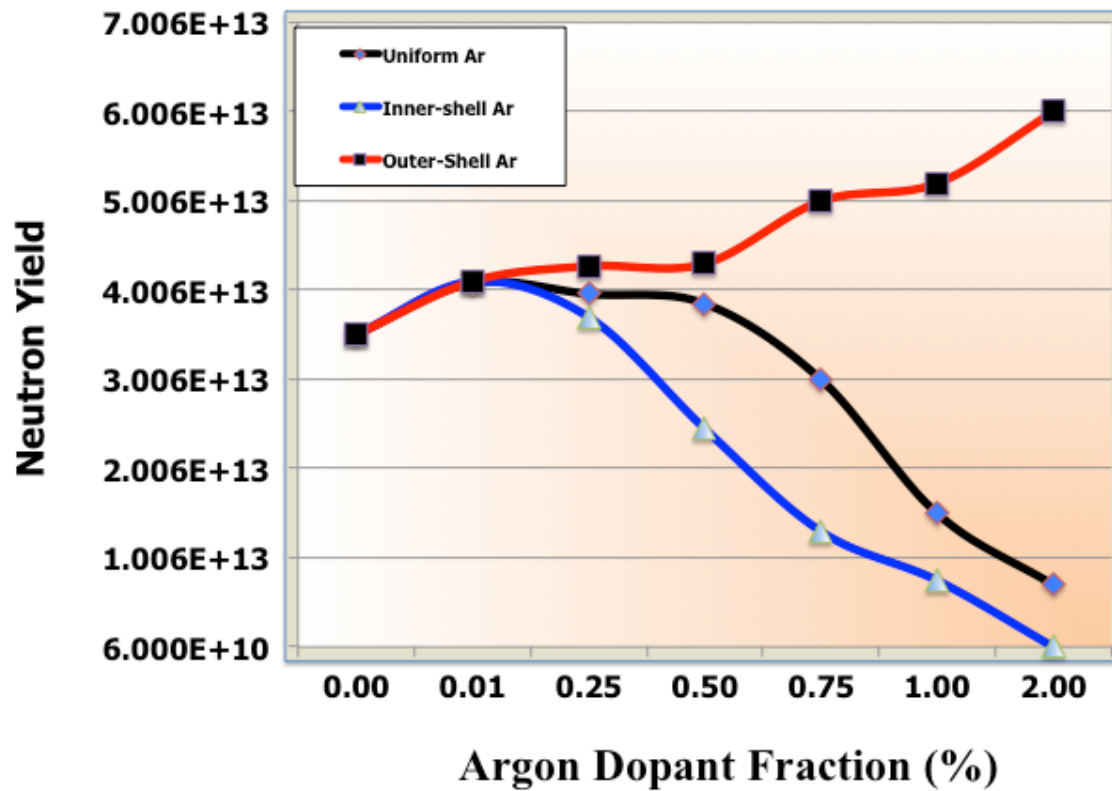


Figure 1. Two dimensional (2D) Mach2+DDTCRE RMHD prediction of total DD thermal neutron yield for Sandia 1234 D-on-D 8cm diameter nozzle as a function of varying argon dopant number fraction for three different dopant distribution profiles: a) uniform, b) inner-shell, and c) outer-shell. For both a) and b), the neutron yield peaks at 0.01% argon dopant while the dopant enhances the outer-shell pusher effect on the neutron emission.

Title: Hypersonic Reactive Flow Modeling
Author(s): G. Goodwin
Affiliation(s): Naval Research Laboratory, Washington, DC
CTA: CFD

Computer Resources: Cray XC30 [AFRL, OH]; SGI ICE X [ARL, MD]

Research Objectives: The objective of this research is to characterize the effect of a high-speed flowfield and unsteady/non-uniform boundary conditions on the ignition and combustion processes in hypersonic air-breathing engines. This research encompasses a broad range of system types, sizes, and scales, from smaller combustors used for analyzing the fine details of the underlying combustion physics to larger applied systems such as ramjets and scramjets in which quantification of combustor efficiency and reliability is a primary goal.

Methodology: One of the predominant challenges in using air-breathing engines for hypersonic flight (typically greater than five times the speed of sound) is that the extremely fast flow speeds through the engine present a challenging environment for reliable ignition of the fuel and stable combustion. The methodology for this research is to use high-fidelity computational fluid dynamics (CFD) to simulate the high-speed reactive flow in the combustors of air-breathing hypersonic vehicles. Boundary conditions, fuel chemistry, combustor geometry, and turbulence levels are varied to catalog the effects of these phenomena on achieving stable ignition and complete combustion. For the results described in this report, a steady, homogeneous mixture of stoichiometric ethylene and oxygen flows into a thin combustor (0.32 cm in height) at Mach 5.25. No-slip walls are used as the top and bottom surfaces and an outflow boundary condition is used at the right. This small combustor size was chosen such that the combustion physics could be simulated with high fidelity and observed in very fine detail.

Results: Due to the high velocity of the reactive mixture, boundary layers form on the walls very quickly. As temperature increases in the boundary layers, the mixture combusts and reacting boundary layers propagate toward the core of the domain. Rayleigh-Taylor (RT) fluid instabilities form as the low-density burned gas compresses the high-density unburned gas. The RT instability arises when the pressure and density gradients across a material interface (here, the interface is the flame) are misaligned. This misalignment in gradients results in the generation of vorticity at the flame and causes it to become turbulent and expand very rapidly. Temperature and pressure increase in the unburned gas as it is compressed by the expanding flame. Shockwaves formed by the hypersonic inflow impacting the boundary layers travel through the domain, further compressing the flame and unburned gas. Eventually, a strong shockwave collides with the turbulent flame and causes the flame to transition to a detonation, or a supersonic combustion wave. This occurs in several locations nearly simultaneously.

DoD Impact/Significance: The impact of this research is an increased fundamental understanding of the fine-scale ignition and combustion physics in hypersonic propulsion systems. Specifically, an inherent fluid instability that arises in hypersonic premixed flames of highly energetic mixtures causes the flames to become turbulent and generate an abundance of shocks. The flames then transition to detonation through shock-flame collisions. This process may be undesirable for some engines and the flow conditions that lead to it occurring can be avoided. In other cases, such as in detonation engines, this process of flame evolution and transition to detonation may be potentially harnessed for the generation of propulsive thrust.

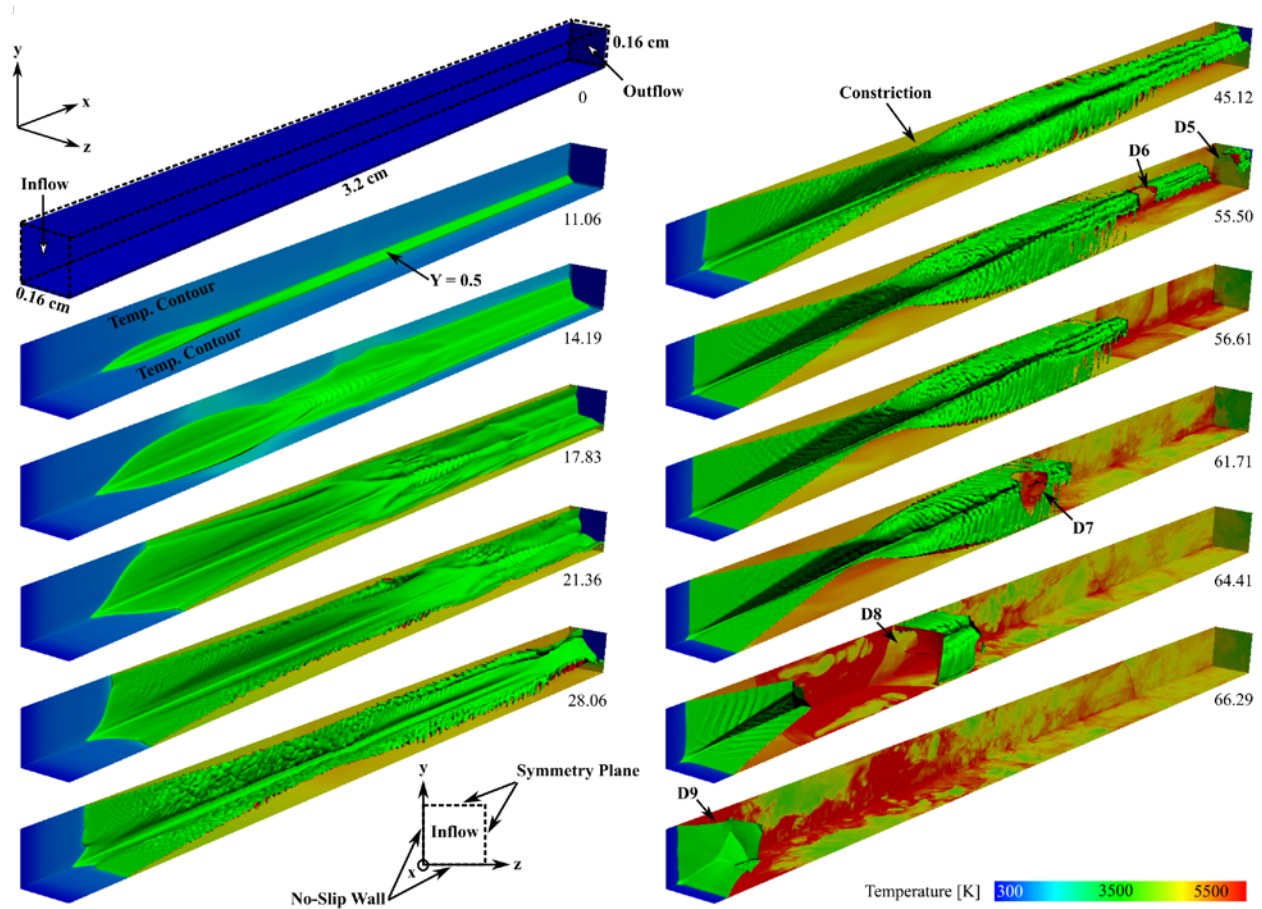


Figure 1. Three-dimensional simulation results for an inflow of stoichiometric ethylene-oxygen at Mach 5.25. Flame contour ($Y = 0.5$ isosurface) and temperature at the walls and outflow plotted as a function of time (time shown in milliseconds in frame corners). Several detonations (D5–D9) are labeled.

Title: Advanced Two Phase CFD Model
Author(s): T.D. Holman
Affiliation(s): Naval Research Laboratory, Washington DC
CTA: CFD

Computer Resources: Cray XC40 [ARL, MD]; Cray XC30 [AFRL, OH]; SGI ICE X [ARL, MD]

Research Objectives: Two-phase heat transfer devices are the state of the art in thermal system architecture, especially the loop heat pipe (LHP) architecture. Due to no moving parts these devices are ideal for use in space environments. Numerically simulating the internal flow of two-phase heat transfer devices will give a better understanding of their behavior in different environments that they are tested and operated in. The primary objectives is to verify physical oscillation mechanisms, design to minimize instability regions, and implement control methods to mitigate unavoidable instability regions through numerical modeling and experimental testing. These oscillations have been shown to precede/cause loop heat pipes to inadvertently shut down, a most undesirable occurrence which is not addressed by existing LHP theory. This inadvertent shut down is often referred to as a LHP failure.

Methodology: To achieve this goal, continued development of numerical and analytical models, continued experimental programs to confirm the accuracy of the analytic and numerical models, and utilizing these models to study and design LHP to mitigate the effects of oscillatory behavior. The end results are tools that will be utilized for design of LHPs for future space assets. The basic approach is: 1) utilize analytical model predicts of oscillations in closed loop two-phase heat transfer systems and experience to narrow down parameter space of mechanisms that cause oscillations. 2) mitigate unavoidable oscillations through closed-loop control. 3) utilize the analytical and numerical model to design proof of concept robust LHP. 4) test proof of concept robust LHP design. This is expected to be an iterative process.

Results: NRL numerical modeling was able to predict correctly 16 of 18 tests done on the NRL POC LHP with oscillations. Numerical simulation of the NRL high-power LHP allowed to link oscillations to partial evaporator dry-outs, which provided deeper understanding of the high-power LHP limitations already experienced during some space missions.

Experimental testing of a high-power LHP (with 13 kg and 45 kg of simulated payload) confirmed the numerical modeling, as shown in Fig. 1, and provided insights toward stabilizing LHP operation to prevent oscillations and partial dry-outs

Active thermal control of the liquid return line and/or LHP reservoir was experimentally and numerically demonstrated to dampen oscillatory behavior in the NRL POC LHP, as shown in Fig. 2. Further, a patent for a novel controlled condenser bypass that can prevent the oscillations has been submitted based on numerical modeling, as shown in Fig. 3. Testing of the bypass is currently being planned for the high-power LHP.

Seven papers have been published and all have been well received, two more have been written but have not yet been published. One patent has been submitted.

DoD Impact/Significance: A unique model has been created that can predict where oscillatory behavior in LHPs can occur and can predict the frequency/amplitude of the oscillations. The model is still being developed to add more features, but once complete this unique tool will allow NRL to design more robust LHPs.

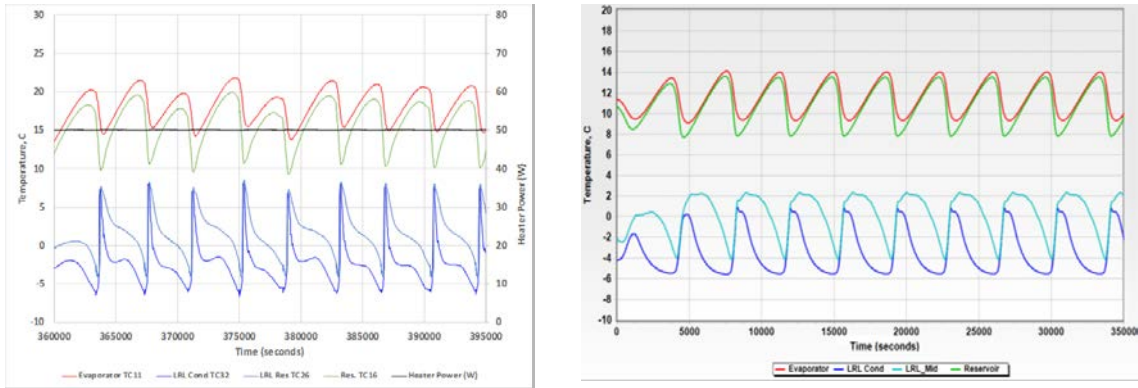


Figure 1. Comparison of LHP model and LHP experimental data.

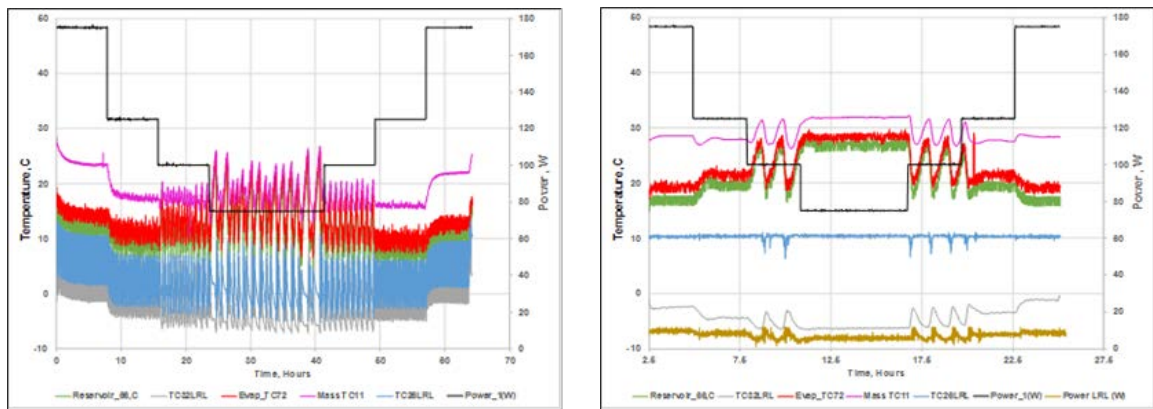


Figure 2. LHP oscillations with and without liquid line heating.

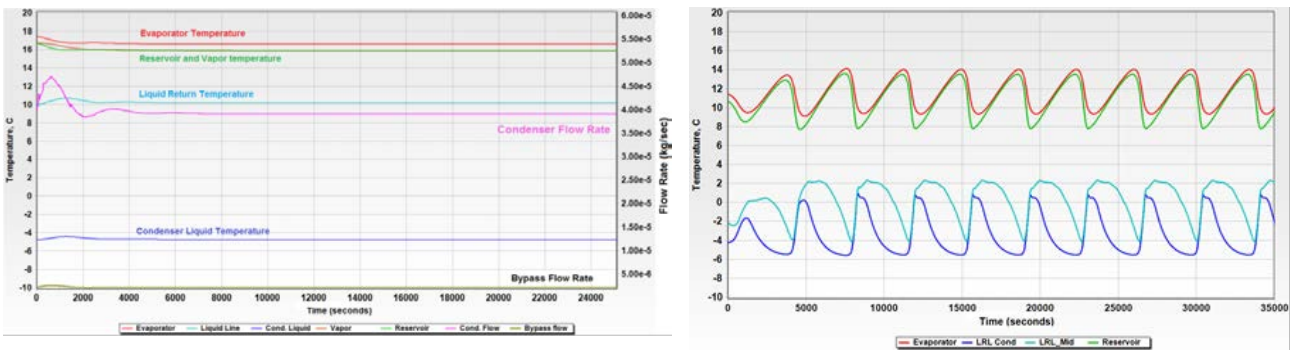


Figure 3. Model predictions for LHP operation with and without condenser bypass.

Title: High-Temperature and Rarefied Gas Dynamics in Hypersonic Flows

Author(s): R.E. Rogers and J.R. Maxwell

Affiliation(s): Naval Research Laboratory, Washington, DC

CTA: CFD

Computer Resources: Cray XC40 [NAVY, MS]

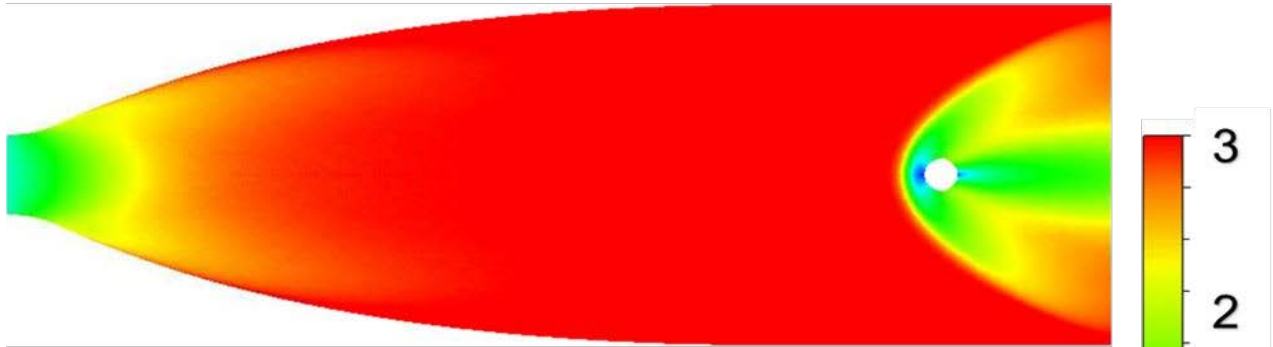
Research Objectives: The objective of the investigations is to better characterize supersonic and hypersonic rarefied flow in a wind tunnel configuration.

Methodology: This research has utilized direct simulation Monte Carlo (DSMC) in the MONACO software suite which requires significant parallel computing to achieve high-fidelity results. To achieve this, flight domains must be created and meshed intelligently with the geometric complexity of the flight vehicle and domain considered. Numerical solutions utilizing high-performance parallel computing are then initiated to solve the domain. For the present research, supersonic wind tunnel flow about a cylinder was studied to investigate the effects of rarefied flow in a wind tunnel configuration. The Knudsen number and surface accommodation coefficients were varied while the Mach number was held constant at 3.

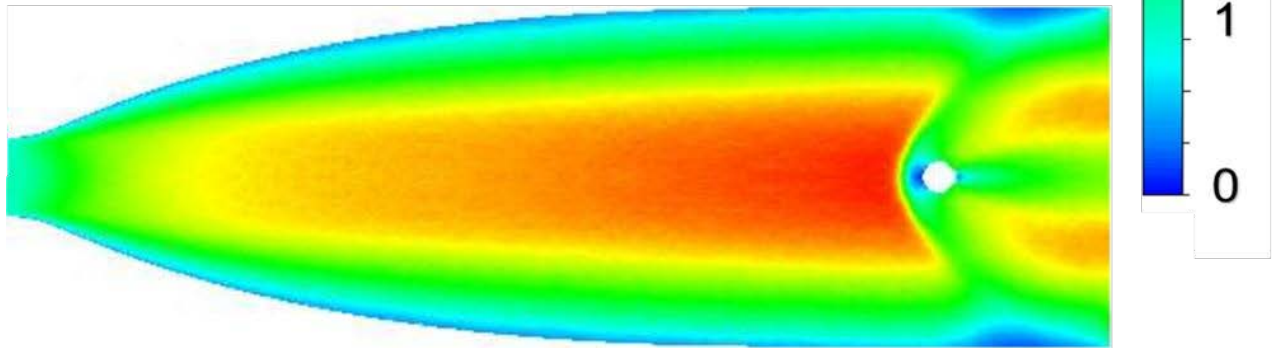
Results: The Knudsen number was shown to inversely affect the test section Mach number with it reaching approximately 10% of the design Mach number for a Knudsen number of 1. Secondly, it was determined that the wall thermal and momentum accommodation coefficients are highly influential on the test section flow quality. The ideal coefficients of zero yield clean and consistent flow, while increasing the values to realistic ranges (i.e. = 0.5) creates significant boundary layer effects. Lastly, the model-referenced Knudsen number is approximately an order of magnitude larger than the nozzle-referenced value. As shown in the attached figure, the flow around a cylinder reached a model-referenced Knudsen number of 0.1 enabling the visualization of rarefaction effects on the flow-field for thermal and momentum accommodation coefficients fixed at 0 (top) and 0.5 (bottom).

DoD Impact/Significance: This research has contributed to the understanding of rarefied flow simulation and experimentation for supersonic and hypersonic flow fields. The critical factors that affect proper simulation and experimentation were determined to be the thermal and momentum accommodation coefficients. Expanding on this newfound knowledge, better modeling of aerodynamic entry vehicles, meteorites, and low-Earth satellites will be possible.

Thermal and Momentum
Accommodation Coefficients = 0



Thermal and Momentum
Accommodation Coefficients = 0.5



Title: Detonations with Multi-Phase Flows for Propulsion
Author(s): D.A. Schwer
Affiliation(s): Naval Research Laboratory, Washington, DC
CTA: CFD

Computer Resources: Cray XC30 [AFRL, OH]

Research Objectives: The main research goal of the present HPC project is to study high- and low-speed reacting flows to further understand advanced engine concepts, with the specific application for detonation engines.

Methodology: We have used two modeling codes for our research into blast and detonation engine simulations. Our main development and simulation code is JENRE. Due to our extensive experience with using the DUSF codes for detonation propulsion, we will continue to use them as a benchmark for comparison with JENRE. JENRE is a new code utilizing unstructured meshes and the Discontinuous-Galerkin-FEM techniques to solve a wide variety of complex fluid dynamical phenomena. It has been built from the ground up at NRL to make efficient use of CUDA, Thread-Building-Blocks, OpenMP, and MPI through the use of the Thrust library. By utilizing unstructured meshes, the solver can be easily coupled to solid structural models and provide a pathway for doing fluid-structure-interaction. Both gas-phase and multi-phase models from our DUSF codes have been incorporated into the JENRE code. Complex geometric obstructions in the DUSF codes are handled through a VCE method.

Results: Rotating detonation engines (RDEs) have been the focus of considerable research over the last several years, but there are still several basic questions regarding using RDEs for propulsion that still need to be addressed. Because detonation engines are a radical departure from the constant combustion processes in current engines and power generation devices, integration of the combustion chamber into those devices requires special care and investigation. Our previous work showed how pressure pulses from a rotating detonation combustor (RDC) propagate upstream through a diffuser in a ram-RDE device. Results this year examined the effect of pressure waves propagating from the combustion chamber through an aerospike nozzle. Aerospike nozzles can be optimized for a range of pressure ratios, and are shown through this work to be a good fit for RDEs. To understand properly the operational stability of the detonation waves in RDEs, a better understanding of interactions between the detonation wave, fill flow, and the deflagration wave that develops between the fill zone and hot gases is necessary. The best way to understand this is through high fidelity simulations using detailed kinetics for both the deflagration and detonation. Research this year focused on validating JENRE with a detailed kinetic model for hydrogen/oxygen/argon detonations under low pressure conditions. This will enable us to examine operational stability in much greater detail than in previous studies. Finally, practical RDEs require direct injection of liquid fuels for efficient operation. Research was conducted this year to improve the modeling of liquid spray detonations in both DUSF and JENRE, and demonstrate the codes' abilities to capture JP10/oxygen spray detonations in multi-dimensions.

DoD Impact/Significance: The physics involved in RDEs and other detonation engines is substantially different than for gas-turbine engines, and also different than more traditional premixed detonation calculations, requiring research into how an RDE can fit into existing frameworks for propulsion and power generation. Our work in computing RDE flow-fields in conjunction with experimental work at the Naval Postgraduate School has helped us to better understand the physics and verify our physical models, and our development of JENRE gives us the capability to explore how best to fit RDEs into these existing frameworks. Through this research the potential of significant efficiency gains for detonation engines can be realized in propulsion and power generation devices.

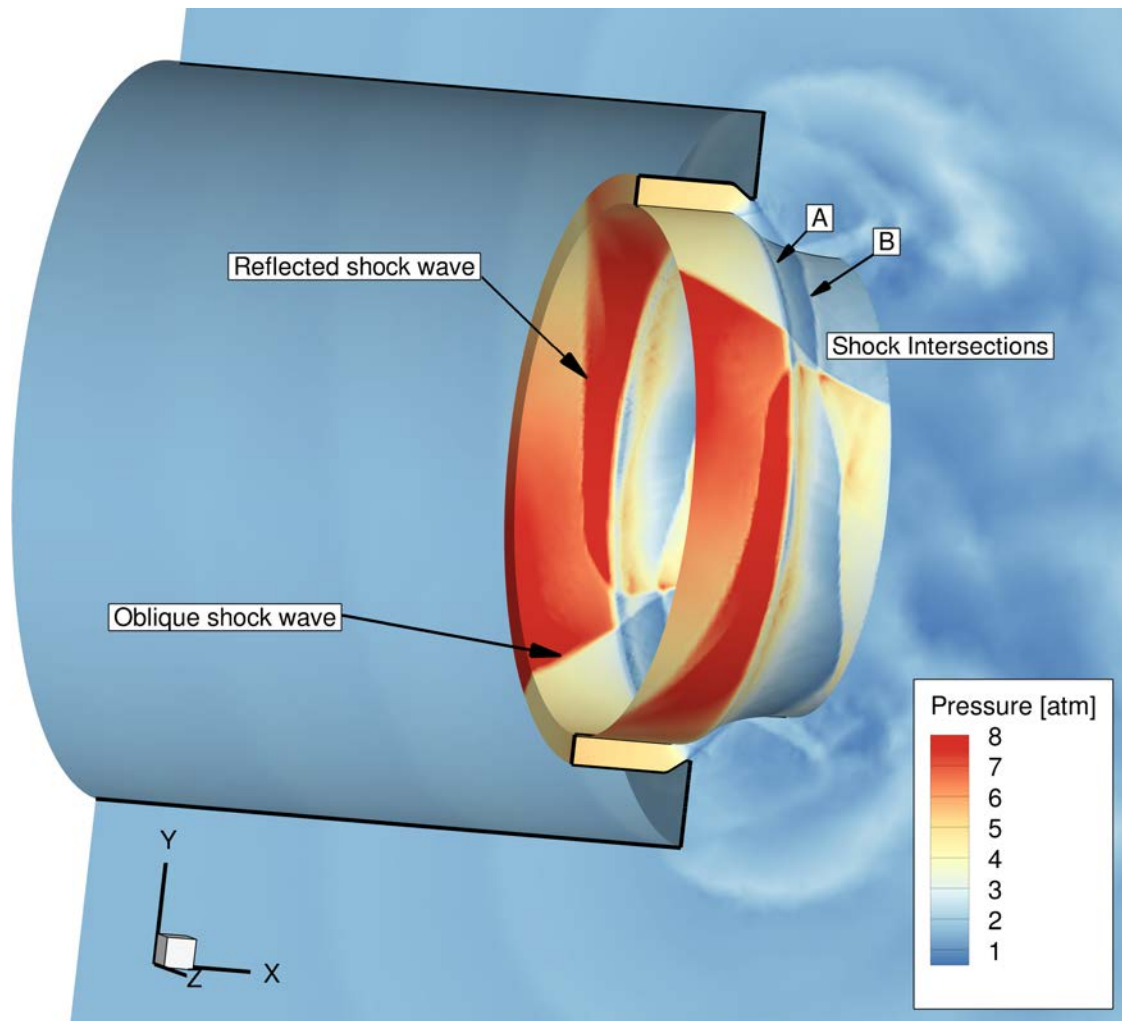


Figure 1. Instantaneous three-dimensional pressure field from outflow of an RDC on an aerospike nozzle showing the complex shock structures that develop on the nozzle, inner RDC wall, and a slice through $z = 0$. RDC conditions for this simulation are $\phi = 0.668$, mass flow rate of 1.067 kg/s, feed pressure of 8.89 atm, and detonation velocity of 1623 m/s.

Title: Simulations of the Ionosphere/Plasmasphere/Thermosphere System

Author(s): J. Krall¹ and J.D. Huba²

Affiliation(s): ¹Naval Research Laboratory, Washington DC; ²Berkeley Research Associates, Springfield, VA

CTA: CFD

Computer Resources: Cray XC30 [AFRL, OH]; SGI ICE X, Cray XC40 [ERDC, MD]

Research Objectives: The objective of this work is to develop space weather forecasting capability; simulate geomagnetic storms and other events of interest in order to understand geospace; develop coupled ionosphere/plasmasphere/thermosphere models for ionospheric specification; and develop a first-principles model of Earth's ionosphere/plasmasphere/thermosphere system.

Methodology: The research primarily uses the NRL code SAMI3 which is a comprehensive three-dimensional (3D) simulation model of Earth's ionosphere/plasmasphere system. Simulations use measured solar wind and irradiance data as input to drive the system. SAMI3 is used with a variety of magnetosphere models, from simple (useful for runs lasting several days) to the more comprehensive RCM code. In some cases we initialize the ionosphere model with thermospheric inputs from the GITM model as well as gravity and infrasound wave inputs.

Results: We used SAMI3 to model the 21 August 2017 total solar eclipse that traversed the continental United States and caused large-scale changes in ionospheric densities. This work supported several related studies. In one, density changes were measured via medium- and high-frequency radio propagation by the solar eclipse citizen science experiment organized by the Ham Radio Science Citizen Investigation (hamsci.org). Eclipse effects, observed for 0.6 hr on 1.8 MHz, 1.5 hr on 3.5 and 7 MHz, and 2 hr on 14 MHz, were consistent with the model. Observations were simulated using ray tracing in conjunction with the SAMI3 model. This and related work was reported at the 2017 Fall AGU Meeting and published in *Geophysical Research Letter*. Moving to high altitudes, the significance of the neutral hydrogen exosphere was studied using SAMI3. Recent work indicates significant uncertainties in the hydrogen density. Specifically, we used SAMI3 and Comprehensive Inner Magnetosphere-Ionosphere (CIMI) models to evaluate scenarios where the hydrogen density is reduced or enhanced, by a factor of two, relative to values given by commonly-used empirical models. We found that the plasmasphere is sensitive to exosphere composition such that more hydrogen in the exosphere leads to faster post-storm recovery. Finally, we showed that the ring current associated with a geomagnetic storm decays more rapidly when H is increased. This work was published in *Space Weather*. Moving still further out into space, SAMI3 was used to examine the physics of a long-lived geomagnetic storm. Specifically, the May 1994 storm lasted 12 days and was associated with a long-lived plasmasphere plume, extending sunward from Earth. The storm was modeled by adding a Kp-driven analytic convection potential to the self-consistent electric potential that is driven by thermosphere winds. Results were compared to measurements of the cold ion density from the 1989-046 spacecraft in geosynchronous orbit. We found that the plume in the magnetosphere was supported by field aligned flows from the ionosphere in excess of 20 km/s. This and related work was reported at the 2017 Fall AGU Meeting, at the 2018 GEM Summer Workshop and published in *Geophysical Research Letter*.

DoD Impact/Significance: The impact of this work includes potential protection of communication satellites and the power grid, support of ongoing experiments in remote sensing of the space environment, and input to ionospheric and thermospheric models.

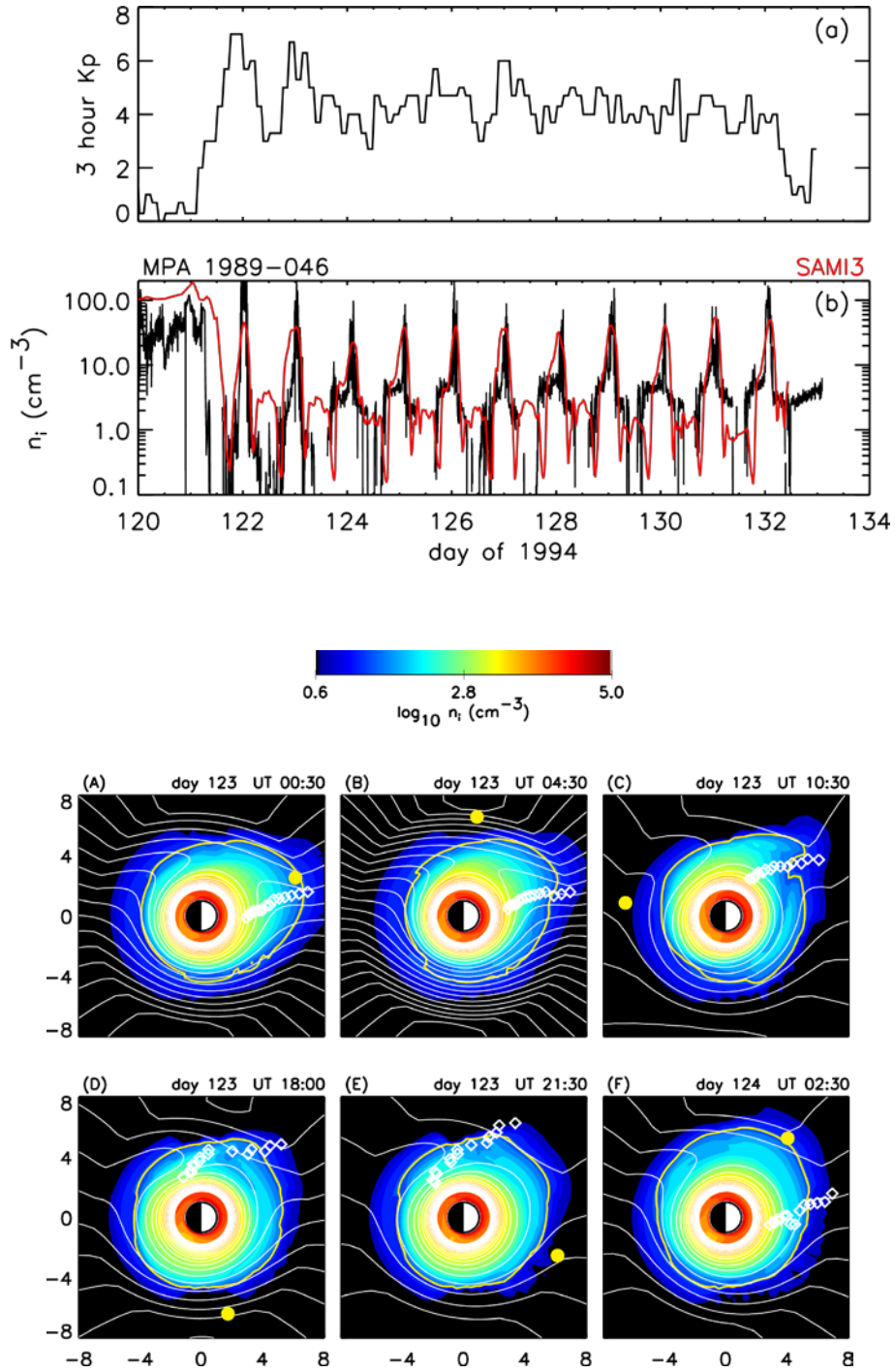


Figure 1. (a) K_p versus time, (b) cold ion density measured at location of satellite 1989-046 (black) and SAMI3 ion density (red), and (A–F) color contours show the log of the SAMI3 ion density in the equatorial plane during day 123. A single thick yellow contour highlights $n_i = 30 \text{ cm}^{-3}$. Contours of the electrostatic potential are plotted as white lines. The satellite position is plotted as a yellow dot. Diamond symbols show the position of the ionosphere “tongue of ionization” (TOI) feature projected along the magnetic field. When the storm is strong (lots of white contours), the TOI lines up with the plume.

Title: Numerical Simulations of Noise Generated by Non-Circular Advanced Military Aircraft Nozzles
Author(s): K. Viswanath and R. Ramamurti
Affiliation(s): Naval Research Laboratory, Washington, DC
CTA: CFD

Computer Resources: Cray XC40 [ARL, MD]; SGI ICE X [ARL, MD]; SGI ICE X [ERDC, MS] Cray XC40/50 [ERDC, MS]

Research Objectives: Use High Performance Computing (HPC) resources to predict details of turbulent flow structures and noise generation in supersonic non-circular asymmetric exhaust jets from representative military aircraft jet engine nozzles. This information will be used to investigate and assess promising jet noise reduction concepts in support of the ongoing testing program.

Methodology: Simulations are performed using the Jet Noise Reduction (JENRE) code developed at the Naval Research Laboratory. JENRE provides unsteady compressible flow solver capabilities that support various numerics, cell-centered finite volume or nodal finite element method, while delivering high throughput on calculations. It was developed with an emphasis on raw performance and the ability to exploit emerging massively parallel, HPC architectures. It supports different HPC parallel programming paradigms for message passing such as MPI, OpenMP, CUDA, and hybrid models depending on the HPC cluster architecture. A key bottleneck of HPC throughput is data input-output (IO). JENRE supports parallel IO via MPI/IO or the adaptable IO system (ADIOS) to further complement the multiple levels of parallelism. JENRE uses an edge-based formulation for all flux integration and limiting algorithms. Taylor-Galerkin finite element method with second order spatial accuracy, for tetrahedral cells, is used with the finite element flux corrected transport (FEM-FCT) method. The multi-dimensional FCT flux limiter provides an implicit subgrid stress model, which ensures monotonicity at shocks and sharp gradients with minimal artificial dissipation.

Results: Simulations of supersonic jets for various operating conditions and different nozzle configurations were investigated to understand their asymmetric noise characteristics and evaluate noise reduction techniques. A rectangular nozzle, with a high aspect ratio of 7.65 shown in Fig. 1, was simulated and its noise production and flow features compared with experimental data from the University of Cincinnati. The grid used for the simulation predicted the farfield noise and the spatial variation of the noise agreeably. Figure 2 shows the temperatures contours of the developed cold jet plume at ideally expanded operating conditions. For this high aspect ratio nozzle, axis switching happens downstream with the jet cross-section at 4D having major axis horizontal, while at 10D it has skewed with the major axis switched in the vertical direction. Despite geometrical asymmetry above and below the nozzle major axis due to the presence of a SERN profile on the nozzle bottom lip, the farfield acoustics recorded were symmetric in both simulations and experiments.

Figure 3 shows the comparison of the shock-cell structures and shock-cell locations near the nozzle exit between time averaged JENRE predictions and the experimental schlieren data. It is seen that the shock-cell structures and shock-cell locations from the simulations agree well with the measurement data.

DoD Impact/Significance: The results of our work will provide better understanding of the noise production for both industrial and military aircraft and will aid the current effort of noise reduction, especially for supersonic aircraft to reduce the impact of jet noise on shipboard health and safety issues. Futuristic nozzles are tending toward non-circular geometries for flexibility in airframe integration, capabilities such a SERN profile, and other potential advantages.

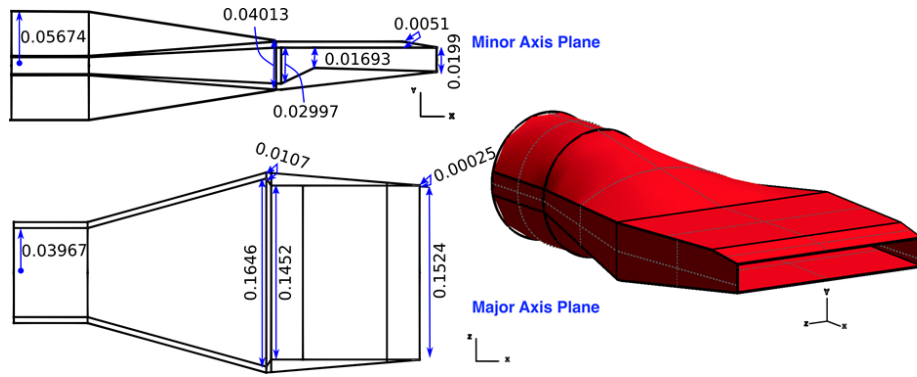


Figure 1. Nozzle geometry cross-sectional views for a high aspect ratio rectangular nozzle.

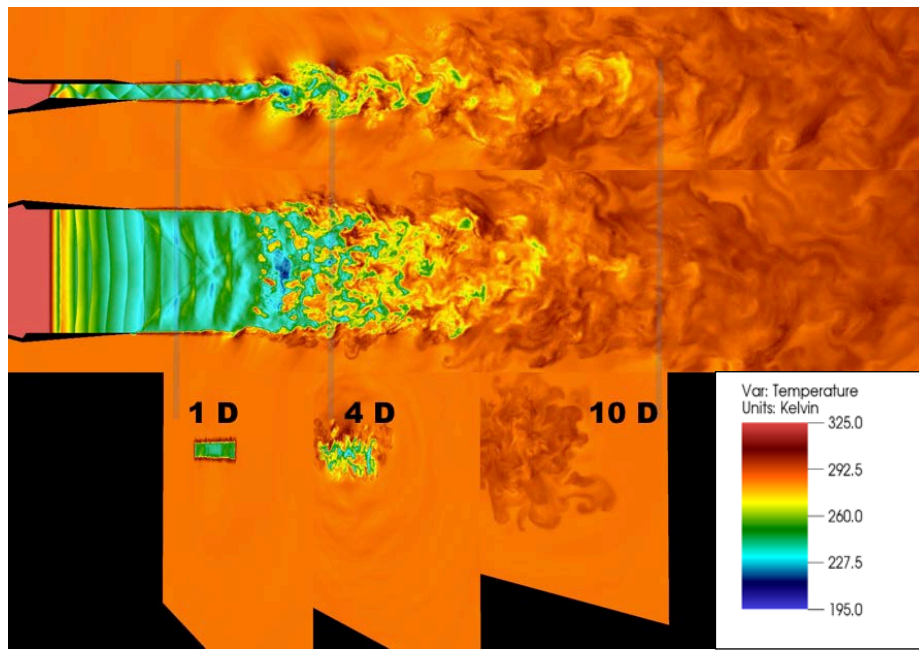


Figure 2. Temperature contours of the high aspect ratio jet. Individual cross-sectional planes are shown at 1D, 4D, and 10D to show the change in the jet profile.

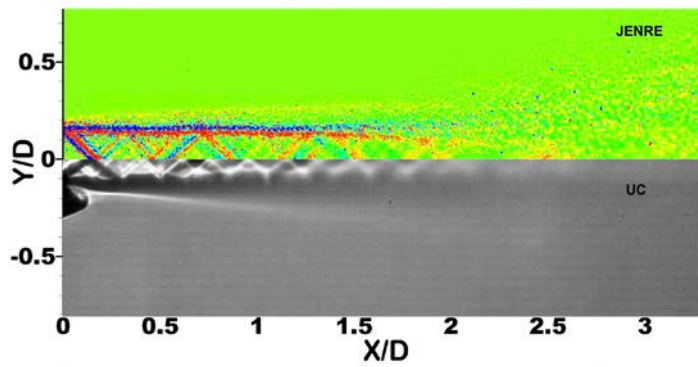


Figure 3. Overlay with schlieren data, from University of Cincinnati, of the time averaged flow field from JENRE simulation.

Title: Applications of FEFLO Incompressible Flow Solver
Author(s): R. Ramamurti
Affiliation(s): Naval Research Laboratory, Washington, DC
CTA: CFD

Computer Resources: SGI Altix ICE [NRL, DC]; SGI ICE X [ARL, MD]

Research Objective: Perform three-dimensional (3-D) numerical simulations of flow past complex configurations. The proposed studies will investigate the use of bio-inspired fins for underwater propulsion and to characterize and control the flow structures generated by these propulsive flapping surfaces with a focus on the interaction between two or more of these surfaces.

Methodology: A finite element solver, called FEFLO, for 3-D incompressible flows based on unstructured grids is used. The flow solver is combined with adaptive remeshing techniques for transient problems with moving grids and is also integrated with the rigid body motion in a self-consistent manner which allows the simulation of fully coupled fluid-rigid body interaction problems of arbitrary geometric complexity in three dimensions. NRL has developed a flapping fin UUV for effective low-speed operations. Limited parametric studies were conducted to improve the performance of that vehicle within the mechanical constraints of that vehicle by varying the spacing and phasing between the flapping fins. The objective of these computations is to investigate the importance of these parameters on the fluid dynamics of force production via proper interaction of the flow structures in order to maximize thrust production and propulsive efficiency.

Results: Based on our previous experience with the bird-wrasse fin and literature on fins based on biological creatures, a trapezoidal bio-inspired fin with an aspect ratio of 3 was selected. A rectangular fin of the same aspect ratio and area was selected to study the effect of the planform. An initial computational study was also performed to understand the effect of the planform on the thrust development. For this purpose, the same kinematics was employed for both the rectangular and the bio-inspired fins at a flapping frequency of 1Hz and the fins were separated by 15cm. For the bio-inspired pair, the rear fin produces a higher mean thrust compared to the front fin. The computational results were validated using the experimentally measured forces. The phase offset between the front and the rear fins were varied. For both the bio-inspired and rectangular set of fins, depending on the axial offset, an optimum phasing of the rear fin with respect to the front fin is found that maximizes the thrust produced by the rear fin. The performance of the bio-inspired fin was also tested at a desired inflow velocity of 1m/s, and showed that by increasing the stroke amplitude within experimental constraints a net positive thrust is achievable.

DoD Impact/Significance: Simulations have enabled characterization of the thrust generation mechanisms in flapping foil propulsion and the interactions of the flow between these propulsors for use in unmanned underwater vehicles. This will provide a tool for improving the performance of existing underwater vehicles and informing the design of future vehicles.

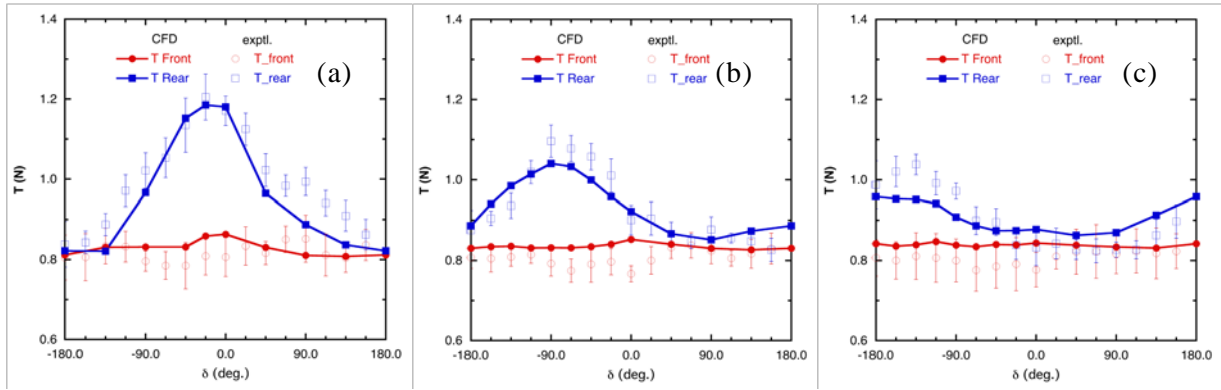


Figure 1. Effect of Phasing and Spacing between the tandem bio-inspired fins, $f = 1\text{Hz}$, at x_{offset} of (a) 11cm, (b) 15cm and (c) 19cm.

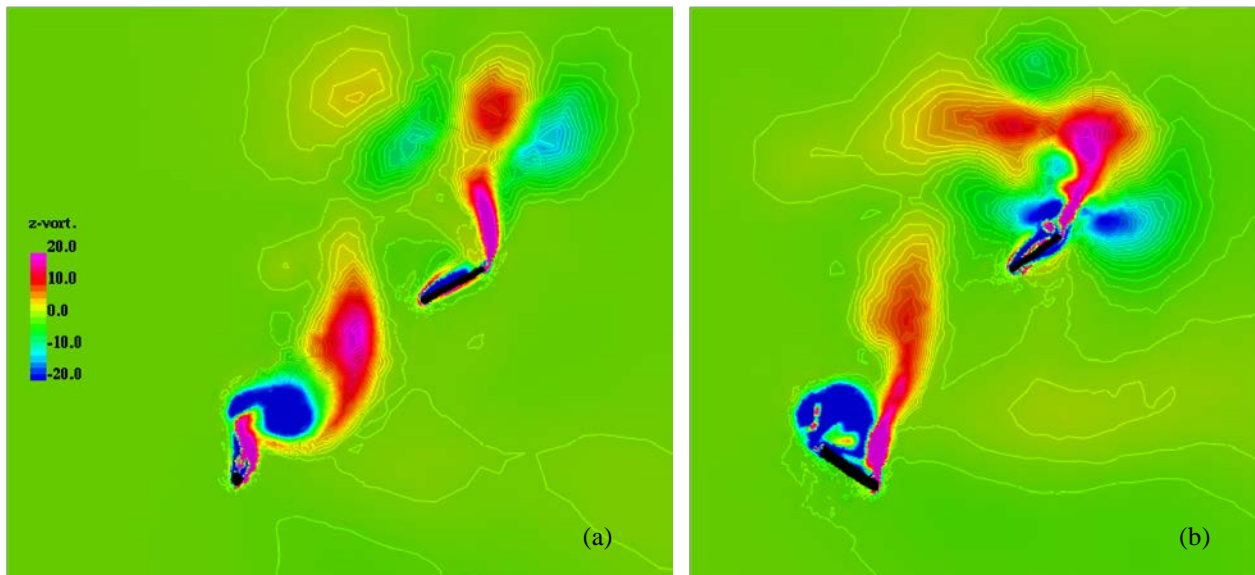


Figure 2. Spanwise component of vorticity along a plane 45% of the span and at an instant 50% of the stroke, for (a) a bio-inspired fin and (b) a rectangular fin.

Title: Particle-in-Cell Simulations of Large-Area Electron-Beam Diodes

Author(s): S.B. Swanekamp, A.S. Richardson, I. Rittersdorf, J.W. Schumer, P.F. Ottinger, and S.P. Obenschain

Affiliation(s): Naval Research Laboratory, Washington, DC

CTA: CFD

Computer Resources: SGI Altix ICE [NRL, DC]; SGI ICE X [ARL, OH]; Cray XC40 [ARL, MD]; Cray XC30 [NAVY, MS]

Research Objectives: The goal is to understand the large-area electron-beam sources that are used to drive high-power excimer laser systems.

Methodology: To pump the high-power excimer lasers that researchers envision for inertial confinement fusion applications, a large-area electron beam is required. The Nike KrF laser, located in the Naval Research Laboratory's Plasma Physics Division, uses a pair of $60\text{ cm} \times 200\text{ cm}$ rectangular electron beam diodes to generate two opposing 150 kA , 600 kV electron beams. The geometry for one of these diodes is shown in Fig. 1. These electron beams are used to uniformly deposit energy into the laser gas medium of the Nike high-power KrF laser system. Experiments and electromagnetic particle-in-cell simulations have shown that the electron flow in these large-area diodes is unstable to the transit-time instability (TTI). The TTI can modulate the electron beam energy delivered to the laser gas medium, create a non-uniform deposition profile, and add to the transverse beam temperature. All of these effects can have negative consequences on the laser beam quality. We are using 2D and 3D electromagnetic particle-in-cell simulations to better understand the TTI. This understanding provided by these simulations is leading to techniques which can mitigate the TTI and improve laser-beam quality.

Results: A distributed transmission line model of the TTI has been developed that allows techniques from microwave engineering to be applied to the unstable diode. The theory suggests that a resistively-loaded, periodic structure of slots in the cathode can stabilize the TTI. The results of the linear analysis shows that the TTI can be mitigated if the slot depth, ℓ , and shunt resistance, R_s , are properly tuned. For best results, the slot depth should be chosen to be $\frac{1}{4}$ of the wavelength of the most unstable mode and the shunt resistance should be chosen to be twice the vacuum wave impedance of the slot, $Z_0 = 377\text{ s/w}$ where s is the slot width. Results from particle-in-cell simulations of the Nike large-area electron-beam diode showing the voltage at the center of the diode are shown in Fig. 2. Particle-in-cell simulations of the Nike diode show that the most unstable TTI mode is about $\lambda = 16\text{ cm}$. Simulation results with a resistively-loaded, slotted cathode structure show that the large-amplitude oscillation in the diode voltage caused by the TTI is virtually eliminated by choosing $\ell \cong \lambda/4$ and $R_s = 2Z_0$.

DoD Impact/Significance: Electron beams generated in modern high-power devices can be used to pump high-power KrF lasers. These lasers are used to study nuclear weapon effects and may one day be used as drivers for inertial-confinement fusion reactors. The particle-in-cell simulations are helping us understand the instabilities in electron flow in large-area diodes. This work is also leading to new diode designs that mitigate the TTI and improve the uniformity of the energy deposited in the Nike KrF laser medium.

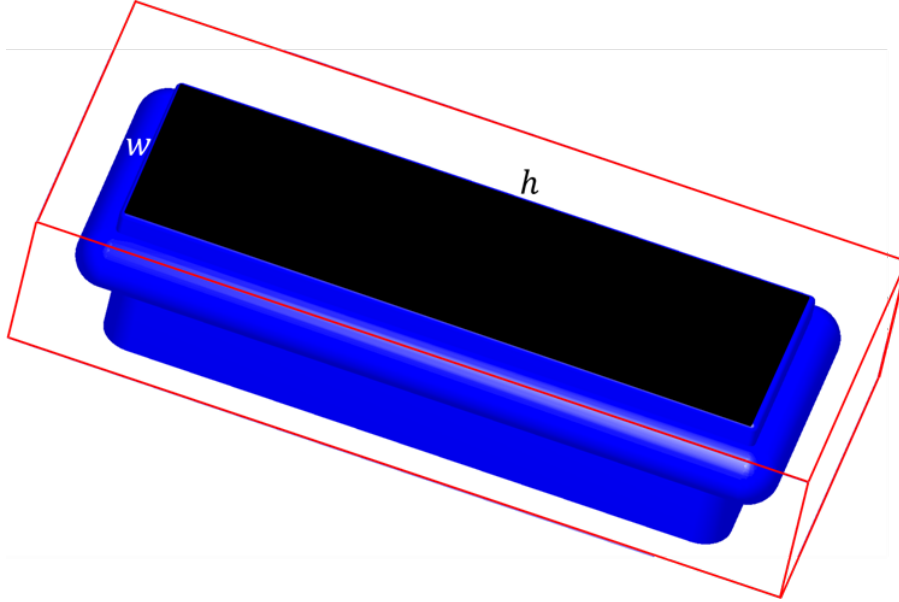


Figure 1. The geometry of the Nike electron-beam diode with $w = 60 \text{ cm}$ and $h = 200 \text{ cm}$. The anode-cathode gap for the Nike diode is $d = 5 \text{ cm}$ and the anode return-current structure is outlined by the red lines.

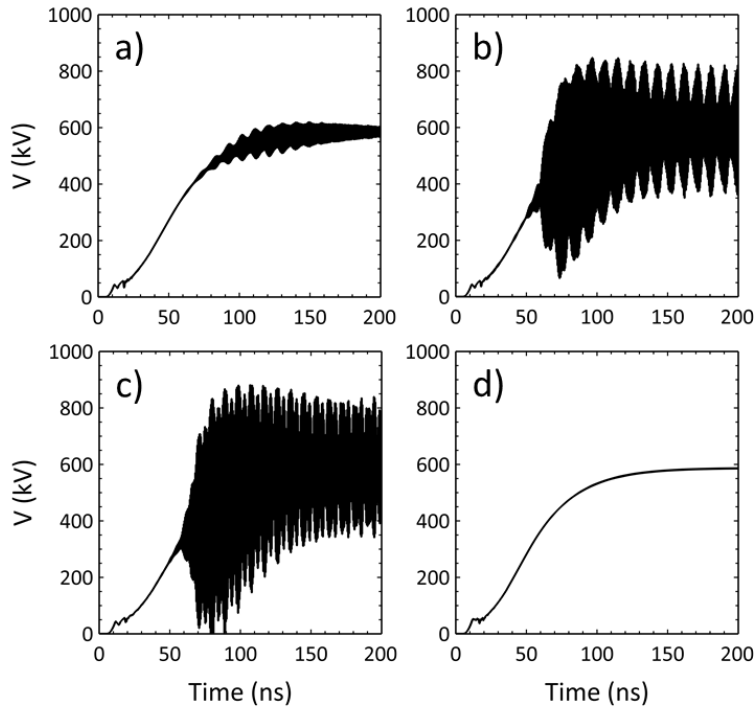


Figure 2. Time histories of the diode voltage with a periodic structure of slots in the cathode for slot parameters: a) $\ell = 4.1 \text{ cm}$ and $R_s = \infty$, b) $\ell = 4.1 \text{ cm}$ and $R_s = 0$, c) $\ell = 7.2 \text{ cm}$ and with $R_s = 2Z_0$, d) $\ell = 4.1 \text{ cm}$ but with $R_s = 2Z_0$.

Title: Fine Scale Structure of the Air-Sea Interface

Author(s): G.B. Smith,¹ R. Leighton,² I. Savelyev,¹ and T. Evans¹

Affiliation(s): ¹Naval Research Laboratory, Washington, DC; ²SRI-International, Ann Arbor, MI

CTA: CFD

Computer Resources: Cray XC30 [AFRL, OH]; SGI Altix ICE [NRL, DC]

Research Objectives: The research objectives of this multi-year effort are to understand the coupling small-scale processes at the air-sea interface to ocean mixed layer process. Much of the efforts have focused on the evolution of Langmuir Circulation, which defines one of the scale generating structures of the mixed layer. Classical theory posits that these structures result from the interaction of ocean wave generated Stokes drift and the surface current due to wind shear. This process is a primary driver in the transport of mass, momentum and heat through the mixed layer, but remains a critical missing element in flux modeling at the interface. The additional objective is developing a model of the interaction of the aqueous turbulence and the thin cool skin observed in the infrared. The specific research objective is to quantify the level of circulation induced surface straining and the impact of that straining on the near surface boundary layer.

Methodology: Two parallel approaches are currently being pursued in this project. In the first approach the numerical simulations are performed using a well-established pseudo-spectral code that can be run in a DNS (Direct Numerical Simulations) or LES (Large-Eddy Simulation) mode. The algorithm has been extended to include the transport of thermal energy and mass, via the Boussinesq approximation and includes an explicit stokes drift term. The simulations are being benchmarked against available in-house infrared imagery of Langmuir circulation. In the second approach a different code is used to simulate a smaller scale “patch” of Langmuir turbulence. This code is also run in a DNS mode, but in this case a passive scaler has been added to the water surface. This passive scaler simulates the behavior of dye on the surface, and is being benchmarked against results from a dye release experiment conducted in October/November 2015.

Results: During the last year we have focused on the scaling associated with the background turbulence, which in this effort is modeled as the turbulence generated by a steady wind shear. Figure 1 shows a typical temperature field at the surface. Note that at a scale of 1.08 by 0.54 meters, the apparent structure in the image will typically be sub-pixel, but disruption of the thermal boundary layer may be visible. In Fig. 2, we present two non-dimensional scalings of the depth averaged temperature field in addition to the dimension form. The first scaling is the dissipation-based scaling used last year. The second scaling is based on relating the dissipation to the production of turbulence and results in a Richardson number-based shear scaling. Aside from an undetermined constant, the scalings are similar and provide a means of determining the potential thermal contrast in the IR due to the disruption of the cool skin.

DoD Impact/Significance: This activity has two potential naval applications. The primary application is in the development of improved flux models for the air sea interface. Specifically, fully coupled air-ocean models, wherein the ocean boundary layer is not fully resolved numerically, would benefit from high-resolution interfacial flux modeling. Other naval applications include the inversion of remote sensing data, specifically combined thermal infrared and visual imagery, for the evaluation of the properties of the ocean mixed layer and the modeling of sea surface clutter in infrared imagery.

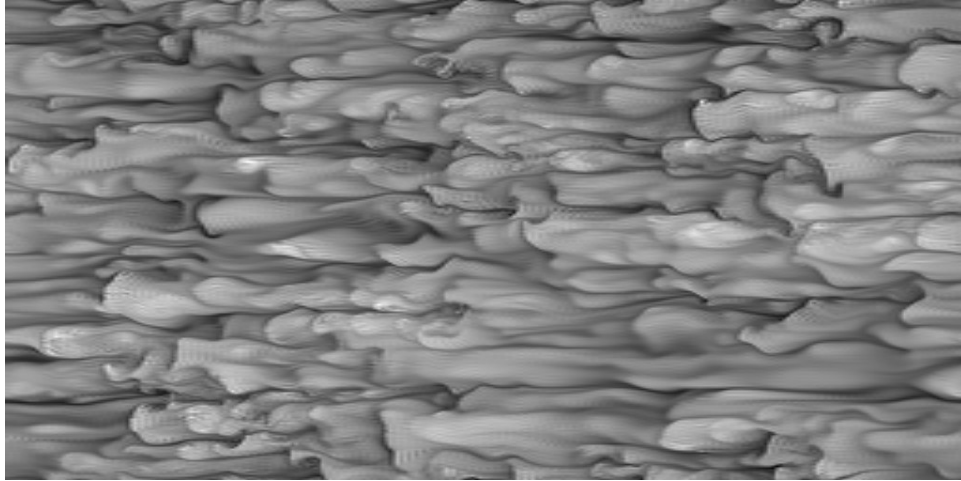


Figure 1. The surface temperature for turbulence wind sheared simulations. Dark grey is cool. Temperature range in image is 0.30 K. The domain size is 0.504 by 1.08 meters.

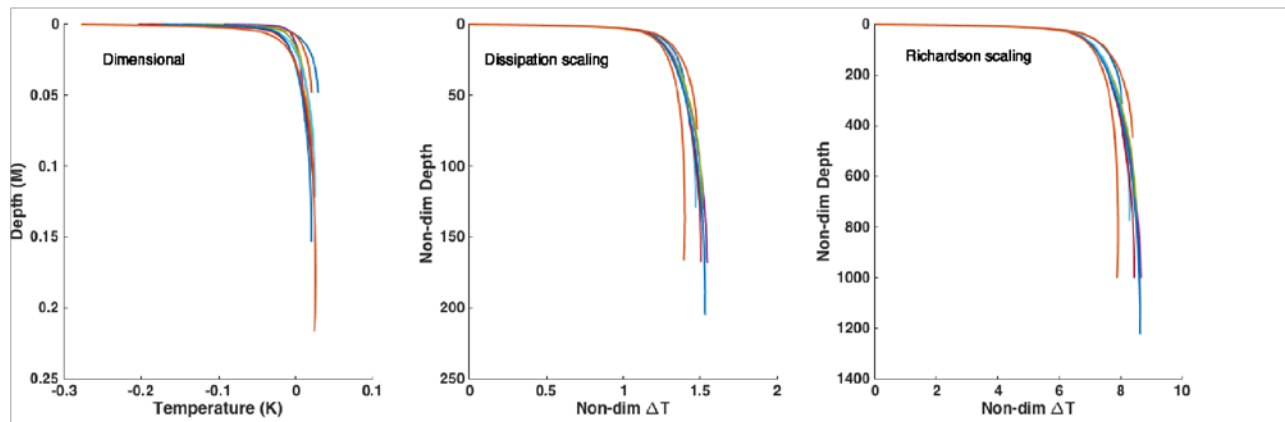


Figure 2. Mean temperature, Θ , as a function of depth for a range of Richardson numbers. The simulated temperature differences between bulk and the surface range from 0.16 K to 0.30 K and the depths range from 0.024 meters to .108 meters. The remaining two images present the temperature increment of the cool skin $\Delta\Theta = (\Theta_{surface} - \Theta)$, scaled by a dissipation (or Kolomogrov) based scaling or by a wind shear based Richardson number. with exception of an undetermined constant, both scalings collapse the data.

THIS PAGE INTENTIONALLY LEFT BLANK

CCM

Computational Biology, Chemistry, and Materials Science

CCM covers computational tools used to predict basic properties of chemicals and materials, including nano- and bio-materials. Properties such as molecular geometries and energies, spectroscopic parameters, intermolecular forces, reaction potential energy surfaces, and mechanical properties are being addressed. Within the DoD, quantum chemistry, molecular dynamics, statistical mechanics, and multiscale methods are used to design new chemical, polymer, nano- and bio-molecular systems, for fuel, lubrication, laser protection, explosives, rocket propulsion, catalysis, structural applications, fuel cells, and chemical defense. Solid-state modeling techniques are employed in the development of new high-performance materials for electronics, optical computing, advanced sensors, aircraft engines and structures, semiconductor lasers, advanced rocket engines components, and biomedical applications. Of recent emerging interest in the Computational Biology, Chemistry, and Materials Science (CCM) CTA are methodologies that cover bioinformatics tools, computational biology, and related areas, such as cellular modeling.

Title: Quantum-Chemical Simulation of Surface-Science Experiments

Author(s): V.M. Bermudez and P.E. Pehrsson

Affiliation(s): Naval Research Laboratory, Washington, DC

CTA: CCM

Computer Resources: SGI Altix ICE [NRL, DC]; Cray XC30 [AFRL, OH]

Research Objectives: The objective of this program is to perform quantum-chemical calculations as an aid in interpreting surface-science experiments and in predicting gas-solid interaction.

Methodology: The QUANTUM ESPRESSO (vers. 5.2 and higher) and CRYSTAL (2014) software packages are used for density functional theory (DFT) calculations on periodic structures. The GAUSSIAN-16 program suite is used for DFT calculations on isolated molecules and clusters.

Results: The removal of toxic industrial compounds (TICs) and chemical warfare agents (CWAs) from air is a subject of great importance. Recent work at the Edgewood Chemical and Biological Center has shown that $Zr(OH)_4$ is significantly more effective than traditional adsorbent materials such as activated charcoal. $Zr(OH)_4$ has a high density of acidic and basic hydroxyl (OH) groups with the former existing as bridges between Zr sites and the latter as OH bonded to a single Zr. The high surface area and high OH density make $Zr(OH)_4$ effective in mitigating toxic agents. Presently the structure and properties of $Zr(OH)_4$ are poorly understood. This has led to a research effort, supported by the Defense Threat Reduction Agency, that is aimed at characterizing $Zr(OH)_4$ and developing a microscopic understanding of interactions with TICs and CWAs. Electronic structure is an important issue affecting photochemistry. However, even the band gap (E_g) of $Zr(OH)_4$ is uncertain, with two studies reporting values of 2.7 and 4.7 eV. The difficulty in obtaining pure samples of $Zr(OH)_4$ complicates an empirical approach, which has led to the present work that addresses the electronic structure computationally.

$E_g = 5.8$ eV is found for pure $Zr(OH)_4$, which, based on tests for cubic ZrO_2 , may be too large by ≤ 0.3 eV. Of the typical impurities in practical $Zr(OH)_4$ (H_2O , carbonate, sulfite and Cl) only sulfite gives states in the gap (~ 0.44 or 0.86 eV above the valence band maximum (VBM)). The defects Zr^\bullet , $Zr-O^\bullet$ and $Zr-O^\bullet-Zr$ (where \bullet is an unpaired electron) have been analyzed. The importance of such defects is suggested by work showing that $Zr(OH)_4$ undergoes loss of H or OH during near-UV irradiation, which could affect the adsorption of agents. The Zr^\bullet (or Zr^{+3}) center, formed by removing an $\bullet OH$ radical from a terminal Zr-OH, has been identified in electron paramagnetic resonance experiments. The other defects are formed by removing $\bullet H$ from a terminal or a bridging OH. All three have a relatively low (endothermic) formation energy, which suggests that all should form fairly easily. The Zr^\bullet center gives a state at ~ 4.4 eV above the VBM, as shown in Fig. 1. The unpaired electron partially delocalizes into the OH vacancy where it interacts with the H atom in a near-by terminal Zr-OH. This is seen in the magnetic moments (MMs) on the Zr, in the vacancy and on the H atom (0.68, 0.16 and 0.09 Bohr magnetons respectively). Thus the defect is largely Zr^{+3} but also involves a $Zr^{+4}(\bullet)$ component where (\bullet) is an electron trapped in the OH vacancy. This is seen clearly in Fig. 1, which shows a contribution to the gap state from both the Zr and the vacancy. The $Zr-O^\bullet$ and $Zr-O^\bullet-Zr$ centers produce states at 3.1 and 1.7 eV, respectively, above the VBM with the unpaired electron localized mainly on the O atom.

DOD Impact/Significance: This study constitutes the first attempt to model quantitatively the electronic structure of $Zr(OH)_4$ and the effects of impurities and defects. The results provide a reliable estimate of E_g for the pure material and identify those foreign species that contribute states in the gap. This in turn provides an improved understanding of the optical properties and the photochemistry of $Zr(OH)_4$ as they relate to adsorption and reaction with TICs and CWAs.

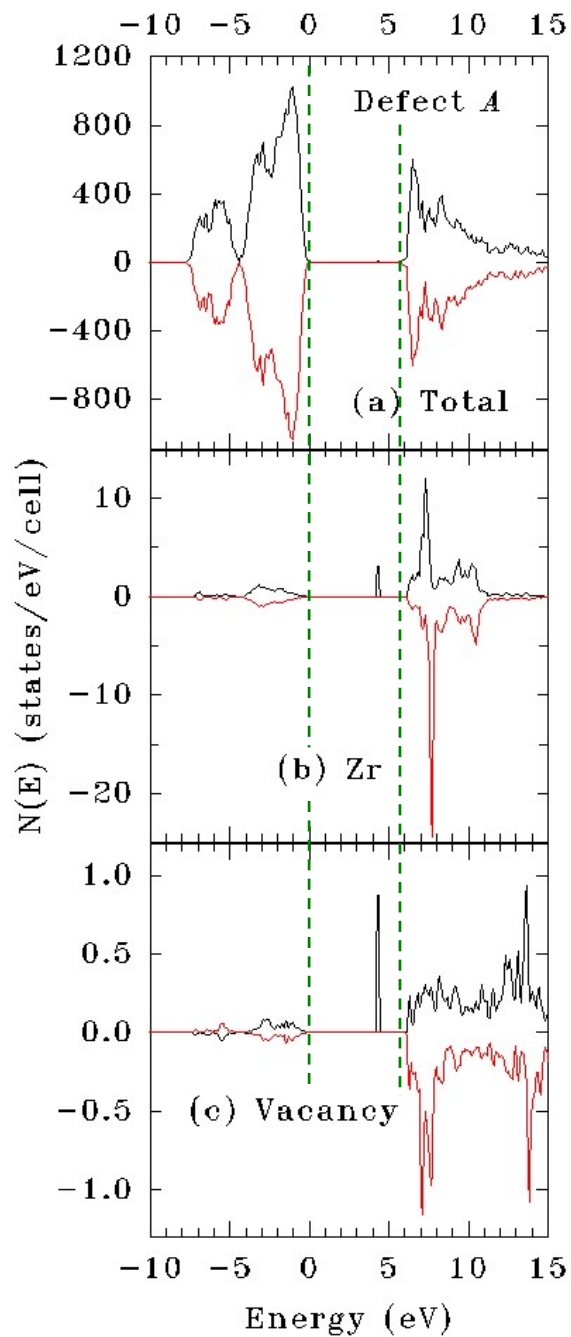


Figure 1. The spin-polarized density of states (DOS) for a 3-layer $\text{Zr}(\text{OH})_4$ model with a Zr^{+3} defect in the middle layer (Defect A). The majority (minority) spin states are shown in black (red) as positive (negative) quantities. The total DOS is shown in (a), and the partial DOS for the Zr and the OH vacancy are given in (b) and (c) respectively. Note the different $N(E)$ scales in the three plots. An occupied defect level appears at 4.4 eV above the valence band maximum (VBM). The dashed green lines show the positions of the VBM and conduction band minimum (CBM). The zero of energy is at the VBM.

Title: Marine Biofilm Metaproteomics

Author(s): W.J. Hervey, IV, C. Ames, M.A. Rimmer, S.M. Colston, D.H. Leary, and G.J. Vora

Affiliation(s): Naval Research Laboratory, Washington, DC

CTA: CCM

Computer Resources: Cray XC30 [AFRL, OH]; SGI ICE X [AFRL, OH]; Cray XC40 [ARL, MD]; Cray XE6m [ERDC, MS]; Cray XC40 [ERDC, MS]

Research Objectives: To implement and maintain a modular data analysis pipeline of selected open-source software applications for biomolecular characterization microbiomes, such as marine biofilm and biofouling microbial consortia. Integration of disparate, large-scale data tiers of biological information on genomic (DNA), transcriptomic (RNA), proteomic (protein), and metabolomics (metabolite) levels is a prerequisite to understanding biofilms at the molecular level.

Methodology: The process of creating large-scale metaproteome inventories of proteins predicted to be present among microbiomes is three-fold: assembly of small DNA pieces into larger contiguous segments, prediction of protein-coding regions from contiguous DNA segments, and *in silico* translation of the genetic information into protein sequence data. Two factors make this workflow computationally-intensive and time-consuming: the large volume of data acquired from complex environmental samples (*eg.* the number of DNA reads and MS/MS spectra acquired) and the diverse species complexity present in the environmental sample. To overcome these computational bottlenecks, we deployed a new metagenome assembler, DISCO, for the assembly of microbial consortia, which leverages both MPI/OpenMPI and large memory access to distribute and process metagenome assembly. The Sipros Ensemble application enables protein identifications from tandem mass spectral measurements of metaproteomes containing several million predicted metaproteome entries. In tandem, these applications have significantly reduced the amount of time required to process large ‘-omics’ data volume. Additionally, Sipros Ensemble employs ensemble machine learning to reduce the number of false positive protein identifications among such large predicted metaproteomes. To improve predicted protein functional annotation among metaproteomes, an application for sequence conversion and annotation with BLAST (seqCAB) enabled characterizations of tens of thousands of proteins tractable across HPC environments. Incorporation of the open-source Unicycler workflow suite and the Canu assembler have enabled assembly of genome reads from state-of-the-art sequencing platforms (Oxford Nanopore Technologies, Pacific Biosciences), ensuring that our workflow is configurable to the latest developments in analytical technologies.

Results: In FY18, HPC allocations enabled publication of the genome sequences of 3 *Vibrio* microbial strains, 2 software applications (DISCO metagenome assembler and seqCAB), and, led to invited oral presentations and multiple conference proceedings.

DoD Impact/Significance: Our HPC subproject is directly applicable to “Sense and Sense-Making” from large-scale biomolecular datasets of considerable DoD interest, particularly with respect to microbiomes, alternative energy sources, and the sustainability of platforms.

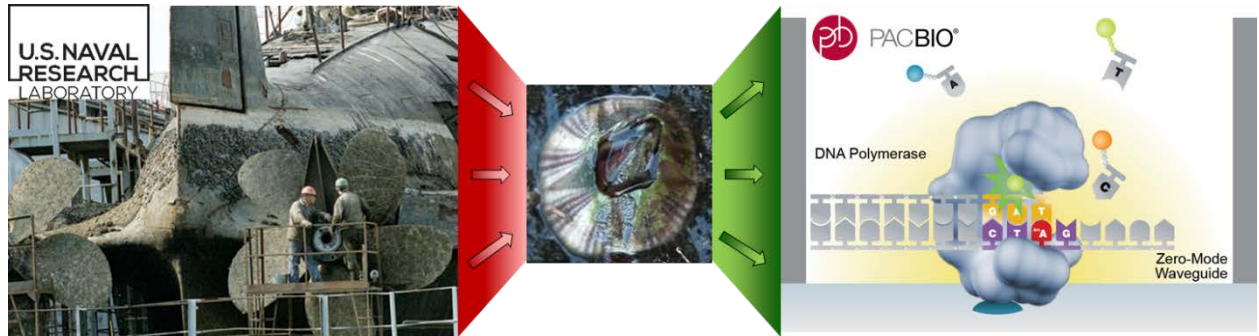


Figure 1. Both macro- and micro-biofilm communities are shown to the left. A macro-fouling organism, *A. amphitrite*, a barnacle species, is shown in the center. Next-generation genome sequencing approaches, such as Pacific Biosciences Smart Cell Technology (PacBio SMRT Cell), are being used to acquire DNA sequence reads of macro- and micro- biofilm communities. One area where HPC allocations are leveraged on this subproject is for the assembly of these DNA reads into a complete genome sequence. (Image courtesy of Chris Spillmann.)

Title: Synthetic Biology for Military Environments

Author(s): W.J. Hervey, IV, D.H. Leary, M.A. Rimmer, S.N. Dean, S.Kim, and G.J. Vora

Affiliation(s): Naval Research Laboratory, Washington, DC

CTA: CCM

Computer Resources: Cray XC30 [AFRL, OH]; SGI ICE X, [AFRL, OH]; Cray XC40 [ARL, MD]; Cray XE6m [ERDC, MS] Cray XC40 [ERDC, MS]

Research Objectives: The primary goal of our synthetic biology research program is to design and implement molecular toolkits for microbial species (or target "chassis") that are directly relevant to military environments, as opposed to solely functioning in laboratory settings. A prerequisite to engineering a synthetic biology platform for this purpose are characterizations and measurements of target microbial genomes (DNA), transcriptomes (mRNA), proteomes (proteins), and metabolomes (small molecules). These high-throughput molecular-level, "wet-lab" measurements allow researchers to compare and contrast synthetic modifications from unmodified microbial strains. Acquisition of disparate '-omics' measurements by multiple analytical modalities results in a very large data volume. To assist with data analysis, a High Performance Computing Applications Software Initiative (HASI) devised a Bioinformatics Workflow for Integrative '-omics' Data Analytics (HPCMO38373A11) which was utilized heavily in FY18.

Methodology: Synthetic biology is a highly multidisciplinary research area that imparts desirable (or "designer") functions into cells from the introduction of simple genetic circuits to complex engineered genetic regulatory networks. Applications of synthetic biology range from design of DNA constructs for sensing and reporting target analytes to the manipulation of enzymatic pathways to improve yield of natural or synthetic products. Our approach is to impart synthetic functions among species that are directly applicable to military environments: the marine microbe, *Vibrio natriegens*; an inhabitant of microbial fuel cell biofilms, *Marinobacter*; and a resident of the human gut microbiome, *Lactobacillus*. A prerequisite to characterizing these species in a robust, high-throughput manner is reproducible sample preparation for proteome profiling. One use of the FY18 HPC allocation has been to determine the efficacy of multiple sample preparation methods among these 3 microbial species.

Results: To impart desirable functions into the host species above, considerable effort has been devoted to developing tractable systems for genetic modification, *in silico* promoter prediction, and measurement of protein coding open reading frames. Mass spectrometry-based proteome profile measurements between genetically unmodified and manipulated microbial species will allow evaluation of the efficacy of the desired functions. To this end, a large peptide-ion library is being constructed for data independent acquisitions of *Vibrio natriegens* proteome profiles. Features measured among the profiles have been extracted using portions of the '-omics' data analysis workflow described above. These robust, quantitative measurements may then be factored into molecular modeling and synthetic circuit design to impart more elaborate functions within *Vibrio*, as well as the other microbial species.

DoD Impact/Significance: Our HPC subproject is directly applicable to "Sense and Sense-Making" from large-scale biomolecular datasets of considerable DoD interest, namely biologically-inspired materials design, synthetic biology, and alternative energy sources.

Figure 1.

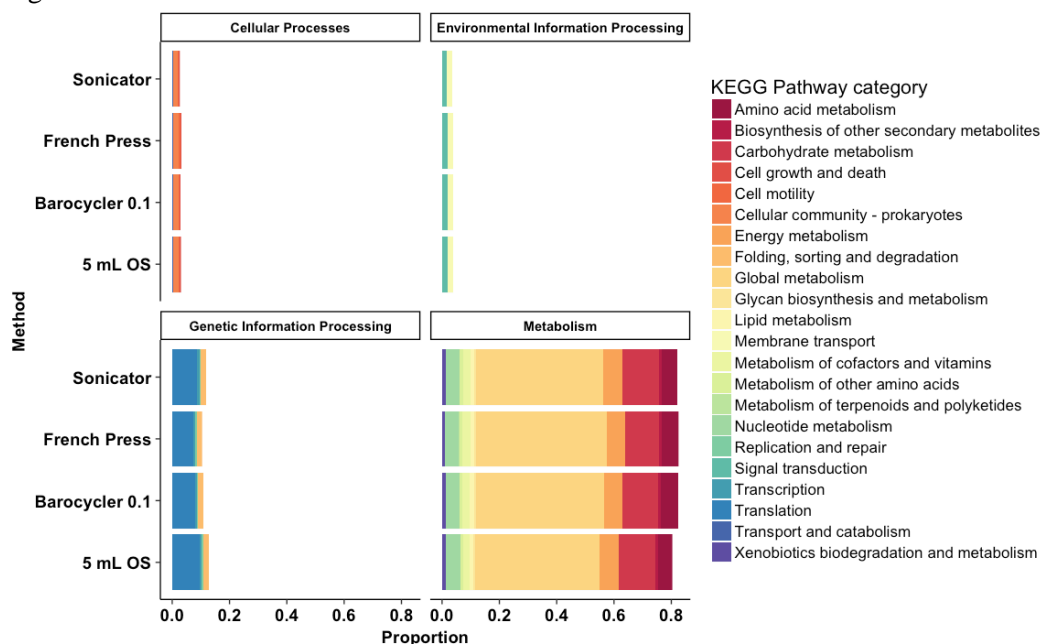


Figure 2.



***Vibrio natriegens* Proteins Identified by Sample Preparation Method.** 1. Predicted functions of identified proteins by sample preparation method. Functional inference is from sequence similarity to the Kyoto Encyclopedia of Genes and Genomes (KEGG). 2. Circos plot of the *Vibrio natriegens* genome illustrating where identified proteins map on the chromosome. (Image courtesy of Mary Ashley Rimmer and Scott N. Dean.)

Title: First-Principles Simulations of Condensed-Phase Decomposition of Energetic Materials

Author(s): I.V. Schweigert

Affiliation(s): Naval Research Laboratory, Washington, DC

CTA: CCM

Computer Resources: Cray XC40 [ARL, MD]; Cray XC30 [AFRL, OH]; SGI ICE X [ERDC, MS]; SGI ICE X [AFRL, OH]; SGI ICE X [ARL, MD]

Research Objectives: To determine phase stability and decomposition mechanisms in energetic materials subjected to elevated temperatures and pressures.

Methodology: Crystal structure optimization and *ab initio* molecular dynamics (MD) simulations are being used to study physical and chemical changes in high-energy-density molecular crystals subjected to elevated temperatures and pressures. These calculations rely on density functional theory (DFT) and periodic-cell models to approximate bulk crystalline environment. Structure optimizations use variable-cell optimization algorithms to determine changes in crystal structures and lattice constants at elevated pressures. *Ab initio* MD simulations use constant-pressure, constant-temperature (NPT) and constant-volume, constant-energy (NVE) integrators combined with multiple replicas to simulate target thermodynamic conditions and probe decomposition mechanisms triggered by these conditions. Python and Perl scripts are being developed to streamline input deck preparation, job execution, and data analysis.

Results: This year, DFT-based crystal structure optimization were completed for hydrostatically compressed pentaerythritol tetranitrate (PETN). Optimizations initiated with the experimental tetragonal PETN I crystal structure were found to preserve the tetragonal symmetry ($a = b \neq c$) of the initial structure, resulting in converged tetragonal structures at all pressures (Fig. 1a). Optimizations initiated with a manually-prepared orthorhombic structure ($a \neq b \neq c$) also resulted in tetragonal structures at lower pressures, but converged to a high-density orthorhombic structure at 30 GPa. We subsequently used the orthorhombic structure relaxed at 30 GPa to re-initialize optimizations at all pressures. These resulting optimizations produced converged orthorhombic structures at progressively lower pressures, until they reverted to tetragonal symmetry below 16 GPa (Fig. 1b). The low-density tetragonal and high-density orthorhombic structures converged at 20 GPa are compared in Fig. 1c. A symmetry analysis confirmed that the tetragonal structure exhibits symmetry of the $P4_2/c$ space group and the orthorhombic structure exhibits symmetry of the $P2_12_12$ space group, in agreement with prior deductions based on experimental data. To assess the relative stability of the two phases as a function of pressure, we calculated the pV -corrected electronic energies (0 K enthalpies excluding zero-point energy) of the optimized structures. The resulting differences in the enthalpies and densities at each pressure computed with various DFT methods are plotted in, respectively, Figs. 1d and 1e. All of these calculations predict that the high-density orthorhombic phase becomes more stable than the tetragonal phase at a sufficiently high pressure, but the predicted transition pressure varies widely from 16 to 23 GPa.

DoD Impact/Significance: PETN is used extensively in detonating fuses and exploding bridgewire detonators. Tailoring its behavior under shock compression and transition to detonation is important for reliability and safety of these devices. A shock-induced transition from its ambient tetragonal phase to a lower-symmetry, high-density phase has been suggested to contribute to detonation initiation in PETN. Our simulations support experimental observations of a stable orthorhombic phase, but predict a higher transition pressure of 16 GPa.

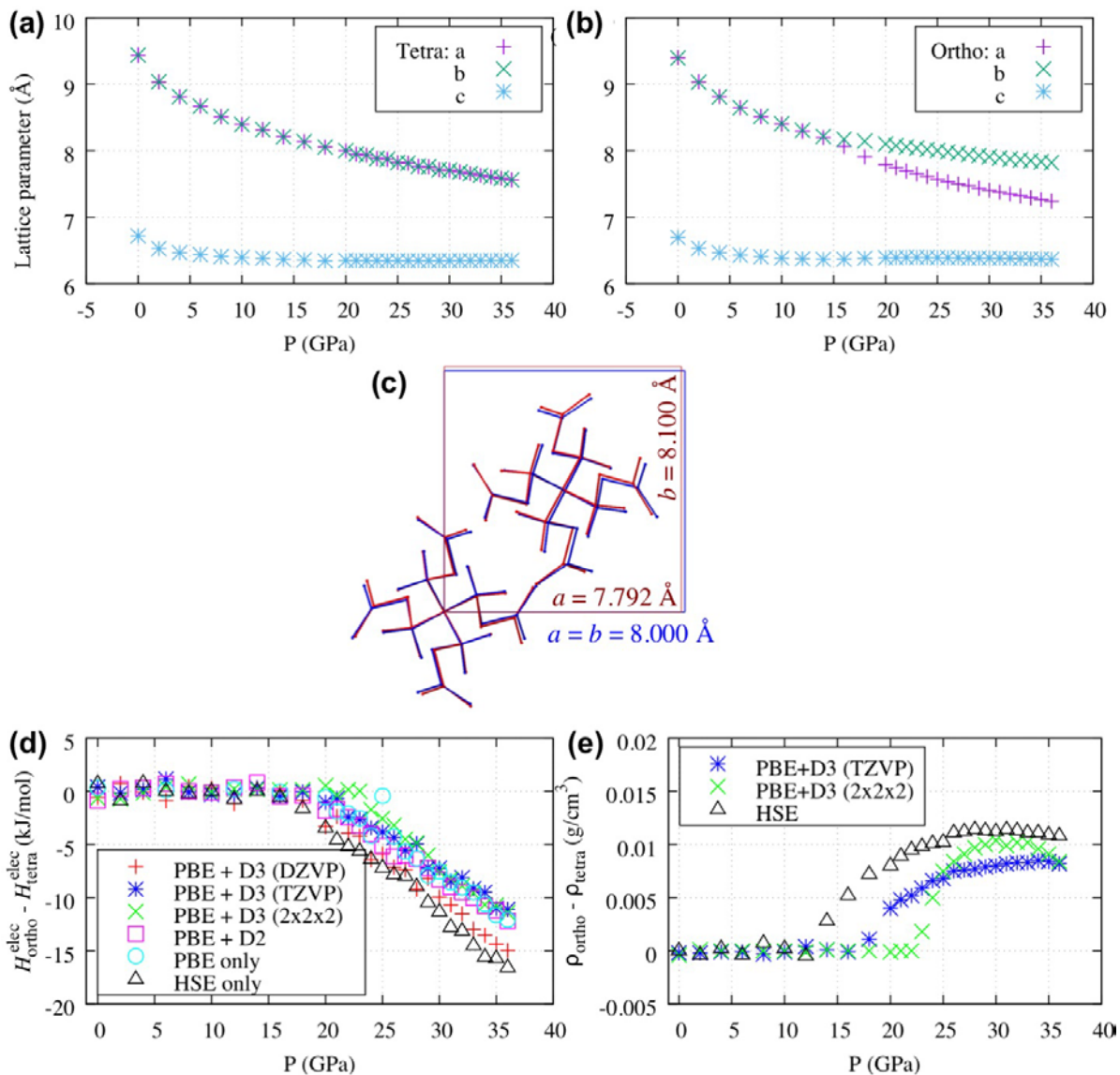


Figure 1. (a) Optimized lattice parameters of PETN based on a tetragonal initial structure. (b) Same but with an orthorhombic initial structure. (c) The low-density tetragonal (blue) and high-density orthorhombic (red) unit cells of PETN optimized at 20 GPa, as viewed down the "c" axis. (d) The difference in enthalpies calculated for optimized crystal structures obtained using initial conditions with tetragonal and orthorhombic symmetry. (e) The difference in densities between the same structures.

Title: Growth and Control of Metal Films on Semiconductor Substrates

Author(s): S.C. Erwin

Affiliation(s): Naval Research Laboratory, Washington, DC

CTA: CCM

Computer Resources: SGI ICE X [AFRL, OH]

Research Objectives: To develop an atomistic model, based on density-functional theory (DFT) and kinetic Monte Carlo simulations, that explains the role of the hydrogen plasma that is commonly used during atomic layer epitaxial growth of aluminum nitride.

Methodology: We used DFT in the generalized-gradient approximation of Perdew, Burke, and Ernzerhof (PBE). Accurate total-energy calculations are required to reveal the most stable configurations of the precursor material, find the relaxed structure of the nanoplatelet, and to identify the reaction paths connecting these states. Highly efficient and precise total-energy and force calculations were critical for the work. The projector-augmented-wave (PAW) method as implemented in VASP is the ideal tool.

Results: We proposed a model for the role of the hydrogen plasma in atomic layer epitaxial growth of aluminum nitride. In the model, the plasma produces atomic hydrogen that participates in chemical reactions on the surface, which is initially covered by methyl radicals left over from decomposition of the precursor molecules used to deliver aluminum. Two simple gas-surface reactions—hydrogen addition and hydrogen abstraction—trigger a chain of reactions that causes some of these methyl radicals to desorb as methane, and others to become trapped in the subsurface region as carbon impurities. We modeled the dynamics of this system—including its dependence on temperature and hydrogen pressure—using rate equations, density-functional theory, and atomistic statistical simulations.

DoD Impact/Significance: This theoretical project complements an experimental New Challenge project, Ultrathin Multicomponent Electronic Materials, based in NRL's Electronics Science & Technology Division. One goal of that program is to use atomic layer epitaxy (ALE), a promising new technique, to grow thin films of nitride-based electronic materials. Despite the promise of ALE, a full understanding of how the commonly used hydrogen plasma affects atomic layer epitaxial growth is not yet in hand. Plasmas produce ions, neutral atoms, electrons, and photons, but the role of these species in the growth remains unclear. We clarify this situation and demonstrate that using a hydrogen plasma has two previously unrecognized consequences, one of which is beneficial and the other detrimental. The resulting picture leads to a proposed solution for the carbon contamination that leaves the main benefit of the plasma unaffected.

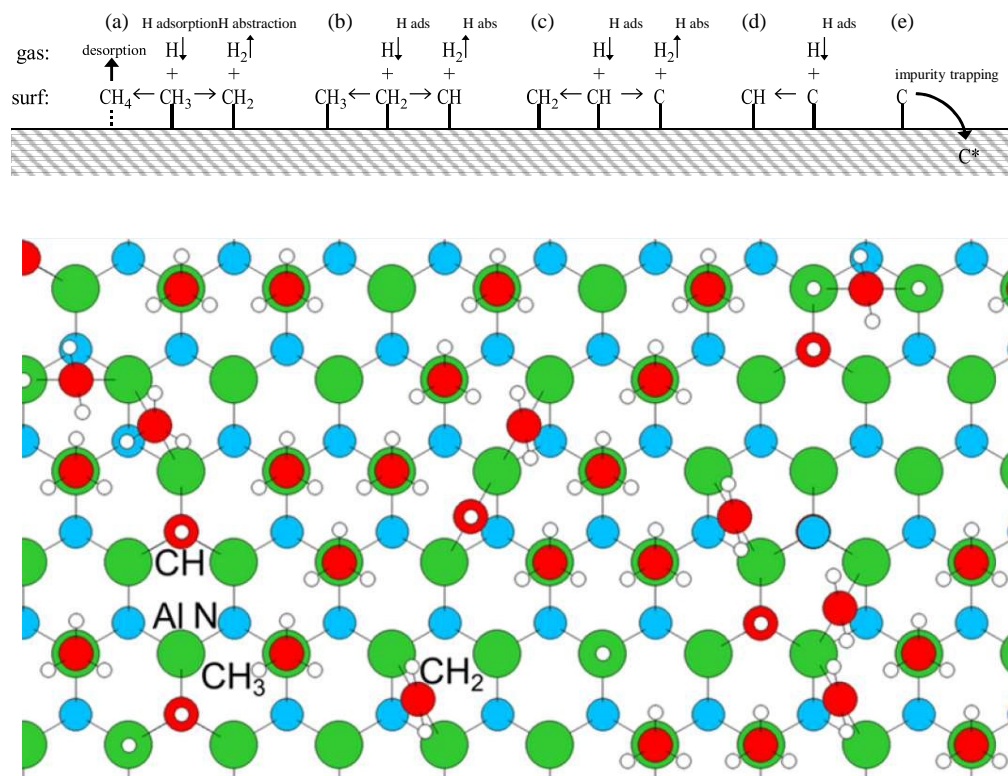


Figure 1. Overview of the chemical reactions considered at the Al-terminated (0001) surface of aluminum nitride after the growth of an aluminum layer from the TMA precursor, $\text{Al}(\text{CH}_3)_3$. Complete decomposition of the TMA molecules leaves the surface covered by strongly bound CH_3 methyl radicals which, if not removed, prevent the growth of the subsequent nitrogen layer. (a–d) Atomic hydrogen, created in the gas phase by the hydrogen plasma, can combine with CH_3 to trigger a sequence of hydrogen adsorption and hydrogen abstraction reactions. This sequence leads to a competition between two terminal processes: (a) desorption of CH_4 and (e) incorporation of atomic C as a trapped subsurface impurity. The five panels illustrate the sequence of reactions, as described in the text. (Bottom panel) Snapshot of surface partially covered by hydrocarbons.

Title: Sequence Clustering

Author(s): D. Zabetakis, J.L. Liu, G.P. Anderson, and E.R. Goldman

Affiliation(s): Naval Research Laboratory, Washington, DC

CTA: CCM

Computer Resources: SGI Altix ICE [NRL, DC]

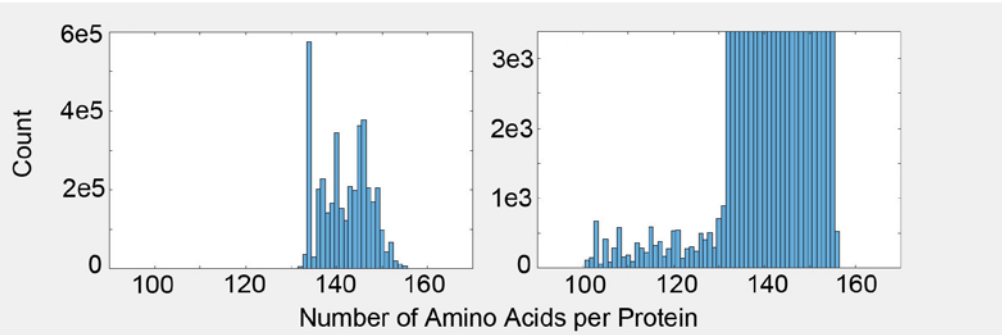
Research Objectives: The purpose of our research is to develop protein reagents for the detection and identification of bio-threat agents of concern to the DoD. Our focus is the single-domain antibody which is a derivative of the natural immune system product of certain species of animal, in this case the llama. Our target pathogen in this project is the virus which causes Dengue fever, a mosquito-borne disease of greatly increasing concern in warm climates. Our process involves the creation of a library of many millions of genes that encode for antibodies from an immunized llama. A small fraction of these antibodies are specific for the target virus protein and must be isolated for study and use as potential detection reagents.

Methodology: An automated method called Next-Generation-Sequencing allows for the recovery of up to 12 million DNA sequences from the library. A major problem is that library construction and sequencing is not a high-fidelity process. Large number of sequence variations are unintentionally introduced. The antibodies themselves also possess (in part) highly variable DNA sequences. In order to resolve this difficulty, it is advantageous to group the antibodies into clusters of highly-related sequences. Each cluster then represents a group that derives from an original unaltered sequence. Since this is an all-against-all comparison, an exceptionally high level of computation resource is necessary when the number of sequences reaches into the millions. A published program, CD-HIT, is available to carry out this function.

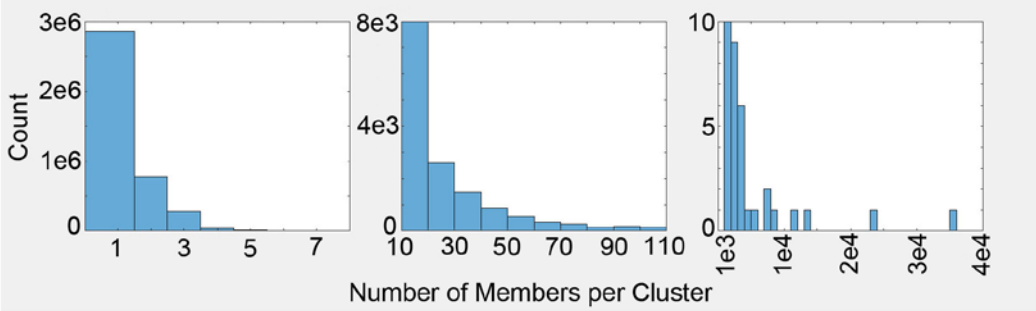
Results: Figure 1 shows a sample of results from our work using the HPCMP resources. Panel 1 shows the results of the CD-HIT clustering with the identity score set to 1. The members of each cluster have identical sequences. Basic information is displayed about the size of the proteins, and the number of members of each cluster. Panel 2 shows a representation of the crystal structure of a single-domain antibody. Panel 3 shows a calculation of the isoelectric point of the proteins represented by each cluster. Panel 4 shows the amino acid sequences of a group of antibodies selected from the extremes of Panel 3. This type of analysis allows for the characterization of the library and will facilitate the recovery of the most suitable antibodies.

DoD Impact/Significance: This work relates to the protection of deployed personnel in regions where infectious diseases are endemic. The three aspects of detection, identification, and therapy all require reagents such as antibodies that effectively interact with specific antigens of the relevant pathogens. Next-Generation-Sequencing and High Performance Computing will assist in finding and developing these reagents.

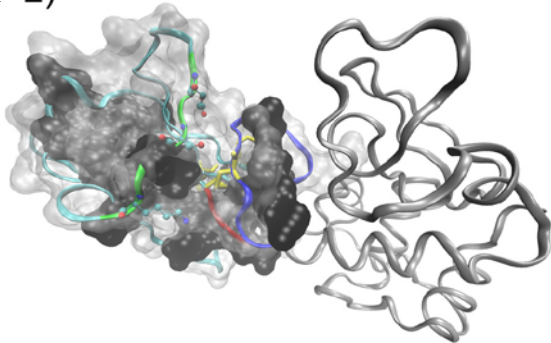
Panel 1 a)



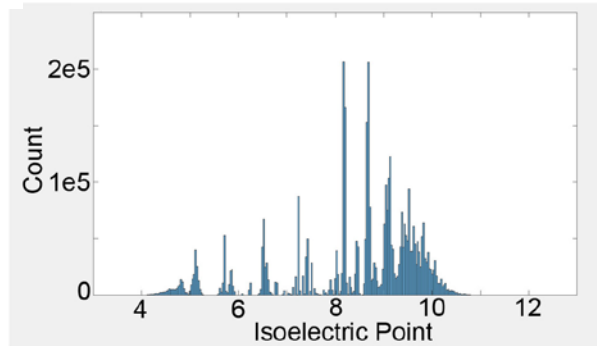
Panel 1 b)



Panel 2)



Panel 3)



Panel 4)

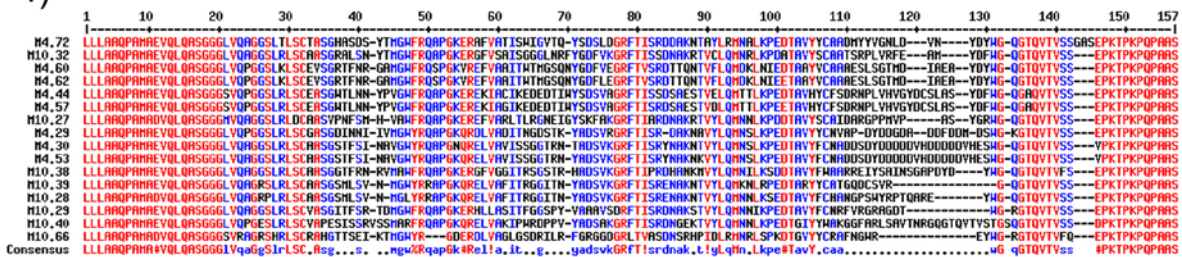


Figure1. Analysis of a library of antibodies against a Dengue virus protein. 1a) Histograms of length of the proteins in the library, shown at two different Y-axis scales. 1b) Histograms of the number of members of each cluster (identity=1) shown at three different scalings of the X- and Y-axes. The majority of clusters have a single member. The few largest clusters have over 10,000 members. 2) Structural representation of an antibody (space-filling model) bound to its antigen (ribbon model). 3) Histogram of isoelectric point calculated for the clusters. 4) Protein sequence alignment of antibodies with isoelectric points near 4 and 11.

Title: Calculation of Materials Properties via Density Functional Theory and Its Extensions

Author(s): J.L. Lyons

Affiliation(s): Naval Research Laboratory, Washington, DC

CTA: CCM

Computer Resources: SGI ICE X [AFRL, OH]; Cray XC40 [ARL, MD]

Research Objectives: The main objective of the project is to understand the roles played by defects, dopants, and interfaces in wide-band-gap semiconductor (WBGs) materials using density functional theory (DFT), as well as related methods (such as hybrid functionals) that overcome the band-gap problem.

Methodology: DFT has long been the method of choice for determining the electronic structure of materials. However, when applied to WBGs, the well-known “band-gap problem” causes difficulties in quantitatively determining not only bulk band structures, but defect properties as well. To overcome this problem, we plan to employ hybrid functional calculations. Hybrid functionals mix in screened Hartree Fock exchange into the exchange-correlation functional, and are capable of quantitative predictive accuracy. Hybrid DFT is used to determine the charge-state transition levels, formation energies, and optical transitions associated with defects and impurities in WBGs.

Results: We investigated the electrical properties of acceptor dopants in Ga_2O_3 using hybrid functional calculations and the VASP code. All impurities were found to have ionization energies in excess of 1.3 eV, meaning that none will be able to give rise to *p*-type conductivity. Furthermore, by examining formation energies as a function of chemical potential we found that Mg_{Ga} followed by Be_{Ga} were the most likely to incorporate into gallium oxide.

We also investigated how carbon impurities incorporate into nitride semiconductors during atomic-layer epitaxy (ALE) growth, using a combination of kinetic Monte Carlo (kMC) simulations together with DFT.

We found that the plasma present during ALE growth, which is crucial for scrubbing methyl species from the surface, also has the effect of dehydrogenating these species. This can lead to atomic C on the nitride surface, which we determined to have moderate barriers to incorporation into the nitride bulk. Based on these results, we provided guidance for how to minimize the amount of C incorporation into ALD-grown nitrides.

DoD Impact/Significance: WBGs such as GaN are utilized a number of devices (including high-power transistors and photodetectors) that play a crucial role in many naval applications, and afford significant cost and weight savings when replacing components based on traditional materials such as silicon or gallium arsenide. Moreover, materials such as Ga_2O_3 have the potential to outperform GaN, but optimizing doping strategies, understanding contaminants, and characterizing unintentionally incorporated defects are crucial steps for improving these materials.

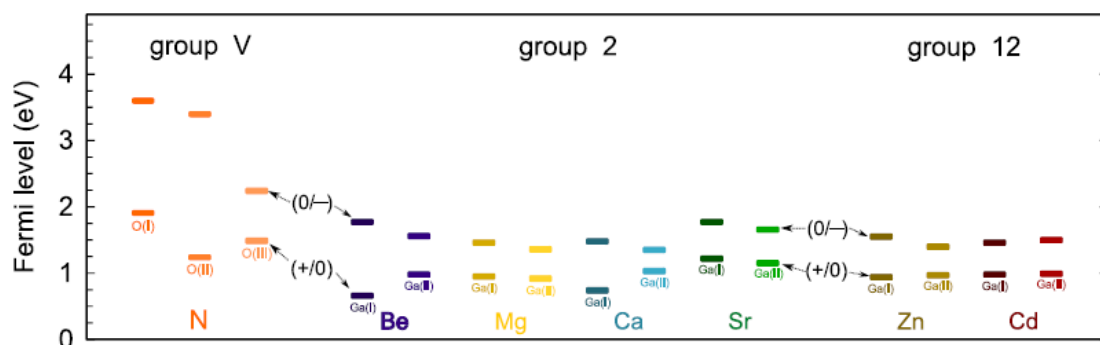


Figure 1. transition levels of acceptor impurities in $\beta\text{-Ga}_2\text{O}_3$

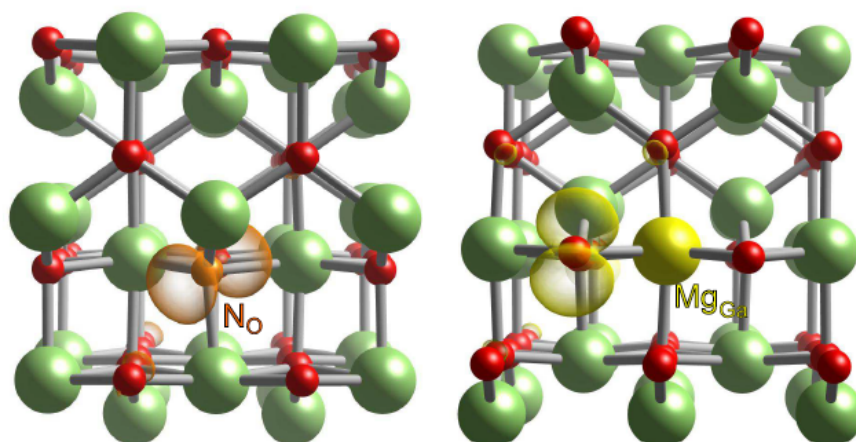


Figure 2. spin densities of anion-site (left) and cation-site (right) acceptors

Title: Materials for Energy Storage and Generation
Author(s): M. Johannes
Affiliation(s): Naval Research Laboratory, Washington, DC
CTA: CCM

Computer Resources: SGI ICE X [ARL, OH]

Research Objectives: The objectives of this program are to use density functional theory (DFT), ab-initio molecular dynamics and machine-learning generated empirical potentials to understand and modify functional materials. More specifically, we strive to design or improve materials for Li-ion batteries and phase change memory devices.

Methodology: First principles pseudopotential methods are employed to calculate the quantities of interest. The majority of the work was done using the Vienna Ab-Initio Software Program (VASP), but a substantial minority was done using the Wien Code which is a full potential LAPW code. Post-processing is done using personal codes. Both standard (static)T=0 DFT calculations and temperature-dependent molecular dynamics (MD) calculations were used. A Gaussian Approximation Potential (GAP) generated via machine learning was employed for large scale temperature-dependent phase change calculations.

Results: In FY18, Li-ion battery research was concentrated on the stability of high voltage cathode materials against outgassing and/or structural degradation due to oxygen release. Previous studies and a predictive methodology developed in last year's project indicate that oxygen release in a given structure depends on the particular transition metal element that serves as the redox couple. According to simulations, Co can be used as the redox center, but it is only barely stable. This year's research showed that "alloying" (~12%) with Fe shifts the redox center to the more stable Fe ion, but also stabilizes the Co that is accessed deeper in the cycle via intra-transition metal bonding.

Studies on phase change materials for non-volatile memory in FY18 produced an empirical potential capable of handling three times the number of atoms at a two orders of magnitude faster computational speed. This allows for examination of phase change phenomena, including phase change fronts and the influence of "seed" crystals in the amorphous phase. Several potentially significant results were found. The first is that N dopants are highly energetically favored to form N₂ molecules which subsequently displaced Ge atoms from their crystallographic sites into interstitials. This occurs even at T=0. At higher temperatures, N atoms may attach to Ge relatively stably and therefore not migrate far enough to find a second N for molecular formation. In this case, clustering of the Ge around one or more N atoms occurs, which may be related to the experimentally observed segregation of N to the grain boundaries.

DoD Impact/Significance: Safety concerns have come to have primacy over rate and power criteria for DoD energy storage devices/materials. While performance in the field is important, safety is essential. This work has helped to describe what causes safety failures in Li-ion batteries and possible routes to stabilize against the factors that catalyze catastrophic breakdown. Non-volatile memory capable of operating at the elevated temperatures of high power applications relevant to many naval operations will be important for future unmanned vehicles, particularly those that are land-based.

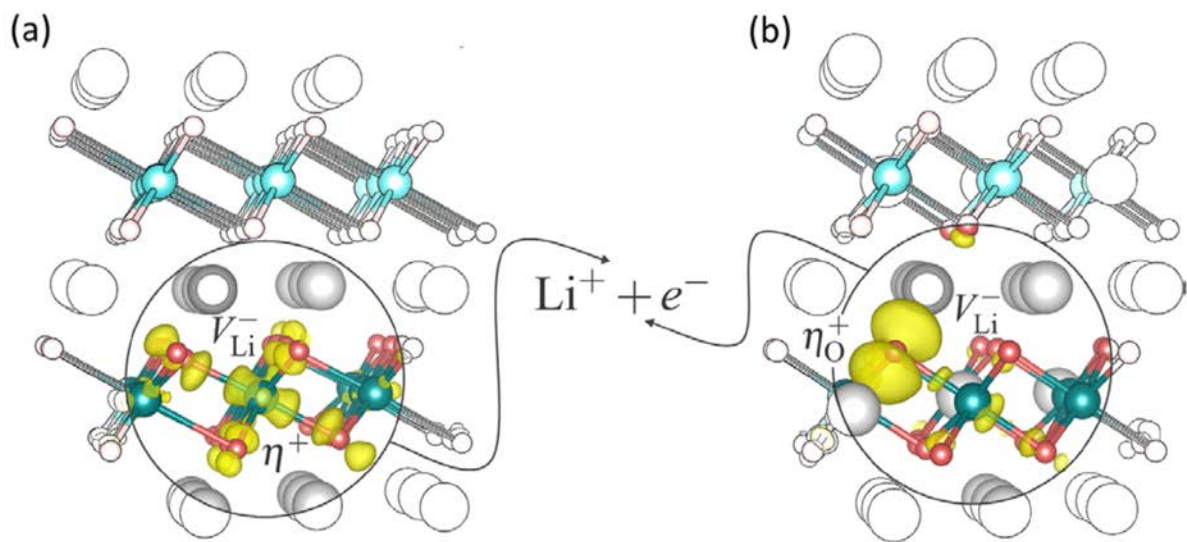


Figure 1. Different redox reactions in LiMnO₂, a high power Li ion battery material. a) Stable electron withdrawal leaves a hole (yellow density) at the Mn site, with minor weight at the oxygen sites. b) Unstable electron withdrawal leaves the hole at the oxygen site, leaving peroxide that is prone to recombination into a more stable O₂ or OH⁻ gas that damages the structure of the cathode.

Title: Surfaces and Interfaces in Oxides and Semiconductors
Author(s): C.S. Hellberg
Affiliation(s): Naval Research Laboratory, Washington, DC
CTA: CCM

Computer Resources: SGI ICE X [AFRL, OH]; SGI ICE X [ERDC, MS]; SGI ICE X [ARL, MD]; Cray XC40 [ARL, MD]; Cray XC30 [AFRL, OH]

Research Objectives: Determine the microscopic origin of electron pairing without superconductivity recently observed in SrTiO₃. Experiments have indirectly shown that the pairing occurs at twin domain walls in the material. We will compute these planar defects to determine their electronic structure and the pairing interaction between electrons at the domain walls.

Methodology: We performed highly accurate first-principles density functional calculations of very large (containing up to 640 atoms) SrTiO₃ computational cells to determine the atomic structure of the twin domain walls. By varying the size of the domain walls, we show that elastic interactions between domain walls extend approximately 3 nm. Fortunately, we are able to separate the domain walls in the calculations by more than 6 nm, well beyond the interaction range. We used the VASP Density Functional Theory (DFT) code at the AFRL, ERDC, and ARL HPC centers.

Results: We find that two types of twin domain walls are stable, as shown in Figure 1. The tetragonal order parameter, indicated by the arrows, is determined from the rotation of the oxygen octahedra using the right-hand rule. The order parameter rotates by approximately 90 degrees as the domain wall is crossed. In the “head-to-tail” domain walls, the order parameter rotates through the normal to the domain wall plane. In the “head-to-head” domain walls (which can be equivalently defined as “tail-to-tail”), the order parameter rotates through the plane of the domain wall. The domain walls are meta-stable—a uniform structure without domain walls has a lower energy. Nevertheless, domain walls form naturally as the material is cooled below the tetragonal transition temperature. Our next steps will be to examine the interaction of conduction electrons with the domain walls.

DoD Impact/Significance: Superconductivity is used for numerous applications. Our current understanding of superconductivity in SrTiO₃ assumes a homogeneous material with no domain walls. There are independent experimental probes suggesting the domain walls may become superconducting at higher temperatures than the bulk material. This research could help the design of metamaterials with elevated superconducting transition temperatures.

Figure 1.

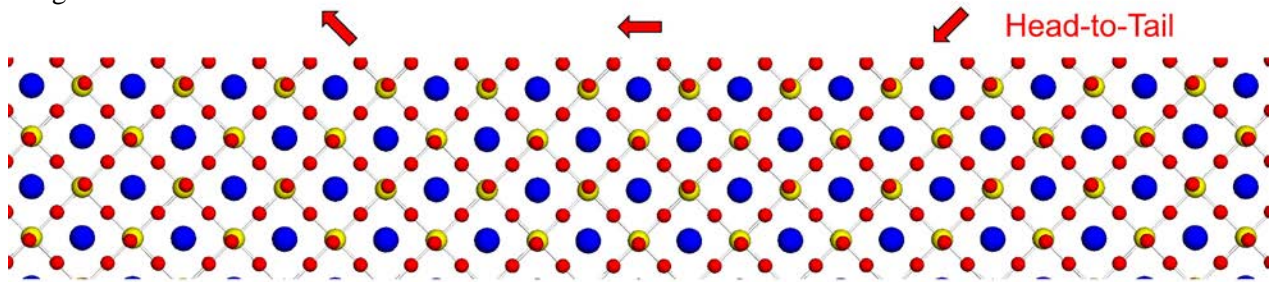


Figure 2.

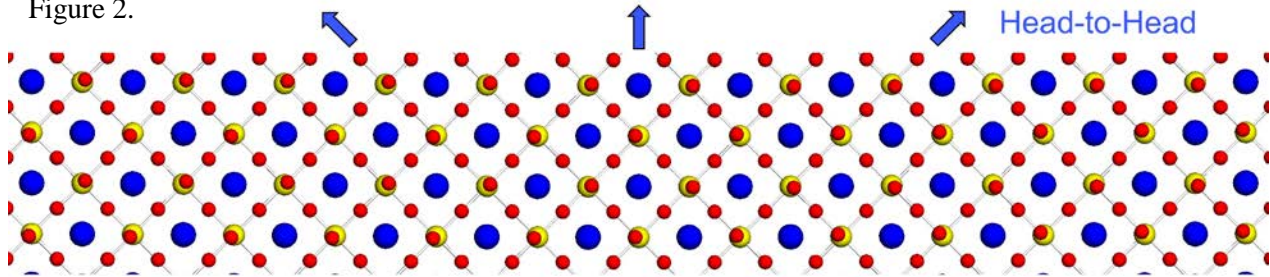


Figure 1. Two types of twin domain walls are stable between tetragonal domains in SrTiO_3 . The domain walls are vertical in the middle of each figure. Sr atoms are blue, Ti atoms are yellow, and O atoms are red. Notice the antiferrodistortive rotation of the red oxygen's relative to the yellow titanium atoms. The tetragonal order parameter, indicated by the arrows, is determined using the "right-hand rule" from the rotation of the oxygen's in one layer. The oxygen's in neighboring layers rotate oppositely. In the "head-to-tail" domain walls, the order parameter is normal to the domain walls, and the oxygen's at the domain wall rotate in the plane of the domain wall. In the "head-to-head" or equivalently "tail-to-tail" domain walls, the order parameter rotates through the plane of the domain wall at its center, and the oxygen's rotate out of the plane of the domain wall.

Title: Multiple Length and Time Scale Simulations of Material Properties

Author(s): N. Bernstein

Affiliation(s): Naval Research Laboratory, Washington, DC

CTA: CCM

Computer Resources: Cray XC40 [ARL, MD]; SGI ICE X [AFRL, OH]; SGI ICE X [ERDC, MS]

Research Objectives: To understand and predict mechanical, structural, and energetic material properties

Methodology: Molecular dynamics (MD) and Monte Carlo (MC) simulations for the time evolution and sampling of atomic configurations. Trajectories use energies and forces from density functional theory (DFT) and interatomic potentials. Nested sampling is used for calculating thermodynamic quantities and phase diagrams. Gaussian approximation potential (GAP) method is used for developing single and multi-species interatomic potentials. The software implementing these methods included VASP for DFT simulations, LAMMPS for interatomic potential MD, ASE and libAtoms/QUIP for GAP development and interfacing between various programs, and pymatnest for nested sampling.

Results: A paper describing the nested sampling method for calculating phase diagrams was published. Work on the method has continued, extending it to multicomponent materials with the possibility of phase separation, evaluating how it scales with simulated system size, and extending it to models of open network materials such as silicon or water. Comparisons of atomistic and coarse-grained models for polymers were completed and published in two papers, and the resulting coarse-grained models are currently being tested with nested-sampling.

A manuscript describing a Gaussian approximation potential (GAP) for silicon is currently under review. This potential shows excellent performance across a very wide range of configurations, and promises to be a revolutionary tool for simulating structural and dynamical properties of Si. Several iterations of the development of a GAP model for GeTe+N were carried out. So far those show excellent performance for GeTe, and are currently being tested for their accuracy in reproducing the interactions of the host material with N and N₂ impurities.

DoD Impact/Significance: Structural and dynamical properties of a wide range of materials impact a wide range of DoD technologies, from structural materials such as metal alloys and polymer-based composites to functional materials for sensors and computing. Machine-learning based interatomic potentials are an emerging approach for fast but accurate descriptions of the interactions between atoms. The work on a potential for GeTe+N will enable design of devices using this phase-change material for fast non-volatile storage and microwave switching. In general, however, developing the database to fit such potentials is laborious and time consuming, and the new approach for automated generation of such data could greatly reduce the effort to develop such potentials.

Of significance is the phase diagram of a material, i.e., its structure as a function of parameters such as temperature, pressure, and composition, controls its properties and therefore its technological applications. The nested sampling method for calculating such phase diagrams is a powerful new tool that could enable design of materials for many applications. Applying it to polymers such as polyethylene (used in armor under brand names such as Spectra and Dyneema), using coarse-grained models to make the problem computationally tractable, will make it possible to determine their atomic structure, and therefore mechanical properties, so they can be optimized. Because the molecules with best properties are very long (UHMW - ultra-high molecular weight), the simulated systems are large, and optimizing the method for such large systems will be required to enable the approach.

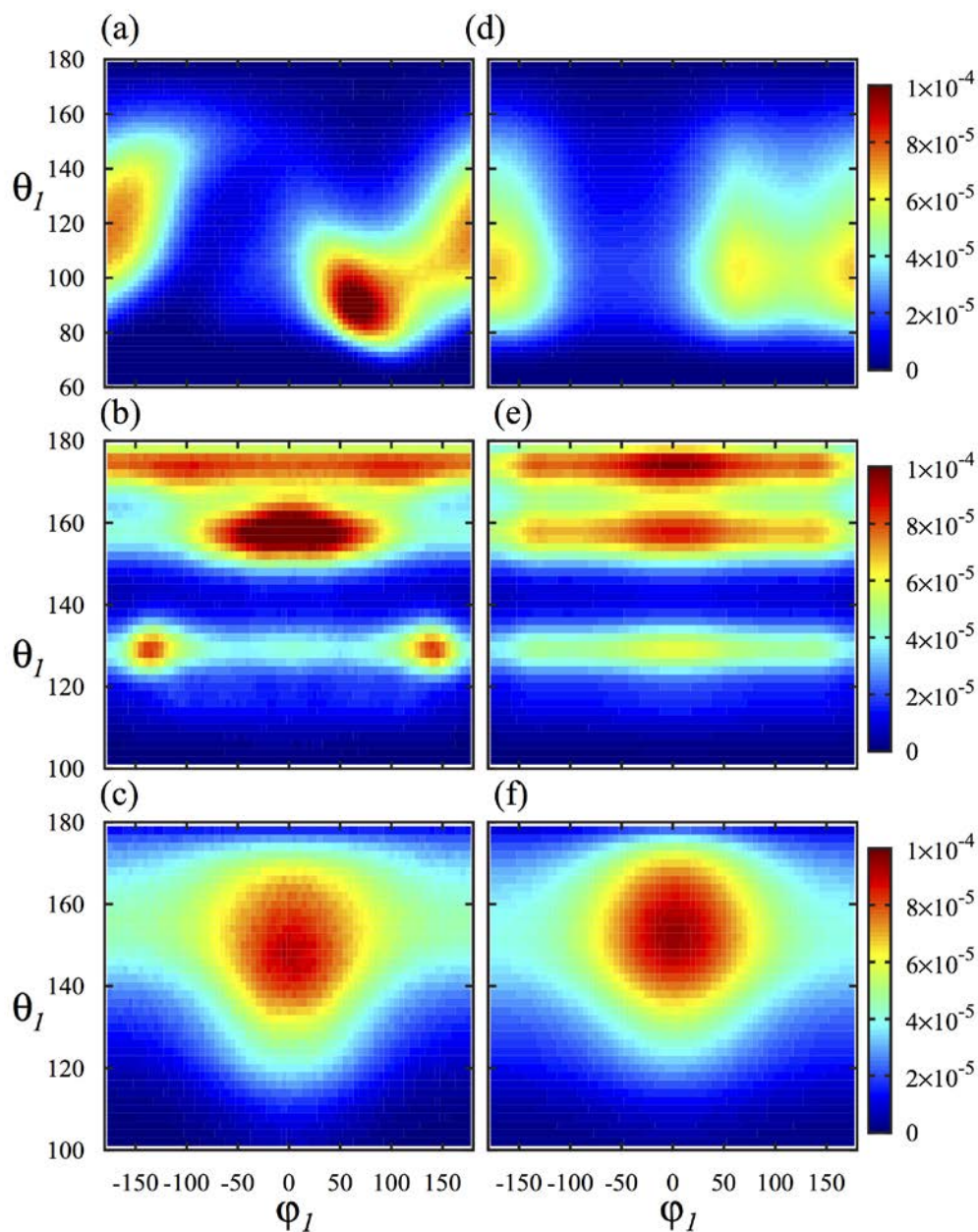


Figure 1. Joint probability distribution functions for coarse grained variables (theta - bond angle, phi - dihedral angle) sampled from atomistic simulation (left) and calculated with a simple independent angle model (right). Differences between left and right panels indicate a deficiency in the conventional independent angle approximation that requires additional correlations be included in the coarse-grained model. Top panels show results for 3-center coarse-grained poly-L-lactic acid, middle panels show 2-center coarse-grained polytetrafluoroethylene (PTFE, Teflon), and bottom panels show 4-center coarse-grained PTFE.

Title: IR Absorption Spectra for Chlorinated Hydrocarbons in Water Using Density Functional Theory

Author(s): S. Lambrakos, ¹L. Huang, ² and L. Massa³

Affiliation(s): ¹Naval Research Laboratory, Washington, DC; ²Volunteer Emeritus; ³City University of New York, NY

CTA: CCM

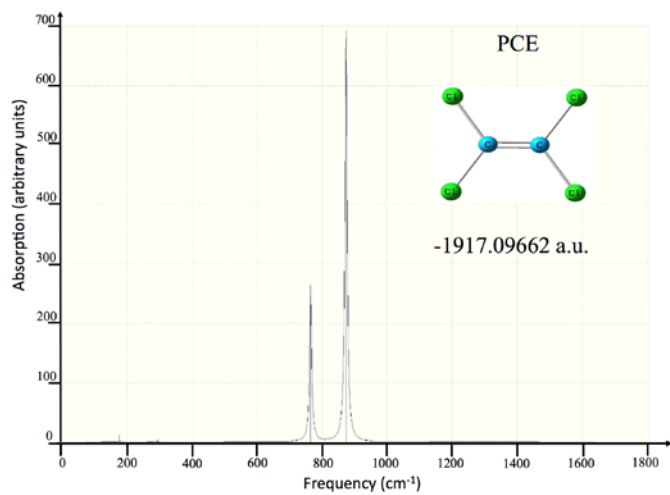
Computer Resources: Cray XC40/50 [ERDC, MS]; SGI ICE X [AFRL, OH]

Research Objectives: IR absorption spectra for PCE-nH₂O, TCE-nH₂O, DCE-nH₂O, VC-nH₂O molecular clusters calculated using density functional theory.

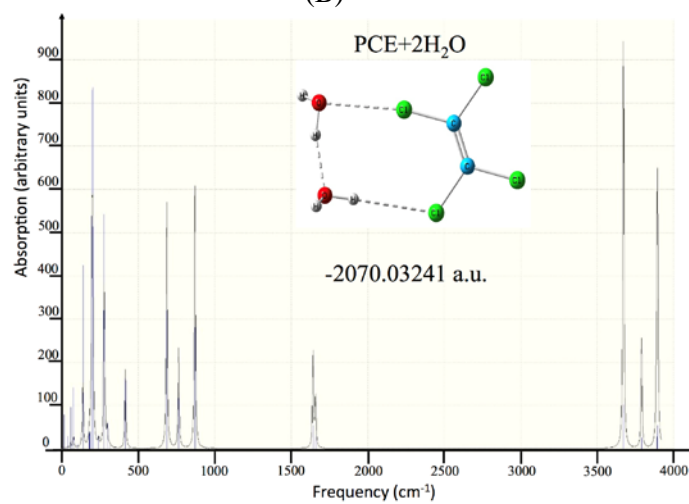
Methodology: The present study examines calculation of infrared (IR) spectra for molecular clusters PCE-nH₂O, TCE-nH₂O, DCE-nH₂O, VC-nH₂O using quantum-theory based calculations, i.e., density functional theory (DFT) and associated software technology, which can potentially provide complementary information to that obtained from spectroscopic measurements. This complementary information should be in terms of the physical interpretation of spectral features with respect to molecular structure, and the prediction of spectral features that are difficult to measure in the laboratory. The present study adopts the software GAUSSIAN09 (G09) for the calculation of IR absorption spectra.

Results: The results of our study are relaxed or equilibrium configurations of PCE-nH₂O, TCE-nH₂O, DCE-nH₂O, VC-nH₂O molecular clusters having different sizes and geometries, ground-state oscillation frequencies and associated IR intensities for molecular-cluster geometries having stable structures, which are calculated by DFT [1]. A graphical representation of the molecular geometry of an isolated molecule of PCE and stable molecular clusters PCE-nH₂O (n=2 and 7) are shown in Figs. 1A-1C, respectively. DFT calculated IR intensities as a function of frequency for these molecular structures are shown in these figures. Comparison of calculated spectra shown in Figs. 1A-1C, shows that spectral features of PCE-nH₂O tend essentially to those of pure water, even for small cluster sizes. These spectral features are consistent with spectroscopic measurements demonstrating the difficulty of detecting low concentrations of the chlorinated hydrocarbon molecules PCE, TCE, DCE and VC in solution.

DoD Impact/Significance: The properties of PCE, TCE, DCE, and VC molecules are of major importance for monitoring and detection of chlorinated hydrocarbons in water. This follows in that PCE, TCE, DCE, and VC, which are part of a specific chemical transformation sequence ending in ethene, are among toxic and carcinogenic contaminants commonly found in the environment, e.g., ground water. The detection of these hydrocarbons, especially in the presence of water, using methods based on (IR) spectroscopy is of particular interest. Specifically, IR spectral signatures, i.e., fingerprint spectra, can be correlated with the presence of these hydrocarbons. Absorption spectra of relatively small molecular clusters, however, represent a separate regime for dielectric response with respect to electromagnetic wave excitation, and thus for detection methodologies, which must consider filtering out of background spectral features. IR absorption spectra within this regime should be better quantified for improved detection methodologies.



(B)



(C)

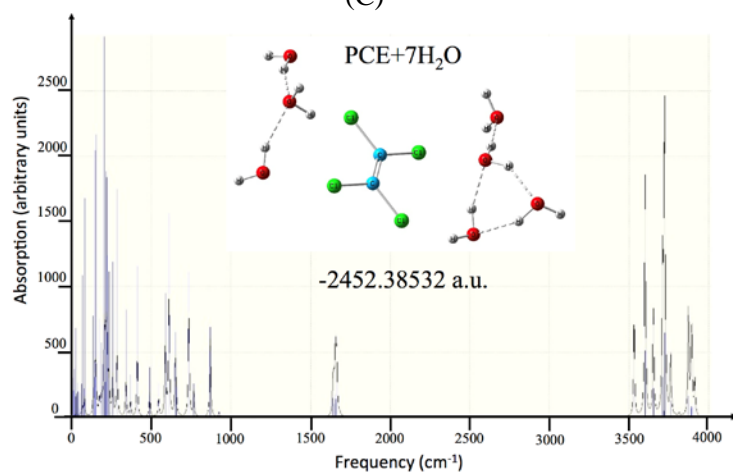


Figure 1. DFT calculated equilibrium geometry, minimal energy and IR spectra of (A) isolated PCE molecule, (B) PCE-2H₂O and (C) PCE-7H₂O.

Title: High-Throughput Search for New Magnetic Materials and Noncollinear Magnetism

Author(s): I. Mazin,¹ and J. Glasbrenner²

Affiliation(s): ¹Naval Research Laboratory, Washington, DC; ²George Mason University, Fairfax, VA

CTA: CCM

Computer Resources: SGI ICE X [ARL, MD]; SGI ICE X [ERDC, MS]; SGI ICE X [AFRL, OH]

Research Objectives: Understanding relativistic and nonrelativistic magnetism, including noncollinear systems, and using high-throughput methods to discover new magnetic materials.

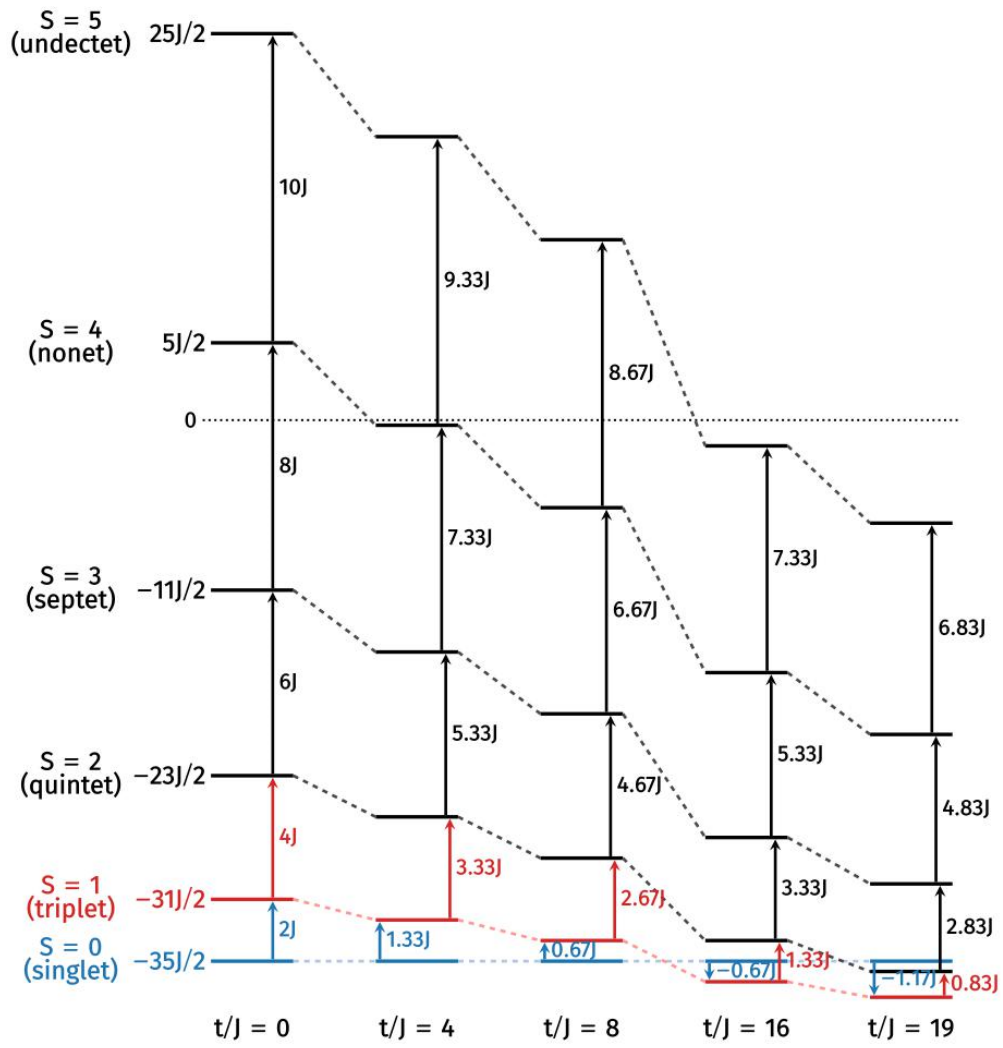
Methodology: We performed *ab initio* density functional theory (DFT) calculations, using the all-electron code ELK and the pseu-dopotential code VASP at the AFRL and ERDC HPC centers. These codes can calculate the total energy for preset magnetic moment directions on each atomic site, as well as full self-consistent relaxation of both the amplitudes and directions of individual magnetic moments, also calculating total energy of incommensurate magnetic spirals. VASP can be also used to efficiently optimize crystal structures.

Results: Together with experimentalists, we followed a prediction we made in an earlier study, that the nearest-neighbor exchange coupling J in $(\text{Ba}_{1-x}\text{K}_x)(\text{Zn}_{1-y}\text{Mn}_y)_2\text{As}_2$, a dilute magnetic semiconductor (DMS) reduces with K x . Our collaborators measured the excitation of the Mn-Mn dimers using neutron scattering for $x = 0-0.20$. We calculated the corresponding spin flip energies, and fitted them to the spectrum of the ideal spin-5/2 dimer with double exchange. This revealed that our model exhibits a degeneracy when J is either 12 or 18 times the hopping t . We found that our DFT calculations overestimate J , likely due to DFT's underestimation of the Hubbard repulsion. Interestingly, the experiment detected a minor decrease in J but observed significant broadening. This suggests that the Mn-Mn interactions in the doped case are not described by the same 2-spin Hamiltonian as in the undoped one. Rather, one should solve the entire problem in the spirit of the Fano model in optics, which leads to complex changes in the excitation lineshape, but only to a very modest energy shift. However, this was beyond the scope of our study.

We also wrapped up and finalized publication of two other projects: (1) Calculations of the collapsed tetragonal phase (CTP) of the $(\text{Ca,Sr})(\text{Fe,Rh})_2\text{As}_2$ Fe-based superconductor (FeBS). We found that subtle variations in the Fe-As geometry strengthened covalent bonding at the expense of exchange splitting, suppressing magnetism, and thus the CTP appears due to a sharp change in the intralayer bond angle, and not As-As bond. (2) Another collaboration with experimentalists, investigating energy and spin susceptibility under pressure of another FeBS, EuFe_2As_2 . Again, we concluded that the observed shrinking of the c lattice parameter around 2.7 GPa is due to an abrupt change in the Fe-As bond length caused by the suppression of magnetism. Experimental evidence was found of novel noncollinear phase close to 2.7 GPa.

DoD Impact/Significance: This DMS is robust and has a high Curie temperature, overcoming the shortcomings of the traditional DMS. It is important to understand these novel systems to design a working DMS, which can be used to create a spin-logic device. The discrepancies between the measurements and calculations+dimer model indicate additional effects that impact magnetism and will require more sophisticated modeling.

Pressure-induced superconductivity is observed in several FeBS and coincides with the collapse of the lattice c parameter. We have shown that the magnetism in CaFe_2As_2 and EuFe_2As_2 , changes rapidly in the pressure region close to superconductivity. For EuFe_2As_2 , there is experimental and computational evidence that the magnetic order at this point may be of a different kind, which would imply different type of spin-mediated superconductivity. For CaFe_2As_2 , we showed that the Fe-As bond controls magnetism, ultimately driving the CTP transition, not the specific details of the As-As bond, as was long believed.



Title: Numerical Studies of Semiconductor Nanostructures

Author(s): T.L. Reinecke¹ and S. Mukhopadhyay²

Affiliation(s): ¹Naval Research Laboratory, Washington, DC; ²National Research Council Postdoctoral Program, Washington, DC

CTA: CCM

Computer Resources: Cray XE6 [ERDC, MS]; Cray XC30 [AFRL, OH]; SGI ICE X [AFRL, OH]

Research Objectives: To calculate the structures and the electronic properties of layered nanomaterials with and without adsorbate atoms and molecules, to guide work on their chemical functionalizations, and to advance their use as chemical sensors and in advanced electronics. To make first principles calculations of the thermal conductivities of semiconductors as a basis for identifying high thermal conductivity materials for cooling in electronics. To calculate the electronic and optical properties of solid state quantum bit systems to advance their implementations in quantum information technology.

Methodology: *Ab initio* density functional calculations are made of the structural and electronic properties of layered nanomaterials with and without chemical functionalization. *Ab initio* density functional methods are used to calculate the phonon frequencies and wavefunctions and the interactions between phonons in semiconductors and in semiconductor nanostructures, and inelastic Boltzmann equation methods are used to calculate their thermal conductivities. Electronic calculations are typically made using QuantumEspresso codes. The properties of optical excitation of quantum dots and other solid state systems in quantum information technology are calculated using density functional theory, finite element techniques, and the diagonalization of large matrices for many-body and optical properties.

Results: New materials with high electrical conductivities and low thermal conductivities are needed for high efficiency thermoelectrics in cooling and power generation. We have developed a new first principles method to calculate thermal conductivities of non-metallic materials and are using it to search for materials with low thermal conductivities. In recent work, calculations have been made for Tl_3VSe_4 and In_3VSe_4 . Exceptionally low thermal conductivities have been found in them and have been traced to their weak Tl and In bonding respectively. This results from subsets of thermal phonons being strongly scattered by other phonons. These results are in good agreement with available experimental results.

Quantum information has opened new opportunities in a range of technologies, including quantum sensing, quantum computing, and navigation. Solid state implementations have the advantages of scalability and integration, and we are developing optically controlled qubit systems based on the single vacancy defect in SiC. In recent work we have calculated the electronic structure and their optical and spin properties needed in resonant optical spin initialization and high-fidelity readout of these defect qubits, and we have shown that the time-dependent properties of the system are in good agreement with the experiment.

DoD Impact/Significance: Chemical functionalization of monolayer systems will open opportunities to control their properties for use in electronics and as chemical and biological sensors. New high thermal conductivity materials and systems make possible their exploitation in thermal management and in thermoelectrics. Understanding the role of interactions and couplings between quantum bits in solid systems opens opportunities to develop fast optical quantum technologies based on them.

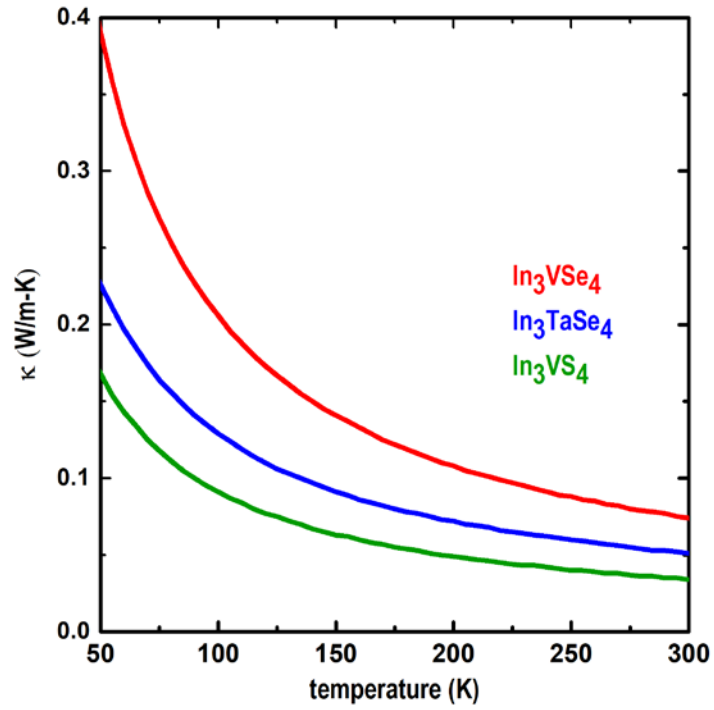


Figure 1. Calculated thermal conductivities of several low thermal conductivity compounds.

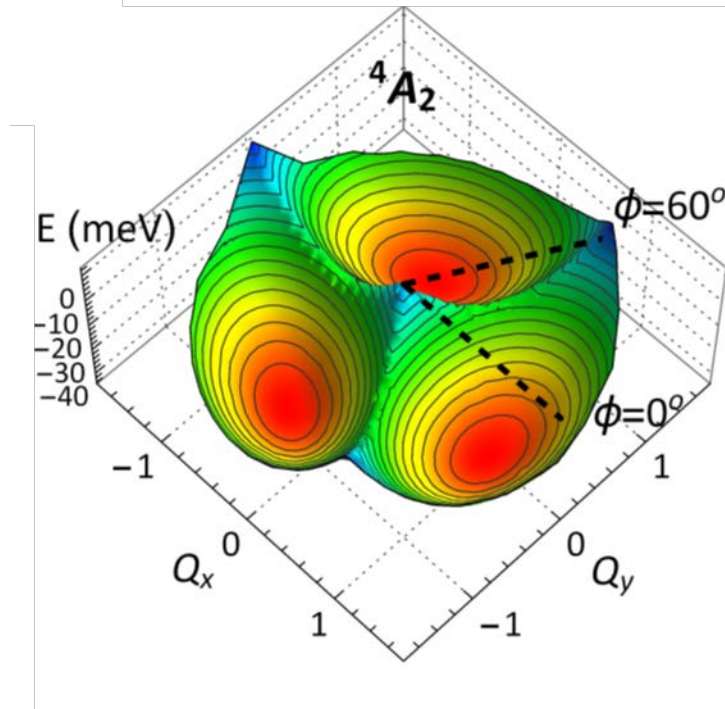


Figure 2. Excitation energy of the Si vacancy defect as a function of position of the excited state electron.

THIS PAGE INTENTIONALLY LEFT BLANK

CEA

Computational Electromagnetics and Acoustics

CEA covers two primary computational disciplines. Computational Electromagnetics covers the high-resolution multidimensional solutions of Maxwell's equations. DoD applications include calculating radiofrequency (RF) sensor performance, radar scattering of tactical ground, air, and sea vehicles, the electromagnetic signature of buried munitions, high power microwave performance, as well as the interdisciplinary applications in magnetohydrodynamics and laser systems. The Computational Acoustics area covers the high-resolution multidimensional solutions of the acoustic wave equations in solids and fluids. DoD applications include the modeling of acoustic fields for surveillance and communication, seismic fields for mine detection, and the acoustic shock waves of explosions for antipersonnel weapons.

Title: Acoustic Parameter Variability over an Ocean Reanalysis (AVORA)

Author(s): J.P. Fabre

Affiliation(s): Naval Research Laboratory, Stennis Space Center, MS

CTA: CEA

Computer Resources: Cray XC40 [NAVY, MS]

Research Objectives: Long time reanalyses of the ocean are becoming available (e.g., NRL 7300) and are potentially extremely useful for understanding the variability of environmental parameters that impact acoustic sensor performance. The objective of this effort is to investigate such potential, provide recommendations for future Navy products to support operations, and to develop prototype products for test and evaluation.

Methodology: Investigate the NRL 20+ year Ocean Reanalysis in conjunction with the necessary atmospheric reanalysis (e.g., NOAAs CFSR) to quantify and understand the variability over various time frames. Investigate the sensitivity of acoustic propagation and proxy parameters to the environmental variability. Investigate and assess appropriate averaging windows for a number of environments. Develop prototype products and make recommendations based on the results for products that could be derived from the described reanalyses. Such products will facilitate improved understanding of acoustic parameter variability in areas of propagation and ambient noise. Develop prototype products and test various ways of storing and accessing large data sets. NRL has been working extensively in the areas of big data and machine learning. We will include such technologies as part of our analysis, testing, and recommendations and incorporate lessons learned into existing products. If successful, these product could become Navy Standard.

Results: Delays in running the ocean reanalysis shifted our focus from running tests to developing scripts and modifying software to be ready for when the ocean reanalysis begins to run. We developed a number of display types and tests for averaging windows, etc. An example is shown in Fig. 1.

DoD Impact/Significance: “In *Joint Vision 2020*, the Department of Defense’s strategic plan to ensure battlespace dominance in the 21st century, a key element is information superiority enabled by emerging technologies...” “An important aspect of information superiority is situational awareness. This implies knowing where you are, where allied and coalition forces are and where enemy forces are. It means understanding the environment, from the sea floor to the top of the atmosphere.” [Heart of ForceNet: Sensor Grid, Advanced Command and Control by RADM Steven J. Tomaszewski]. Our efforts will directly inform environmental variability as it applies to acoustics.

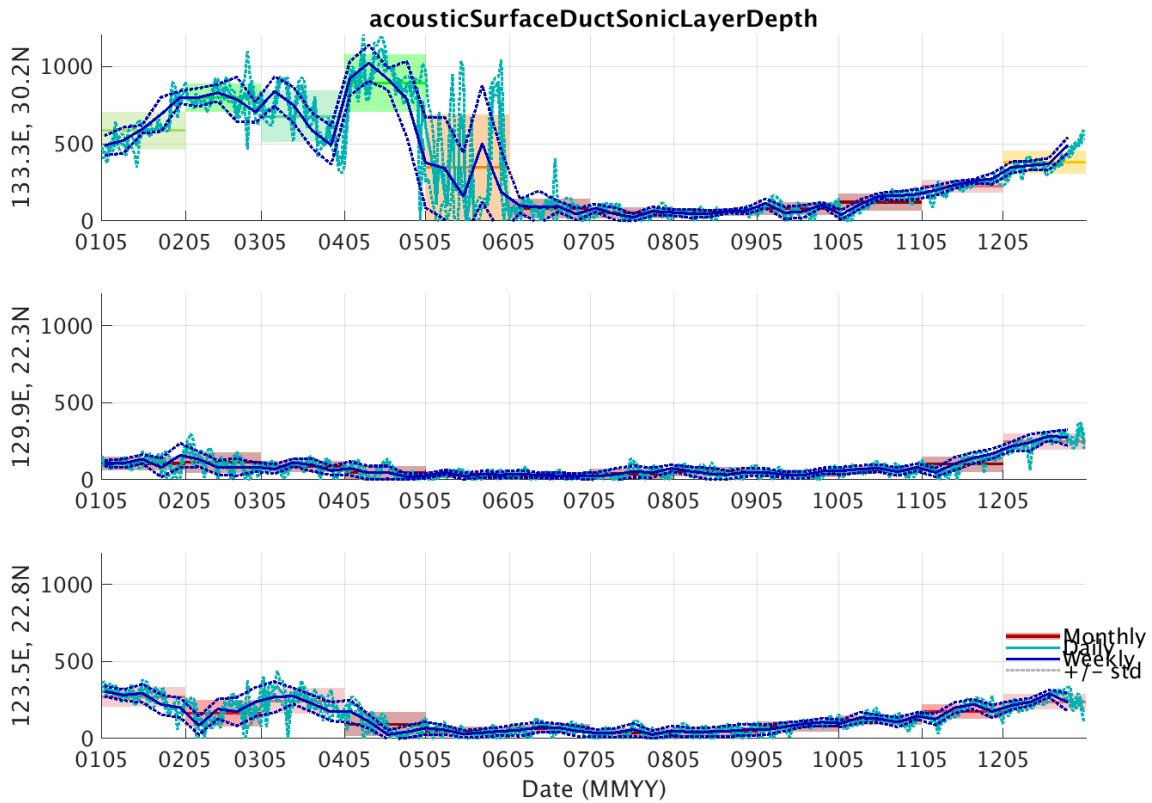


Figure 1. Averages of Sonic Layer Depth for 2005 at three specific locations is shown. Solid lines show monthly (red), daily (light blue) and weekly (dark blue averages). The blue dashed lines are +/- 1 standard deviation from the daily and weekly means. The colored boxes are +/- 1 standard deviation from the monthly mean. This sort of plot allows the user to envision the variability over various scales across a significant time period for planning purposes.

Title: Forward Simulations of Diffusive Wave Algorithms
Author(s): D. Photiadis
Affiliation(s): Naval Research Laboratory, Washington, DC
CTA: CEA

Computer Resources: SGI ICE X [AFRL, OH]

Research Objectives: Develop forward numerical simulation models in disordered, acoustic media which can be used to test and further develop diffusive wave based detection algorithms.

Methodology: Effective multipole expansion method for the prediction of the late time response in a medium with random disorder.

Results: The straightforward simulation of diffusive wave algorithms fails because the required medium size, determined by the mean free path of the random medium, is too large. In the current year, simulations based on an effective multipole expansion for randomness described by assumed point scatterers was carried out. This approach, scaling with the number of scatterers rather than the total number of acoustic degrees of freedom in the volume is much smaller and at least for the smaller problems of Navy interest, can be carried out with current high performance computing (HPC) resources. In the current year a test simulation was carried out in a uniform acoustic medium with a homogeneous distribution of random scatterers.

With the computational capability in hand, testing of the diffusive wave algorithm based on the Aubry-Derode multiple scattering filter (MSF) was carried out. This simulation consists of embedding a target, itself a point scatterer with a strength ten times larger than that of a typical scatterer, in the medium a distance R from an array with N -elements. The N -elements are then used to search for the target using conventional beam forming and the Aubry-Derode MSF.

The simulation results show clearly the failure of conventional beam forming at this range (such failure is expected for any distance greater than a mean free path). On the other hand, the success of the MSF algorithm is unambiguous.

DoD Impact/Significance: The simulation results testing the diffusive wave algorithm discussed above are the first such reported numerical simulations.

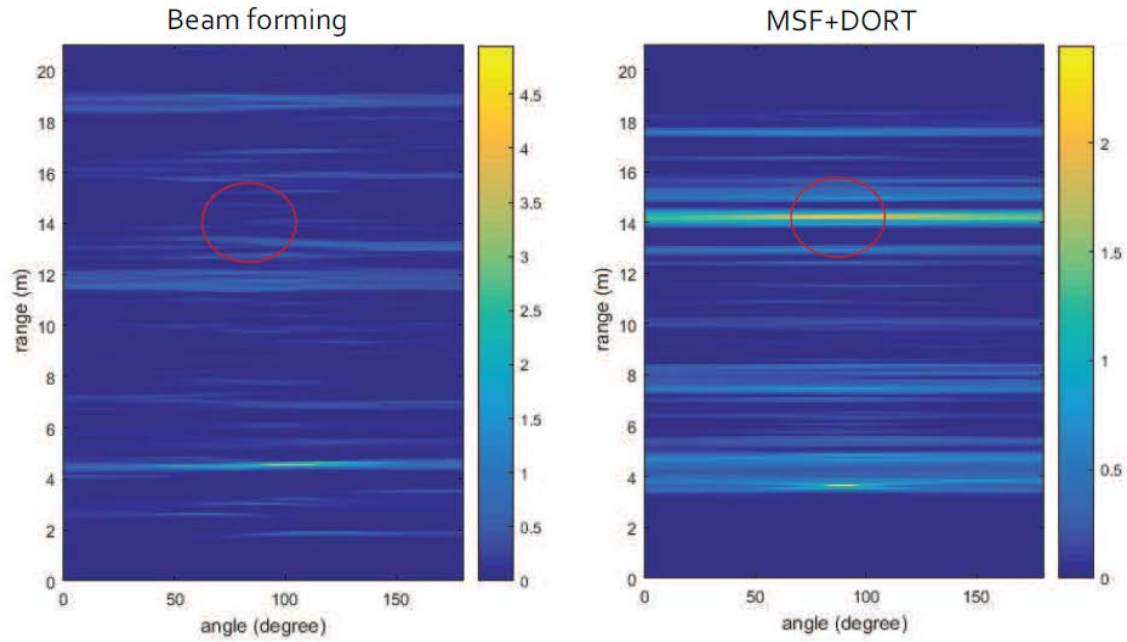


Figure 1. Target detection with diffusive wave processing compared to beam forming (conventional imaging); detection strength shown by yellow. The target is indicated by the red circle. Distances are scaled by a factor of ten and the mean free path is 100m; the range of the target is thus $1.4l_{\text{mfp}}$.

Title: Flowfield and Transport Models for Navy Applications
Author(s): W.G. Szymczak, and A.J. Romano
Affiliation(s): Naval Research Laboratory, Washington, DC
CTA: CEA

Computer Resources: SGI ICE X [AFRL, OH]; SGI ICE X [ERDC, MS]

Research Objectives: Provide resources for computational fluid dynamics simulations, as well as optimization and inverse problems, supporting a variety of Navy applications. Examples include flow through acoustic sensors, flow and transport over passive filter shelters, and the extraction of anisotropic stiffness coefficients of white matter in brains of both healthy controls and patients with mild to severe traumatic brain injury (TBI).

Methodology: The extraction of stiffness parameters using wave guide elastography (WGE) was performed using a mixed model inversion (MMI) algorithm to treat both the anisotropic and isotropic regions within a human brain. WGE utilizes magnetic resonance elastography (MRE) and diffusion tensor imaging (DTI) measurements processed with an orthotropic anisotropic inversion algorithm. Within the anisotropic white matter regions, the orthotropic inversion provides nine independent stiffness coefficients including the three longitudinal terms C_{11} , C_{22} , C_{33} , three shear coefficients C_{44} , C_{55} , C_{66} , and three off-diagonal stiffness terms C_{12} , C_{13} , C_{23} . The algorithm was implemented using message passage interface directives with work balancing based on the ratios of isotropic to non-isotropic voxels being sent to each processor.

Results: The WGE-MMI code was run using 1152 cores (32 nodes with 36 cores per node) reducing the execution time from 48 hours (using a single node with 36 threads) to under 15 minutes. In FY18 we performed approximately 200 analyses using over 40 datasets provided by the Mayo Clinic in Rochester, MN, Washington University in St. Louis, and Charité-Universitätsmedizin in Berlin. Figure 1 shows the white matter fiber tracts derived from the DTI data colored by displacements from the MRE extracted from a healthy volunteer. Segmentations of the white matter tracts were used to perform statistical comparisons of the stiffness values obtained over a group of subjects. For example, it was found that among healthy subjects provided by Charité, the value of C_{66} was significantly larger ($p \leq 0.01$) than either C_{44} or C_{55} in several segments including the Forceps minor, Cortico-spinal tract, Fornix, and Uncinate fascicle. Figure 2 shows the white matter tracts of the Forceps minor colored by shear stiffness values in the patient with values closest to the mean of the group.

DoD Impact/Significance: The WGE-MMI provide a unique capability in extracting anisotropic stiffness values of white matter structures. These values, within different segmented brain structures, provide features which are currently being prepared for machine learning algorithms to distinguish between healthy controls and TBI patients. Thus, it has the potential to be used as a non-invasive test for diagnosing conditions of warfighters exposed to blunt, ballistic, or blast impacts.

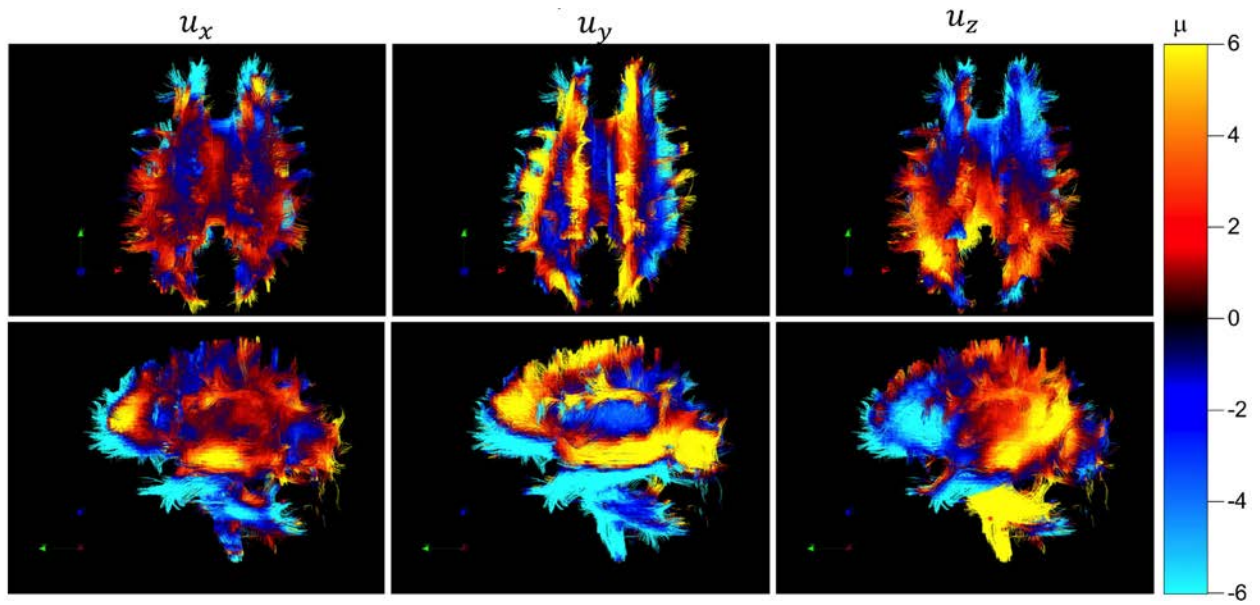


Figure 1. White matter pathways colored by MRE displacement values in the three coordinate directions at 60 Hz excitation. The top and bottom rows of images show the top and lateral views, respectively.

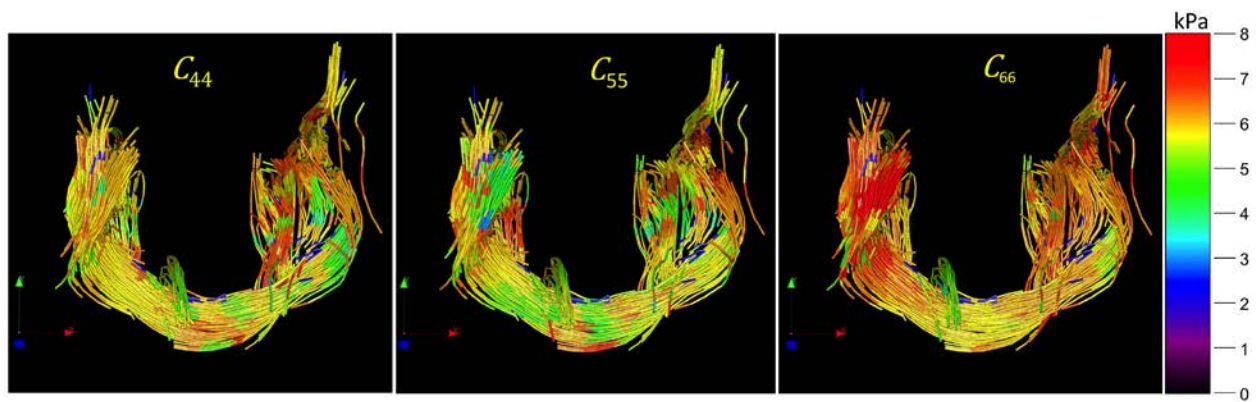


Figure 2. Forceps Minor tracts colored by shear stiffness indicating larger values for C_{66} .

Title: Intense Laser Physics and Advanced Radiation Sources

Author(s): D.F. Gordon,¹ J. Penano,¹ L. Johnson,¹ D. Kaganovich,¹ Y. Chen,¹ M. Helle,¹ B. Hafizi,¹ and Y. Khine²

Affiliation(s): ¹Naval Research Laboratory, Washington, DC; ²Engility Corporation, Chantilly, VA

CTA: CEA

Computer Resources: Cray XC40 [ARL, MD]; Cray XC40 [ERDC, MS]; Cray XC30 [AFRL, OH]

Research Objectives: The primary objectives of this program are to model the propagation of intense, short-pulse lasers in plasmas and other nonlinear media, and to provide computational support for experiments on the NRL Terawatt-Femtosecond-Laser (TFL). Current areas of research include plasma based accelerators, novel sources of short pulse infrared radiation, ultra-high field physics, and hypersonic flow modeling.

Methodology: High performance computing (HPC) resources are utilized using several codes. turboWAVE is an object oriented framework that contains modules designed to solve a variety of problems. Both fully explicit and ponderomotive guiding center particle-in-cell modules are used to model relativistically intense laser pulses propagating in plasmas. Quantum optics modules are used to describe the interaction of the laser pulse with atoms or ions. Fluid modules (SPARC) are used to describe hypersonic flow and shock propagation in gas targets. Optimization for the latest computer architectures requires exploiting three levels of hardware parallelism: vector arithmetic units, shared memory threads, and distributed memory processes. The framework universally supports all of these using a combination of OpenMP directives for vector and loop parallelism, and the message passing interface for distributed processes. Some modules support general purpose graphics processing units via OpenCL.

HELCAAP solves a paraxial wave equation with a large number of source terms representing atmospheric turbulence, dispersion, and various nonlinear processes. HELCAAP simulates the propagation of short pulse and high energy laser pulses, including adaptive optics. It is often useful to run a large statistical ensemble of initial conditions. For this purpose, embarrassingly parallel methodology is effective.

Results: We carried out CFD simulations of vortex flows for plasma optics applications. Runs were made using CFD++ and SPARC. The CFD++ runs solved the steady flow problem using Reynolds-averaged Navier-Stokes equations, the SPARC runs solved the time dependent problem neglecting small scale turbulence. Understanding of the requirements of the outflow nozzles was developed and applied to an actual device. We carried out HELCAAP runs modeling nonlinear and high average power laser propagation in various turbulent atmospheres. These runs helped clarify the role of thermal blooming in high repetition rate short pulse laser propagation. Runs quantifying the usefulness of adaptive optics for beam control in turbulent atmospheres were also carried out.

DoD Impact/Significance: Laser propagation in turbulent atmospheres is relevant for directed energy. High power pulsed sources of long wavelength radiation may also be relevant for directed energy. Laser-driven accelerators and radiation sources have potential applications for ultrafast (femtosecond) imaging of chemical and biological systems. High energy electron beams might be useful as a gamma ray source for detection of special nuclear materials (SNM). High-energy ions might also be useful for SNM detection or for cancer therapy.

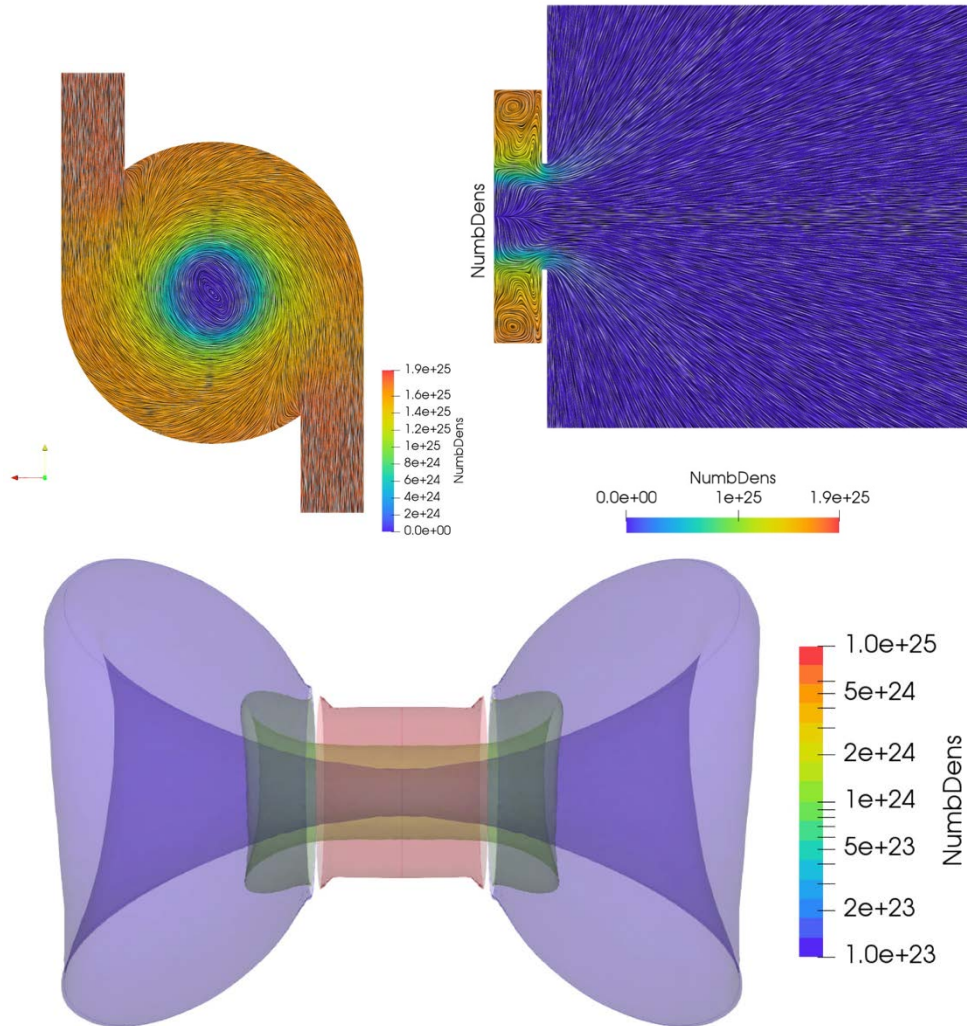


Figure 1. CFD++ 17.1.1 model of flow through a gas lens. The top two images show perpendicular cross-sections of the gas number density with lines indicating the flow field. There is a large rotational flow that creates the on-axis density minimum and the optical lensing effect. The bottom image shows a side-on view of surfaces of constant number density. These flows are driven by a constant mass flow rate which empties into a near-vacuum chamber.

Title: Optomechanical Systems

Author(s): M. Zalalutdinov, S. Carter, and S. Dey

Affiliation(s): Naval Research Laboratory, Washington, DC

CTA: CEA

Computer Resources: SGI ICE X [ARL, MD]; Cray XC40 [ARL, MD]; SGI Altix ICE [NRL, DC]; SGI ICE [ERDC, MS]; Cray XC40/50 [ERDC, MS]; SGI ICE X [AFRL, OH]

Research Objectives: Optomechanical coupling in vibrating nanophotonic structures was explored using finite element modeling. Radiofrequency (MHz range) mechanical response of photonic crystals (PhC) and optical waveguides implemented in ultra-thin GaAs suspended films was studied in order to interpret experimentally observed features in photoluminescence spectrum of InAs quantum dots (QD) embedded in vibrating GaAs photonic devices. The quantitative analysis of strain-induced variations in the energy of QD-bound excitons requires explicit knowledge of three dimensional elastic field generated by the flexural deformation in vibrating plates at the locations of the QD and is not feasible without numerical methods, given the complexity of the device geometry.

Methodology: Eigenfrequency study of the PhC structures modeled using shell elements was used to identify spatial patterns for various components of the strain tensor that correspond to various modes of vibrations in the 1-15MHz frequency range.

Results: Three dimensional tensor components of the motion-induced strain patterns were determined. The magnitude of the in-plane elastic strain attainable for a given amplitude of displacement was shown to be in agreement with the time-variable wavelength shifts in QD photoemission spectrum.

DoD Impact/Significance: The effort is motivated by applications in nanomechanics that will rely on QD as nanoscale optical transducers for local strain readout. New capabilities are expected to emerge from the abundance of self-assembled QD distributed across the nano-opto-mechanical structure, ability to access individual QD optically (one dot at a time) and high spatial resolution limited only by QD dimensions (~20nm).

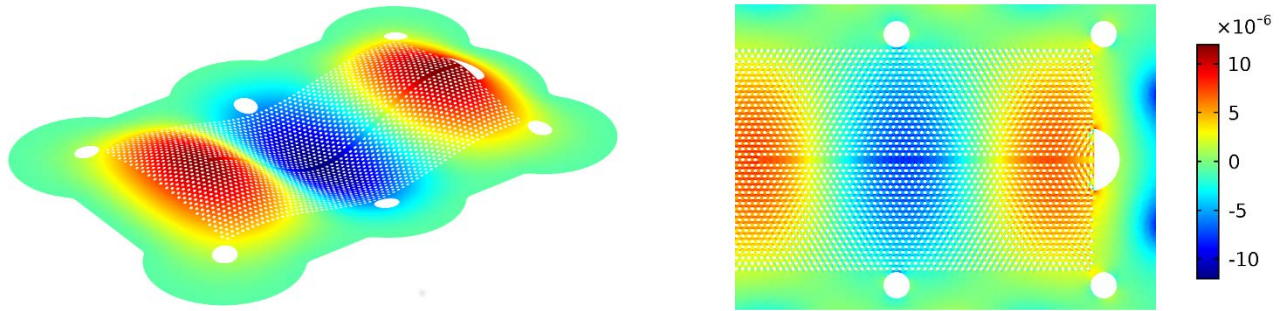


Figure 1. Left: out-of-plane displacement shown for the fourth overtone ($f_{\text{res}}=11\text{MHz}$) of the PhC implemented in 200 nm-thick suspended GaAs plate. The period of the PhC structure is 240 nm, full extent $15 \times 8.5 \mu\text{m}^2$. Right: amplitude of in-plane strain ($\epsilon_{xx} + \epsilon_{yy}$) imposed on QD by 11 MHz vibrational mode, normalized for 1nm maximum displacement.

Title: Small-Slope Approximation Rough-Surface Back-Scattering Analysis

Author(s): J. Alatishe

Affiliation(s): Naval Research Laboratory, Washington, DC

CTA: CEA

Computer Resources: SGI ICE X [ARL, MD]; Cray X30 [NAVY, MS]; IBM Power 8 [MHPCC, HI]

Research Objectives: To determine and characterize the spatial coherence effects that are inherent in sea clutter by numerically analyzing the associated response at the antenna port of a monostatic radar. The sea-surface coherence effects are examined with respect to the associated antenna characteristics and the surface properties.

Methodology: The surface model used is based on empirical data as represented by the ocean wave-number spectrum for a fully developed sea, from which statistical realizations of the ocean surface are generated. Once the response from the surface has been computed, the properties of the simulated sea-clutter responses are characterized. The surface scattering amplitude (SA) characterizes the spatial coherence. Once the SA has been computed, the response at the antenna port is determined and the coherence effects due to the surface are examined. Numerical integration was used to determine the antenna response from the rough-surface profile. The SA has a nonlinear relationship with the surface profile, which is evaluated by the Fourier transform of a linearized sea-surface model that employs the ocean wave-number spectrum. The surface non-linearities are incorporated via the choppy wave model, which accounts for the wave-wave interaction observed in ocean surfaces and accurately models the Doppler response in sea-clutter analyses. The ocean wave-number spectra were represented by the Elfouhaily ocean wave-number spectrum over a range of wind speeds and wind directions. With both the SA and surface model calculated, the response at the antenna port was computed for each antenna aspect angle. The codes used to execute these steps were first written in MATLAB and then converted into Fortran 90. The codes were then parallelized using the message passing interface and run on 1024 processors or up to 32 graphics processing units at the NRL high-performance computing facility. Simulations were conducted for a given sea state at X-band (10 GHz).

Results: Data obtained from published accounts of sea clutter were used as the baseline for comparison. These sea-clutter values were measured at various wind speeds and wind directions for given antenna aspect angles (elevation and azimuth) and polarizations of the antennas. The simulated received sea-clutter responses were computed for various elevation angles for vertical and horizontal polarizations. The simulation generated a 4096-point frequency response of the sea surface for a given sea state for an observed time increment. The fast Fourier transform convolution was used to generate the complex time-dependent echo, which is the spectral product of the associated sea-surface frequency response and the transmitted waveform. As a result of the previous step, multiple coherent processing intervals were generated for analysis as depicted in Fig. 1. The number of spatial samples of the sea surface was set to 8191 in the down-range, and 8191 in the cross-range, dimensions. The simulation results showed that the range-Doppler properties are similar to real sea clutter with the correct frequency offset and spectral structure (see Fig. 2). In addition, some sea-spike phenomena are present in the simulated data and the statistics of the clutter appears to closely match that of real data. Further investigation of the simulated data is still required.

DoD Impact/Significance: Understanding the spatial coherence effects in radar sea clutter provides further insight into the phenomenology of back scattering from the ocean, which will be useful in devising algorithms for detecting threats over the sea.

Example results:

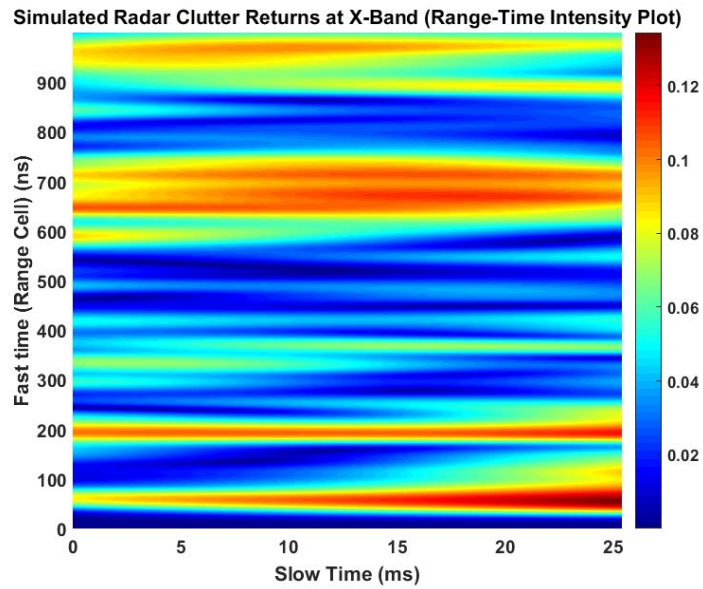


Figure 1. Range-time intensity plot of X-band sea-clutter returns for VV polarization at 65° elevation. Pulsewidth is 100 ns, pulse repetition interval (PRI) is 200 μ s, and wind speed is 10 m/s away from the radar.

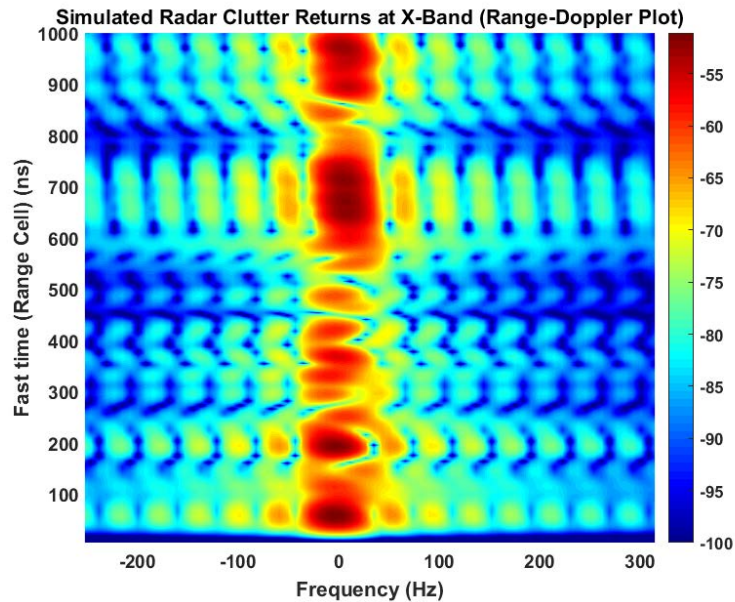


Figure 2. Range-Doppler plot of X-band sea-clutter returns for VV polarization at 65° elevation. Pulsewidth is 100 ns, PRI is 200 μ s, and wind speed is 10 m/s away from the radar.

Title: Multidimensional Particle-in-Cell Modeling of Ultrashort Pulse Laser with Solid Targets

Author(s): G.M. Petrov

Affiliation(s): Naval Research Laboratory, Washington, DC

CTA: CEA

Computer Resources: Cray XC30, [NAVY, MS]; SGI ICE X [ERDC, MS]

Research Objectives: Multidimensional particle-in-cell (PIC) modeling and simulations of the interaction of short pulse laser with micro- and nano-materials for better understanding the dynamics of particle acceleration and generation of x-ray and gamma radiation.

Methodology: Intense lasers interact with matter in a wide range of time scales. For processes occurring on a picoseconds time scale, multidimensional PIC models provide proper description. Such models are the primary computational tool for laser-produced plasmas since they provide a self-consistent description of the electromagnetic fields and response of the material. Nowadays, PIC models are used extensively for modeling laser-matter interaction on a micro- and nano-scale. We use a two-dimensional relativistic PIC code for laser-matter interaction, which was developed in-house at the Plasma Physics Division at NRL.

Results: The PIC code was extensively used to study particle acceleration and x-ray/gamma-ray generation from thin (sub-micron) foils covered with nano-material irradiated by ultrashort (fs-ps) high-intensity (10^{19} - 10^{20} W/cm²) laser pulses. The code provided valuable insight into the physical processes occurring during the interaction and was employed to analyze experiments done at the University of California San Diego, which were conducted to gain understanding of target performance. We did a systematic study by varying laser parameters (intensity, duration and focal spot size) and target parameters (material, thickness, surface coverage) in order to optimize targets and guide experiments, which are very expensive and time consuming. Such experiments were conducted on the Hercules laser at the University of Michigan and the Texas Petawatt Laser in Austin, Texas. The target layout is shown in Fig. 1. Typical simulation results for Au foil irradiated by an ultra-short pulse laser (peak intensity 1.5×10^{21} W/cm², duration 32 femtoseconds, wavelength 0.8 μ m, spot size 1.5 μ m and energy 2 Joules) are shown in Fig. 2, which displays proton spectra and maximum proton energies versus number of nanowires per focal spot, N. We found that (1) the nanowires greatly enhance the coupling of laser energy to the target and (2) the interaction is optimum for $1 < N < 2$.

DoD Impact/Significance: This modeling and the results are of significant interest to the Navy and DoD as it is directly related to problems such as generation of x-rays and gamma rays, as well as directed particle beams (neutrons, protons, radioactive ion beams), all of which can be used for both fundamental research and practical applications such as detection of nuclear materials and improvised explosive devices. The research is also of great interest to the scientific community dealing with high energy density plasmas, laser nuclear physics and laser-matter interactions. The simulations have been used to guide experiments related to laser-matter interaction. The payoff of the computational efforts is that long, arduous, and expensive experiments have been modeled and guided using "virtual experiments" on computers, thus saving time and resources.

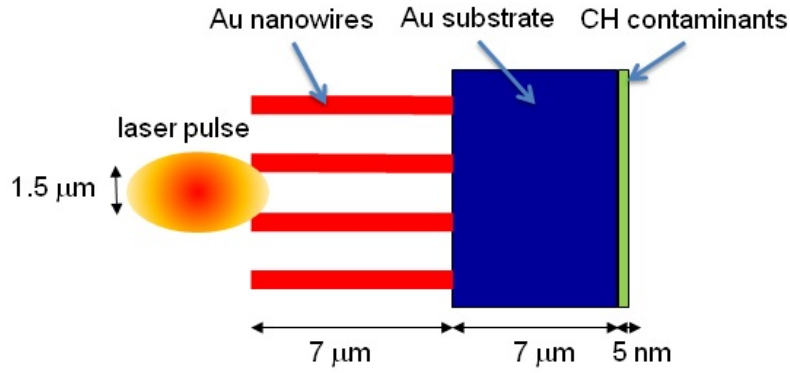


Figure 1. Interaction of short pulse laser with targets covered with nanowires.

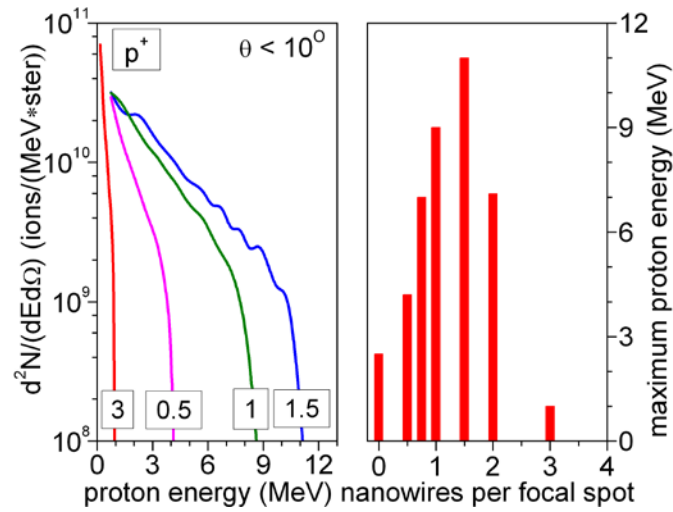


Figure 2. PIC simulations for targets with different number of nanowires per focal spot N . Left panel: proton spectra in forward direction. Red: $D=0.2 \mu\text{m}$, $S=0.5 \mu\text{m}$, $N=3$; blue: $D=0.4 \mu\text{m}$, $S=1 \mu\text{m}$, $N=1.5$; green: $D=0.6 \mu\text{m}$, $S=1.5 \mu\text{m}$, $N=1$; magenta: $D=1.2 \mu\text{m}$, $S=3 \mu\text{m}$, $N=0.5$. Parameters D and S are the nanowire diameter and distance between nanowires. The substrate thickness and nanowire length are $L=7 \mu\text{m}$. Right panel: maximum proton energy vs. N . $N=0$ corresponds to a flat target (no nanowires).

Title: Low Grazing Angle Radar Backscatter
Author(s): J.V. Toporkov, M.A. Sletten, and J.D. Ouellette
Affiliation(s): Naval Research Laboratory, Washington, DC
CTA: CEA

Computer Resources: Cray XC40 [ERDC, MS]; Cray XC40 [ARL, MD]; Cray XC30 [AFRL, OH]

Research Objectives: Sea surface reflections are present in many shipborne, coastal, and airborne radar systems. They are often regarded as clutter that masks a target echo, but also can be a source of information about the ocean environment. Understanding the properties of sea backscatter and how they depend on the environmental parameters, as well as identifying their distinctions from those of man-made target echoes is key to improving or even enabling performance of such radar systems and applications. We investigate detailed characteristics of radar returns from the ocean surface with the possible presence of embedded targets. We use direct numerical simulations to solve the scattering problem and, where appropriate, numerical implementations of approximate scattering models.

Methodology: We combine physics-based models for ocean surface and floating target evolution with computationally efficient, exact evaluation of the scattered electromagnetic (EM) field. A wind-driven surface is represented by realizations of a Gaussian random process defined by the Elfouhaily wave spectrum. Interactions between surface harmonics affecting shape and motion of small ripples (that have great impact on scattering of centimeter-scale EM waves) are modeled by the Creamer transformation applied to a Gaussian realization. The motion of a semi-submerged round target is defined by the orbital wave current (derivable from the known surface profiles) at the location of its center. The EM field scattered by a “time-frozen” scene (surface with the broached part of the target, if present) at a particular frequency is found by iteratively solving a boundary integral equation for the induced surface current. This first principles approach automatically accounts for many phenomena (multiple scattering, shadowing) known to be problematic for analytical treatment. The calculations can be conducted at a number of frequencies covering certain bands to simulate pulse scattering. The procedure is repeated for every surface or “surface+target” profile in the sequence representing temporal evolution. The simulations are limited to the two-dimensional space but have direct relevance to commonly occurring three-dimensional geometries (e.g., incoming long-crested waves).

Results: To support an investigation of feasibility of passive remote sensing of a sea state using illumination from geostationary communications satellites, time-varying simulations were performed for continuous-wave, time-harmonic S-band signals with vertical (VV) and horizontal (HH) polarizations using the setup shown in Fig. 1. Consistent with an anticipated satellite position, the incidence angle was fixed at 45° . All scattering directions within the upper half-space were considered, although low grazing angles around $\theta_s = -80^\circ$ are of most interest. Doppler spectra cf. Fig. 2 were obtained from a Monte Carlo ensemble of 2000 simulated 5-second data records. The first two moments of the Doppler spectra are compared to the results from similar simulations based on a popular approximate scattering model (Fig. 3). Notably, the discrepancies emerge and grow as the scattering angle approaches grazing. Several more realizations of the range-resolved, time-varying X-band backscatter from sea surface with and without floating targets were generated and provided to the Radar Division for further analysis and use.

DoD Impact/Significance: More comprehensive and detailed characterization of sea clutter will help in design and performance assessment of the Navy radar systems operating in Low Grazing Angle (LGA) regime. Bistatic configurations provide covertness for a passive receiver asset and could further yield performance enhancements due to peculiar scattering characteristics of surface and targets that do not emerge in the conventional monostatic case.

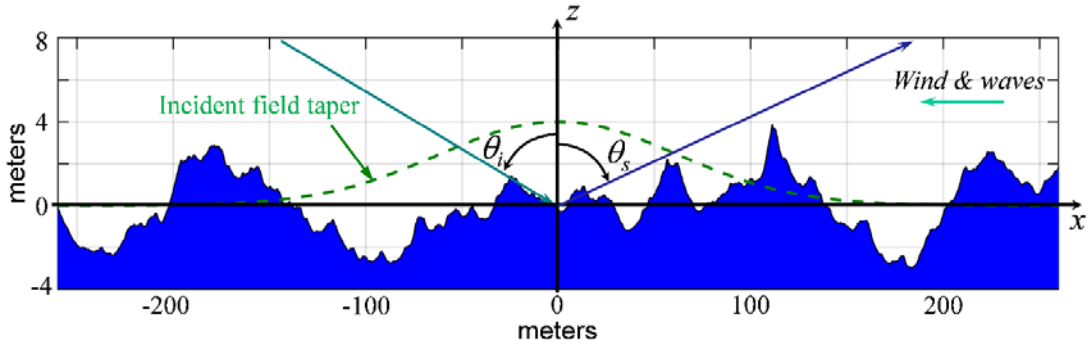


Figure 1. Setup for bistatic scattering simulations from evolving surface. Incidence angle θ_i is fixed at 45° .

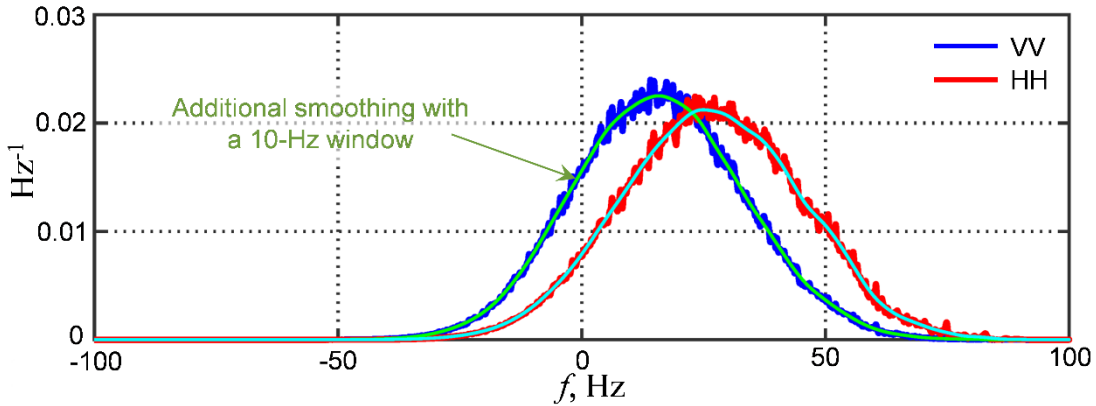


Figure 2. Examples of Doppler spectra (normalized to unit area) obtained from direct numerical scattering simulations. S band (2.3 GHz), 16-m/s wind, $\theta_i = 45^\circ$, $\theta_s = -80^\circ$, averaging over 2000 realizations.

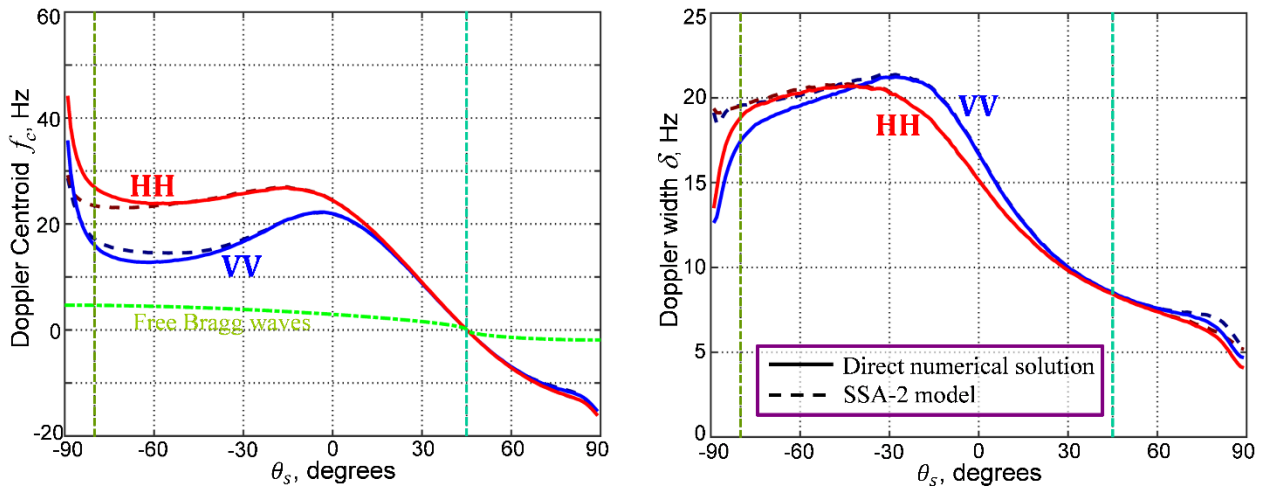


Figure 3. Mean shifts (left) and widths (right) of the Doppler spectra of the simulated bistatic sea echoes as functions of scattering angle. S band (2.3 GHz), 16-m/s wind, $\theta_i = 45^\circ$. Solid lines indicate results from exact numerical solution of the scattering problem, while their dashed counterparts correspond to the data simulated using the 2nd-order Small Slope Approximation (SSA-2). Same set of 2000 surface realizations was used in both cases. Vertical lines highlight forward scattering direction $\theta_s = 45^\circ$ as well as the near-grazing scattering angle $\theta_s = -80^\circ$ considered in Fig. 2.

Title: Computer-Aided Design of Vacuum Electronic Devices

Author(s): G. Stantchev,¹ S. Cooke,¹ J. Petillo,² A. Jensen,² and S. Ovtchinnikov²

Affiliation(s): ¹Naval Research Laboratory, Washington DC; ²Leidos, Billerica, MA

CTA: CEA

Computer Resources: Cray XC40 [ARL, MD]; Cray XC40, [NAVY, MS]; SGI ICE X [ERDC, MS]; SGI ICE X [AFRL, OH]; Crazy XC40/50 [ERDC, MS]

Research Objectives: 1. Modify, enhance, and refactor the MICHELLE charged particle beam optics code to take advantage of DoD HPC hardware and software architectures, in order to enable significantly larger simulations, optimizations, and sensitivity studies, reduce simulation times and amplify user productivity in the design and development of vacuum electronic components and systems of interest to the DoD. 2. Employ the new capability in the design of new vacuum electronic components with optimized performance characteristics.

Methodology: MICHELLE is being extended to a flexible heterogeneous computing framework that can be deployed on distributed memory HPC clusters, and that can also use computational accelerators such as multi-core CPUs and Graphics Processing Units (GPUs). In addition, we have developed interfaces with existing DoD HPC mesh generation, visualization, simulation environments, and productivity tools.

MICHELLE is a 2D and 3D finite-element, conformal mesh, Electrostatic (ES) Particle-in-Cell (PIC) code, written primarily in C++, that provides both steady-state (“gun-code”) and time-domain initial-value algorithms to predict with high accuracy the formation and transport of high-current charged particle beams in complex electric and magnetic field geometries. The code provides a comprehensive set of advanced, self-consistent emission models including thermionic (spanning space charge limited to temperature limited regimes), thermal-beam, field emission, photoemission, and secondary emission (true and backscattered).

In order to address the challenges necessary to bridge the software gap, we have the following two broad objectives for the software improvements, specifically targeting the HPCMP objective of exploiting technologies to maintain RDT&E leadership:

- I. **Exploitation of Heterogeneous Computing Architectures:** Leveraging existing and emerging DoD HPC architectures to take advantage of distributed memory HPC clusters and per-node computational accelerators such as multi-core CPUs, GPUs, and Intel PHIs.
- II. **Integration of MICHELLE into existing DoD HPC ecosystem for Mesh Generation, Visualization and Productivity:** This integration brings in the DOD CAPSTONE CAD/Mesh generation software (CREATE-MG), and DoD HPC tools including AFRL’s Galaxy Simulation Builder (GSB), and Kitware’s ParaView visualization software, available and supported through the Data Analysis Assessment Center (DAAC). Figure 1 illustrates the integration of the MICHELLE code under GSB along with CAPSTONE invoking the Sandia DAKOTA optimization library.

Results: The focus of the project during FY18 has been on continuing the integration of the HPC version of MICHELLE as well as the integration with the productivity tools. Figure 2 shows a proof of principle multi-objective genetic algorithm optimization, Fig. 3 shows how complex pipelining of the codes under GSB can be simplified using scripting, Fig. 4 shows hybrid meshing capability, and Fig. 5 shows multi-scale domain decomposable meshing capability. In this project, DoD HPC resources have also been used in support of the DARPA INVEST program researching the latest trends in emission surface physics. Extensive parameter scans have been performed on the AFRL and ARL systems, where simulation sets required hundreds of MICHELLE runs, each lasting from 3 to 5 hours.

DoD Impact/Significance: This development has impacted three DARPA and four NRL programs in Vacuum Electronics by providing the ability to perform rapid analysis and optimization of mission-critical Vacuum Electron devices, previously deemed intractable via state-of-the-art methods.

Galaxy Simulation Builder (GSB) and DoD High Performance Computing (HPC)

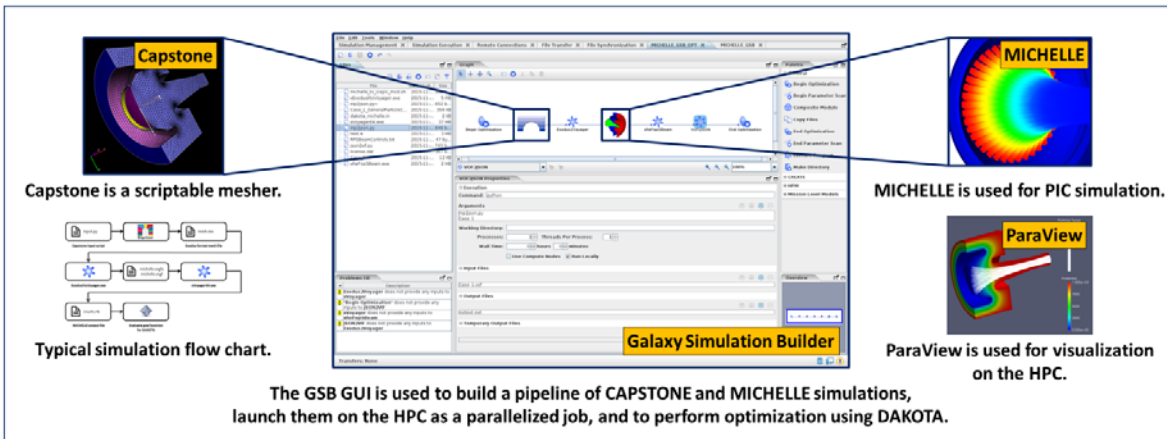


Figure 1

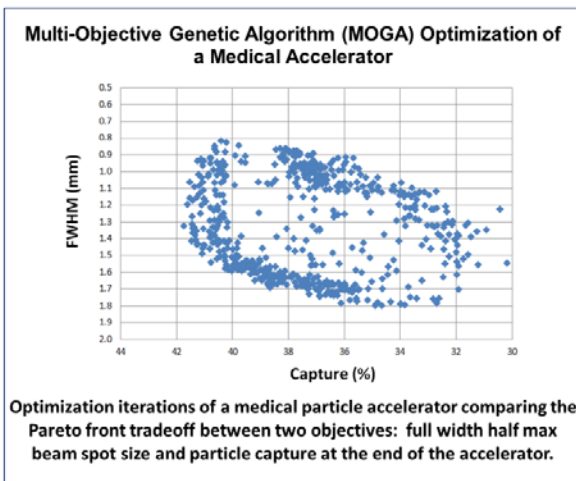


Figure 2

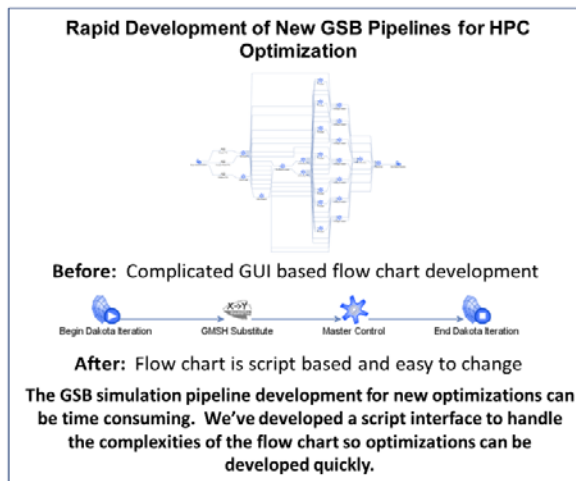


Figure 3

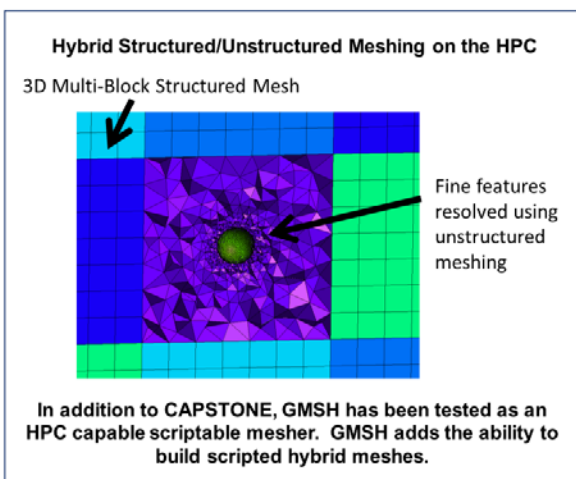


Figure 4

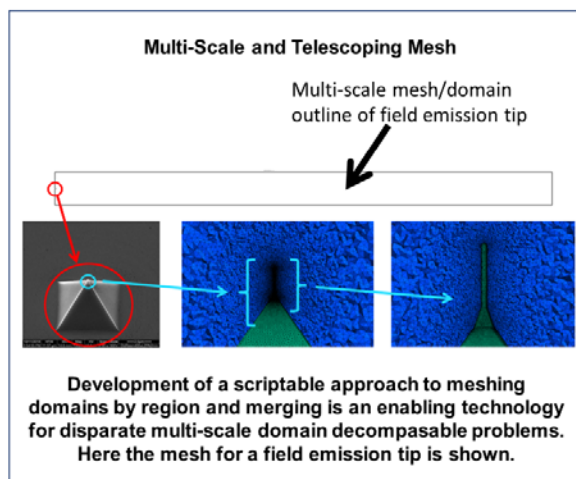


Figure 5

THIS PAGE INTENTIONALLY LEFT BLANK

CWO

Climate Weather Ocean Modeling

CWO focuses on the accurate numerical simulation of the Earth's atmosphere and oceans on those space and time scales important for both scientific understanding and DoD operational use. This CTA includes the simulation and forecast of atmospheric variability (e.g., temperature, winds, pressure, relative humidity, cloud cover, precipitation, storms, aerosols and trace chemicals, surface fluxes, etc.) and oceanic variability (e.g., temperature, salinity, currents, tides, waves, ice motion and concentration, sediment transport, optical clarity, etc.). Numerical simulations and real-time forecasts are performed from the very top of the atmosphere to the very bottom of the ocean. CWO also includes the development of numerical algorithms and techniques for the assimilation of in-situ and remotely sensed observations into numerical prediction systems. CWO has DoD applications on a daily basis for specific warfare areas, mission planning, and execution (air, ground, sea, and space), as well as for flight and sea safety, search and rescue, optimal aircraft and ship routing, and weapon system design. This CTA provides DoD with: (1) real-time, high-resolution weather and oceanographic forecasts leading to incisive decision making and enhanced operational capability in adverse weather and ocean conditions and (2) realistic simulations of the dynamic oceanic and atmospheric environment to permit effective mission planning, rehearsal and training, and materiel acquisition.

Title: Data Assimilation Studies Project
Author(s): W.F. Campbell and B. Ruston
Affiliation(s): Naval Research Laboratory, Monterey, CA
CTA: CWO

Computer Resources: Cray XC30 [NAVY, MS]; Cray XC40 [NAVY, MS]; Cray XC30 [AFRL, OH]; SGI ICE X [AFRL, OH]

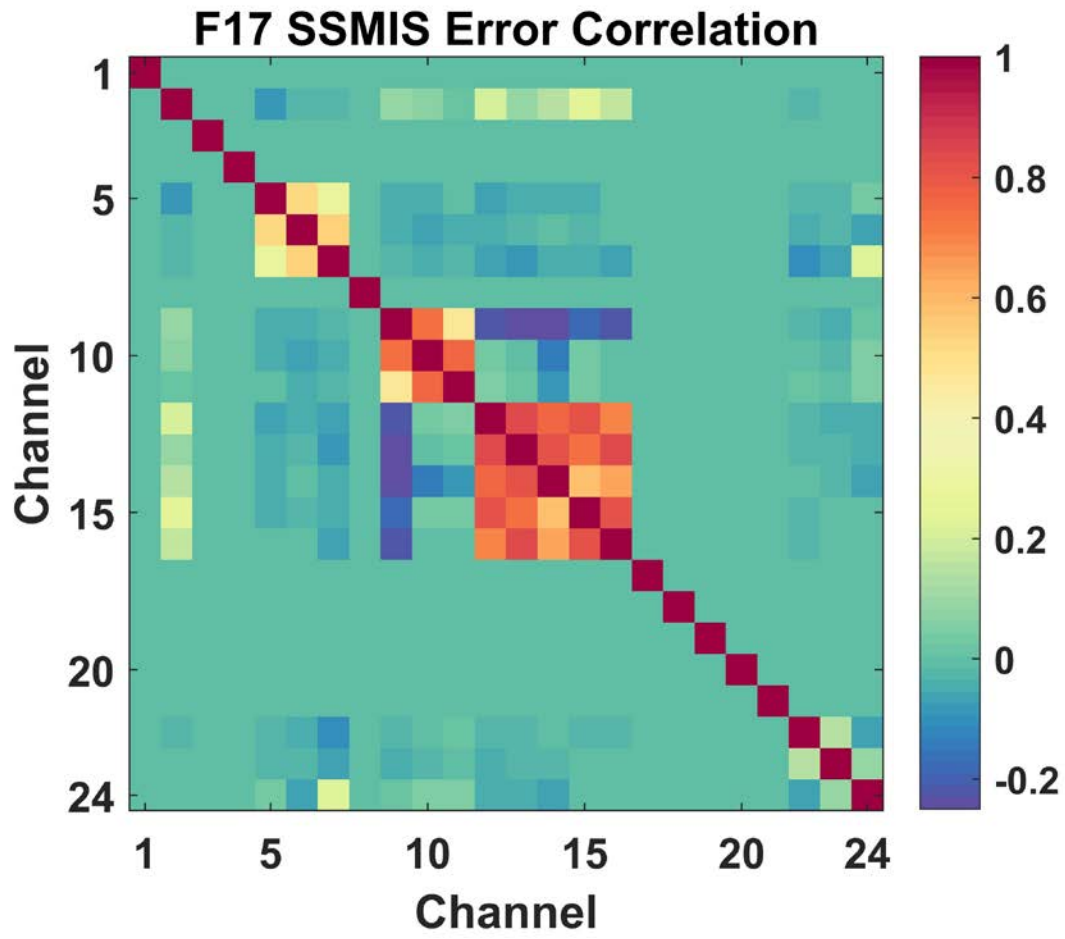
Research Objectives: Data assimilation (DA) corrects model analyses of the atmosphere, ocean or surface using non-homogenous observations. This project develops, tests, and improves: 1) our four dimensional variational (4DVAR) assimilation system, which is coupled to the atmospheric global model NAVGEM (Navy Global Environmental Model); 2) fully ensemble-based data assimilation; 3) hybrid ensemble/4DVAR data assimilation; 4) 4DVAR data assimilation for COAMPS[®]; 5) adjoint, tangent linear, and forecast sensitivity to observations; 6) coupled DA (atmosphere and ocean together); and 6) prepare for and test assimilation of new data types, both satellite and conventional. Our goal is to assimilate traditional data (generally in-situ, i.e., weather balloons, ship or buoy reports) as well as data from a variety of new sources (often space-borne) efficiently and effectively, to provide the best atmospheric analysis, and ultimately improve numerical weather forecast performance. HPC resources are a critical testbed for assimilation studies to move to next generation fully coupled atmosphere/land/ocean/sea-ice systems.

Methodology: A variety of experimental setups are used to develop and test our global and regional models and DA systems, as well as large datasets of in-situ and satellite-based observations for several summer and winter months.

Results: A broad spectrum of research takes place under this project, using the Navy's latest global (NAVGEM 1.4.3 and Middle Atmospheric NAVGEM (HA-NAVGEM)) and mesoscale (COAMPS) models, along with our global (NAVDAS-A, hybrid NAVDAS-AR, and coupled hybrid NAVDAS-AR) and mesoscale (COAMPS-AR) DA systems. Results from FY18 research include: 1) continued development of ensemble-based tangent linear model, a novel alternative to existing TLM and ADJ atmospheric models, 2) development of correlated error matrices for microwave imagers, 3) COAMPS 4DVar assimilation of Navy shipboard defense radar data into the ship-following COAMPS to improve hazardous weather prediction near Navy ships, 4) continued testing of Holm transform for the moisture control variable in hybrid NAVGEM, 5) development of new bias drift mitigation technique for NAVGEM radiance data, 6) testing of near real time ensemble aerosol forecasting system ENAAPS, 7) testing of the coupled ocean-atmosphere system with the addition of surface-sensitive infrared radiance data, and 8) development and testing of full spectral resolution CrIS DA.

DoD Impact/Significance: DoD HPCMP computing platforms provide a common environment for collaboration and the rapid development of NRL's DA systems. Large common datasets can be stored there and accessed by many researchers. Collaboration between NRL scientists at different locations (Monterey, Stennis, and DC) and among other scientists is greatly facilitated. The advancements of NAVDAS-AR, NAVGEM (including hybrid NAVGEM and HA-NAVGEM), and COAMPS-AR systems have been accelerated by the HPCMP systems. The core and future of Navy data assimilation capabilities are being mostly, and in many cases solely, developed using the resources provided by HPCMP. In summary, the ability to access the HPCMP resources is critical to prepare technology for successful transfer to operations.

¹COAMPS[®] is a registered trademark of the Naval Research Laboratory



Title: Bio-Optical Modeling and Forecasting

Author(s): J.K. Jolliff, S. Ladner, T. Smith, and J. Dykes

Affiliation(s): Naval Research Laboratory, Stennis Space Center, MS

CTA: CWO

Computer Resources: Cray XC40 [NAVY, MS]

Research Objectives: To develop and validate three-dimensional, coastal optical prediction systems that leverage results from the Coupled Ocean Atmosphere Mesoscale Prediction System (COAMPS[®]) and the Navy Coastal Ocean Model. The modeling system will forecast the emergence and transport of near shore turbidity plumes and the eruption/propagation of turbidity in the benthic boundary layer. This forecasting capability will be validated and prepared for transition to the Naval Oceanographic Office to be used in support of Navy missions.

Methodology: Ocean physics is fundamental to all else. Without the correct frictional boundary layer dynamics, current field velocities, and simulated turbulence (diffusivities), the optical models that depend upon the underlying physics will not yield results that have fidelity to observations. Accordingly, these projects focus on the application of the COAMPS in air-sea and coupled surface gravity wave (air-sea-wave) modes. HPC resources were essential to run the hierarchy of wave models required to implement the nested COAMPS air-sea-wave system, and to run high-resolution inner nests for the COAMPS itself. Inner nest horizontal spatial resolution was achieved at a range of 800 down to 50-meter horizontal grid spacing for domains in the northern Gulf of Mexico. These results were used to examine a variety of integrated physical-optical processes and assess requirements for predictive capabilities.

Results: The salient and summary results from this year's research is that observed and ephemeral optical features in the coastal zone (temporally submesoscale: ~24-48 hours duration) emerge as a result of physical processes that are only capably resolved utilizing the air-sea or air-sea-wave coupling features of COAMPS. First, accelerating northerly winds associated with metrological fronts (cold fronts) in the northern Gulf of Mexico, when combined with rapid thermal energy loss from the coastal ocean to the atmosphere, results in a dynamical and optical frontal boundary that is clearly discernable in satellite imagery (Fig. 1). COAMPS air-sea capably resolves the hourly evolution of the physical and coupled air-sea dynamics giving rise to this observed feature. Second, under a different set of seasonal dynamics, the sediment-laden bottom boundary layer may ventilate along the seaward side of a buoyancy plume under the conditions of sustained "down-front" winds, i.e., the wind direction is in the same as the buoyancy current propagation. COAMPS is not capable of resolving this process without the integration of the wave model because the simulated bottom boundary layer dynamics are substantially impacted by the wave model perturbations.

DoD Impact/Significance: This research falls directly within the Naval S&T Strategic Plan Focus Area "Assure Access to the Maritime Battlespace" under the "Match Environmental Predictive Capabilities to Tactical Planning Requirements" objective. The ability to forecast the coastal ocean optical environment, as it may impact EO/LIDAR and other Navy systems, is dependent upon high-resolution COAMPS output fidelity to real world physical dynamics. Whereas COAMPS output will continue to be used as the physical basis for optical forecast models, this research also suggests that optical-based observations from satellite or UAV platforms may be used to identify the location and occurrence of physical features, such as frontal boundaries, and this information may be used to correct feature position/evolution within physical model simulations.

¹COAMPS[®] is a registered trademark of the Naval Research Laboratory

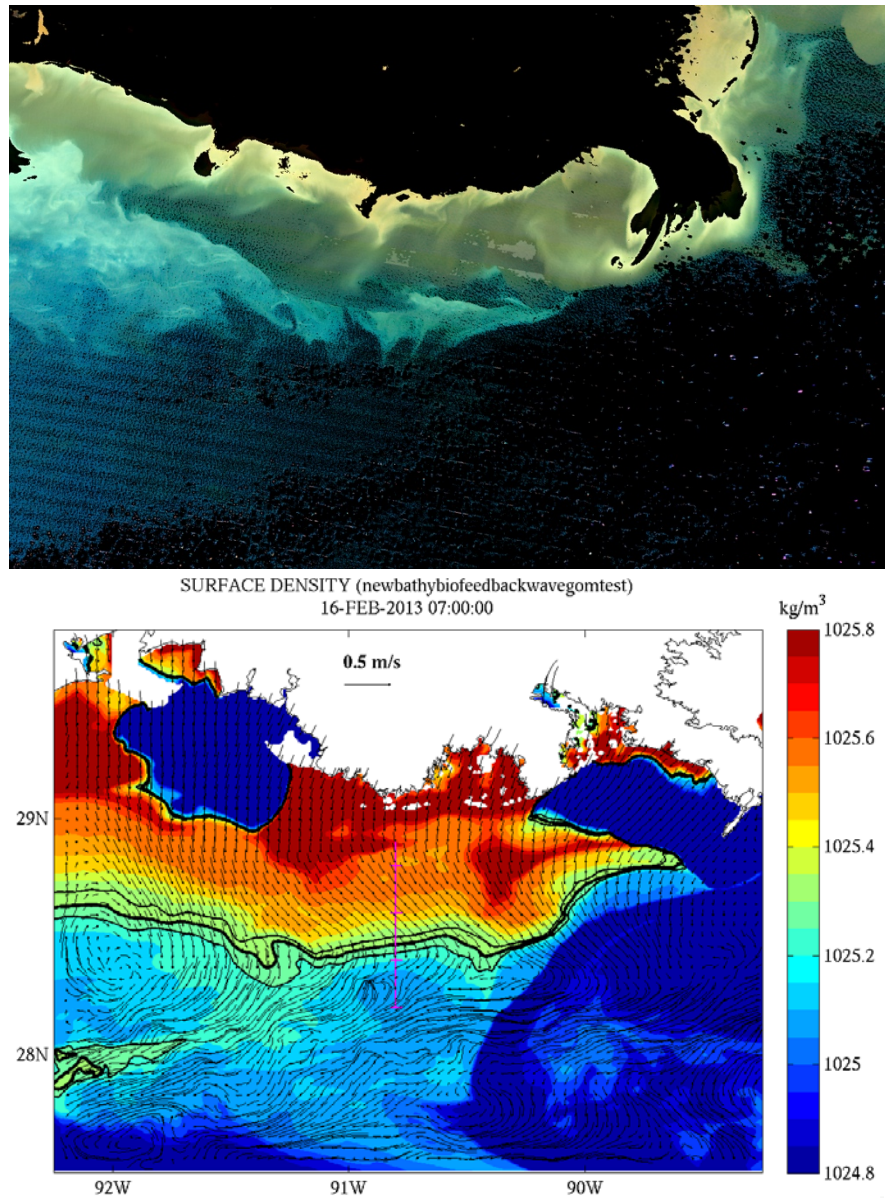


Figure 1. Top: Moderate Resolution Imaging Spectroradiometer (MODIS) (Terra) true color projection, 16 February 2013, based on remotely sensed reflectance. (Jolliff et al., 2018a) Bottom: COAMPS simulated density with surface current overlay: although the river effluent from the Atchafalaya is prominent near the coast, the temperature-driven shelf front density gradient (indicated by contours) occurs approximately where the blue-shifted turbidity appears in the satellite images. (Jolliff et al., 2018b)

Title: Modeling Cloud-Aerosol Interactions in Long-Lived Polluted Clouds

Author(s): P. Caffrey and S. Rabenhorst

Affiliation(s): Naval Research Laboratory, Washington, DC

CTA: CWO

Computer Resources: SGI ICE X [ARL, MD]; SGI ICE X [ERDC, MS]

Research Objectives: Observations of dust-infused baroclinic storm (DIBS) clouds have revealed Saharan and Asian storm systems with mineral dust mixed with overrunning cirrus shield clouds at altitudes of 8 - 10 km. The unique characteristics observed in these clouds, including intense cloud-aerosol lidar with orthogonal polarization lidar backscatter and large daytime 3.9- to 11- μm brightness temperature differences (indicating relatively small ice crystals), have prompted this modeling study to determine the mineral dust pathway and dynamics, if any, through an observed DIBS.

Methodology: We use the advanced weather research and forecasting (WRF) model with the chemistry model (WRF-Chem) and constrained with the WRF data assimilation system (WRF-DA) to conduct a reanalysis of an East Asian DIBS from 6 to 11 April 2010. Desert dust emission via the global ozone chemistry aerosol radiation and transport dust emission scheme and transport from both the Taklimakan and Gobi deserts is simulated within WRF-Chem with the model for simulating aerosol interactions and chemistry aerosol treatment. In-line air mass trajectories were used to source and trace dust transport from the storm spin-up through dissipation four days later.

Results: Results show rapid dust transport from the Gobi desert to cirrus cloud tops via the warm conveyor belt mechanism, with the dust mixed throughout the cloud at altitudes from 5 to 10 km. Results are verified by good qualitative agreement with cloud-aerosol lidar with orthogonal polarization observations at several different moments in the DIBS cycle, including an elevated layer of dust that remains after storm cloud dissipation. These results confirm the potential for routine and significant dust-cloud processing in DIBS cases, affecting both cloud properties and identifying a previously unidentified pathway for long-range transport of dust.

DoD Impact/Significance: Using HPC resources to unravel observations of newly discovered and unexplained features of specific storm/cloud events (DIBS) furthers our understanding of the limitations of existing Navy/DoD weather prediction systems. DIBS and other unique polluted cloud types are not properly understood or identified properly, and current weather models do not account for their effects on cloud microphysical properties and lifetimes. Understanding these systems will lead to their proper treatment in weather predictions systems, with improvements then in cloud prediction, visibility, and aviation forecasts, among others.

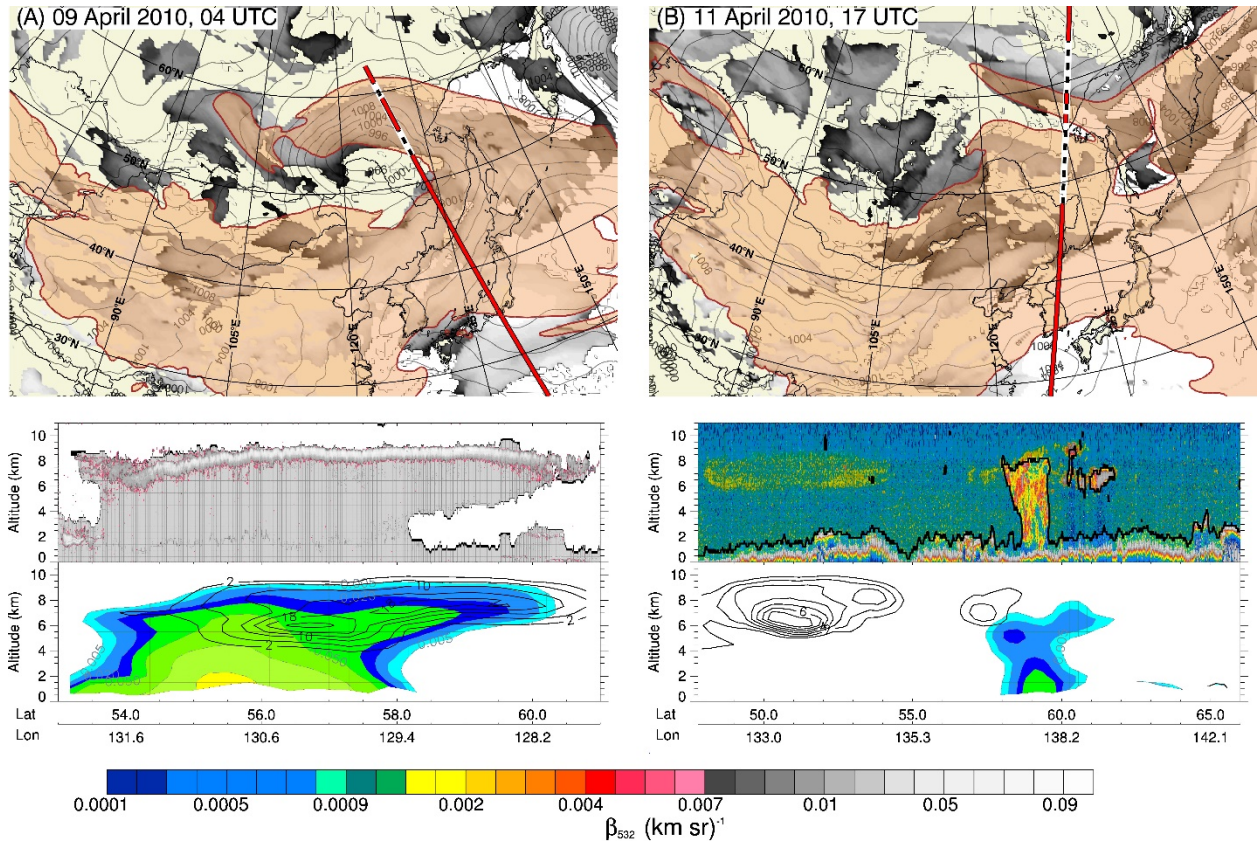


Figure 1. WRF-Chem Results: DIBS evolution, (A) mature and (B) decay phase. Top panels present WRF-Chem results at the time of the Cloud-Aerosol Lidar and Infrared Pathfinder Satellite Observations (CALIPSO) overpasses, with contour lines of sea level pressure, cloud-top pressure (clouds) in gray scale, and the dust plume overlain in semi-transparent brown. Dust is indicated as the vertically integrated dust mass greater than 0.5 mg m^{-2} . Bottom panels compare the WRF-Chem dust and cloud results with the measurements of CALIPSO and CloudSat along the satellite track depicted in the top panel by the black and white hatched line. CALIPSO lidar backscatter as indicated by colorbar, but limited here for clarity for backscatter greater than $0.005 \text{ km}^{-1} \text{ sr}^{-1}$ in (A), and the CloudSat cloud mask product in gray to indicate measured cloud volumes. Below those are the corresponding WRF-Chem results, with dust aerosol mass concentrations ($\mu\text{g m}^{-3}$) in black contour lines, and clouds as total water content (sum of ice, snow, and liquid water (in g m^{-3})) in the filled, colored contours.

Title: Atmospheric Process Studies

Author(s): N.P. Barton,¹ T. Whitcomb,¹ J. Ridout,¹ K. Viner,¹ J. McLay,¹ W. Crawford,² M. Liu,¹ and C. Reynolds¹

Affiliation(s): ¹Naval Research Laboratory, Monterey, CA; ²American Society for Engineering Education, Washington, DC

CTA: CWO

Computer Resources: Cray XC30 [NAVY, MS]; Cray XC30 [AFRL, OH]; Cray XC40 [NAVY, MS]; Cray XC40 [ARL, MD]; Cray XC40 [ERDC, MS]

Research Objectives: To improve our understanding of the fundamental dynamical and physical processes that operate in the atmosphere and to develop and test a state-of-the-art global atmosphere prediction system that includes data assimilation and ensembles.

Methodology: We focus on improving the accuracy and efficiency of the Navy global environmental model (NAVGEM). NAVGEM is the Navy's current global atmosphere operational numerical weather prediction model, and is used for basic and applied atmospheric research. We aim to improve the representation of physical processes in the model. As initial conditions are very important to numerical systems, NAVGEM is developed in conjunction with its data assimilation capability, NAVDAS-AR. In addition, seamless prediction across multiple temporal scales and earth system components is the next frontier of numerical prediction, and NAVGEM is being developed and tested when tightly coupled with the hybrid coordinate ocean model (HYCOM) and the Los Alamos community sea ice code (CICE) using the earth system modeling framework (ESMF) tools under the earth system prediction capability (ESPC) national program. Seamless prediction across temporal scales requires additional research and development on probabilistic prediction and diagnostics using ensembles.

Results: This year's advances largely fall into the categories of (1) workflow management development, (2) NAVGEM 2.0 testing, and (3) ensemble forecasting with NAVGEM stand-alone and the coupled model. (1) For workflow management, our effort focuses on implementing the Cylc workflow manager to aid our operational partners in modernizing their run control as well as updating our R&D workflows for better use of HPCMP resources through more accurate resource allocation and error handling. This development with our operational partners will remove technical barriers that slow the transition of our science to operational Navy weather prediction systems. (2) NAVGEM 2.0 testing mainly addressed changes to physics-dynamics coupling, subgrid scale vertical mixing, and preparation for transition; this requires long periods of cycling the system to obtain statistically significant differences relative to NAVGEM 1.4. A major result of this testing was a major improvement in the representation of low level clouds in NAVGEM 2.0, which has major implications for downstream ocean prediction through modified surface radiative forcing. Preliminary results show considerable improvements in the tropical storm track error over the currently operational system (Fig. 1). (3) For the ensemble prediction system, a new capability to account for model error during the ensemble forecast was developed under these resources. The model error is derived from analysis increments in the data assimilation scheme and fed into the forecast model throughout the forecast. The modification proved beneficial to the earth prediction system and has been submitted to our operational partner for transition. This method may also be used in the coupled model ensemble system.

DoD Impact/Significance: Continued development of our global forecast system is making significant positive impacts on weather forecasts and DoD predictions dependent on weather forecasting (i.e., ocean modeling, wave modeling, and ship routing). Developments in coupled modeling and extended range probabilistic forecasting increase the utility of the forecast and potential number of users. This development provides an improved modeling system for studying the dynamical and physical processes in the atmosphere.

TROPICAL STORM TRACK ERRORS

NAVGEN 2.0 Test Configuration versus NAVGEN 1.4.3

July 1 – September 15, 2017

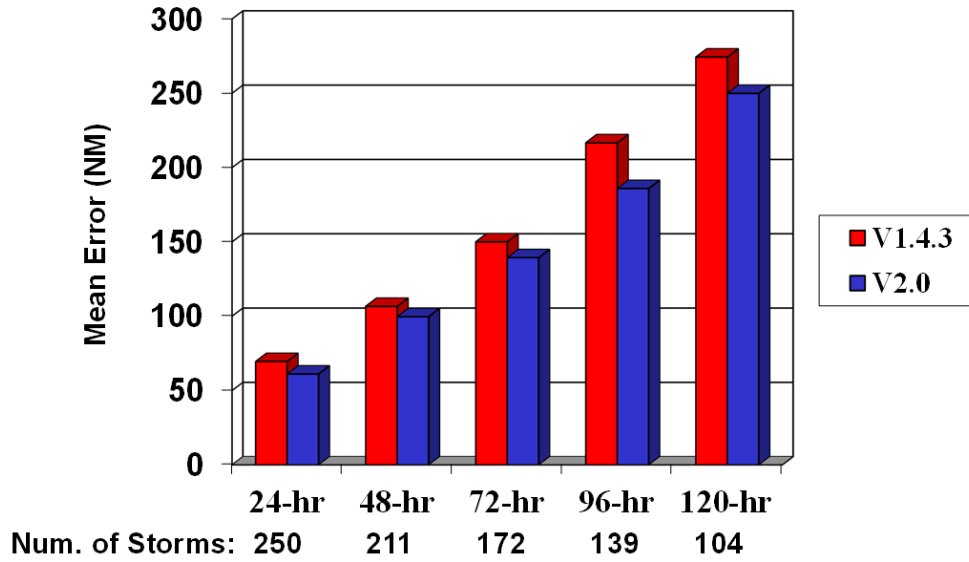


Figure 1. Tropical storm track errors in nautical miles between a test configuration of NAVGEN 2.0 at the T681L60 resolution against the current operational NAVGEN 1.4.3 (T425L60). Track error is on the y-axis and forecast hour is on the x-axis. As shown, the NAVGEN 2.0 has smaller track errors at all forecast hours.

Title: Multi-scale Characterization and Prediction of the Global Atmosphere from the Ground to the Edge of Space using Next-Generation Navy Modeling Systems

Author(s): J.P. McCormack,¹ S.D. Eckermann,¹ C.A. Barton,^{1,3} F. Sassi,¹ M.A. Herrera,^{1,3} K.W. Hoppel,¹ D.D. Kuhl,¹ D.R. Allen,¹ J. Ma,² and J. Tate²

Affiliation(s): ¹Naval Research Laboratory, Washington, DC; ²Computational Physics, Inc., Springfield, VA; ³National Research Council Postdoctoral Research Fellow, Washington, DC

CTA: CWO

Computer Resources: Cray XC40 [ARL, MD]; Cray XC40 [NAVY, MS]; Cray XC40 [ERDC, MS]; Cray XC30 [NAVY, MS]; SGI Altix ICE [NRL, DC]; SGI Altix ICE [ARL, MD]

Research Objectives: To develop and test new seamless atmospheric specification and prediction capabilities from 0-500 km altitude for a future Navy Earth System Prediction Capability (ESPC) linking the ocean, atmosphere, and space over time scales from hours to decades.

Methodology: This project develops and tests key components of state-of-the-art systems required for the improved modeling, prediction and analysis of the extended operational environment for Navy applications, focusing on the atmosphere, the near space and the geospace. Specific systems under development are: (a) a high altitude version of the Navy global environmental model (NAVEM-HA), based on an upward extension of the Navy's operational global numerical weather prediction (NWP) system; (b) the NRL atmospheric variational data assimilation system – accelerated representer (NAVDAS-AR), the Navy's four-dimensional variational (4DVAR) data assimilation algorithm; (c) the coupled ocean-atmosphere mesoscale prediction system (COAMPS[®]), the Navy's operational regional NWP system, and; (d) the whole atmosphere community climate model extended version (WACCM-X), a ground-to-space global model of Earth system climate and part of the National Center for Atmospheric Research community earth system model (NCAR CESM).

Results: Major results during FY18 include: (a) development and testing of new modeling and data assimilation techniques to determine relative roles of resolved and parameterized sub-grid-scale gravity wave drag on atmospheric circulations in the stratosphere and mesosphere (see Fig. 1); (b) first decadal free-running NAVEM-HA simulations that generate and sustain a quasi-biennial oscillation (QBO) in equatorial stratospheric winds; (c) improved forecasts of equatorial stratospheric winds out to 100 days using a high-vertical resolution version of the NAVEM-HA forecasts/analysis system for northern winters of 2013-2014, 2014-2015, and 2015-2016; (d) production runs of NAVEM-HA meteorological analyses extending from the surface to 100 km altitude over the 3-year period 2014-2016 for comprehensive studies of atmospheric dynamics in collaboration with observational field campaigns; (e) use of NAVEM-HA analyses for specification of lower atmosphere dynamics in WACCM-X model simulations showing the impact of atmospheric observations in the 50-100 km altitude region on the ability to specify and predict thermospheric tidal circulations that, in turn, drive day-to-day variability in high-frequency radio wave propagation within the ionospheric E and lower F regions (100-300 km altitude).

DoD Impact/Significance: This research develops and tests new high-altitude atmospheric specification and prediction capabilities that together will comprise bridge technology to a future Navy ESPC by 2020. This project provides the Navy with logistical support to install an accurate high-altitude (e.g., 10-100 km) specification and forecast capability in next-generation Navy NWP systems, which can ultimately provide improved near-space specification and prediction capabilities to the warfighter over both tactical and strategic time frames.

¹COAMPS[®] is a registered trademark of the Naval Research Laboratory

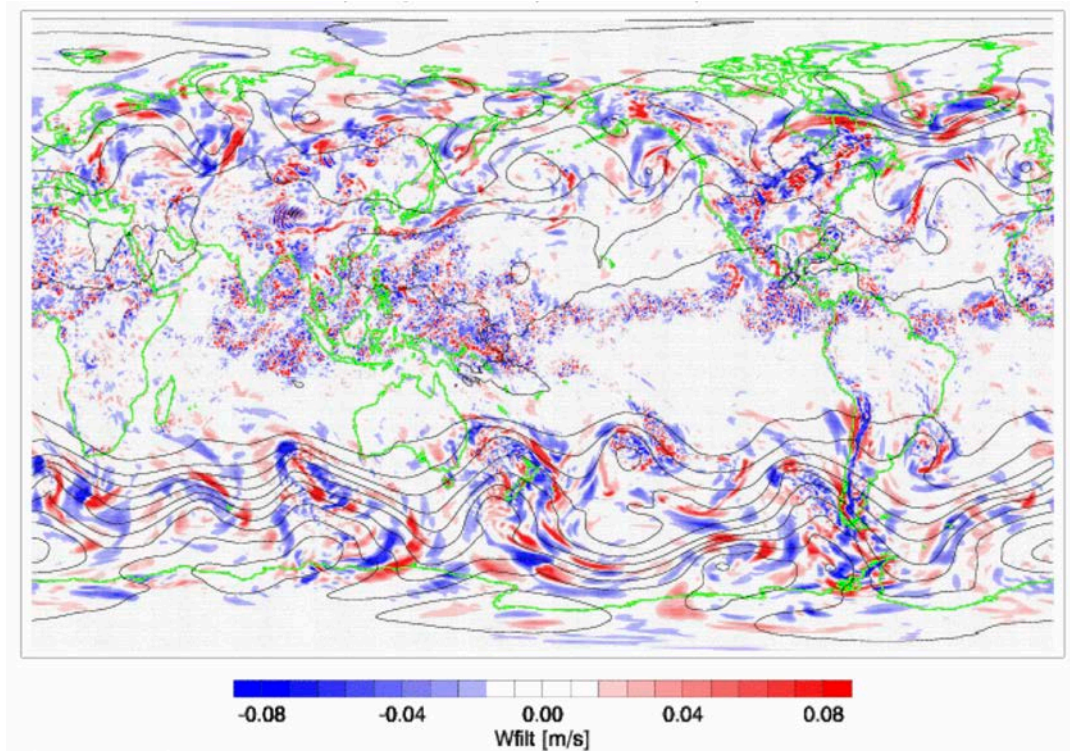


Figure 1. Shading indicates sources of resolved gravity (buoyancy) waves in NAVGEM-HA analyses valid 00 UT 1 July 2014 calculated from spatially filtered vertical winds at 500 hPa (approximately 5 km altitude) with total wavenumber 22 or greater. Contours indicate geopotential height at 500 hPa.

Title: Variational Data Assimilation

Author(s): S. Smith,¹ C. Amerault,² C. Barron,¹ T. Campbell,¹ M. Carrier,¹ J. D'Addezio,³ J. Dastugue,¹ S. DeRada,¹ E. Douglas,¹ P. Martin,¹ J. May,¹ W. Mulberry,⁴ H. Ngodock,¹ J. Osborne,⁵ C. Rowley,¹ R. Schaefer,⁵ J. Shriver,¹ O. Smedstad,⁶ T. Smith,¹ I. Souopgui,⁷ and P. Spence⁶

Affiliation(s): ¹Naval Research Laboratory, Stennis Space Center, MS; ²Naval Research Laboratory, Monterey, CA; ³University of Southern Mississippi, Stennis Space Center, MS; ⁴University of North Carolina, Greensboro, NC; ⁵American Society for Engineering Education, Stennis Space Center, MS; ⁶QinetiQ North America, Stennis Space Center, MS; ⁷University of New Orleans, Stennis Space Center, MS
CTA: CWO

Computer Resources: Cray XC30 [NAVY, MS]; Cray XC40 [NAVY, MS]

Research Objectives: The scope of this project is to advance the analysis and prediction capability of the Navy's environmental modeling and forecasting systems through the improvement of the assimilation software. This project used three different variational assimilation systems: 1) Relo NCOM (3DVAR), 2) the multi-scale 4DVAR, and 3) the NCOM-4DVAR. There were 8 funded NRL projects that focused on either adding or improving capabilities of 4DVAR in FY18, and the experiments performed under this HPC project went toward satisfying these efforts.

Methodology: This HPC project helped advance the NCOM-4DVAR assimilation system in FY18 through the following funded NRL projects: (1) The 6.4 Ocean Data Assimilation (ODA) project tested the NCOM-4DVAR within the operational COAMPS5 system and in the highly nonlinear regimes of the U.S. East Coast and Western Pacific. (2) The 6.4 RTP Coupled Ocean-Atmosphere Variational Assimilation and Prediction System project merged the 4DVAR capabilities of the atmospheric and oceanic components of the Coupled Ocean/Atmospheric Mesoscale Prediction System (COAMPS) to create a coupled 4DVAR capability. (3) In the 6.4 RTP Coupled Ocean-Acoustic Assimilative Model project, a number of validation experiments were performed of the coupled 4DVAR-NCOM and 4DVAR-RAM system. (4) The 6.2 Smart Glider Teams for Rapid Update of Local Analysis project tested the multi-scale 4DVAR for accurately assimilating coordinated teams of gliders. (5) The 6.1 Propagation and Dissipation of Internal Tides on Coastal Shelves project continued the study of the year-long NCOM-4DVAR experiment on the Northwest Australia Shelf to resolve the generation of internal tides. (6) The 6.4 Validation and Verification of NCOM-4DVAR project performed experiments in the South China Sea to prepare its transition into an operational setting. (7) The 6.2 Submesoscale Prediction of Eddies through Altimeter Retrieval (SPEAR) project performed 3DVAR and 4DVAR experiments in the North Arabian Sea to test high-resolution assimilation (1 km) of future observation types (Wide Swath Altimetry and Satellite Sea Surface Salinity) to improve the resolution of submesoscale features. (8) The NCOM-4DVAR was used to provide real-time support for field experiments for a CMRE Collaboration.

Results: Numerous 3DVAR, NCOM-4DVAR, multi-scale 4DVAR experiments were performed under this FY18 HPC project with the overall result of further improving the analysis accuracy, prediction skill, portability and robustness of the system in various regions of interest. A few of the specific advancements that were made include: assimilating at very high resolution, coupling assimilation systems from different models, using multi-scale, and assimilating velocities, SWOT, and SSS observations.

DoD Impact/Significance: The 3D and 4D variational systems that were tested under this project went toward improving the Navy's capability for forecasting the ocean environment. Various validation studies for the 4DVAR-NCOM were performed and they showed more accurate analyses and model forecast fields than its predecessor, NCODA_VAR. Additionally, the work on coupling the assimilation systems for the ocean, atmosphere, and acoustic models made significant progress this fiscal year and these coupled systems will ultimately further improve the forecast skill of all three environments.

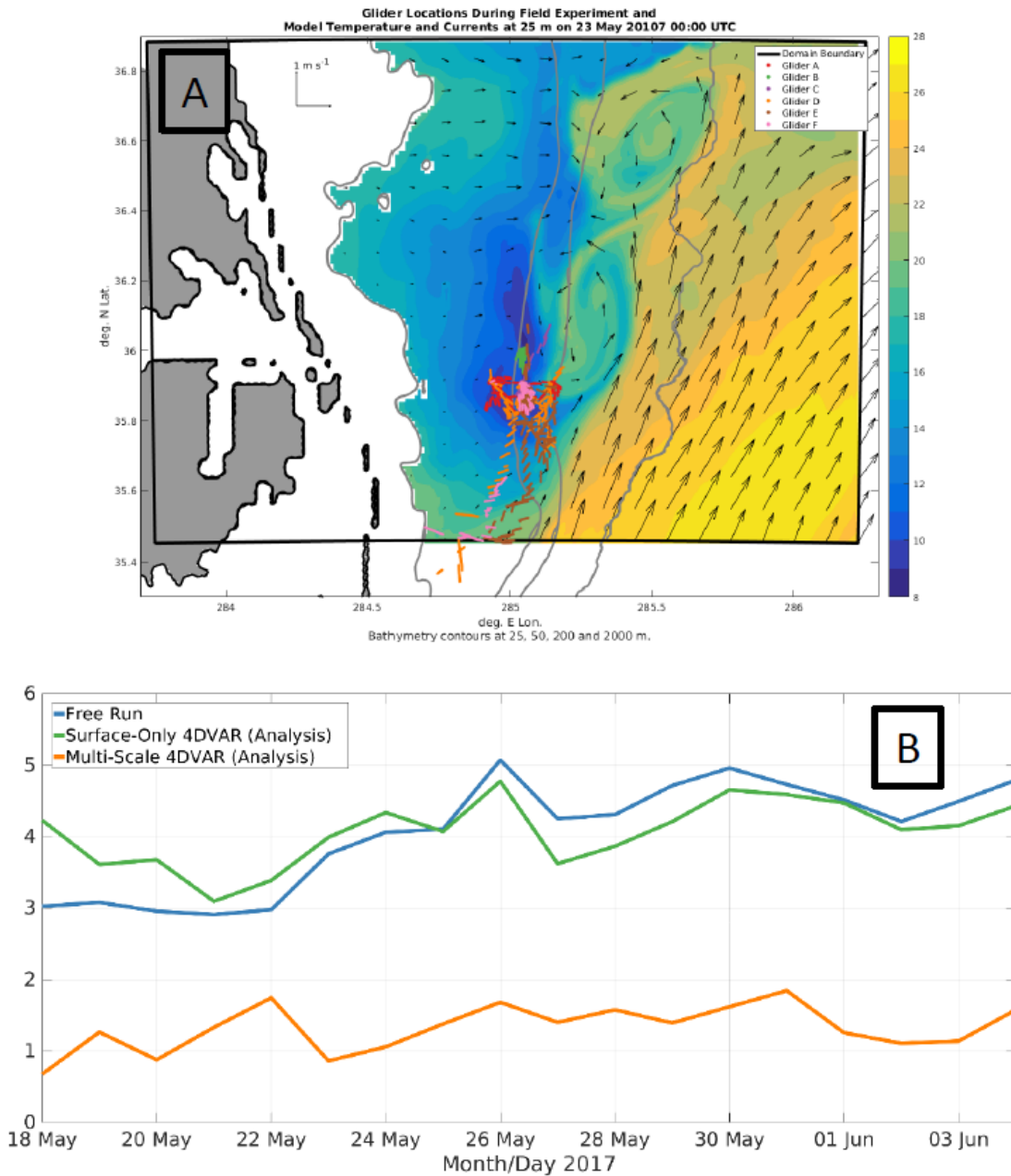


Figure 1. Temperature and salinity profiles from 6 gliders were assimilated into a Relocatable Navy Coastal Ocean Model (RELO NCOM) with a “multi-scale” four-dimensional variational (4DVAR) approach. Gliders were deployed north of Cape Hatteras (US East Coast) and inshore of the Gulf Stream in a field experiment from 17 May until 4 June 2017 (Panel A). The comparison of root mean square errors from non-assimilative, normal 4DVAR, and multi-scale 4DVAR assimilation experiments show that multi-scale 4DVAR significantly improves the ability to assimilate glider data (Panel B).

Title: Rogue Wave Probability Estimator for WAVEWATCH III

Author(s): M. Orzech,¹ J. Simeonov,¹ and M. Manolidis²

Affiliation(s): ¹Naval Research Laboratory, Stennis Space Center, MS; ²National Research Council Postdoctoral Research Associate, Naval Research Laboratory, Stennis Space Center, MS

CTA: CWO

Computer Resources: Cray XC40 [ARL, MD]; Cray XC40 [NAVY, MS]; Cray XC40/50 [ERDC, MS]

Research Objectives: Overall objective is to develop a configurable module for WAVEWATCH III to forecast the likelihood of rogue waves around the world. The probability estimation system will operate in a broad range of wave environments, using metrics to account for multiple extreme-wave contributors based on established theory and extensive analysis of representative sea states. FY18 objectives include: (1) Analyze and quantify the effects of current gradients on rogue wave formation with the CFD model NHWAVE. (2) Configure and utilize the continuum mechanics model OpenFOAM to simulate airflow over a highly nonlinear, wavy water surface on which rogue wave formation is imminent; determine whether wind is playing a role in either damping or augmenting the rogue development.

Methodology: For objective (1), generate waveforms based on a JONSWAP spectrum in a numerical wave tank and allow them to propagate against current gradients of known strength, monitoring wave characteristics throughout the process in a series of simulations. Quantify changes in the wave groups by tracking both total energy E and significant wave height H_s . Compare these results to estimates of wave evolution in currents based on both linear and nonlinear theory. Measure the degree of nonlinearity of the wave groups using the Benjamin-Feir Index (BFI ; Benjamin & Feir, 1967). Use simulation results to determine an empirical relationship expressing the change in BFI as a function of current gradient strength. For objective (2), conduct a series of simulations including both air and water phases, varying model resolution in the vicinity of the air-sea interface. Adopt a computationally efficient approach based on the Reynolds-Averaged Navier Stokes (RANS) equations with a k-epsilon closure model estimating the turbulent kinetic energy and the turbulent eddy viscosity throughout the air and the water phases.

Results: We verified that waves gain energy from the underlying flow field as they travel against current gradients, and the simulated level of energy increase was comparable to that predicted by earlier studies of the nonlinear Schrödinger equation. Based on simulation results, we determined that the BFI for waves propagating against a current gradient can best be expressed in terms of the initial index, BFI_o , as

$$BFI = BFI_o \exp(C_o \Delta U / c_g)$$

where $C_o = 3.59$ is an empirical coefficient, ΔU is the net change in the opposing current velocity from initial to final location, and c_g is the wave group velocity.

We have made progress toward overcoming two related computational difficulties in the proposed RANS wind-wave simulations. To initialize the fully developed turbulent wind flow in the air phase, we implemented full/partial logarithmic wind profiles at locations where the water interface was below/above mean sea level, respectively. To limit the excessive production of turbulent kinetic energy damping near the interface, we modified the k-epsilon model to completely suppress the turbulence below the water interface. We are currently working on implementing a second modification of the k-epsilon model to include stability functions above the interface that damp the excessive production of turbulence in the air phase.

DoD Impact/Significance: Accurate prediction of environmental hazards is important to tactical and strategic operations in the world's oceans. The results obtained from these simulations will form the core of the configurable WAVEWATCH III prediction module, which will enhance the safety of naval missions and reduce the potential for damage or loss of Navy assets in rogue wave events.

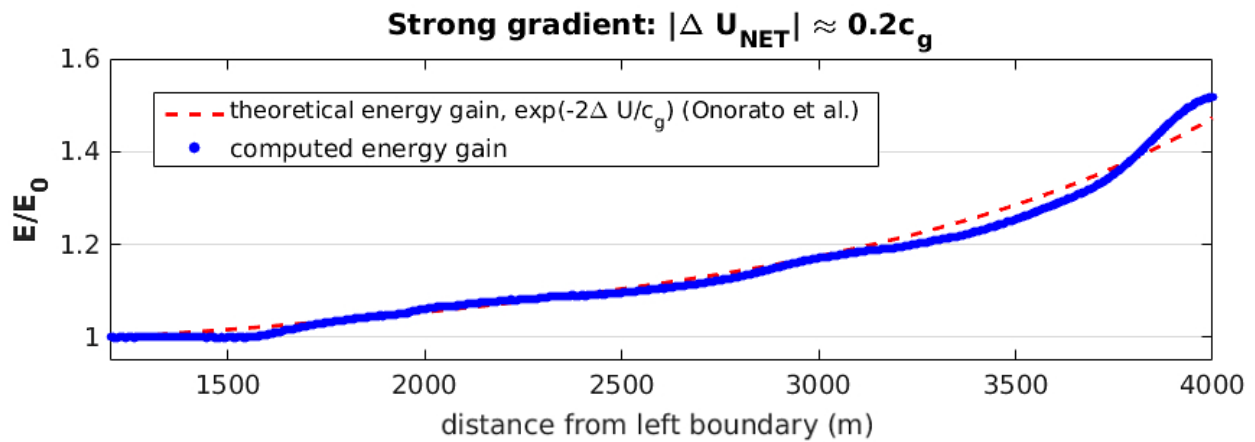


Figure 1. Evolution of relative total wave energy, E/E_o , for waves propagating against a current gradient. Current is constant before $x = 1200$ m, after which it begins to increase. The total increase in the opposing current velocity across the entire domain (i.e., from $x = 1200 - 4000$ m) is 0.2 times the wave group velocity c_g . Computed energy gain (blue line) is well matched by nonlinear theory (red dashed line).

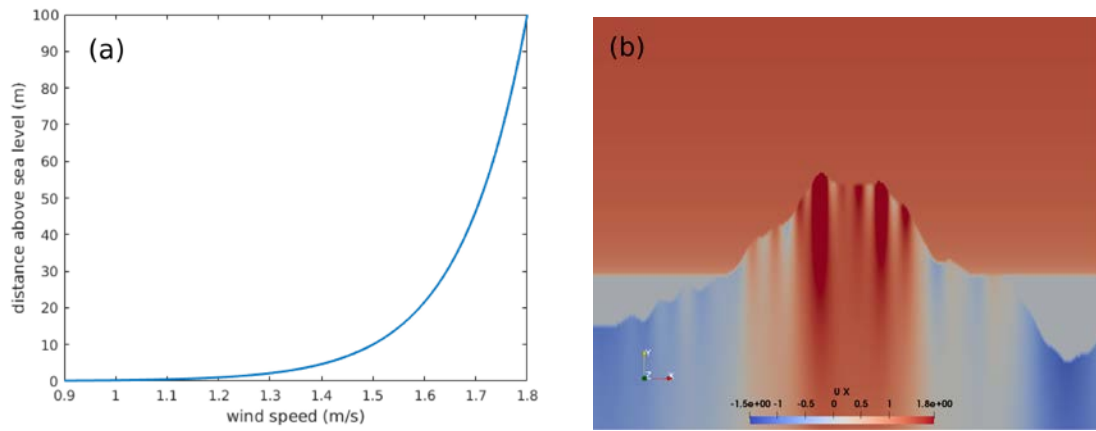


Figure 2. (a) Logarithmic wind velocity profile with $U_{10} = 1.5$ m/s. (b) Detailed view of the air-water interface with a 1:10 scale in the horizontal direction.

Title: Dynamics of Coupled Models

Author(s): I. Shulman, B. Penta, S. Cayula, and C. Rowley

Affiliation(s): Naval Research Laboratory, Stennis Space Center, MS

CTA: CWO

Computer Resources: Cray XC40 [NAVY, MS]

Research Objective: Improve our understanding of coupled bio-optical and physical processes in the coastal zone and the variability and predictability of the coastal ocean's optical properties on time scales of 1-5 days. Investigate the coupled dynamics of ocean bio-optical, physical, and atmospheric models. Provide a foundation for the development of scientifically valid, dynamically coupled atmosphere-ocean models.

Methodology: The approach is based on using nested, coupled physical-bio-optical models of the coastal region together with bio-optical and physical in-situ and remotely sensed observations. Data assimilation techniques for both physical and bio-optical fields are being used to examine project research issues and objectives. Approach is also based on joint studies of the bioluminescence (BL) potential and inherent optical properties (IOPs) over relevant time and space scales. Dynamical, biochemical, physical and BL potential models are combined into a methodology for estimating BL potential and night-time water leaving radiance (BLw).

Results: We published a refereed paper describing a novel, ensemble-based approach to specify observational error covariance in the data assimilation of satellite bio-optical properties. The proposed choice of observational error covariance gives observational errors less than 35% of the mean observed value at observational locations in relatively more productive areas (where the ensemble mean values are approximately more than 2.5 mg/m³), and observational errors more than 35% at observational locations in less productive areas of the modeling domain. Comparisons demonstrated that data assimilation with the proposed observational error covariance has smaller or comparable errors than the data assimilation run with the assumption that observational errors equal 35% of the ensemble mean (JGR Oceans, 2018). We developed an ensemble approach for modeling bioluminescence (BL) potential. The proposed approach has been applied to modeling of the BL potential changes in the area of the submesoscale filament, which developed during the upwelling event in the Monterey Bay area, California. We demonstrated that BL potential dynamics are impacted by the submesoscale processes due to the interaction between warm anticyclonic eddy and cold jet in the Monterey Bay area, and due to the interaction between buoyant river outflow with cold and saline upwelled water in the Delaware Bay area.

DoD Impact/Significance: Emerging Navy Electro-Optical (EO) systems under development and Special Operations missions require an improved understanding of the ocean optical environment. This is critical for operations and weapon deployment, especially in the coastal and littoral zones. Improved basin scale to mesoscale forecast skill is critical to both military and civilian use of the oceans, particularly on the continental margins.

Combining bioluminescence potential and coupled bio-optical, physical models

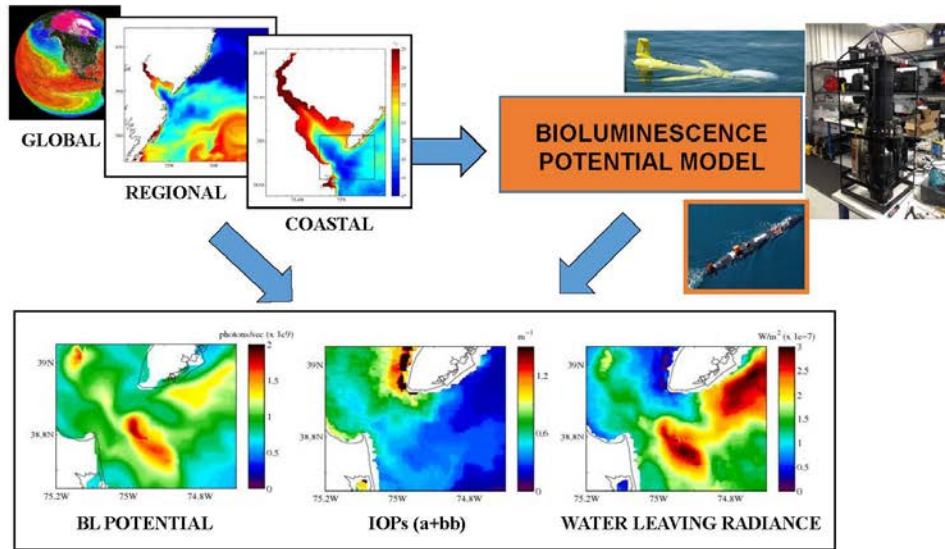


Figure 1. Approach for bioluminescence (BL) potential modeling and forecasting. Bio-optical, physical, data assimilative, nested models are merged with BL potential model and observations into predictions of BL potential and water leaving radiance due to stimulated BL potential.

Title: Probabilistic Prediction to Support Ocean Modeling Projects

Author(s): C.D. Rowley,¹ L.F. Smedstad,¹ C.N. Barron,¹ R.S. Linzell,² M. Yaremchuk,¹ J.C. May,¹ J.M. Dastugue,¹ P.L. Spence,² T.L. Townsend,¹ T.A. Smith,¹ J.J. Osborne V,³ G.G. Pantelev,¹ N. VandeVoorde,² B.P. Bartels,² and B.R. Maloy¹

Affiliation(s): ¹Naval Research Laboratory, Stennis Space Center, MS; ²Perspecta, Stennis Space Center, MS; ³Naval Research Laboratory Postdoctoral Program, Stennis Space Center, MS

CTA: CWO

Computer Resources: Cray XC40 [NAVY, MS]

Research Objectives: Develop ocean and air-sea coupled ensemble generation, ensemble data assimilation, and probabilistic prediction capabilities using the Coupled Ocean Atmosphere Mesoscale Prediction System (COAMPS[®]), Navy Coastal Ocean Model (NCOM), and Hybrid Coordinate Ocean Model (HYCOM). Extend ocean data assimilation capabilities and test and implement new types/platforms of ocean and air/ocean surface observational data.

Methodology: Current operational capability for regional ocean ensemble forecasts is being extended to global ocean and regional and global coupled air-ocean-ice-wave extended-range forecast systems. We face new technical challenges due to the size and scale of global ocean and global coupled ensembles in the Earth System Prediction Capability (ESPC) program. Work consisted of global coupled system ensemble initialization and metrics development; support for NRL modeling and data handling; testing of systems for operational use with new types of input data; NCOM/NCODA system development to support NAVOCEANO operational modeling; assimilation tests comparing adjoint-free and standard 4dVar; and a series of assimilation runs to advance gaussianization methodology in application to ice concentration and ice thickness assimilation in NCODA (static covariance formulation). Testing and simulations of the Global Heterogenous Observation Systems (GHOST) system were performed to utilize the GHOST system for support of new platforms and the Smart Glider Teams project.

Results: We continue to support transitioned operational NCOM/NCODA systems at NAVOCEANO using the allocation in this project. Multi-scale four-dimensional variational data assimilation methods for teams of autonomous ocean-observing platforms were tested. High-resolution COAMPS modeling was performed for the ICoBOD project with 1000-point nests run at both 125 m and 50 m resolution. HPC support used by our satellite sea surface temperature (SST) work supported evaluations of assimilative forecasts using new SST data streams from GOES-16, Meteosat-8, and Meteosat-11.

DoD Impact/Significance: These HPC resources support research and development efforts on coupled data assimilation and ensemble forecasting. Higher resolutions and larger ensembles are needed to ensure forecast reliability and accurate risk assessment in areas such as antisubmarine warfare, nuclear-chem-bio hazard prediction and monitoring, and search and rescue. Development of extended-range coupled forecasts depends on probabilistic forecasting, due to the inherent limitations of deterministic forecasts at extended forecast times, and on new coupled-assimilation techniques to improve initial conditions. Operational systems are becoming more embedded with new types in data obtained from autonomous systems, and more interest on the air-sea interface requires more understanding of the assimilation capabilities that will improve modeling in these areas. Controlling larger amounts of autonomous systems requires more complex algorithms and interface from outside of the DSRC environment which has led to complicated system development.

¹COAMPS[®] is a registered trademark of the Naval Research Laboratory

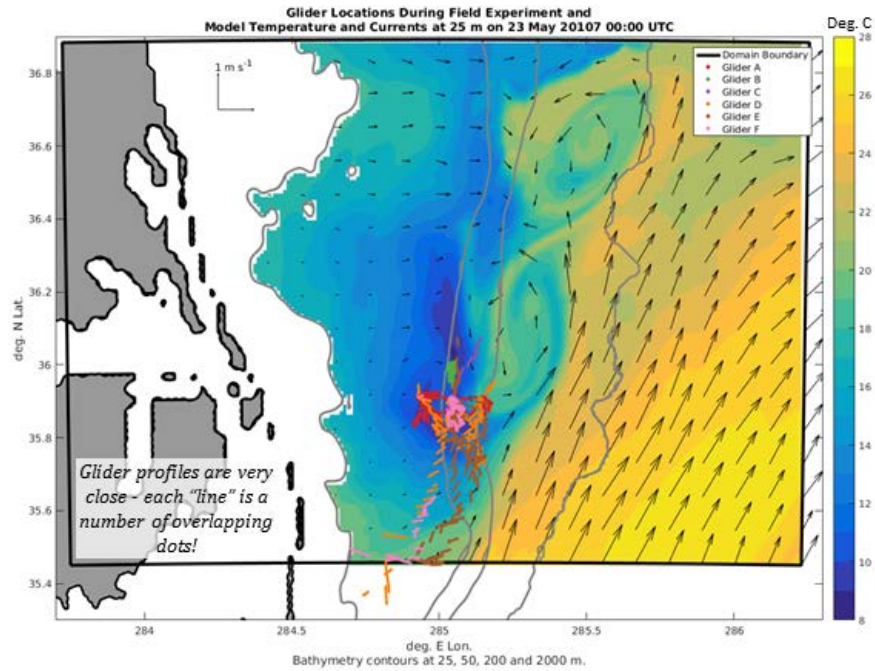


Figure 1. Six U.S. Naval Research Laboratory (NRL) autonomous undersea “gliders” were deployed off the North Carolina coast in a field experiment in May and June 2017, collecting over 14000 vertical profiles of ocean temperature and salinity. NRL scientists have developed new ways to assimilate this data with ocean models. Shown here are, at midnight on 23 May 2017, temperature at 25 m depth (blue-yellow field), water velocity at 25 m (arrows), and glider locations during the entire field experiment (colored dots/lines). New data assimilation methods tested in FY18 result in more accurate forecasting of cold water (just north of glider positions).

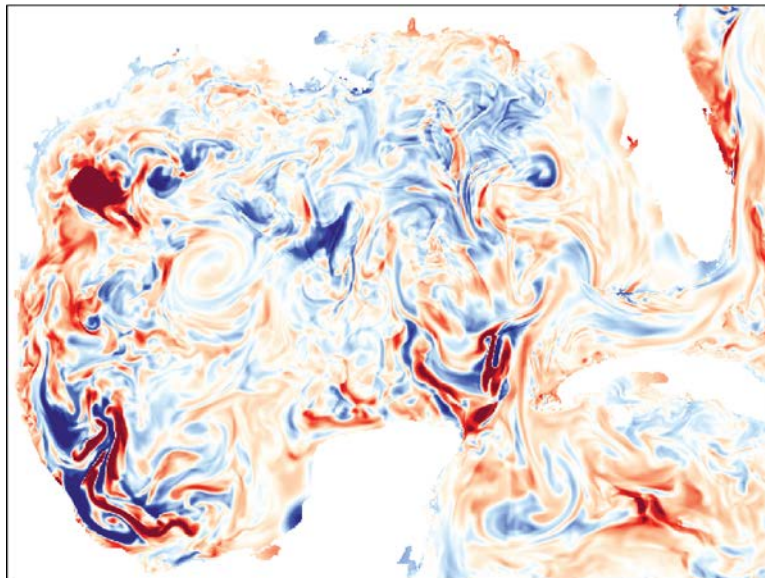


Figure 2. HPC hours supported evaluations of new satellite sea surface temperature (SST) data streams. The figure above shows the difference in SST in the Gulf of Mexico on 14 August 2018, subtracting SST of the ocean model forecasts assimilating NPP VIIRS data from the run assimilating GOES-16 observations.

Title: Guidance for Heterogeneous Observation Systems (GHOST)

Author(s): L.F. Smedstad,¹ C.N. Barron,¹ G.A. Jacobs,¹ P.L. Spence,² C.J. DeHaan,² T.A. Smith,¹ R.S. Linzell,² B.P. Bartels²

Affiliation(s): ¹Naval Research Laboratory, Stennis Space Center, MS; ²Perspecta, Stennis Space Center, MS

CTA: CWO

Computer Resources: Cray XC40 [NAVY, MS]

Research Objectives: GHOST determines water-sampling plans for a suite of unmanned observation systems under active Navy control. The data are targeted to optimize battlespace environment forecasts. Accurate use of the data is through ocean data assimilation capabilities that should be extended and tested in order to implement new types/platforms of ocean and air/ocean surface observations.

Methodology: Several experiments were performed to determine appropriate influence scales of incoming platform observations. A symbiotic relationship exists between the platforms and models, and the best use of platform data must be determined. When observations are used to regularly correct ocean model initial conditions, there is a constraint on the scales that are predicted in the forecast. Larger scales that are well resolved have lower prediction errors than small scales not resolved. The scales at which there is skill in the forecast are “constrained” while smaller scales are not constrained. The regular corrections made to the initial condition through the data assimilation have a prescribed decorrelation length scale, which does vary spatially, and this scale must be consistent with the constrained scales. A series of ocean forecast experiments are set up with a range of decorrelation scales that average from 9 km to 140 km (Fig. 1). The scales constrained in the model experiments are not the same as the decorrelation scale of the assimilation process.

Results: Model runs with a range of prescribed influence or decorrelation scales show that small decorrelation scales (12 to 20 km) produce many localized corrections (left frames of Fig. 1) that do not influence the larger scale circulation and do not provide improvement in forecast currents. Medium scales (50-100 km) produce more physically realistic corrections to the model forecast initial conditions. Long decorrelation scales (150 km) result in unrealistically correcting very broad scales (right frames of Fig. 1) that do not reflect the ocean features affecting Navy operations.

DoD Impact/Significance: Ocean forecasts are critically reliant on regular corrections of initial conditions on a daily basis via use of environmental observations. We must optimize the parameters controlling the influence scales of observations to produce accurate forecasts. This influences the accuracy of battlespace environment forecasts for the operational Navy missions. These include antisubmarine Warfare (ASW) operations where sound speed is critical, currents that affect Naval Special Warfare (NSW) and mine warfare (MIW). Search and rescue (SAR) operations are also dependent on accurate ocean forecasts. HPC resources support research and development efforts on data assimilation and forecasting.

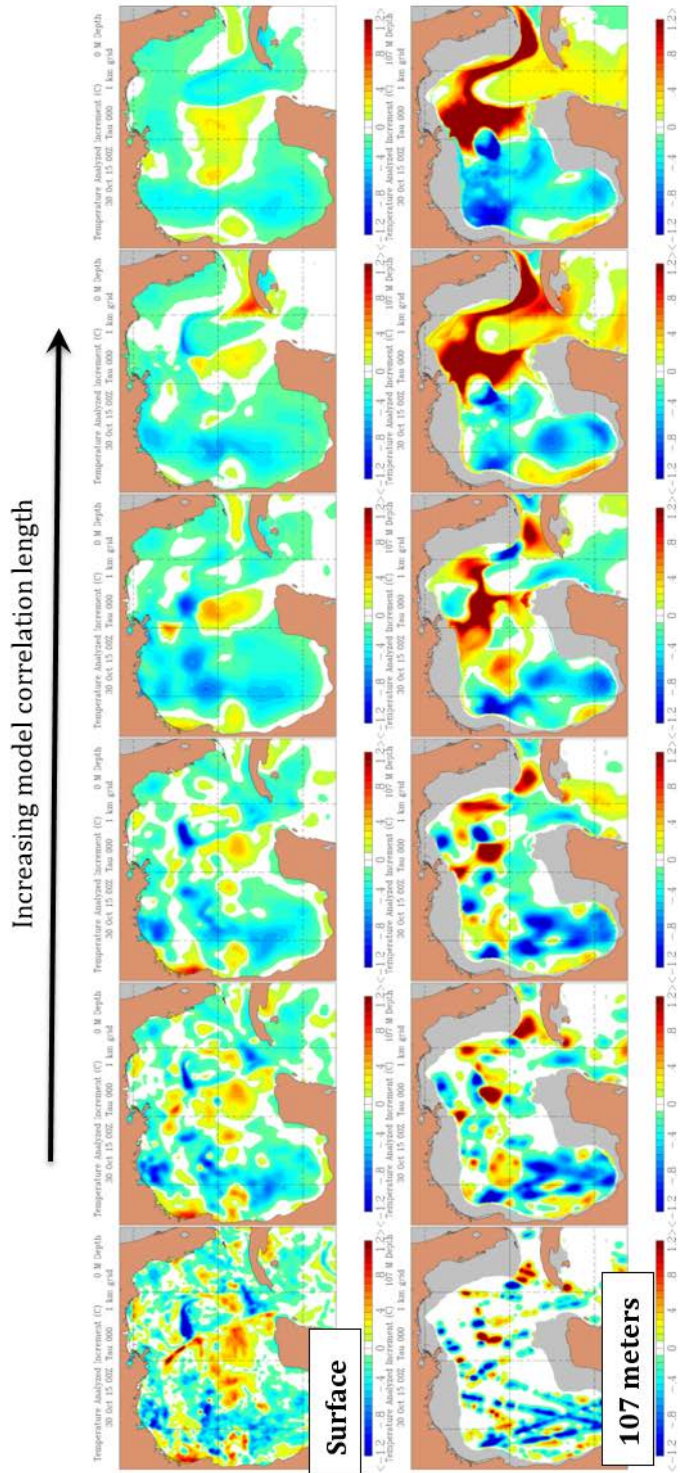


Figure 1. Temperature corrections to model initial state on 30 October 2015 after observation assimilation. Reds are warming the model temperatures and blues are cooling. As model correlation length increases, so does the area affected by the temperature correction.

Title: Coupled Ocean-Wave-Air-Ice Prediction System

Author(s): R. Allard,¹ T. Campbell,¹ J. Crout,² D. Hebert,¹ T. Jensen,¹ T. Smith,¹ and E. Rogers¹

Affiliation(s): ¹Naval Research Laboratory, Washington, DC; ²Perspecta, Stennis Space Center, MS

CTA: CWO

Computer Resources: Cray XC40 [NAVY, MS]

Research Objectives: Perform research studies with the Coupled Ocean Atmosphere Mesoscale Prediction System (COAMPS[®]) which is six-way coupled with the Navy Coastal Ocean Model (NCOM), WaveWatch-III (WW3) and spectral wave model (SWAN) wave models and the COAMPS atmospheric model. Utilize the fully coupled system to perform applied research in areas such as the North Arabian Sea, Bay of Bengal (BoB) and Arctic Seas.

Methodology: For accurate simulation and prediction we are using various configurations of the fully coupled atmosphere-ocean-wave model system COAMPS with very high spatial and temporal resolution. For the Indian Ocean (IO) and South China Sea (SCS), four different models were used. The atmospheric component has 60 vertical levels. The ocean model has a 0.5 m resolution in the upper 10 m, 45 sigma levels and up to 15 z-levels for a total of 60 levels in water deeper than 330 m and includes 8 semi-diurnal and diurnal tidal components. The numerics apply 3rd order upstream differencing schemes, 4th order pressure gradient and Coriolis terms for increased accuracy. The turbulent closure scheme is the Kantha-Clayson 2.5 that includes Stokes drift from the wave model. For these configurations we use the spectral wave model (SWAN) with 10 km spatial resolution, 34 frequency bands and 48 directions. Coupling interval for data exchange between each of the 3 models is 6 to 10 min. The NASCar-COAMPS coupled regional model area covers the western IO north of 18°S, eastward to 80°E with a horizontal resolution of about 3.5 km in the ocean and up to 9 km in the atmosphere. In FY18, this model was expanded eastward to cover the entire tropical IO and SCS to 127°E (Fig. 1).

Results: The COAMPS-MISO-BoB for the tropical Indian Ocean domain has been run daily in a hindcast mode since 10 March 2018. Daily websites are maintained for ONR and NRL scientists including the SCS PISTON and IO (MISO-BoB). The websites are updated daily (see <https://www7320.nrlssc.navy.mil/PISTON/> and <https://www7320.nrlssc.navy.mil/MISO/>) and provide daily averages of 10-m winds, sea surface, temperature and salinity, net surface heat flux and 100-m temperature, salinity and currents, as well as daily rainfall rate, 850 mb wind and total precipitable water. During RV Thompson cruises in August 2018 the BoB model results were sent daily to scientist onboard the ship to help with measurements planning and interpretation. The large anti-cyclonic eddy south of Sri Lanka seen in Fig. 1 was first seen in the model, and later confirmed by seagliders released in the area. A regional 1km CICE domain was set up to support the Year of Polar Prediction (YOPP). COAMPS was run in a 27/9/3 km nested configuration providing daily 48-hour forecasts to drive the regional CICE model. The YOPP domain was operational for a 90-day period beginning 1 July 2018 as part of the YOPP Special Observing Period II where additional rawinsonde observations were assimilated in near real-time into the atmospheric model. Figure 2 shows the evolution of the ice edge during this period.

DoD Impact/Significance: The development of a coupled air-ocean-wave prediction system can have a pronounced effect on Navy forecasting by improving ASW performance, tropical cyclone prediction, search and rescue and mission planning. The relocatable COAMPS-CICE system will provide high-resolution Arctic forecasting of ice thickness, ice drift and concentration to support navigation.

¹COAMPS[®] is a registered trademark of the Naval Research Laboratory

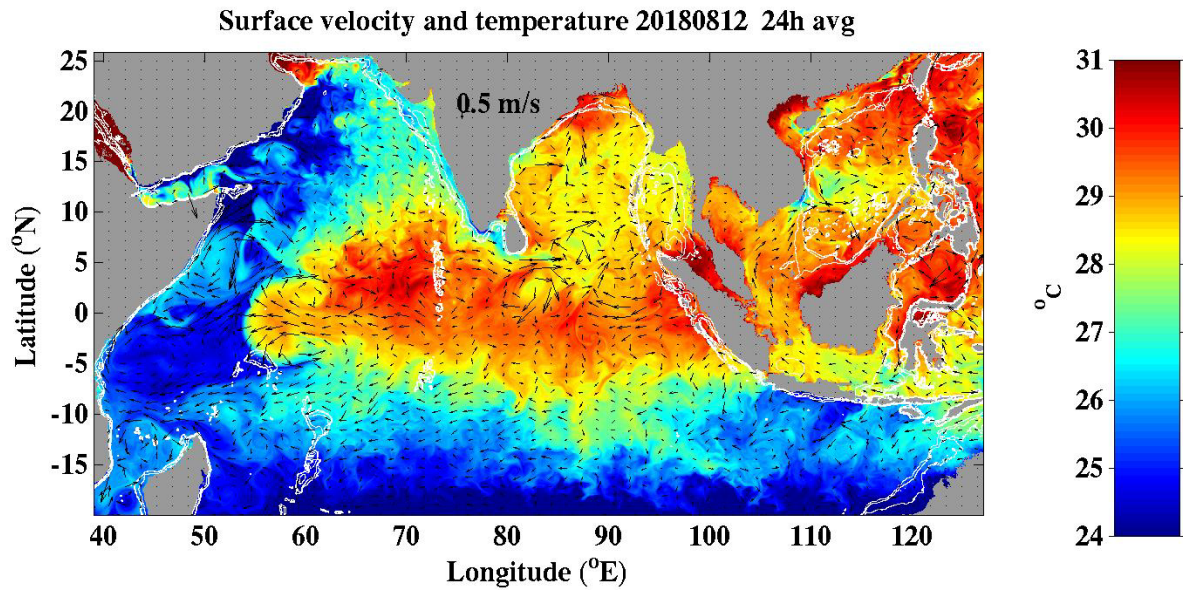


Figure 1. Daily averaged Sea Surface Temperature (SST) in $^{\circ}$ C, from the coupled MISO-BoB COAMPS on 12 August 2018. Prominent features are strong SST gradients in the western equatorial Indian Ocean promoted by advection, and intense anti-cyclonic eddies south of Sri Lanka and south of Vietnam.

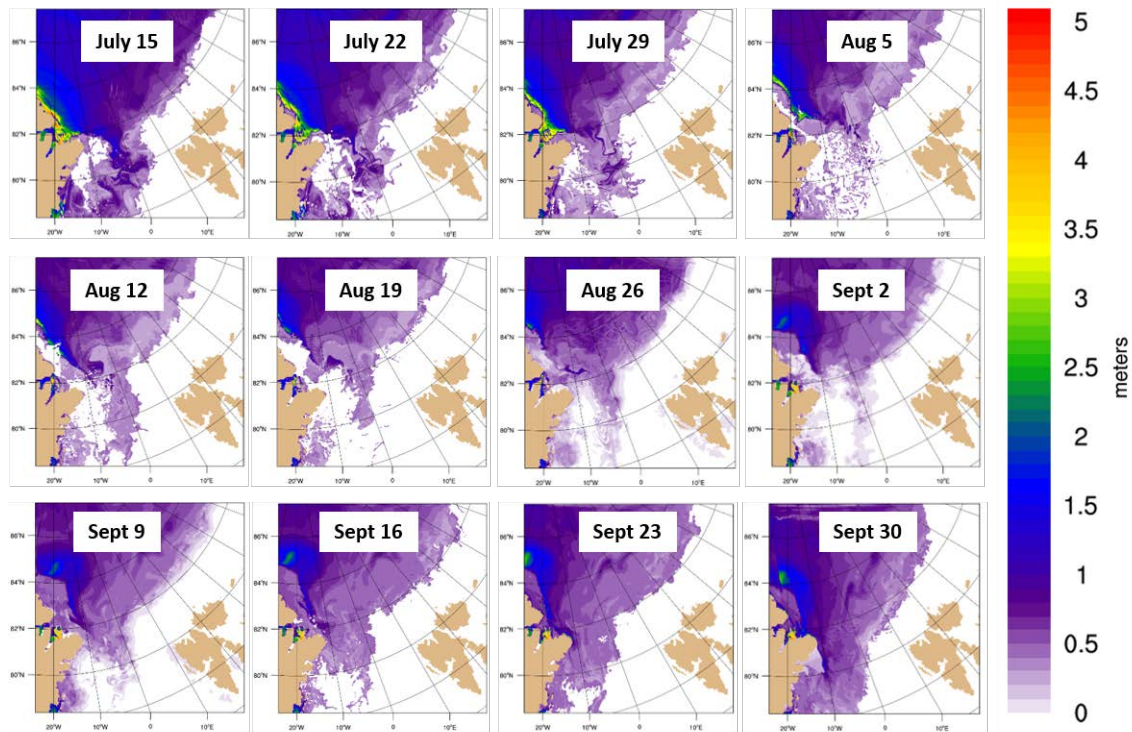


Figure 2. Weekly Ice thickness (m) from regional CICE (1km) analyses for Fram Strait YOPP for the period of 15 July–30 September 2018. The ice edge is much farther north of Svalbard than in recent years.

Title: The Effect of Langmuir Turbulence in Upper Ocean Mixing
Author(s): Y. Fan, E. Rogers, and T. Jensen
Affiliation(s): Naval Research Laboratory, Stennis Space Center, MS
CTA: CWO

Computer Resources: Cray XC40 [NAVY, MS]

Research Objectives: The goal of this project is to understand the effect of Langmuir turbulence (LT) in upper ocean mixing within a broad parameter space and during complex oceanic conditions through extensive ocean, wave, and Large Eddy Simulation (LES) modeling studies. The results from this project will provide a greater understanding of the generation, growth and decay of the LT, how it is affected by the mesoscale and submesoscale structures and its impact on vertical and horizontal momentum and heat fluxes within the ocean on larger scales.

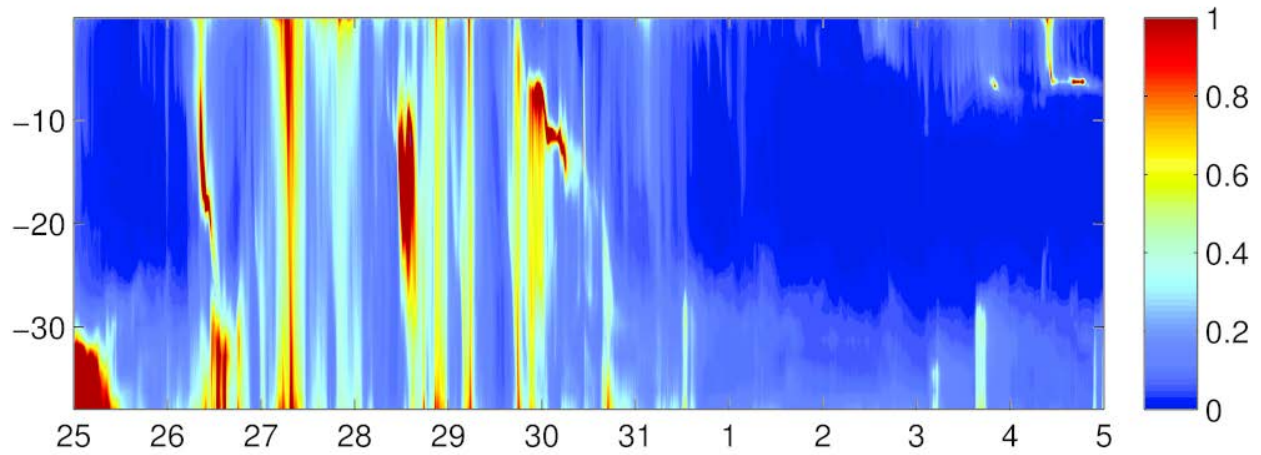
Methodology: The NCAR Large Eddy Simulation (LES) model, a widely used model in the science community to study wave-current interaction and LT, is used in this study. A suite of numerical experiments was conducted for the Casper East field measurements using the NCAR LES to investigate the generation, growth and decay of LT and its interaction with large scale ocean dynamics. Due to the strong fluctuations of river inflow into this research region with fresh and cold waters, temperature and salinity varies significantly both spatially and temporally. In order to conduct LES studies in this region, a new module was implemented to the NCAR LES model to relax the model T, S profiles to glider observations. To avoid the influence of the relaxation on the small scale turbulence in the model, the domain mean temperature and salinity are first computed and then used to calculate the mean T, S differences between the model and observations. Then, the mean T, S differences are used to adjust the T, S profiles at every grid point in the model domain.

Results: The Casper East field experiments are conducted in the Gulf Stream region with strong submesoscale activities and is significantly impacted by fresh water inflow from several nearby rivers. A suite of LES experiments was conducted for the Casper East experiment with and without Stokes drift, and with and without temperature and salinity relaxation in the model simulation to determine the effect of large scale temperature and salinity variations on Langmuir turbulence, and the interaction between Langmuir turbulence and deep convection. Analysis of turbulence intensity, which is defined as the magnitude of the turbulent current divided by the magnitude of the mean current, indicates that the turbulence is actually stronger without Stokes drift during strong convections events, indicating that the Langmuir circulation may be able to inhibit or reduce the extent of deep convection. All current existing LT parameterizations enhance turbulence under all circumstance, and thus are not appropriate for strong convective situations. Apparently, more dynamics and physics are needed to correctly parameterize the LT effect in ocean circulation models. Non-dimensional variables using the Buckingham Pi theory were constructed based on the insights from these experiments. Their correlations with various turbulent kinetic energy components were analyzed using the LES simulations. Parameterization for Langmuir turbulence with better physical representation of the ocean state is under way.

DoD Impact/Significance: This study can help us improve the Battlespace Environment forecasting accuracy for both ocean and atmosphere (HYCOM, NCOM and COAMPS®). Better understanding of the mechanism, growth and dissipation of LT will help us improve the air-sea interaction process in our coupled models (i.e. COAMPS and ESPC), which will lead to more accurate vertical thermal profile simulations in the ocean models and better predication of acoustic and optic properties in the upper ocean.

¹COAMPS® is a registered trademark of the Naval Research Laboratory

With Stokes drift



Without Stokes drift

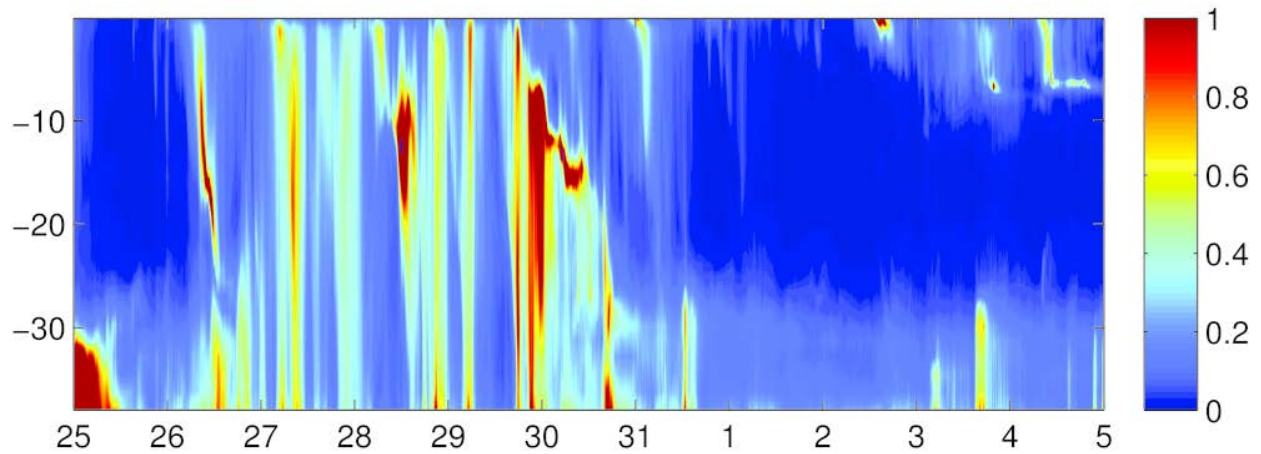


Figure 1. Turbulent intensity $((u'^2 + v'^2 + w'^2)/\sqrt{U_m^2 + V_m^2 + W_m^2})$ for LES simulation (a) with Stokes drift, and (b) without Stokes drift from 25 October to 5 November 2015. Here, u' , v' , and w' are the turbulent velocities in the x, y, and z direction respectively, and U_m , V_m , and W_m are the mean velocities in the x, y, and z directions respectively. Notice the turbulent intensity around 30 October when it is much smaller in the case with Stokes drift.

Title: Eddy-Resolving Global/Basin-SOM

Author(s): E.J. Metzger,¹ J.F. Shriver,¹ M. Buijsman,² and C.H. Jeon²

Affiliation(s): ¹Naval Research Laboratory, Stennis Space Center, MS; ²University of Southern Mississippi, Stennis Space Center

CTA: CWO

Computer Resources: Cray XC30 [NAVY, MS]; Cray XC40 [NAVY, MS]; Cray XE6m [ERDC, MS]; Cray XC40/50 [ERDC, MS]

Research Objectives: Modeling component of a coordinated 6.1-6.4 effort on the problem of eddy-resolving global and basin-scale ocean modeling and prediction. This includes increased understanding of ocean dynamics, model development, model validation, naval applications, oceanic data assimilation, ocean predictability studies, observing system simulation studies, and nested models.

Methodology: The appropriate choice of vertical coordinate is a key factor in ocean model design. Traditional ocean models use a single coordinate type to represent the vertical, but no single approach is optimal for the global ocean. Isopycnal (density tracking) layers are best in the deep stratified ocean, Z-levels (constant depths) provide high vertical resolution in the mixed layer, and terrain-following levels are often the best choice in coastal regions. The HYbrid Coordinate Ocean Model (HYCOM) has a completely general vertical coordinate (isopycnal, terrain-following, and Z-level) via the layered continuity equation that allows for an accurate transition from the deep to shallow water.

Results: 13 refereed articles, 3 non-refereed articles published or in press in FY18.

Global modeling: During the Global Ocean Forecast System (GOFS) 3.1 Operational Test (OPTEST) at Fleet Numerical Meteorology and Oceanography Center, ocean instabilities were discovered in the Philippine Seas. These were traced to a data assimilation implementation issue and a HYCOM abyssal layer instability. Numerous assimilative reanalyses and non-assimilative simulations were integrated that eventually led to a correction of the problem. A new spin-up was also provided to get the OPTEST back on track. GOFS 3.1 was declared operational on 18 September 2018. A year-long GOFS 3.5 (1/25° HYCOM/CICE with tides) reanalysis and sequence of forecasts were also integrated for use in its Validation Test Report.

Improving tides in global HYCOM: M2 surface tides in 1/25° global HYCOM have relatively large height errors in the shallow coastal zone. To improve the local and global surface tides, two-way nesting has been implemented in barotropic HYCOM simulations using the nesting package OASIS3-MCT. Simulations were performed with seven 1/75° two-way nests in various regions across the globe. For each nest, not only the local tides, but also the remote tides are generally improved (see figure).

Earth System Prediction Capability (ESPC): The Navy's ESPC presently includes atmosphere, ocean, and sea ice components in fully coupled mode. We again participated in the Sea Ice Prediction Network's Sea Ice Outlook using a 10 member time-lagged ESPC ensemble using initial conditions from early May, June, and July 2018 to make forecasts of the September 2018 mean sea ice extent of 5.9, 4.7 and 4.3 Mkm², respectively. The observed sea ice extent was 4.7 Mkm². Results are at <https://www.arcus.org/sipn/sea-ice-outlook>.

DoD Impact/Significance: Data assimilative eddy resolving models are important components of global ocean and sea ice prediction systems. Ocean forecasts are valuable for tactical planning, optimum track ship routing, search and rescue operations, and the location of high current shear zones. The sea ice environment has become increasingly important for strategic and economic reasons given the diminishing trend in sea ice extent and thickness and the potential summertime opening of the Northwest Passage and Siberian sea routes. Fractures, leads and polynya forecasts are also valuable to the naval submarine community.

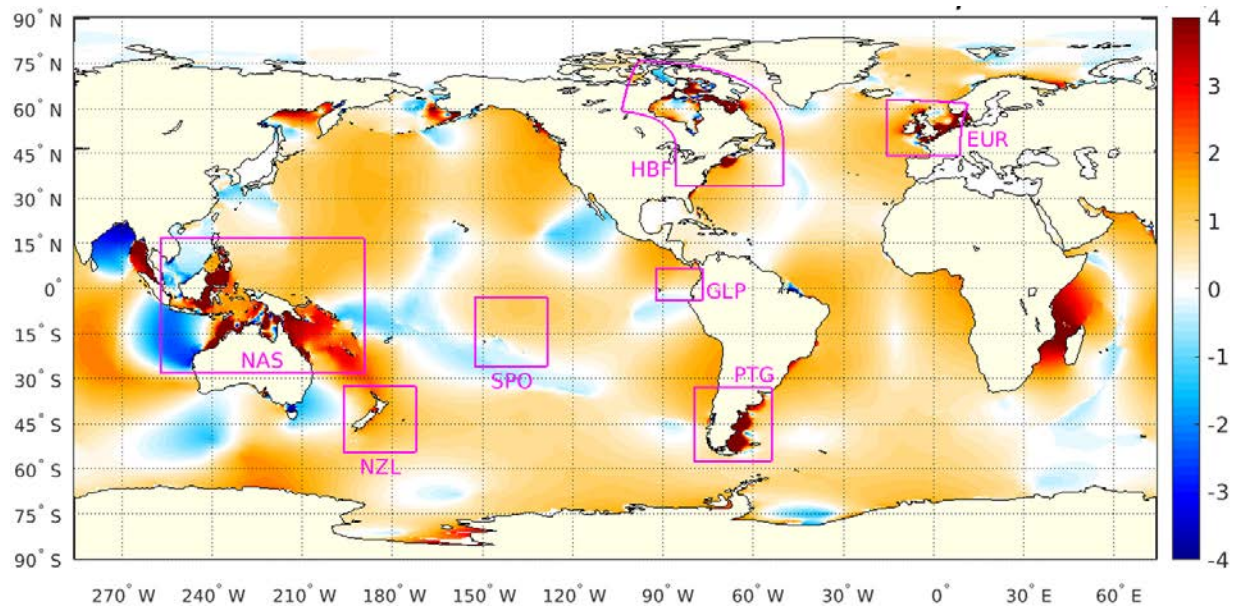


Figure 1. Change of predictability (Δ RMSE, cm) of M2 surface tides in $1/25^\circ$ global HYCOM due to two-way nesting in the seven $1/75^\circ$ regions outlined by magenta, i.e., RMSE for the simulation with two-way nesting minus RMSE for the simulation without nesting. Tides are compared against the Finite Element Solution 2014 tide model. For each nest, not only the local tides, but also the remote tides are generally improved. Positive values indicate improvement in tidal prediction while negative values indicate worsening. RMSE is improved by $\sim 16\%$ averaged across the globe.

Title: Coastal Mesoscale Modeling - COAMPS-TC Intensity Prediction

Author(s): J.D. Doyle

Affiliation(s): Naval Research Laboratory, Monterey, CA

CTA: CWO

Computer Resources: Cray XC40 [NAVY, MS]; Cray XC40 [ARL, MD]; SGI ICE X [ARL, MD]; Cray XC30 [NAVY, MS]; Cray XC40/50 [ERDC, MS]; Cray XC30 [AFRL, OH]; SGI ICE X [AFRL, OH]

Research Objectives: Tropical cyclone (TC) track forecasts have improved in a steady manner over the past several decades, but intensity forecasting has shown much slower increase in skill over the same time period. This is due, in part, to our limited ability to properly model physical process controlling tropical cyclone structure and intensity, but also to the inherent sensitivity that tropical cyclone forecasts exhibit to initial conditions. The objective of this project is to further advance and demonstrate Coupled Ocean/Atmosphere Mesoscale Prediction System Tropical-Cyclone (COAMPS-TC), a state-of-the-science numerical weather prediction (NWP) system designed for the simulation of tropical cyclones in support of Navy and DoD operations, and for civilian applications. The COAMPS-TC system is operational at Fleet Numerical Meteorology and Oceanography Center (FNMOC) and has undergone yearly upgrades since 2013. The overall goal is to improve the COAMPS-TC tropical cyclone intensity predictions through improved vortex initialization and representation of physical processes.

Methodology: There are two types of COAMPS-TC simulations and forecasts performed. The first type of application is used to facilitate rapid development and testing. The prototype testing needs to be rigorous and involves running approximately 500 or more individual cases to assess the performance of the system in a statistically meaningful manner. Each change in the development process needs to be tested through this procedure. This rapid testing process is needed to develop and evaluate the new version that will be run operationally at FNMOC. A second type of application involves the real-time execution of a more advanced experimental version which contains more advanced capabilities than the FNMOC version, on the DSRC. The testing of the experimental COAMPS-TC system is performed for all tropical cyclones worldwide.

Results: Several configurations of COAMPS-TC were tested over a suite of storms in the Atlantic and Pacific Ocean basins based on several previous TC seasons. A new version with improvements was transitioned to operations at FNMOC in May 2018. These improvements included the use of high horizontal resolution (4 km), along with upgrades to the physical parameterizations and vortex initialization. Figure 1 shows a real time 5-day forecast of accumulated precipitation from the new version initialized at 0000 UTC 13 September 2018 for the period in which Hurricane Florence made landfall and caused catastrophic flooding in North and South Carolina. The observed precipitation from the National Weather Service is shown in Fig. 1 as well. The COAMPS-TC makes use of two moving nested grid meshes (12-km and 4-km resolution) that follow the storm. The forecasts of precipitation for Florence correctly predicted the potential for flooding, and provided excellent guidance for forecasters. COAMPS-TC continues to be one of the top performing tropical cyclone prediction models in the world in 2018.

DoD Impact/Significance: Tropical cyclones remain the most disruptive and devastating environmental threat that impact U.S. Navy operations. We anticipate that an increase in accuracy of tropical cyclone forecasts will result in significant cost benefit to the Navy through better sortie decisions and avoidance of hazardous winds and seas. Real-time testing and development of the system at HPC DSRCs have led to significant improvements in the data assimilation and predictive skill of COAMPS-TC and more rapid transitions to operations at FNMOC. These improvements will inform future directions of tropical cyclone and mesoscale model and data assimilation development, particularly as computational power increases allowing for higher resolution capabilities.

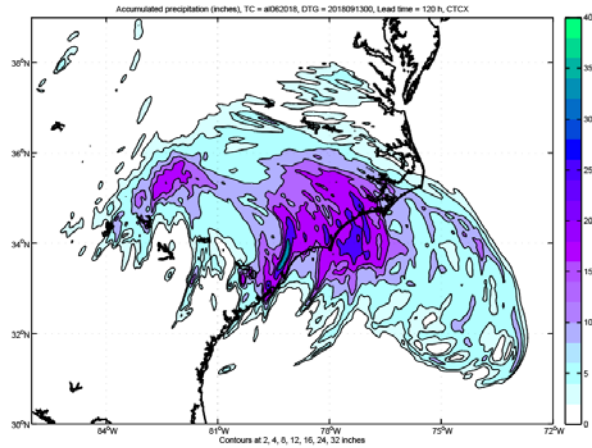
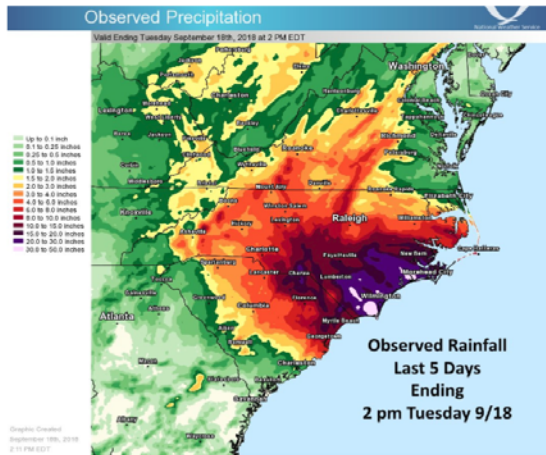


Figure 1. Observed precipitation (inches) from Hurricane Florence (National Weather Service) (top). COAMPS-TC accumulated precipitation (inches, color scale) from a 120-h forecast for Florence initialized at 0000 UTC 13 September and extending through 0000 UTC 18 September.

Title: Coastal Mesoscale Modeling
Author(s): P.A. Reinecke
Affiliation(s): Naval Research Laboratory, Monterey, CA
CTA: CWO

Computer Resources: Cray XC30 [NAVY, MS] Cray XC40 [NAVY, MS]; Cray XC4050 [ERDC, MS]; Cray XC40 [ARL, MD]; Cray XC30 [AFRL, OH]; SGI ICE X [AFRL, OH]; SGI ICE X [ARL, MD]

Research Objectives: Our objective is to develop and validate a fully coupled coastal/littoral prediction system that can be used to provide high-resolution (<5 km) data assimilation (DA) and short-term (0-48 h) forecast guidance for tactical sized areas of the world. This system can also be used for basic and applied research leading to an improvement in our understanding of atmospheric and oceanic processes. Improvements to the mesoscale prediction and DA systems will result from this research.

Methodology: The Coupled Ocean/Atmosphere Mesoscale Prediction System (COAMPS^{®1}) is being developed further for independent and coupled simulations of the atmosphere and ocean for the mesoscale. The atmospheric component of COAMPS is made up of a DA system; an initialization procedure; and a multi-nested, nonhydrostatic numerical model. This model includes parameterizations for moist processes, surface and boundary-layer effects, and radiation processes. The NRL Coastal Ocean Model (NCOM) is currently being used for the simulation of the mesoscale ocean circulation response to the COAMPS forcing in one-way and two-way interactive modes. Ocean coupling is being developed using the Earth System Modeling Framework (ESMF). A new tropical cyclone capability has been developed for COAMPS, referred to as COAMPS-TC. Development and testing of the Navy's next generation prediction system, NEPTUNE (Navy's Environmental Prediction System Using the NUMA Engine) is underway. This system uses a spectral element based approximation to the atmosphere and can scale to over 1,000,000 cores.

Results: In FY18, COAMPS was demonstrated to be an accurate DA and forecast system capable of predictions and simulations on a variety of horizontal scales of less than 1 km for land-sea effects, topographically driven flows, and tropical cyclones. Numerous studies were performed to explore the impact of the ocean and the sea-state on the atmospheric boundary layer. Figure 1 shows the result of one such study which used Large Eddy Simulations to model the dependence of the atmospheric boundary layer on the sea-state swell. Of particular interest is the dependence of gradients in temperature and water vapor on the direction and amplitude of the sea swell, which is shown in Fig. 1. Compared to the calm sea-state (top row), the case in which the flow coincides with the direction of the swell (bottom row) shows a significant reduction in the depth of the boundary layer and stronger vertical gradients of both potential temperature and water vapor, which can significantly impact wave ducting layers and modify electromagnetic propagation properties. Development of the Navy's next generation global NWP system, NEPTUNE, continued in 2018 with systematic testing of real-data initial condition forecasts using full physics parameterizations.

DoD Impact/Significance: COAMPS continues to play a significant role in providing atmospheric forecasts in support of Navy missions involving the deployment of weapons systems, strike warfare, radar propagation, and search and rescue. Research and development performed at HPC DSRCs have led to significant improvements in the predictive skill of COAMPS that will greatly benefit the operational performance of COAMPS. The HPC DSRCs will be the primary computing resources in FY2018 and beyond for the development of the fully coupled COAMPS system including the emerging tropical cyclone and ensemble capabilities for COAMPS as well as NEPTUNE, the next generation global and mesoscale modeling system.

¹ COAMPS[®] is a registered trademark of the Naval Research Laboratory.

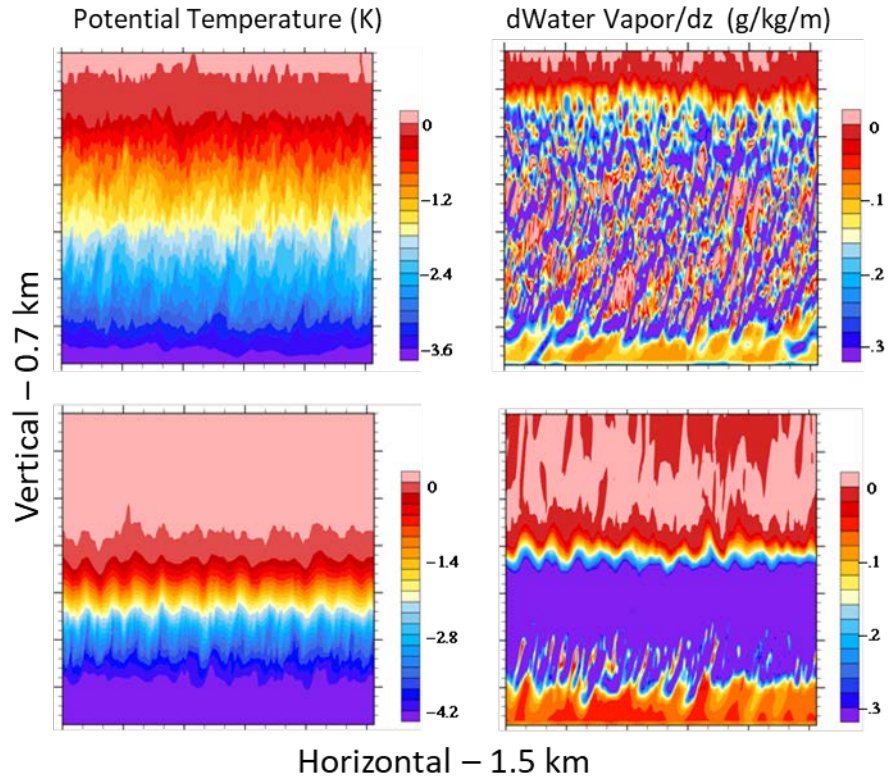


Figure 1. Vertical cross sections of potential temperature (left column) and vertical gradient of water vapor specific humidity (right column) from a Large Eddy Simulation of air flowing from left to right over a calm sea state (top row) and in the direction of a monochromatic swell (bottom row). The horizontal and vertical grid spacing is 3 m and 1 m, respectively.

THIS PAGE INTENTIONALLY LEFT BLANK

SIP

Signal Image Processing

SIP covers the extraction of useful information from sensor outputs in real time. DoD applications include surveillance, reconnaissance, intelligence, communications, avionics, smart munitions, and electronic warfare. Sensor types include sonar, radar, visible and infrared images, and signal intelligence (SIGINT) and navigation assets. Typical signal processing functions include detecting, tracking, classifying, and recognizing targets in the midst of noise and jamming. Image processing functions include the generation of high-resolution low-noise imagery, and the compression of imagery for communications and storage. The CTA emphasizes research, evaluation, and test of the latest signal processing concepts directed toward these embedded systems. Usually such processors are aboard deployable military systems and hence require hefty packaging, minimum size, weight, and power. System affordability is expected to improve an order of magnitude through the development of scalable codes running on flexible HPC systems. This will enable the traditional expensive military-unique “black boxes” required to implement high-speed signal/image processing to be replaced by COTS HPC-based equipment.

Title: Reducing the Burden of Massive Training Data for Deep Learning

Author(s): L.N. Smith, S.N. Blisard, and K.M. Sullivan

Affiliation(s): Naval Research Laboratory, Washington, DC

CTA: SIP

Computer Resources: SGI Altix ICE [NRL, DC]; Cray XC40/50 [ERDC, MS]; IBM Power8 [MHPCC, HI]

Research Objectives: The successes of deep learning in the past several years rely on three pillars: faster computer hardware, lots of labeled training data, and new algorithms. In this basic research project, we design, develop, and evaluate novel deep learning algorithms for training deep neural networks that significantly reduces the training time and eliminates the current requirement for massive labeled training datasets in order to allow application of deep networks in situations where labeled data is scarce or expensive.

Methodology: Our methodology is primarily based on the following process: based on our understanding, we develop hypotheses, which often requires experimenting with many variations of neural networks and hyper-parameters to determine which of those hypotheses are beneficial, when they are beneficial, and to develop a new understanding as to why they work. The majority of the work done was in the most popular deep learning frameworks—TensorFlow, Caffe, Torch, and PyTorch. Hence it is valuable that the HPC staff installs and maintains these frameworks.

Typically our experiments build on previous work so the first step is to download code from github.com, replicate previous results, and then test our own hypotheses.

Results: Our current research in deep neural networks has already discovered several substantial innovations.

In FY18 the majority of the work on this project concerned using dynamic hyper-parameters in place of the typical static hyper-parameters. For example, we showed that dynamic learning rates could speed up the training of networks on the standard Cifar-10 dataset by approximately an order of magnitude (see Fig. 1). We named this phenomena “super-convergence.” One of the key elements of super-convergence is training with one learning rate cycle and a large maximum learning rate. Figure 1 also shows that the super-convergence training curve (red) is fundamentally of a different shape than the typical training curve (blue) and attains a higher test accuracy. Others have built on our super-convergence work to win public contests where both performance and speed of training are emphasized (i.e., Kaggle and Stanford’s DAWNBench competition).

In FY18 we have also done significant work on few shot learning. Based on the literature, we have tested several several implementations and settled on two: prototypical networks and Model Agnostic Meta Learning (MAML). We improved on the state-of-the-art and are continuing to test new hypotheses and develop innovative methods.

DoD Impact/Significance: Our work on significantly speeding up the training of neural networks and reducing the amount of labeled training data needed are fundamental achievements focused on the three pillars of deep learning and is having far reaching impacts in the field and future applications. In addition, the understanding gained by the experiments on the HPC GPU servers build on all the previous understandings gained from earlier experiments and this understanding is crucial for our future progress in the field.

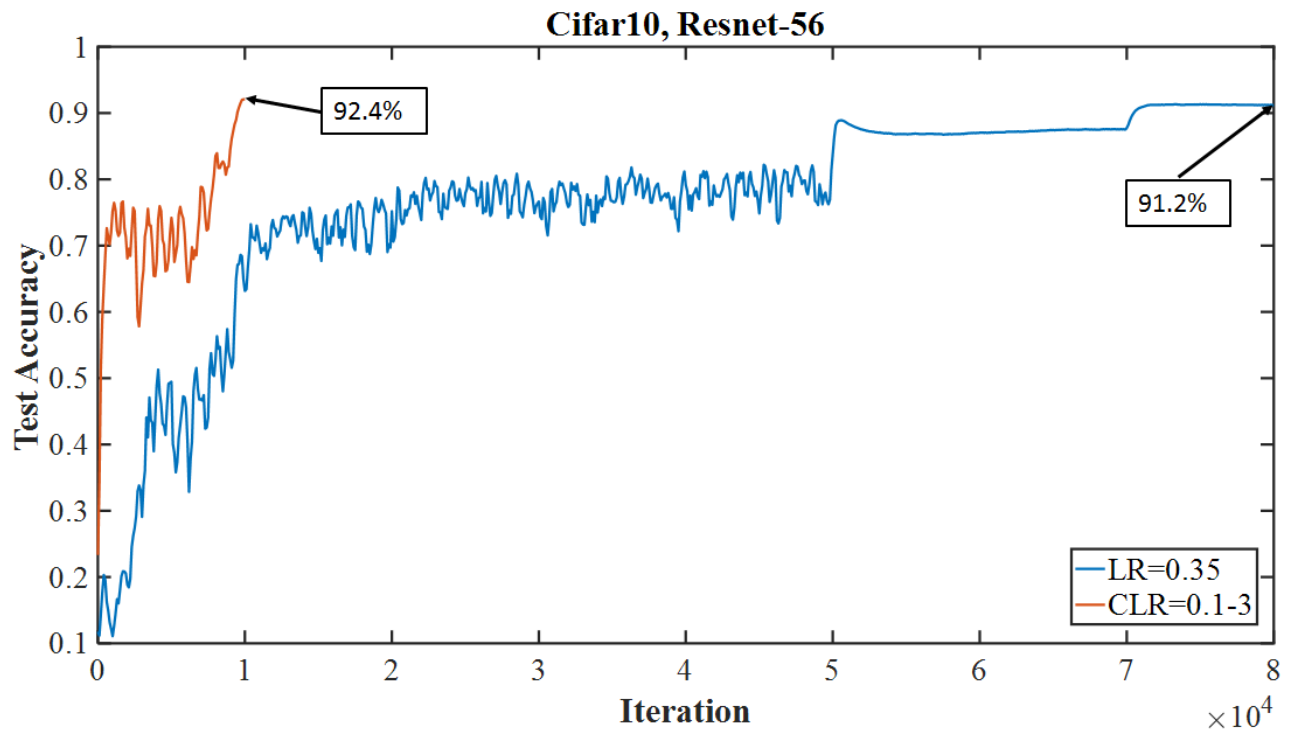


Figure 1. Examples of super-convergence with Resnet-56 on Cifar-10. Comparison of test accuracies of super-convergence example (red curve) to a typical training regime (blue curve). Training with super-convergence is an order of magnitude faster than the typical training methods.

Title: Common Ground Learning and Explanation (COGLE)

Author(s): L.N. Smith,¹ M. Youngblood,² M. Stefik,² and B. Krivacic²

Affiliation(s): ¹Naval Research Laboratory, Washington, DC; ²Palo Alto Research Center (PARC, a Xerox Company), Palo Alto, CA

CTA: SIP

Computer Resources: SGI ICE X [ARL, MD]

Research Objectives: In this DARPA-sponsored basic research project, we will design, develop, and evaluate novel accounting extensions to deep learning algorithms. These accounting extensions and the local data used in the learned policies will be used to generate manifold abstractions from the learning process and locally embed salient data for use in introspective explanation. These explanation data are used in an external tool as explanations to humans (see Fig. 1), which is intended and evaluated for mental model induction used for situational behavior predictions. We utilize an ArduPilot derived simulation environment to simulate an Unmanned Autonomous System (UAS) with a single fixed-wing agent as the behavioral actor. Thus learning, explanation, and human model induction involve a single, simulated UAS that is performing search and rescue missions on many types of terrain. Self-explaining drone technology is valuable to the DoD to increase usability, trust, evaluation, and incorporation of current and future UASs into mission, support, and training operations.

Methodology: Our primary methodology is empirical, which requires experimenting with many UAS configurations, learning algorithms, explanation extensions, and mission scenarios. Some behavioral abstractions capture the variations and patterns of the permutations, which are useful in explanation.

Our cluster use will be focused on training deep reinforcement learning agents built on custom Python code and common libraries (e.g. TensorFlow) as needed. Our methodology involves data extraction and abstraction techniques embedded in the learning process that leaves localized explanation data linked in the learned policy network. Large numbers of agent runs are performed in an embedded, stochastic simulation environment to develop the learned policy with embedded explanation information. Those trained policies with explanation primitives are then used in a user-facing tool to test utility in human subject experiments.

Results: We are currently evaluating our self-generated explanations with human subjects with regard to their utility for future behavioral prediction. We anticipate initial results by 22 October 2018 (approx. 20 participants), and a complete full-powered results (up to approx. 60 participants) by 7 December 2018.

DoD Impact/Significance: Explainable AI (XAI) is likely to set the standard for all future AI systems to present their decision rationale.



Figure 1. Introspective explanations from a UAS flight in our user-facing test interface *Exigisi*.

THIS PAGE INTENTIONALLY LEFT BLANK



Space and Astrophysical Science

Space and Astrophysical Sciences (SAS) research and development advances understanding, specification and prediction of Earth's atmospheric and space domains to exploit the extended operational environment for military advantage and to minimize environmental impacts on military operations. The SAS Computational Technology Area (CTA) embodies the use of mathematics, computational science, and engineering in the analysis, design, identification, modeling, and simulation of the space and near-space environment, and of all objects therein, whether artificial or natural. The SAS CTA encompasses foundational discovery research to study the atmospheres of the sun and the earth, including solar activity and its effects on the earth's atmosphere, ionosphere, and near-Earth space, and the unique physics and properties of celestial sources. SAS employs an extensive array of physical and empirical models and analysis tools to integrate observations and theoretical understanding, for ever-improving DoD enterprises within, and exploitation of, the extended operational environment. The CTA melds the strengths of a broad range of physical sciences—atomic and molecular physics, materials science, plasma physics, applied optics, radiation survivability, electronic warfare, directed energy technology, astronautics and space propulsion, orbital mechanics, space situational awareness, and remote sensing—into a structure that helps the DoD multiply force combat effectiveness.

Title: Radiative Signatures and Dynamical Interactions of AGN Jets

Author(s): M.T. Wolff,¹ and J.H. Beall²

Affiliation(s): ¹Naval Research Laboratory, Washington, DC; ²St. John's College, Annapolis, MD

CTA: SAS

Computer Resources: SGI Altix ICE [NRL, DC]

Research Objectives: The scientific goal of this research is to investigate the physical processes that occur as an astrophysical jet interacts with the ambient galactic interstellar medium through which it propagates. This interaction accelerates the ambient plasma, heating and entraining the material, ultimately producing radiation signatures that can be modeled with computer simulations. Such astrophysical jets can be subsonic, supersonic, or relativistic, and are believed to originate from the accretion environment surrounding supermassive black holes in the cores of active galactic nuclei (AGN). During FY18, we completed a series of large-scale, three-dimensional (3D), relativistic, magneto-hydrodynamic jet simulations in order to explore the jet parameter space so we can better understand the many modes of jet-ambient-medium interaction.

Methodology: For these large-scale numerical simulations, we use the PLUTO code, which has the capability of simulating hydrodynamic (HD), magneto-hydrodynamic (MHD), and relativistic, magneto-hydrodynamic (RMHD) processes. The PLUTO code has proven to be a robust platform for simulating astrophysical jets and we are continuing to explore jet evolution in the relativistic hydrodynamic, and relativistic magneto-hydrodynamic regimes. We plan to incorporate “microscopic” plasma processes, including the two-stream instability, the parametric instability, and the ion-acoustic instability, into these simulations. These processes remove energy from the jet during its interaction with the ambient medium and enhance the transfer of momentum and kinetic energy from the jet to the ambient medium. Their inclusion provides for a more realistic jet simulation. These jet-ambient medium simulations can then provide a self-consistent estimation of the expected thermal radiation and synchrotron emission from the jet structures.

Results: We have ported, compiled, and run highly parallelized versions of PLUTO for the largest simulation thus far (1024x1024x1024). We have successfully simulated a RMHD 3D jet including external force terms that simulate the gravity from the accretion disk environment, as well as the deceleration effects from plasma processes. Jet velocities of 0.5c to .998c, where c is the velocity of light, have been simulated extensively. During our latest detailed simulation runs we have moved to 512x512x512 cells with PPM and Runga-Kutta solvers and are currently testing the stability of these solutions. We have also used post-processing algorithms to estimate the 10 GHz radio emission that results from these simulations. Figure 1 shows the fully 3D, relativistic hydrodynamic simulation of the jet-ambient medium radio emissivity from a volumetric rendering at a time of 40 million years, with a jet bulk velocity of $v=0.5c$. This simulation of the radio emission utilizes 128x128x512 grid cells. Note the well-developed Rayleigh-Taylor instabilities at the jet-ambient medium boundary and the Kelvin-Helmholtz instabilities in the jet column. The simulation size is ~65 kpc lengthwise and at ~23 kpc on a side at the base. We show the structure after ~100 million time steps. In this simulation, the jet-to-ambient medium density ratio is 0.01 and the ratio of jet input pressure to ambient medium pressure is 0.005.

DoD Impact/Significance: Many U.S. government agencies, in addition to the DoD, have an interest in developing a robust capability to hydrodynamically model plasma and fluid systems in a highly anisotropic medium. A related and closely following interest is in developing the ability to model radiative transfer in such a multi-dimensional plasma and fluid environment. These calculations will advance the science of modeling astrophysical and near-earth space plasma environments.

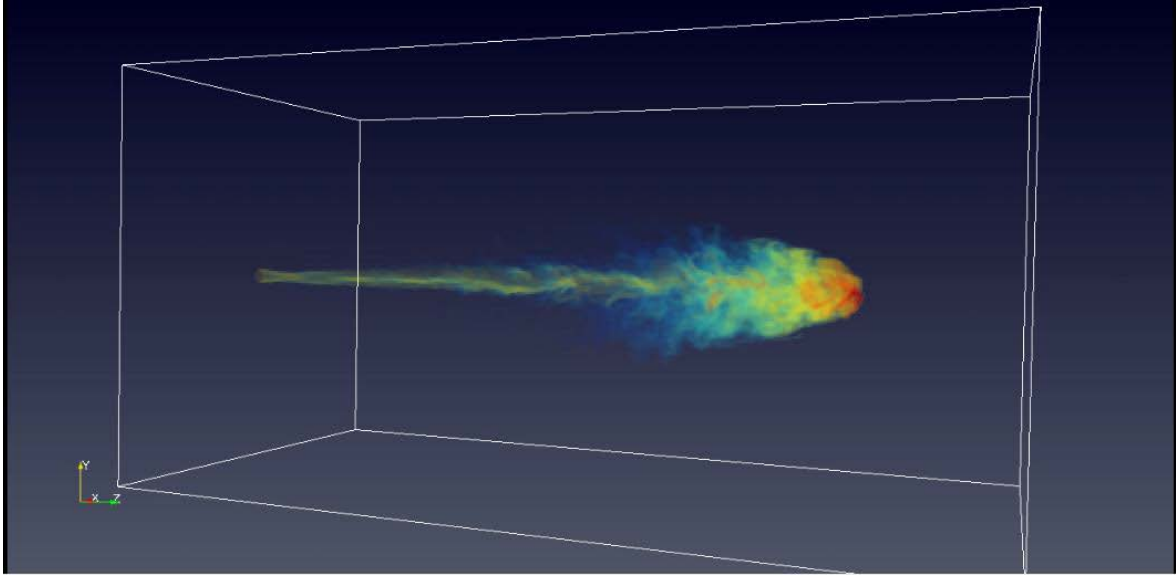


Figure 1 shows the fully 3D, relativistic hydrodynamic simulation of an astrophysical jet radio emissivity seen with a volumetric rendering at a time of 40 million years, with a jet bulk velocity of $v=0.5c$. This simulation utilizes $128 \times 128 \times 512$ grid cells. Note the well-developed Rayleigh-Taylor instabilities at the jet-ambient medium boundary and the Kelvin-Helmholtz instabilities in the jet column. The simulation size is ~ 65 kpc lengthwise and at ~ 23 kpc on a side at the base. We show the structure after ~ 100 million time steps. In this simulation, the jet-to-ambient medium density ratio is 0.01 and the ratio of jet input pressure to ambient medium pressure is 0.005.

Title: Development of a Weather Model of the Ionosphere

Author(s): S.E. McDonald,¹ F. Sassi,¹ C.A. Metzler,¹ D.P. Drob,¹ J.L. Tate,³ M.S. Dhadly,² and B.D. Curtis⁴

Affiliation(s): ¹Naval Research Laboratory, Washington, DC; ²National Research Council Postdoctoral Fellow, Naval Research Laboratory, Washington DC; ³Computational Physics, Inc., Springfield, VA; ⁴Praxis, Inc., Arlington, VA

CTA: SAS

Computer Resources: Cray XC30 [AFRL, OH]; Cray XC30 [NAVY, MS]; Cray XC40 [ARL, MD]

Research Objectives: The scientific goal of the proposed research is to characterize and simulate the physical processes that are important for improving numerical forecasting of high-frequency (HF) radio wave propagation through Earth's atmosphere and ionosphere across the range of conditions relevant to DoD operations. To achieve the objectives of this project, we have developed a fully coupled atmosphere-ionosphere model. In FY18, the main objectives were to complete the development of the fully coupled model, perform validation studies, and investigate lower atmospheric effects on the ionosphere.

Methodology: We have developed the Navy Highly Integrated Thermosphere and Ionosphere Demonstration System (Navy-HITIDES), which consists of SAMI3, a state-of-the-art NRL model of the ionosphere, along with couplers that use the Earth System Modeling Framework (ESMF) for interpolation between the atmosphere and ionosphere grids. Navy-HITIDES has been integrated with the Whole Atmosphere Community Climate Model eXtended (WACCM-X); it is also being designed to work with any NUOPC (National Unified Operational Prediction Capability) and ESMF-compliant whole atmosphere model that includes a thermosphere.

Results: In FY18, we improved the high-latitude of Navy-HITIDES by adding a parameterization for solar wind – magnetosphere coupling to the ionosphere, which improves the simulation of geomagnetically active periods. Validation studies of the high latitude thermospheric winds are underway to study coupling of the ionosphere-thermosphere. We also conducted validation studies of the Northern Hemisphere winter periods in 2009-2010, 2012-2013 and 2015-2016 using Navy-HITIDES coupled to WACCM-X and using meteorological forcing from the Navy Global Environmental Model - High Altitude (NAVEM-HA). These validation studies have illustrated how thermospheric variability is crucial for a correct representation of the ionospheric structure. As an example, Fig. 1 shows that during boreal winter 2016, and at times following a major stratospheric warming event at 30 km of altitude at the beginning of January 2016, the thermospheric day-to-day variability is characterized by an enhancement of a diurnal non-migrating tide (DE3) and a fast kelvin wave. These waves are generated by lower atmospheric weather and have been shown to affect ionospheric variability and longitudinal structure.

DoD Impact/Significance: This effort will lead to a better understanding of the physics, dynamics, and chemistry of the bottomside ionosphere, with direct implications on future capabilities for nowcasting and forecasting of the environment relevant to DoD/Navy systems.

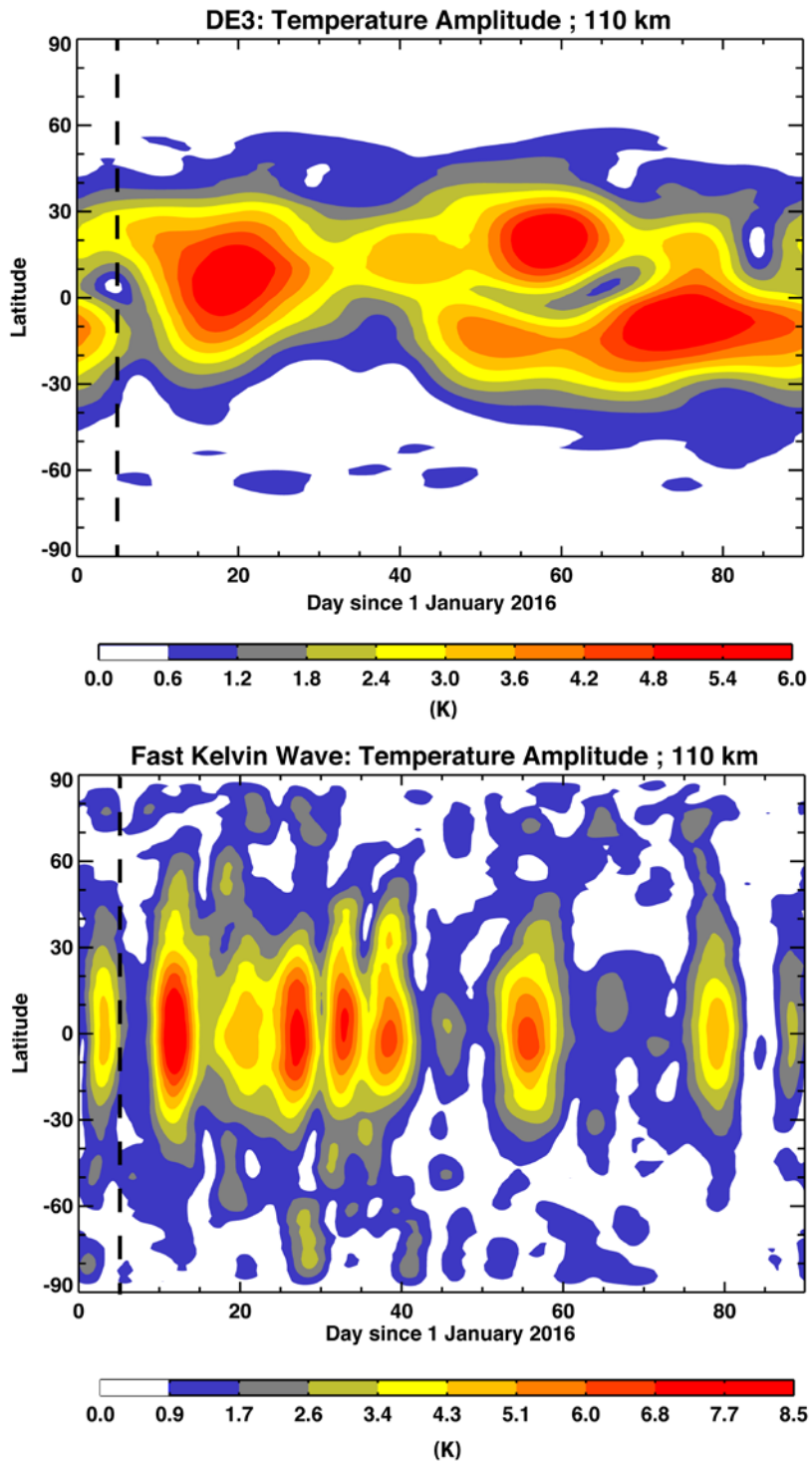


Figure 1. Amplitude of neutral temperature variability at 110 km during January, February, and March 2016 for (top) the diurnal non-migrating, eastward propagating, zonal wavenumber 3 solar tide, and (bottom) for a fast Kelvin wave at zonal wavenumber 1. The vertical dashed line identifies the time of the stratospheric warming.

Title: Navy Ionosphere Model for Operations

Author(s): S.E. McDonald,¹ C.A. Metzler,¹ J.L. Tate,² B.D. Curtis,³ R.K. Schaefer,⁴ P.B. Dandenault,⁴ A.T. Chartier,⁴ G. Romeo,⁴ G.S. Bust,⁴ and R. Calfas⁵

Affiliation(s): ¹Naval Research Laboratory, Washington, DC; ²Computational Physics, Inc., Springfield, VA; ³Praxis, Inc., Arlington, VA; ⁴The Johns Hopkins Applied Physics Laboratory, Laurel, MD; ⁵The University of Texas at Austin Applied Research Laboratories, Austin, TX

CTA: SAS

Computer Resources: Cray XC30 [NAVY, MS], Cray XC40 [NAVY, MS]; Cray XC40 [ARL, MD]; Cray XE6m [ERDC, MS]; SGI Altix ICE [NRL, DC]

Research Objectives: The objective of this effort is to develop a physics-based ionosphere model coupled to an ionospheric data assimilation system that provides global and regional electron density specifications and short-term forecasts (0 – 2 hour). This capability will form the basis of a future Navy operational ionospheric forecasting system, running at multiple resolutions and fully coupled to operational atmospheric forecast models. In FY18, the main objectives were to port the data assimilation system to the HPC environment, begin coupling the data assimilation system with the ionosphere model, and perform initial validation studies.

Methodology: The Navy Ionosphere Model for Operations (NIMO) is a physics-based model, the Navy Highly Integrated Thermosphere and Ionosphere Demonstration System (Navy-HITIDES), and a 3DVAR ionospheric data assimilation system (IDA4D) that can ingest a wide variety of ionospheric datasets. Navy-HITIDES consists of SAMI3, a state-of-the-art NRL model of the ionosphere, along with couplers that use the Earth System Modeling Framework (ESMF) for interpolation the ionosphere and data assimilation grids. IDA4D currently uses an empirical ionosphere, the International Reference Ionosphere (IRI), as its background model and has thus far only been used for ionospheric specification. For NIMO, IRI is being replaced with Navy-HITIDES, which will enable improved specifications and short-term forecasts. The MPI-enabled Earth System Modeling Framework (ESMF) interpolation routines are used to interpolate between the unstructured IDA4D grid and the geomagnetic field-aligned Navy-HITIDES grid.

Results: IDA4D has been successfully ported to several HPC systems and we have identified algorithms within the code that will need to be optimized within the next two years. To couple Navy-HITIDES with IDA4D, we have utilized ESMF interpolation libraries; however, an intermediate grid is required in order to handle interpolation from the unstructured grid in IDA4D to the Navy-HITIDES grid. In FY18 we have successfully completed a one-way coupling in which IDA4D uses the Navy-HITIDES electron densities as the background state. Full coupling to Navy-HITIDES will be completed in early FY19. Navy-HITIDES simulations have been performed for several periods in 2010, 2014, and 2017 that will be used for validation studies as well as determining biases in the code. To prepare for transition of Navy-HITIDES to operations, we are also continuing to optimize the code. With the support of HPCMP User Productivity Enhancement, Technology Transfer and Training (PETTT) program, we have successfully implemented MPI in a second dimension within Navy-HITIDES, which significantly improves the scalability of the code.

DoD Impact/Significance: The development of an operational ionospheric forecast model will aid in the numerical forecasting of high-frequency (HF) radio wave propagation through Earth's atmosphere and ionosphere across the range of conditions relevant to DoD/Navy operations.

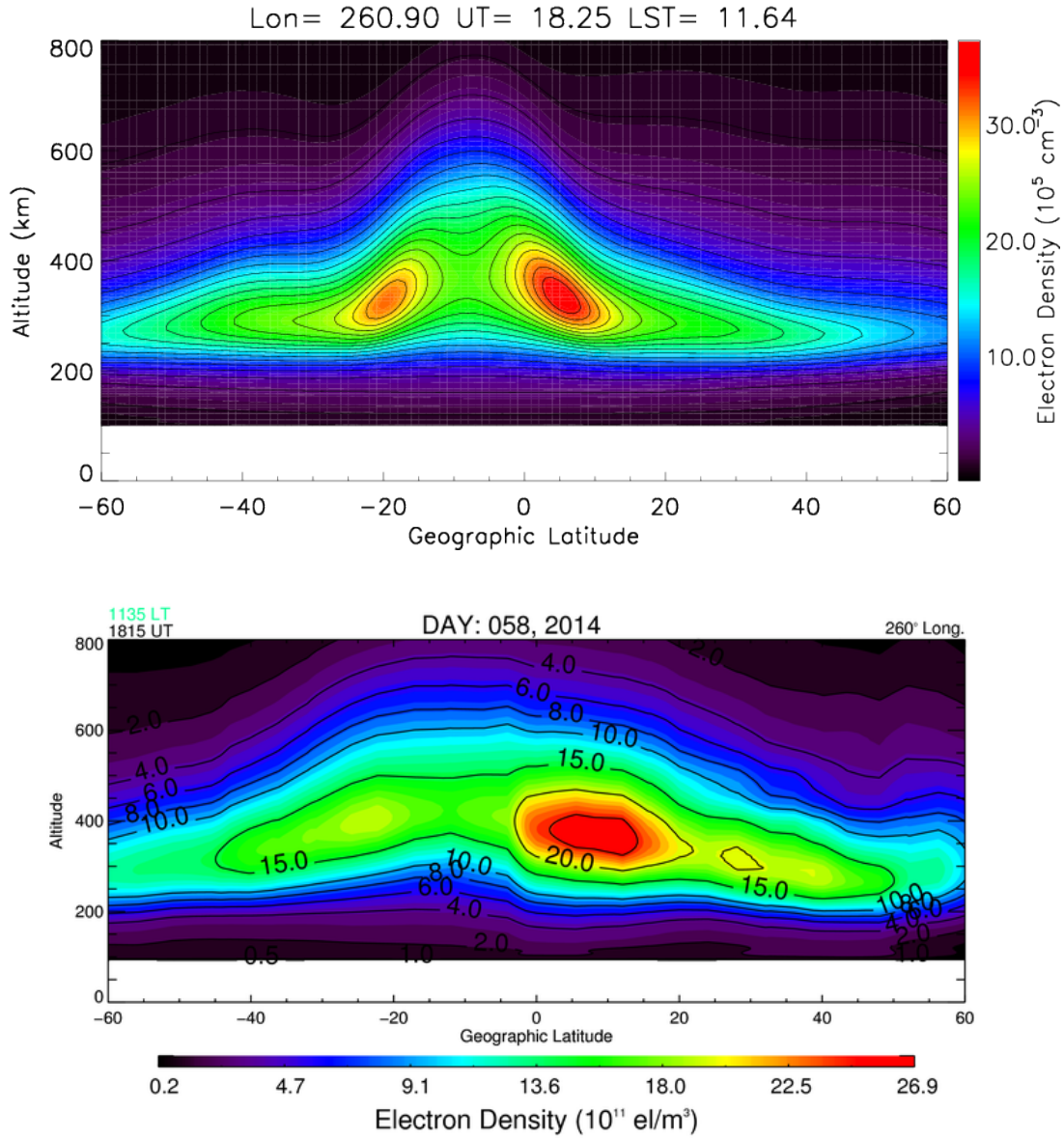


Figure 1. (Top) Navy-HITIDES simulation of electron density as a function of geographic latitude and altitude near noon local time at 260° longitude on 27 February 2014. (Bottom) IDA4D reconstruction of the electron density at the same location and time. In NIMO, IDA4D will use Navy-HITIDES as the background model and to generate short-term (less than 24 hours) forecasts of the ionosphere.

Title: Meteorology and Climatology of the Thermosphere

Author(s): D.P. Drob,¹ M. Jones,¹ and M. Dhadly²

Affiliation(s): ¹Naval Research Laboratory, Washington, DC; ²National Research Council Postdoctoral Program, Washington, DC

CTA: SAS

Computer Resources: SGI ICE X [AFRL, OH]; SGI ICE X [ERDC, MS]; Cray XC40/50 [ERDC, MS]

Research Objectives: Improved knowledge is needed on how the earth's thermosphere and ionosphere is perturbed by tides, planetary waves, and sub-grid scale fluctuations from below, in concert with variable X-ray and extreme ultraviolet (EUV) flux from the sun above. The latter heats the thermosphere and creates the ionosphere. This knowledge is sought for encapsulation into improved first-principles numerical models of the mass, momentum, and energy of the thermosphere for DoD space weather and ionospheric applications.

Methodology: This involves solving the fully coupled neutral thermosphere and ionosphere major species transport equations accounting for radiative transfer, atmospheric chemistry, electric fields, and ion-neutral coupling effects. The fundamental governing equations are encapsulated in the open source distributions of the National Center for Atmospheric Research (NCAR), Thermosphere Ionosphere Mesosphere Electrodynamics General Circulation Model (TIME-GCM).

Results: In order to investigate the effects that drive of the thermosphere and ionosphere from below we performed several numerical experiments to dynamically constrain the TIME-GCM between 35 to 85 km with 3-hourly global output from the High Altitude Navy Global Environmental Model (HA-NAVEM) system. A technique known as 4D tendency nudging was utilized to synchronize TIME-GCM with HA-NAVEM without introducing spurious waves or dynamical artifacts (see Fig. 1). Several case studies for a 3-month period in 2010 were performed to evaluate different model coupling techniques and the results compared to ionospheric observations. A paper has been submitted to the *Journal of Advances in Modeling Earth Systems*.

The effect of the Great American Solar Eclipse of 21 August 2017 on the ionosphere and thermosphere was also investigated. Eclipse-induced solar EUV flux variations were precomputed over space and time using the Naval Observatory Vector Astrometry Software (NOVAS) software library. Space-based EUV images of the solar disk from the NASA Solar Dynamics Observatory Satellite were used to further account for brightness variations across the solar disk. A control simulation of the upper atmosphere and ionosphere was then performed for the 24-hours before and after the event. The eclipse effects were then computed from the solar flux perturbations. The eclipse results in cooling of ~40 K between ~200 to 500 km altitude over ~45 minutes that promptly recovers over about the same timescale. This cooling causes an associated synoptic-scale wind surge in excess of ~50 m/s. Unlike earlier theoretical calculations it was discovered that the eclipse induced temperature and wind perturbations continue to propagate well into the nighttime regions for several hours after the eclipse. Our prediction was confirmed by ground-based 250-km wind and temperature observations obtained in Brazil during the event. A paper was published in *Geophysical Research Letters*. The TIME-GCM output was then used to drive the NRL SAMI3 model to study the eclipse effects on the daytime plasmasphere (see Fig. 2).

DoD Impact/Significance: The coupled physical-based thermosphere-ionosphere model validation studies performed here address the DoD/Navy long-term needs of the environmental prediction of space weather effects for tactical planning purposes, as well as the maximization of DoD HF and Space systems performance through adaptation to the variable environment (ref: SECNAVINST 2400.2A).

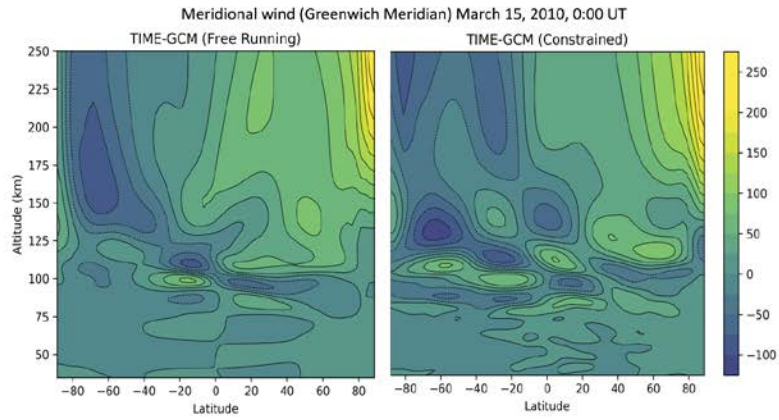


Figure 1: Comparison of meridional (north-south) wind component (m/s) at Greenwich Meridian for March 15, 2010 00:00 UT from the free running TIME-GCM with constant geomagnetic and solar forcing (*left*) and TIME-GCM driven with HA-NAVEM between 35 and 85 km (*right*).

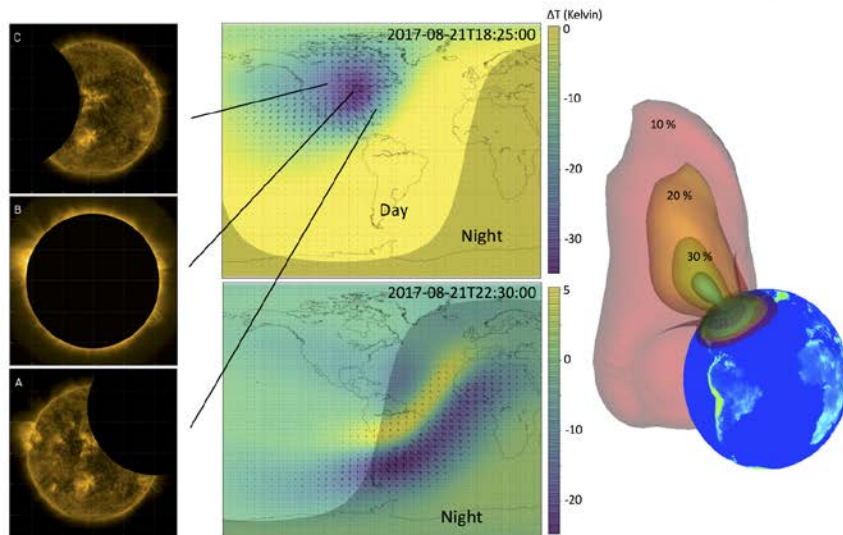


Figure 2: (Left) Eclipse circumstances for 3 times near the point of maximum totality. (Middle) Temperature and wind perturbations at 400 km altitude near maximum totality (*top*) and several hours after with effects well into the nightside (*bottom*). (Right) Ionosphere/plasmasphere electron density perturbations (%) computed with NRL SAMI3 driven by TIME-GCM for the event.

Title: Electromagnetic Pulses from Hypervelocity Impacts on Spacecraft

Author(s): A. Fletcher

Affiliation(s): Naval Research Laboratory, Washington, DC

CTA: SAS

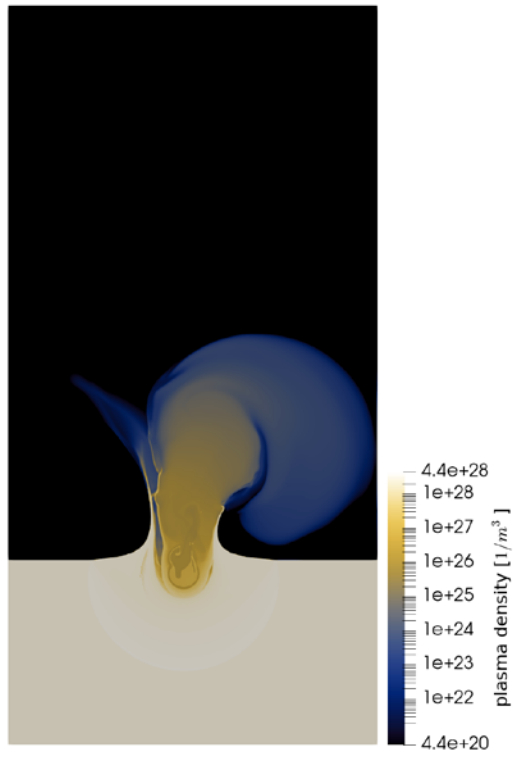
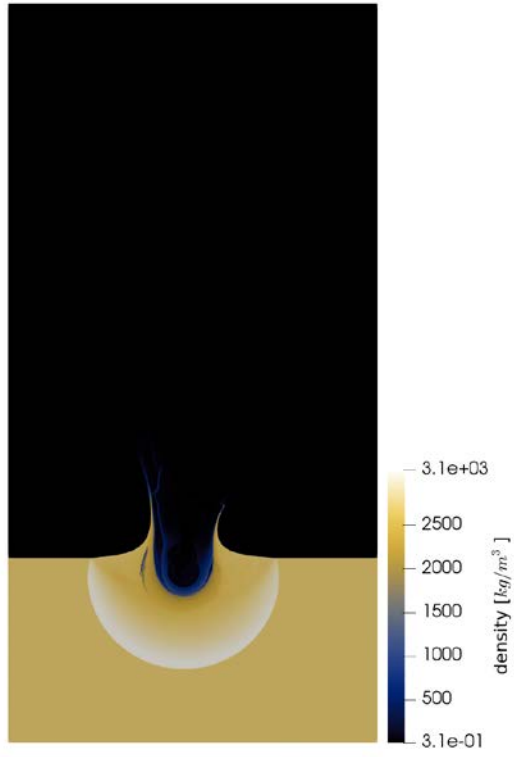
Computer Resources: SGI ICE X [ARL, MD]

Research Objectives: The objective of this project is to use large-scale simulations to understand electromagnetic pulses (EMPs) that are associated with hypervelocity impacts (HVIs) on spacecraft and develop mitigation strategies. HVIs from meteoroids and orbital debris can produce EMPs that threaten satellite electronics. For energetic impacts that occur at a sensitive location on the spacecraft, these EMPs can result in complete loss of mission. While the EMP has been measured experimentally in ground-based experiments, the physical process that produces the EMP and thus the threat posed to spacecraft is not well understood. Countermeasures against hypervelocity impacts of micro-projectiles on DoD space assets depend on the knowledge of the electromagnetic power and frequency spectrum of the impact-associated EMPs. The parametric dependence of the power and spectrum will be determined with a semi-analytic approach in combination with simulations.

Methodology: The problem is split into two regimes (impact and EMP) for which we run separate codes. ALEGRA, a hydrocode from Sandia National Laboratories, is used to simulate the impact and plasma generation. ALEGRA is a hydrocode that solves the continuum dynamics equation, and includes solid mechanics (elasticity, plasticity, and fracture), phase change, and magnetohydrodynamics. JABBERWOCK, a particle-in-cell code from Naval Research Laboratory, is used to simulate the plasma expansion and generation of the EMP. JABBERWOCK is a particle-in-cell code that solves the Vlasov-Maxwell system of equations, and includes kinetic physics, non-equilibrium behavior, and free space electromagnetic radiation. The hydrocode simulation provides boundary and initial conditions for the particle-in-cell simulation. Both codes are fully parallelized with MPI.

Results: We ran a series of simulations to verify the predictive capability of the simulation pipeline by validating against ground-based Van de Graaff accelerator impact experiments. These simulations were consistent with a number of impacts from these experiments, specifically in plasma temperature, plasma density, charge production, and EMP frequency. The simulations also reproduced the EMP mechanism predicted by theoretical calculations, including the broadband spectrum. However, unlike the theory, the simulations exhibited dampening which subsequently narrowed the frequency spectrum. The addition of Earth's magnetic field in both codes altered the expansion of the plasma plume from the impact site. Additionally, the presence of an ambient magnetic field led to the formation of a diamagnetic cavity. The formation of this cavity, as well as the snap-back effect once the plasma diffuses, seems to enhance lower frequency power within the EMP frequency spectrum. We also examined new target and projectile materials beyond the tungsten used in the impact experiments. Specifically, we began running cases of iron and ice meteoroids striking an aluminum spacecraft surface. The aforementioned dampening process, the impact angular dependence, as well as velocity space instabilities triggered in the impact plasma will be explored further in future simulations. As part of this effort, the JABBERWOCK code also underwent significant development, testing, and parallelization.

DoD Impact/Significance: Protection of critical DoD space assets from impact EMPs is necessary to assure uninterrupted C4ISR capability, which is critical for operational success as envisioned in the Navy's S&T strategic plan for information dominance. Impact EMPs can produce electromagnetic fields that overwhelm existing mitigation if the impact is near a sensitive component, driving currents and creating electrostatic potentials in spacecraft electronics.



Title: Dynamic Phenomena in the Solar Atmosphere
Author(s): M.G. Linton
Affiliation(s): Naval Research Laboratory, Washington, DC
CTA: SAS

Computer Resources: SGI ICE X [AFRL, OH]; Cray XE6m [ERDC, MS]; Cray XC30 [AFRL, OH]; Cray XC40 [ARL, MD]; Cray XC40 [ERDC, MS]

Research Objectives: The goal of this HPC program is to investigate the solar drivers of the space weather that disrupts DoD and civilian communications and navigation systems. The program is focused on understanding, and ultimately predicting, the initiation processes of the two key solar drivers: coronal mass ejections (CMEs) and solar flares. The fundamental questions that we are investigating are how flux emergence and photospheric twisting or shearing drive CMEs and flares, and how the reconnection which releases energy in these events occurs in both coronal and chromospheric conditions.

Methodology: Our work focuses on the emergence of magnetic fields from the convection zone into the solar corona, with the goal of determining how solar activity is generated. We investigated how the emergence of twisted magnetic fields into the corona generates flaring active regions known as delta-spots. We also advanced our data-driving capabilities, developing methods to incorporate observed photospheric magnetic field information into magnetohydrodynamic (MHD) simulations. We also studied how photospheric convective motions can send MHD waves into the corona, both driving reconnection in the corona, and heating coronal fields. For these studies, we used our MHD code LAREXD for two dimensional (2D) and three dimensional (3D) simulations.

Results: We have simulated the formation of coronal current sheets and bands of heating along current sheets due to the conversion of MHD waves at coronal null points. We have shown how these waves convert between modes at the coronal nulls, and how trapping of these converted waves in the nulls turns the nulls into current sheets. Reconnection at these current sheets then releases stored coronal magnetic energy, and heats the corona along critical surfaces separating different magnetic field domains. This work helps explain how the corona is heated to higher temperatures than the underlying photosphere, and provides possible diagnostics for detecting wave heating at magnetic domain boundaries. We have further developed MHD wave characteristic methods for driving the photospheric boundary of chromospheric and coronal MHD simulations with observed photospheric magnetic fields and velocities. We have derived the characteristics-based boundary conditions required to drive our MHD simulation in an internally self-consistent manner. This has been implemented in LARE3D, and successfully tested on standard shock-wave problems in the one dimensional limit. Current work will extend testing to three dimensions. We have simulated the formation of solar delta-spots, a type of active region that makes up only a minority of sunspots, but which accounts for the majority of large solar flares. We have shown that twisted magnetic flux ropes, when they emerge into the corona, show all of the classic traits of delta-spot evolution, namely: spot rotation, magnetic field twist, and compact structure. We are now investigating how flare active these simulated structures can be. The simulations will be extended further into the convection zone, to capture the critical early evolution of these structures before they emerge.

DoD Impact / Significance: These numerical simulations are providing new insight into how solar flares and coronal mass ejections are driven by photospheric flux emergence, and how wave driving energizes and heats the chromosphere and corona. Furthering understanding of how solar activity is generated is a critical step toward building space weather prediction models, and mitigating dangers of space weather.

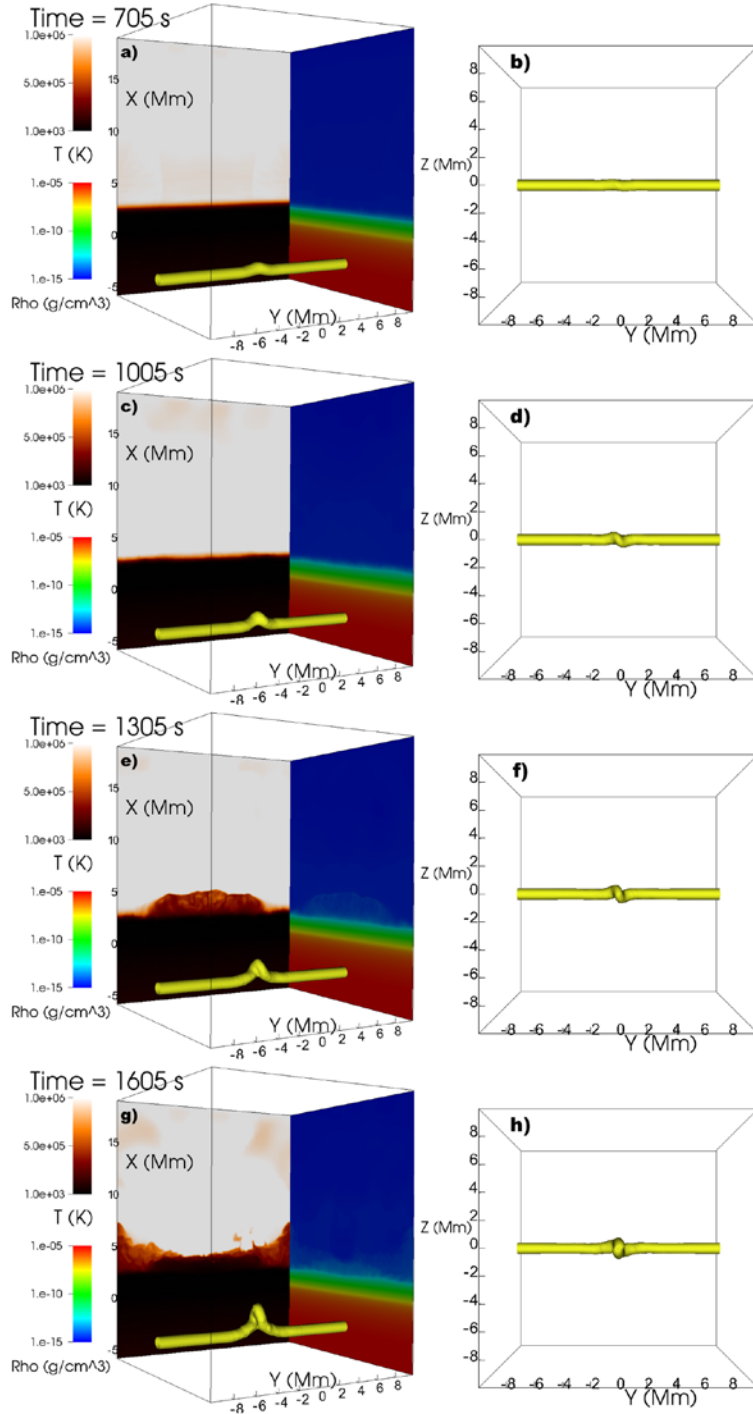


Figure 1. This figure illustrates the evolution of the helical, current-driven kink instability in a twisted magnetic flux rope as it rises and expands through the solar convection zone. The panels show isosurfaces of magnetic field at a strength of 1 kG (yellow surfaces), from the side (a, c, e, g) and top (b, d, f, h) perspectives. The side perspectives also show the temperature (brown color scale) and the density (rainbow color scale) on the side surfaces. This figure shows how the flux rope, which is perturbed with a buoyancy term, rises at its center, and then kinks in a helical fashion as it nears the photosphere ($X=0$ Mm).

Title: Radio and Gamma-ray Searches for Millisecond Pulsars and Radio Transients*

Author(s): P.S. Ray and J. Deneva

Affiliation(s): Naval Research Laboratory, Washington, DC

CTA: SAS

Computer Resources: SGI Altix ICE [NRL, DC]

Research Objectives: The purpose of this project is to search for millisecond pulsars in gamma-ray data from NASA's *Fermi* Large Area Telescope as well as pulsars and radio transients in ground based data from the Robert C. Byrd Green Bank Telescope in West Virginia and the Arecibo telescope in Puerto Rico. These searches require high performance computing resources because of the massive parameter spaces that must be searched.

Methodology: We use custom codes to search for pulsations in our radio and gamma-ray data sets. These correct for frequency-dependent delays caused by interstellar dispersion and variable Doppler shifts caused by orbital acceleration in a binary system then search over a broad range of candidate frequencies using very large Fourier transforms and harmonic summing. We split up the trials over a set of nodes on the cluster.

Results: During FY18 we searched 300 hours of data from the 327 MHz Arecibo drift pulsar survey (AO327). This survey began in 2010 and aims to cover the part of the sky accessible to the Arecibo telescope. It is currently the largest conducted with the Arecibo telescope, both in terms of sky coverage and observing time allocation. Our code for automatically selecting radio transient candidates based on their likelihood of originating from an astrophysical source discovered 4 new objects: 2 pulsars and 2 rotating radio transients. In addition, students looking through candidates from our periodicity search found 2 new pulsars, including one millisecond pulsar. We are carrying out additional observations with the Arecibo telescope to determine whether the millisecond pulsar is a stable enough rotator for inclusion in Pulsar Timing Arrays (PTAs) aiming to detect nanohertz gravitational waves. We also searched 29 hours of Green Bank Telescope data at 2 GHz and 6 GHz from a search for pulsations in 15 steep-spectrum radio sources in the Galactic Center. A population of millisecond pulsars in the Galactic Center is one of two competing explanations for the excess of gamma-ray emission detected in that region by the *Fermi* spacecraft. Although there were no new pulsar discoveries from this project, a pulsation search is a necessary step toward determining the type of compact radio sources in the Galactic Center whose spectra are similar to those of known pulsars.

DoD Impact/Significance: The main goal of AO327 is to find millisecond pulsars that are very stable rotators and therefore useful for detecting gravitational waves with a PTA. Among the ~2700 known pulsars, only 35 fit this criterion and any addition to this set is a significant contribution to the nanohertz gravitational wave detection effort as it improves the sensitivity of the PTA. The PTA approach to gravitational wave detection is complementary to LIGO and sensitive a different range of gravitational wave frequencies. To date, AO327 has contributed two such discoveries to the PTA. Another major goal of the survey is to catalog the local pulsar population at 327 MHz, which would contribute to improved models of the pulsar population and evolution in the Galaxy as a whole. Our searches are part of a worldwide campaign to understand the nature of the large population of unidentified gamma-ray sources being uncovered by *Fermi*. The large population of millisecond pulsars in short-period interacting binaries (the black widows and redbacks) has been a real surprise. This work is an important contribution to the science return of the major NASA mission and will help us understand the physics and astrophysics of neutron stars, one of the most extreme environments anywhere in the universe.

* This work was supported by NASA.

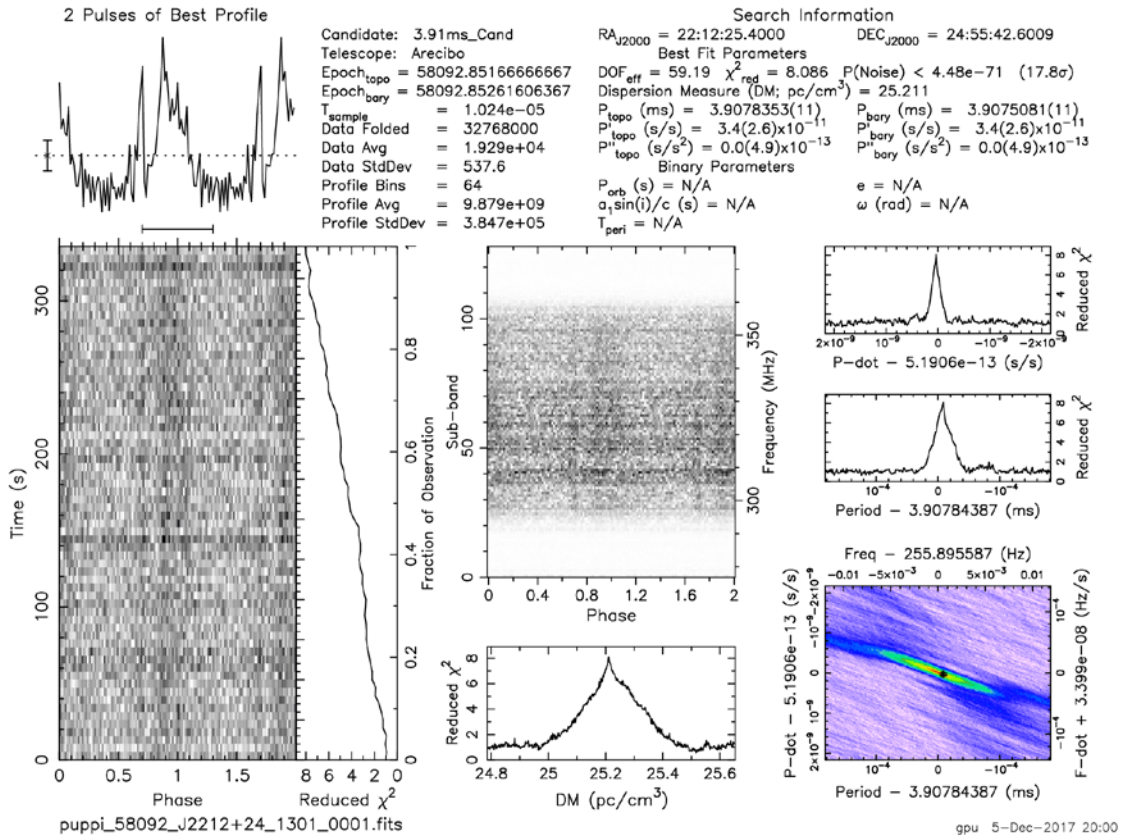


Figure 1. Discovery of the millisecond pulsar J2212+24 in the AO327 survey for radio pulsars and transients. This pulsar has a rotation period of 3.91 ms. The pulsar's sharp resolved features in its pulse profile make it a good candidate for inclusion in Pulsar Timing Arrays with the goal of detecting nanohertz gravitational waves.

THIS PAGE INTENTIONALLY LEFT BLANK

OTH

Other

Work that is not easily categorized as one of the other computational technology areas.

Title: Simulation of High Energy-Radiation Environments
Author(s): J. Finke and A. Hutcheson
Affiliation(s): Naval Research Laboratory, Washington, DC
CTA: OTH

Computer Resources: SGI Altix ICE [NRL, DC]; SGI ICE X [AFRL, OH]; Cray XC30 [AFRL, OH], Cray XC40, [ARL, MD]; Cray XC40/50 [ERDC, MS]

Research Objectives: Apply 3-D Monte Carlo methods to simulate the transport of high-energy particles for use in space applications and for modeling detection systems, radiation environments, and the operational concepts relevant to the detection of Special Nuclear Materials and other radiological/nuclear materials in maritime and urban scenarios of interest to DoD and other civilian agencies.

Methodology: Our studies involve using three industry-standard ionizing radiation transport codes: two 3-D Monte Carlo packages, Geant4 (CERN) and MCNP (Los Alamos National Lab), and one discrete ordinates package, Denovo (Oak Ridge National Lab). We use an NRL-developed front-end package called SoftWare for Optimization of Radiation Detectors (SWORD) to quickly prototype geometries and radiation environments for running our simulations.

Results: Many of the simulations conducted were in direct support of Defense Threat Reduction Agency (DTRA) and the Department of Homeland Security's Countering Weapons of Mass Destruction office (DHS/CWMD) operational scenarios and/or exercises and were classified FOUO or higher. We have supplied extensive simulations in support for optimizing upgrades to radiation detection capabilities on Stryker armored vehicles for Space and Naval Warfare Systems Command (SPAWAR) and DTRA. In addition, we have continued support of the Data Mining, Analysis and Modeling Cell (DMAMC) program at DHS/CWMD. As part of our effort to supply measured radiation background spectra to DMAMC, we have performed simulations to understand instrument response to various background configurations. Along with supporting these agencies, two additional simulations are discussed here. First, in support of investigations at the National Institute of Standards and Technology (NIST) research reactor, we performed modeling and simulations of both thermal and cosmogenic neutrons in an experiment "cave" to help determine residual backgrounds. Second, we have investigated using the gamma-ray spectra of active galactic nuclei to measure the extragalactic background light (EBL) and the cosmic star formation rate (SFR) as a function of redshift. We used Markov Chain Monte Carlo (MCMC) fits to the gamma-ray opacity measurements with a model that allows a parameterized SFR to vary. A result can be seen in Fig. 1. The squares represent a variety of SFR data from ultraviolet (UV) and Lyman break galaxy (LBG) surveys. The shaded blue and green regions represents the 68% confidence interval SFR from MCMC fits to the gamma-ray data with two different methods. This is the first point source-independent measurement of the SFR; it has been accepted for publication by the journal *Science*.

DoD Impact/Significance: The ability to produce accurate predictions of radiation detection instrument effectiveness reduces risk and cost in development. Similarly, simulation of radiation detection concepts of operation allows assessment of their effectiveness in realistic environments. The ability to provide timely answers to the questions posed by DHS/CWMD, DTRA, NASA and other government sponsors is also important for the continued success in supporting the DoD mission. In addition, the science addressed by ionizing radiation simulations such as the studies described above is often impractical or not cost effective to study in any manner other than simulation. The results of these studies directly address our understanding of the high-energy radiation environment in which we live and operate.

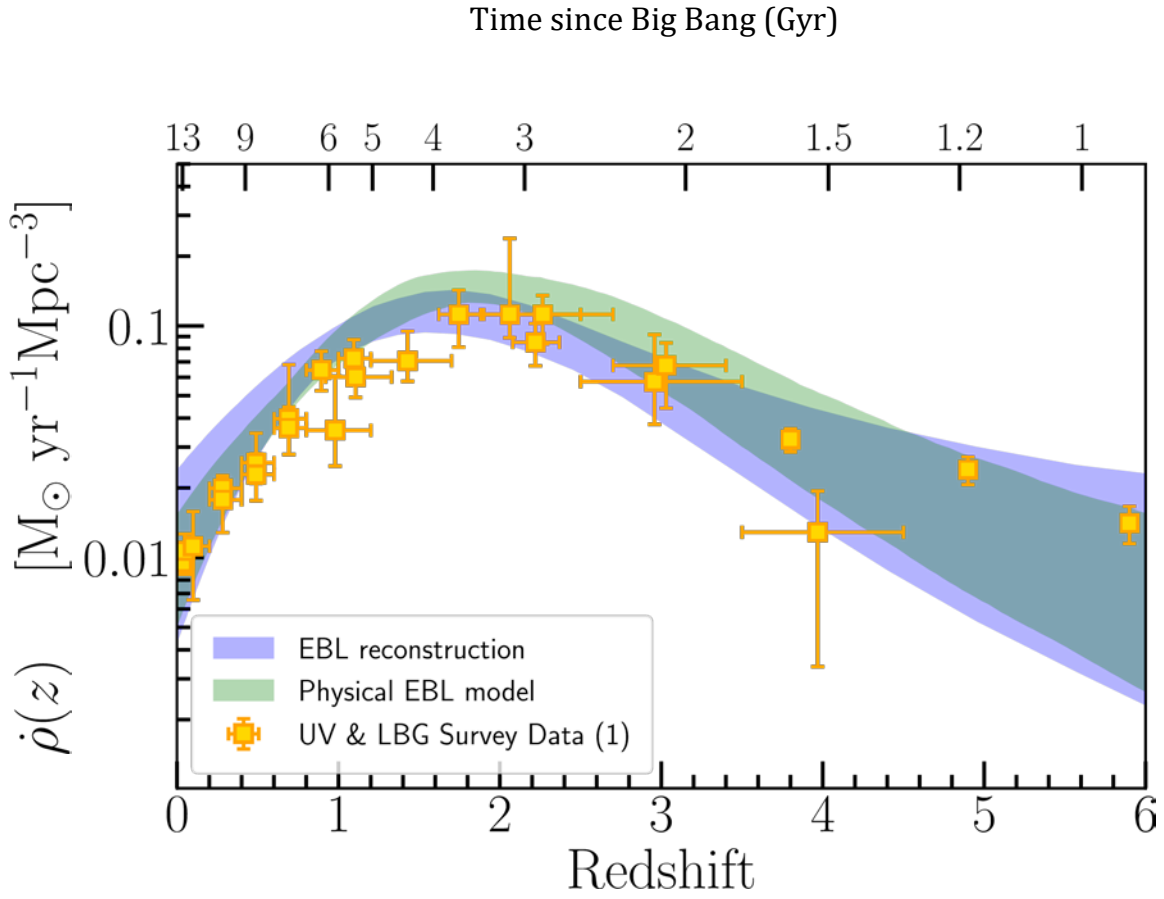


Figure 1. The Star Formation Rate (SFR) as a function of redshift, or equivalently, the time since the big bang. The yellow squares are the SFR measured from UV and LBG surveys. The green and blue shaded regions represent the 68% confidence intervals from MCMC fits to the gamma-ray data with two different methods.

THIS PAGE INTENTIONALLY LEFT BLANK

Author Index

Achuthan, A.----- 6	deRada, S.----- 104
Alatishe, J.-----84	Dey, S.----- 82
Allard, R.----- 114	Dhadly, M.S. ----- 134, 138
Allen, D.R.----- 102	Douglas, E. ----- 104
Amerault, C.----- 104	Doyle, J.D.----- 120
Ames, C.-----48	Drob, D.P.----- 134, 138
Ananth, R.-----10	Dykes, J.-----96
Anderson, G.P.-----56	
Arcari, A.----- 6	Eckermann, S.D.----- 102
	Erwin, S.C.----- 54
Bartels, B.P.----- 110, 112	Evans, T. ----- 42
Barron, C.N.----- 104, 110, 112	
Barton, C.A.----- 102	Fabre, J.P.----- 74
Barton, N.P.----- 100	Fan, Y.----- 116
Bateman, S.P.-----12	Finke, J. ----- 148
Beall, J.H. ----- 132	Fletcher, A. ----- 140
Bermudez, V.M.-----46	Franke, J.R.-----6
Bernstein, N.-----64	
Blisard, S.N. ----- 126	Gamezo, V.N. ----- 18
Buijsman, M. ----- 118	Geltmacher, A.B. -----6
Bust, G.S. ----- 136	Glasbrenner, J. -----68
	Goldman, E.R.----- 56
Caffrey, P.-----98	Goodwin, G. ----- 26
Calantoni, J.----- 12	Gordon, D.F.----- 80
Calfas, R.----- 136	
Campbell, T.----- 104, 114	Ha, V.-----4
Campbell, W.F.-----94	Hafizi, B.----- 80
Carrier, M. ----- 104	Hasler, D.J. -----6
Carter, S. ----- 82	Hebert, D. ----- 114
Cayula, S. ----- 108	Hellberg, C.S. ----- 62
Chartier, A.T.----- 136	Helle, M. ----- 80
Chen, Y. ----- 80	Herrera, M.A.----- 102
Chong, Y.K. -----24	Hervey, W.J., IV ----- 48, 50
Colston, S.M.-----48	Holman, T.D.----- 28
Cooke, S.-----90	Hoppel, K.W.----- 102
Corrigan, A.-----16	Horton, D.J.-----6
Crawford, W. ----- 100	Hou, W. ----- 14
Crout, J.----- 114	Huang, L. ----- 66
Curtis, B.D. ----- 134, 136	Huba, J.D.----- 34
	Hutcheson, A. ----- 148
D'Addezio, J.----- 104	
Dandenault, P.B.----- 136	Jacobs, G.A.----- 112
Dastugue, J.M.----- 104, 110	Jensen, A. ----- 90
Dean, S.N.-----50	Jensen, T. ----- 114, 116
DeHaan, C.J.----- 112	Jeon, C.H.----- 118
Deneva, J. ----- 144	Johannes, M.----- 60

Author Index

Johnson, L. -----	80		
Johnson, R.F. -----	16, 22		
Joliff, J.K. -----	96		
Jones, M. -----	138		
Kaganovich, D. -----	80		
Kercher, A.D. -----	20, 22		
Khine, Y. -----	80		
Kim, S. -----	50		
Krall, J. -----	34		
Krivacic, B. -----	128		
Kuna, L.P. -----	6		
Kuhl, D.D. -----	102		
Ladner, S. -----	96		
Lambrakos, S. -----	66		
Leary, D.H. -----	48, 50		
Leighton, R. -----	42		
Levenson, A. -----	12		
Linton, M.G. -----	142		
Linzell, R.S. -----	110, 112		
Liu, J.L. -----	16, 56		
Liu, M. -----	100		
Lyons, J.L. -----	58		
Ma, J. -----	102		
Maloy, B.R. -----	110		
Mancias, J.A. -----	6		
Manolidis, M. -----	106		
Martin, P. -----	104		
Martin, T.J. -----	6		
Massa, L. -----	66		
Matt, S. -----	14		
May, J.C. -----	104, 110		
Maxwell, J.R. -----	30		
Mazin, I. -----	68		
McCormack, J.P. -----	102		
McDonald, S.E. -----	134, 136		
McLay, J. -----	100		
Metzger, E.J. -----	118		
Metzler, C.A. -----	134, 136		
Michopoulos, J.G. -----	6		
Mott, D.R. -----	20		
Mukhopadhyay, S. -----	70		
Mulberry, W. -----	104		
		Ngodock, H. -----	104
		Obenschain, S.P. -----	40
		Orzech, M. -----	106
		Osborne, J.J. -----	104, 110
		Ottinger, P.F. -----	40
		Ouellette, J.D. -----	88
		Ovtchinnikov, S. -----	90
		Pehrsson, P.E. -----	46
		Penano, J. -----	80
		Penta, B. -----	108
		Penteleev, G.G. -----	110
		Petillo, J. -----	90
		Petrov, G.M. -----	86
		Photiadis, D. -----	76
		Poludnenko, A.Y. -----	18
		Rabenhorst, S. -----	98
		Ramamurti, R. -----	16, 36, 38
		Ray, P.S. -----	144
		Reinecke, P.A. -----	122
		Reinecke, T.L. -----	70
		Reynolds, C. -----	100
		Richardson, A.S. -----	40
		Ridout, J. -----	100
		Rimmer, M.A. -----	48, 50
		Rittersdorf, I. -----	40
		Rogers, E. -----	114, 116
		Rogers, R.E. -----	30
		Romano, A.J. -----	78
		Romeo, G. -----	136
		Rowley, C.D. -----	104, 108, 110
		Ruston, B. -----	94
		Sassi, F. -----	102, 134
		Savelyev, I. -----	42
		Saunders, R.N. -----	2, 4, 6
		Schaefer, R.K. -----	104, 136
		Schumer, J.W. -----	40
		Schweigert, I.V. -----	52
		Schwer, D.A. -----	22, 32
		Shriver, J.F. -----	104, 118
		Shulman, I. -----	108
		Simeonov, J.A. -----	12, 106

Author Index

Sletten, M.A.	88
Smedstad, L.F.	104, 110, 112
Smith, G.B.	42
Smith, L.N.	126, 128
Smith, S.	104
Smith, T.	96, 104, 110, 112, 114
Souopgui, I.	104
Spence, P.J.	104, 110, 112
Stantchev, G.	90
Stefik, M.	128
Sullivan, K.M.	126
Swanekamp, S.B.	40
Szymczak, W.G.	78
Tan, X.G.	2
Tate, J.L.	102, 134, 136
Teferra, K.	4
Toporkov, J.V.	88
Townsend, T.L.	110
VandeVoorde, N.	110
Viner, K.	100
Viswanath, K.	36
Vora, G.J.	48, 50
Whitcomb, T.	100
Wimmer, S.A.	6
Wolff, M.T.	132
Yaremchuk, M.	110
Youngblood, M.	128
Zabetakis, D.	56
Zalalutdinov, M.	82
Zhuang, X.	10

Site Index

DSRC's

AFRL 2, 4, 6, 10, 16, 18, 20, 22, 26, 28, 32, 42, 46, 48, 50, 52, 54, 58, 62, 64, 66, 68, 70, 76, 78, 80, 82, 88, 90, 94, 100, 120, 122, 134, 138, 142, 148

ARL 2, 12, 14, 16, 20, 22, 24, 26, 28, 36, 38, 40, 48, 50, 52, 58, 60, 62, 64, 68, 80, 82, 84, 88, 90, 98, 100, 102, 106, 120, 122, 128, 134, 136, 140, 142, 148

ERDC 2, 4, 6, 12, 16, 18, 22, 24, 34, 36, 48, 50, 52, 62, 64, 66, 68, 70, 78, 80, 82, 86, 88, 90, 98, 100, 102, 106, 118, 120, 122, 126, 136, 138, 142, 148,

NAVY 24, 30, 40, 74, 84, 86, 90, 94, 96, 100, 102, 104, 106, 108, 110, 112, 114, 116, 118, 120, 122, 134, 136

MHPCC 84, 126

ARC's

NRL 2, 38, 40, 42, 46, 56, 82, 102, 126, 132, 136, 144, 148

Division/Branch Index

Systems Directorate (Code 5000)

Navy Center for Applied Research In Artificial Intelligence (Code 5510) 126, 128

Radar Division (Code 5300)

Surveillance Technology (Code 5340) 84

Information Technology Division (Code 5500)

Center for Computational Science (Code 5590)..... 80

Materials Science and Component Technology Directorate (Code 6000)

Laboratory for Computational Physics and Fluid Dynamics
(Code 6040) 16, 18, 20, 22, 32, 36, 38, 40, 56, 80

Chemistry Division (Code 6100)

Center for Corrosion Science and Engineering (Code 6130) 6
Surface Chemistry (Code 6170)..... 46
Navy Technology Center for Safety and Survivability (Code 6180) 10, 52

Materials Science and Technology Division (Code 6300)

Multifunctional Materials (Code 6350) 2, 4, 6, 80
Center for Computational Materials Science (Code 6390)..... 6, 54, 58, 60, 62, 64, 66, 68

Plasma Physics Division (Code 6700)

Radiation Hydrodynamics (Code 6720) 24, 86
Laser Plasma (Code 6730) 40
Charge Particle Physics (Code 6750) 140
Pulsed Power Physics (Code 6770) 40
Beam Physics (Code 6790)..... 34, 80, 128

Electronics Science and Technology Division (Code 6800)

Microwave Technology (Code 6850) 90
Electronic Materials (Code 6870)..... 46, 70, 82

Center for Biomolecular Science and Engineering (Code 6900)

Senior Scientist for Biosurveillance (Code 6905) 56

Laboratory for Biosensors and Biomaterials (Code 6910)	48, 50
Laboratory for Biomaterials and Systems (Code 6920)	56

Ocean and Atmospheric Science and Technology Directorate (Code 7000)

Acoustics Division (Code 7100)

Physical Acoustics (Code 7130)	76, 78, 82
Acoustics Signal Processing and Systems (Code 7160)	78
Acoustics Simulation, Measurements and Tactics (Code 7180)	74

Remote Sensing Division (Code 7200)

Remote Sensing Physics (Code 7220)	88, 98, 102
Coastal and Ocean Remote Sensing (Code 7230)	42
Image Science and Applications (Code 7260)	88

Oceanography Division (Code 7300)

Ocean Dynamics and Prediction (Code 7320)	96, 104, 106, 108, 110, 112, 114, 116, 118
Ocean Sciences (Code 7330)	14, 96, 104, 108

Marine Geosciences Division (Code 7400)

Seafloor Sciences (Code 7430)	12, 106
-------------------------------------	---------

Marine Meteorology Division (Code 7500)

Probabilistic Prediction (Code 7504)	100
Atmospheric Dynamics and Prediction (Code 7530)	94, 100, 104, 120, 122

Space Science Division (Code 7600)

Geospace Science and Technology (Code 7630)	102, 134, 136, 138
High-Energy Space Environment (Code 7650)	132, 144, 148
Solar and Heliospheric Physics (Code 7680)	142

Naval Center for Space Technology Directorate (Code 8000)

Spacecraft Engineering (Code 8200)

Space Mechanical Systems Development (Code 8220)	26, 28, 30
--	------------

REVIEWED AND APPROVED
NRL/PU/5594--19-653
RN: 19-1231-3335
November 2019

Brian J. Cadwell (Acting)
Superintendent, Information Technology Division